Carbon dynamic in New Caledonia mangroves : Past, present, futur

Adrien Jacotot

École Doctorale du Pacifique - ED 469

THÈSE

Pour l'obtention du titre de

DOCTEUR DE L'UNIVERSITÉ DE LA NOUVELLE-CALÉDONIE

Spécialité : Sciences de la Terre et de l'Univers

présentée par

Adrien JACOTOT

Dynamique du carbone dans les mangroves de Nouvelle-Calédonie : Passé, présent, futur

Sous la direction de

Cyril MARCHAND, Chargé de Recherche HDR, IRD Nouvelle-Calédonie

Michel ALLENBACH, Professeur de l'Université de la Nouvelle-Calédonie

COMPOSITION DU JURY

Cyril MARCHAND	Chargé de Recherche HDR, IRD Nouvelle-Calédonie	Directeur
Michel ALLENBACH	Professeur, Université de la Nouvelle Calédonie	Directeur
Andrea C. ALFARO	Professeur, Faculty of Health and Environmental Sciences	Rapporteur
Shing Yip Joe LEE	Professeur, Griffith School of Environment, Australia	Rapporteur
Yves LETOURNEUR	Professeur, Université de la Nouvelle Calédonie	Examinateur
Luc DELLA PATRONA	Chargé de Recherche HDR, IFREMER Nouvelle-Calédonie	Examinateur

SOUTENUE LE 11 DÉCEMBRE 2017

École Doctorale du Pacifique - ED 469

THÈSE

Pour l'obtention du titre de

DOCTEUR DE L'UNIVERSITÉ DE LA NOUVELLE-CALÉDONIE

Spécialité : Sciences de la Terre et de l'Univers

présentée par

Adrien JACOTOT

Dynamique du carbone dans les mangroves de Nouvelle-Calédonie : Passé, présent, futur

Sous la direction de

Cyril MARCHAND, Chargé de Recherche HDR, IRD Nouvelle-Calédonie

Michel ALLENBACH, Professeur de l'Université de la Nouvelle-Calédonie

Histoire du Mont Mou et du Mont Karikaté

C'était au temps où les humains se confondaient avec la nature. Les hommes étaient en même temps montagne ou rocher, les femmes plaine ou source. Et c'est ainsi que le Mont Mou était le grand chef de la région. L'eau qui sortait de ses flancs était autant de femmes qui fertilisaient les champs… Quand le grand chef voulait s'entretenir avec ses ancêtres, il se couvrait de nuages et personne n'osait le déranger.

Au bord de mer vivait le Mont Karikaté, avec son clan pêcheur. En ce temps-là, le lagon était riche : poissons, coquillages, on n'avait pas besoin d'aller très loin pour les pêcher, la mangrove grouillait de crabes. Les gens du littoral se contentaient de prendre au jour le jour leur nourriture. Voyant cette abondance, le Mont Karikaté se dit :

— Tiens, je vais m'attirer les bonnes grâces du grand chef Mont Mou. Je vais m'approcher de lui avec ma mer, mes poissons, mes coquillages et mes crabes et ses femmes n'auront plus qu'à se pencher pour se servir.

Sitôt dit, sitôt fait. Il se déplaça avec sa mer, ses poissons, ses crabes et ses coquillages, et arriva très vite à côté du Mont Mou.

Or, ce jour-là, le grand chef Mont Mou était de mauvaise humeur, le sorcier lui avait donné de fort mauvaises nouvelles de son fils aîné parti guerroyer dans le sud. Et il digérait mal son repas. Il eut des nausées et se mit à crier :

— Tu m'incommodes avec ton odeur de poisson et de coquillage ! Vas-t-en, éloigne-toi de moi ! Retourne d'où tu viens avec ta mer, tes poissons, tes coquillages et tes crabes ! Tout ça sent mauvais !

Le Mont Karikaté, surpris et étonné d'entendre dire qu'il sentait mauvais, ne bougea pas.

Alors le grand chef se fâcha :

— Si tu ne pars pas je vais te frapper !

L'autre recula vers la plaine et s'arrêta en narguant le Mont Mou.

Le grand chef prit alors sa sagaie de pêche taillée dans le bois de karive[1] *et la lança à la tête de Karikaté. Celui-ci para le coup à l'endroit que l'on appelle Ko Tàbwòo-re*[2] *(« là où il a paré le coup »). Mais il ne fut pas assez rapide car la sagaie se planta dans sa tête. Fou de douleur, il cassa une branche de palétuvier et, de toutes ses forces, il la lança à la tête du Mont Mou. Il prit une motte de boue et l'envoya aussi sur la tête de son adversaire. Puis il s'en*

---

[1] Arbre endémique, espèce du Sud

[2] Toponyme, région de Païta

retourna avec sa mer, ses poissons, ses crabes et ses coquillages, au milieu des siens.

Longtemps après, quand chacun d'eux prit sa condition définitive de montagne, et ne bougea plus, la tige de karivé poussa et devint un arbre, et la tige de palétuvier prit racine dans la motte de boue.

Aujourd'hui, si vous vous promenez à Karikaté, vous apercevrez un beau karivé qui pousse au milieu des essences du littoral. De même, si vous faites l'ascension du Mont Mou, vous risquez de vous trouver nez à nez avec un palétuvier qui pousse dans sa motte de boue. Ce sont des arbres qui ne devraient pas se trouver là. Le karivé, qui pousse actuellement en bas du Mont Karikaté, provient de là-haut, sur le Mont Mou. Le palétuvier est un arbre de la région du littoral, et pousse actuellement sur le Mont Mou.

Du bois périssable jaillit la vie qui en perpétue la mémoire.

Voilà ce que nous ont raconté les « vieux ».

Récit de Mme Yvonne Païta, recueilli par Tadahilo Shintani,
et réécrit par l'association Bècaa-jíí küü yë.

In Textes en Nráa drùbea, I.L.C.A.A., 1992.

Nrè tàa jíí a jíè nrókû-mú pá káavùu ké nrè ngímè-nrí.
Káavùu kââ.
Wè tó pèe nrè tètèrî nrí a-wí jíè nrókû-káríkáté.
Nrókû- káríkáté a nyí ábórú ké pèe wècáaxíí.
Nròpwe nyí mwà té mèe vèngí-re drákánrìa nrècóxè re nrí mí xée íyà-re nrí mí púu re nrí mí bée re nrí mí nrúxée íyá-re nrí.
Wè jíkââ pàa káavùu nrókûmù mwà nrìí yò nrí mè vê rùu mè kí vè kû ké tètèrî rá.
Kó béè jáanrí-re mè kí té tóre tètèrî rá wê téè múu a-kââ.
Mú nrècóxè mí mú nrúxée íyà-re mí mú púu-roo mú bée-roo mú-nrí a-kââ.
Kó béè jáanrí.
Vè rúu mè kí mítò-mwéré kwé nrè ngímòo mè kí vêmwéré kwé pèe wècáaxíí lè kí tó wê ngí áúré-roo.
Wè jíè káríkáté pá béè jáanríwârá-re vée re nrí.
Nyí pá tóò.
Nrókû-mú mwà pérú.
Jíè káavùu-kââ mwà pérú.
Nyí mwà pérú.
Wè kí béè jáanrí-vê-re nròpwe kó mwà nrè yè-roo mè kí vê kû ké yè.
Jíè káavùu-kââ pwé trò.
Nyí pwé ví cè-nrí tàa címwávîrá.
Nyí pwé tróo té cí yè té cí nrì védrée-nrí karívé.
Pwé tróo té cí yè.
Nyí pwé pwéré.
Nyí mwà yúu ngì kàríkáté.
Nyí pwé pwéré tó nrè nrókù kàríkáté.
Wè kàríkáté pwé tábwòo.
Wè jíè mwá pwéré-roo té cí tó kû nrókû-nrí.
Jíè kàríkáté pwé pérú.
Wè nyí pwé ví tàa míídùu.
Wè nyí pwé yúu ngì jíè nrókû-mú.
Wè nyí pwé pwéré tó pàa nrè nrókû jíè nrókû-mú.
Wè nyí pwé ví tàa î-pârâ úíété ké pèe nrècóxè.
Wè nyí pwé pèpàa tó pàa nrè nrókû jíè nrókû-mú.
Wé kùre té wèvìee nrá mwà úì wè jíè kàríkáté mwà mítò-mwéré.
Mwà vì-mítò-mwéré cóo-nrí cóxè mí púu re nrí mí bée re nrí mí nrúxée íyà-re nrí.
Nyí mwà mítò-mwéré kwé pèe wècáaxíí.
Wè ké wê té jíí yè tó pàa nrè nrókû-mú mwà a-wì tàa dùu nyí té túu-re wê mí tàa párâ úíété kóò jèpàa-re kàríkáté tó kû nrókû-nrí.
Nrà tó pèe kû nrókû- kàríkáté a té cí kárívé mwà túu.
Tó pèe té cí kárívé yè máà áúrékââ pá té nrómwe tùâ-re.
Máà áúrékââ té kwíí-re té xírikê yè.
Nrì pá té nròmwe tùâ-re té kárívé yè.
Nyí mwà túu tó pèe kù nrókù-kàríkáté yè.
Nrà yáa mè gòo ká túu tó wê.
Mè pá ká túu tó nrè kúré tó nrè nrókû-mú.
Nrà té míídùu jíè kàríkáté té yúu-ngì-re nrí nyí mwà túu tó pàa nrè nrókû-mù.
Nyí pá béè trôkô túu-re tó nrè nrókû-mú.
Mè gòo ké nrè wècáaxíí.
Kó mwà cókwà.

À mes parents, Joëlle et Eric,

pour votre soutien sans faille dans mes choix et mes projets, ainsi que votre amour indéfectible

À Inès,

pour la tolérance, la patience et l'affection que tu me montres, jour après jour, et surtout, pour ta présence à mes côtés

À ma grande sœur, Emilie,

qui m'a toujours soutenu, et qui a supporté mes humeurs tout au long de cette aventure

À mes grands-parents,

pour votre affection, et pour tous les souvenirs que vous m'avez apportés

À mes neveux, Kilian et Valérian,

vers qui j'espère pouvoir passer un peu plus de temps dans le futur

Remerciements

Arrivé à la fin de mon parcours de doctorant, je repense au temps passé et à tous les moments qui sont venus ponctuer ces dernières années, très souvent de manières inattendues. Ce travail de doctorat ne se constitue pas essentiellement de ma simple production, mais reflète aussi tout l'enrichissement et l'investissement que les nombreuses personnes que j'ai un jour côtoyé y ont apporté. Ce sont toutes ces personnes pour qui mes pensées vont aujourd'hui et à qui j'adresse ces remerciements.

Je tiens tout d'abord à remercier très chaleureusement mes deux directeurs de thèse, Cyril Marchand et Michel Allenbach, pour l'intérêt et le soutien qu'ils m'ont apporté et leur considérable investissement dans ce travail. Cyril, merci pour toutes les connaissances que tu m'as enseignées, pour m'avoir transmis ta passion pour ce métier, et pour la mangrove, ainsi que pour m'avoir appris à ne jamais laisser tomber. Merci aussi pour tout le temps que tu as passé à travailler avec moi dans ce projet. Michel, merci pour m'avoir montré la réalité du métier, pour toutes les facilités que vous m'avez apportées, administratives et personnelles, ainsi que pour les nombreuses heures de vacation à l'UNC qui auront su aiguiser davantage mon intérêt et mes envies pour l'enseignement.

Je remercie également les membres du jury, Andrea C. Alfaro, Shing Yip Joe Lee, Yves Letourneur et Luc Della Patrona, pour l'honneur qu'ils me font d'évaluer et de corriger ce travail.

Merci à l'équipe administrative de l'IRD, Catherine, Christine, Reine-Claude, pour votre aide. Merci à Nicaise, Jean, Marcel, pour leur appui technique. Merci à Jenny, Denise, Jean-Paul et Soraya. Merci à Jacky pour les nombreuses sorties en mangrove, et pour toutes les discussions que l'on a pu avoir, qui ont considérablement augmenté mes connaissances. Merci à Diana de Mont Dore Environnement pour les vérifications quotidiennes de l'installation. Je remercie également Monik Lorfantfant pour les moments partagés.

De même, je remercie profondément Vinh et Nho pour m'avoir fait découvrir le Vietnam à travers toutes les histoires que vous m'avez racontées. Votre rencontre et nos partages resteront parmi les moments le plus forts de ce parcours. Je voudrais aussi remercier Benjamin, Laura et Sylvain pour toutes les soirées que nous avons passées ensembles. Je remercie aussi très fortement Vincent et Marine pour votre amitié. Merci beaucoup à Laure

pour tous les moments que nous avons pu partager ensembles. Merci également à toutes les personnes que j'ai pu fréquenter, dans, et en dehors du travail, et qui, par leur présence, leurs partages et leur aide, ont contribué à rendre ce parcours inoubliable. Merci à vous tous.

Je remercie sincèrement Deirdre Bean pour la gentillesse qu'elle a eu de partager avec moi ses dessins botaniques d'*Avicennia marina* et de *Rhizophora stylosa*.

Finalement, mais pas des moindres, je tiens à remercier plus que tout Elisabeth et Dominique, aka Kalamity Tours. Votre amitié m'est très précieuse.

Avant-propos

Ce manuscrit de thèse synthétise trois ans de travail sur les stocks et les flux de carbone dans les mangroves de Nouvelle-Calédonie. Il a été réalisé au sein de l'Institut de Minéralogie, de Physique des Matériaux et de Cosmochimie (IMPMC UMR 7590) rattaché à **l'Institut de Recherche pour le Développement (IRD) de Nouméa**, et à l'Institut des Sciences Exactes et Appliquées (ISEA EA 7484) rattaché à l'**Université de la Nouvelle-Calédonie**.

La bourse de thèse qui a permis la réalisation de ce travail a été attribuée par la **Province Sud de la Nouvelle-Calédonie** grâce au **Prix d'Encouragement à la Recherche**. Les autres partenaires qui ont participé au financement de ce travail sont (par ordre alphabétique) : la **Fondation d'Entreprise Air Liquide**, le **Grand Observatoire du Pacifique Sud** (GOPS), l'**Initiative Française pour les Récifs Coralliens IFRECOR, Koniambo Nickel SAS**, la **Province Sud de la Nouvelle-Calédonie, VALE NC et** la **Ville du Mont-Dore**.

Ce document est rédigé sous la forme de thèse sur publication, signifiant qu'une partie des informations présentées est en cours de préparation pour soumissions dans des journaux scientifiques internationaux. Une liste des publications est disponible à la fin du mémoire.

Foreword

This thesis manuscript summarizes three years of studies on carbon stocks and fluxes in New Caledonian mangroves. It was realized at the Institute of Mineralogy, Physics of Materials and Cosmo-chemistry at the **French Institute for the Sustainable Development** of Noumea, and at the Institute of Exact and Applied Sciences of the **University of New Caledonia**.

The thesis grant was attributed by the Southern Province of New Caledonia. The others financial partners that contributed to the founding of this study, are (in alphabetical order): the **Air Liquide Foundation**, the **French Initiative for Coral Ecosystems** (**IFRECOR**), the **Grand Observatory of the South Pacific** (GOPS), **Koniambo Nickel SAS**, the **City of Mont-Dore**, the **Southern Province of New Caledonia**, and **VALE NC**.

This manuscript is written as a publication base, meaning that a part of the presented information is in preparation for submission to international scientific journals. A list of publications is available at the end of the manuscript.

Sommaire

A. Problématique

Les émissions anthropogéniques de carbone vers l'atmosphère ont considérablement augmenté depuis l'ère préindustrielle, au point que les émissions actuelles ont atteint des taux sans équivalents depuis les 66 derniers millions d'années (Zeebe *et al.*, 2016). Par conséquent, les concentrations en CO_2 atmosphérique ont bondi de 280 ppm (parties par millions) en 1880 à plus de 400 ppm aujourd'hui (Betts *et al.*, 2016), le plus haut niveau atteint depuis les 800 000 dernières années (Lüthi *et al.*, 2008). Les différentes projections pour l'évolution de ces concentrations au cours du XXI^{e} siècle ne montrent pas de décroissance, malgré le développement croissant des énergies alternatives aux combustibles fossiles. Les différents scenarii envisagés pour le futur prévoient que les concentrations en CO_2 atmosphérique atteindront des valeurs comprises entre 794 et 1150 ppm à la fin du XXI^{e} siècle (Collins *et al.*, 2014).

Du fait de ces récents changements globaux, et en prévision des futurs, différentes communautés internationales se sont intéressées aux possibilités d'atténuation des émissions anthropogéniques de carbone. La mise en place de stratégies de réduction des émissions est alors devenue une des possibilités les plus évidentes. Cependant, une autre approche a été avancée, mettant en lumière les effets bénéfiques, sans toutefois être suffisants (Mcleod *et al.*, 2011), que pourraient avoir les écosystèmes naturels en fixant et en piégeant de grandes quantités de carbone sur des très longues échelles de temps. Néanmoins, ce service écosystémique ne pourra être accompli que si la préservation et l'expansion de ces écosystèmes est assurée (Canadell and Raupach, 2008). Si les recherches se sont préliminairement concentrées sur les océans ainsi que sur les écosystèmes forestiers terrestres, les plus récentes études ont permis de souligner la grande efficacité des écosystèmes côtiers végétalisés, tels que les herbiers marins, les marais salants tidaux et les mangroves à séquestrer le carbone dans leur sol sur le long terme (Bouillon *et al.*, 2008; Chmura *et al.*, 2003; Duarte *et al.*, 2010). Du fait de leurs capacités exceptionnelles, ces trois écosystèmes ont ainsi été nommés écosystèmes à « Carbone Bleu » (Mcleod *et al.*, 2011). Toutefois, une très grande partie des surfaces couvertes par ces écosystèmes a disparu au cours des dernières centaines d'années et disparaît encore actuellement à des taux alarmants, compris entre 0,7 et 7% par an (voir références dans Mcleod *et al.*, 2011), surlignant l'urgence

de comprendre leur fonctionnement afin d'adopter les stratégies de conservation les plus performantes possibles.

La mangrove a été reconnue comme étant le plus efficace de ces puits de « Carbone Bleu » (Donato *et al.*, 2011; Kauffman *et al.*, 2011). Cette spécificité résulte d'une combinaison de nombreux paramètres dont (i) une très forte production primaire, estimée en moyenne à 218 ± 72 Tg de carbone par an (Bouillon *et al.*, 2008), (ii) une grande capacité de séquestration, avec 15% de la production primaire enfouis dans les sols (Breithaupt *et al.*, 2012), ou (iii) des conditions très anoxiques du sol qui diminuent la vitesse de dégradation de la matière organique (Kristensen *et al.*, 2008). Les mangroves sont un véritable réservoir de carbone qui peut être séquestré sur des échelles de temps s'étendant jusqu'à plusieurs milliers d'années (*e.g.* Lallier-Verges *et al.*, 1998). Du fait de l'effet stimulant des augmentations des concentrations de CO_2 atmosphérique sur l'activité photosynthétique et sur la croissance des palétuviers (Ball *et al.*, 1997; Farnsworth *et al.*, 1996; McKee and Rooth, 2008; Reef *et al.*, 2016, 2015), ce stock de carbone séquestré pourrait être encore plus important dans le futur.

Toutefois, au-delà de l'aspect bénéfique que semblent avoir les augmentations des concentrations de carbone dans l'atmosphère, les autres implications environnementales qu'elles impliquent pourraient avoir des répercussions négatives sur l'évolution de l'écosystème. Les émissions anthropogéniques de carbone induisent un réchauffement global important (Cook *et al.*, 2016) qui, en retour, provoque une augmentation du niveau marin global, principalement par la fonte des glaces terrestres (Meier *et al.*, 2007; Radić and Hock, 2011), mais aussi par l'expansion (dilatation) thermique des océans (Zickfeld *et al.*, 2017). Les projections actuelles s'accordent sur une augmentation du niveau marin global entre 0,26 m et 0,98 m pour la fin du XXI^{e} siècle (Church *et al.*, 2013). De par sa position sur la zone intertidale, la mangrove est directement concernée par cette hausse du niveau marin. Si l'accrétion verticale du sédiment semble être une possibilité performante pour assurer à la mangrove sa survie et sa croissance (Kirwan and Megonigal, 2013), cette capacité est dépendante de nombreux facteurs, notamment anthropiques, et les mangroves pourraient bien ne pas pouvoir suivre le rythme actuel d'élévation marine. C'est notamment le cas pour la région Indopacifique où 69% des mangroves qui y ont été étudiées risquent de finir submergées (Lovelock *et al.*, 2015). Une autre possibilité est la migration de l'écosystème vers d'autres espaces d'accommodation (Di Nitto *et al.*, 2014; Gilman *et al.*, 2008), mais cela dépendra des

barrières, anthropiques ou naturelles, situées en périphérie des zones intertidales (Lovelock *et al.*, 2015). Dès lors, les mangroves actuelles risquent d'être soumises à une modification de leurs cycles d'immersion.

Les informations disponibles sur la réponse de la mangrove face aux changements à venir restent très limitées. Les quelques études qui ont été menées se sont concentrées sur certaines espèces régionales de palétuvier, ainsi que sur un nombre restreint de paramètres environnementaux, tels que la salinité, l'enrichissement en nutriments, ou encore la compétition (Ball *et al.*, 1997; Farnsworth *et al.*, 1996; McKee and Rooth, 2008; Reef *et al.*, 2016, 2015). Toutefois, ces études ne sont pas suffisantes, à l'heure actuelle, pour proposer des scenarii d'évolution de l'écosystème et les défis techniques que posent les installations de simulation des changements climatiques sont majoritairement responsables du manque actuel d'informations. On peut néanmoins constater un investissement croissant de la communauté internationale dans ce domaine, avec l'émergence de nouvelles installations analytiques de haute performance telles que les serres à atmosphère contrôlée pour la simulation directe du changement climatique, les instrumentations *in situ* comme les tours à flux pour des mesures par Eddy-Covariance (*e.g.* Leopold *et al.*, 2016) et les tables d'élévation des horizons de surface (RSET) (*e.g.* Lovelock *et al.*, 2015).

Par ailleurs, même si les processus de décomposition de la matière organique dans les sols de mangrove sont moins efficaces que pour d'autres sols du fait qu'ils sont gorgés d'eau, cette minéralisation des produits de la productivité des palétuviers induit la production et l'émission de gaz à effet de serres. Ainsi, il a été montré que les mangroves pouvaient être des sources de GES vers l'atmosphère réduisant d'autant leur rôle dans l'atténuation du changement climatique (*e.g.* Allen *et al.*, 2007; Chauhan *et al.*, 2015; Chen *et al.*, 2016; Oertel *et al.*, 2016). Toutefois, ces émissions restent faiblement caractérisées et nécessitent plus d'études pour comprendre leur amplitude réelle. Notamment, les mangroves sont immergées régulièrement par les marées, causant une alternance des conditions oxiques et anoxiques dans leurs sols pouvant influer sur la production et l'émission de GES. Cependant, les émissions depuis les forêts de mangrove durant les cycles d'inondation n'ont, à ce jour, pas fait l'objet d'études spécifiques. Ces dernières sont d'autant plus importantes, qu'en considérant l'augmentation du niveau marin global induit par les futurs changements climatiques, la fréquence des cycles d'inondation par les marées devrait augmenter.

B. Principaux objectifs de l'étude

Afin d'apporter des éléments de réponse à la compréhension de l'évolution de l'écosystème, et plus spécifiquement à sa capacité à être un puits pour les gaz à effet de serre, avec les futurs changements climatiques, différents objectifs ont été définis. Il s'agit de :

a. Déterminer les répercussions des variations eustatiques passées sur la distribution de la végétation de surface, et par la même sur les stocks de carbone organique enfouis dans les sols d'une mangrove se développant sous climat semi-aride, dans le but de pouvoir estimer l'impact de la hausse prochaine du niveau marin sur les capacités de séquestration du carbone de l'écosystème.
b. Contribuer à enrichir les connaissances sur l'amplitude des émissions de gaz à effet de serre depuis les sols et la colonne d'eau dans les forêts de mangrove. Dans cette partie, différents sous-objectifs ont été définis. Il s'agit de (i) donner une estimation des émissions atmosphériques de CO_2 et de CH_4 sous climat semi-aride, (ii) d'évaluer les paramètres physiques et biologiques qui contrôlent ces émissions, et (iii) de comprendre comment la marée influe sur l'amplitude de ces émissions. Ce dernier objectif permettra notamment d'évaluer l'impact des futures prolongations des périodes d'inondations causées par l'élévation du niveau marin.
c. Déterminer l'impact de l'augmentation des concentrations en CO_2 atmosphérique et du niveau marin sur la physiologie et la croissance de jeunes plants de palétuviers caractéristiques des mangroves de la zone Indopacifique, *Avicennia marina* et *Rhizophora stylosa*. Leur aptitude à utiliser le surplus en carbone atmosphérique, ainsi qu'à lutter contre une immersion tidale prolongée apporteront des éléments qui permettront de comprendre les futures capacités de résilience de l'écosystème ainsi que sa faculté à conquérir de nouveaux espaces.

C. Déroulement du manuscrit

Ce manuscrit comporte au total cinq chapitres, comprenant une introduction et une synthèse générale, qui permettent de répondre aux différents objectifs fixés. Ces chapitres peuvent être résumés comme suit :

Le chapitre I permet de définir succinctement la mangrove dans son contexte général avec une partie dédiée au cycle du carbone au sein de cet écosystème. Il contient également une présentation des mangroves en Nouvelle-Calédonie.

Le chapitre II s'intéresse à l'influence de la régression marine de l'Holocène tardif (-5000 ans à actuel) sur la séquestration en carbone organique dans la mangrove de La Foa, située sur la côte ouest de la Nouvelle-Calédonie. Une évaluation du stock en carbone organique enfoui est proposée, ainsi qu'une rétrospective de l'évolution de cette mangrove durant cette période. Ce chapitre a pour objectif d'être soumis dans la revue *Marine Geology*.

Le chapitre III met en évidence la variabilité des émissions de gaz à effet de serre, principalement le CO_2 et le CH_4, depuis les sols de mangrove vers l'atmosphère. Ce chapitre est décomposé en deux parties, dont la première s'intéresse aux émissions à marée basse, en tentant d'identifier les différentes sources de production de ces gaz dans le sédiment. Cette partie est en cours de préparation pour le journal *Soil Biology and Biochemistry*. La seconde partie met en relation les émissions de CO_2 et de CH_4 durant les cycles d'inondation tidaux dans la mangrove. Cette étude originale et inédite fait l'objet d'une courte communication, actuellement en préparation pour la revue *Science of the Total Environment*.

Le chapitre IV propose d'examiner l'impact des futurs changements climatiques, particulièrement des augmentations de CO_2 atmosphérique et du niveau marin sur la physiologie des deux espèces de mangrove les plus répandues en Nouvelle-Calédonie ainsi que dans toute la zone Indopacifique, *Avicennia marina* et *Rhizophora stylosa*. Ce chapitre devrait faire l'objet de deux publications parallèles, dont la première se focalisera sur les échanges gazeux foliaires, et la seconde, en format courte communication, sur la croissance, la biomasse et la qualité géochimique des tissus. Toutes deux sont en préparation pour le journal *Ecosystems*.

Enfin, le chapitre V est une synthèse générale. Elle permet, sur la base du travail réalisé, d'apporter des éléments de réponse quant à l'impact des changements climatiques sur l'évolution de la mangrove et sa capacité à piéger les gaz à effet de serre. Elle contient également une proposition de perspectives de recherche qui s'inscrivent dans la continuité de ce travail.

CHAPITRE I État de l'art sur les mangroves et le cycle du carbone

I.1. La mangrove : généralités

La mangrove est un écosystème forestier de la zone intertidale des environnements tropicaux et subtropicaux, localisée le plus souvent le long des estuaires, en fond de baie ou le long des côtes protégées par un lagon adjacent. Elle est composée des seules plantes ligneuses halophytes connues au monde, qualifiées de palétuviers. Les palétuviers se répartissent en 20 familles comprenant 28 genres et plus de 70 espèces à travers le monde (Alongi, 2009; Hogarth, 1999). Parmi eux, 9 genres sont considérés comme strictement inféodés à l'écosystème mangrove (Tomlinson, 1986). Les genres les plus diversifiés sont les *Rhizophora* et les *Avicennia* avec 8 espèces chacun, suivis par le genre *Bruguiera* avec 6 espèces (Kathiresan and Bingham, 2001).

Les mangroves se développent dans des conditions extrêmes, *e.g.* salinité variable (jusqu'à trois fois la salinité de l'eau de mer), une influence forte de la marée (alternance entre hydromorphie et dessication du sédiment), des vents et une houle forts, des températures élevées, un sédiment bien souvent anoxique, et un fort indice UV. Pour faire face à ces facteurs naturels de stress, les palétuviers ont développé des mécanismes adaptatifs morphologiques et physiologiques exceptionnels. Les échanges gazeux avec l'atmosphère se font à travers les nombreuses lenticelles du système racinaire. La lutte contre la salinité élevée est assurée soit par une membrane racinaire qui filtre le sel et maintient une pression osmotique interne hautement négative, autorisant l'absorption de l'eau (Parida and Jha, 2010; Smith and Snedaker, 1995), comme c'est le cas chez les *Rhizophora*cées, soit par l'intermédiaire des glandes foliaires excrétant le sel qui cristallise à la surface des feuilles par évaporation. Cette dernière adaptation se retrouve notamment dans la famille des *Avicennia*cées. Finalement, le système racinaire latéral abondant ancre les arbres dans le sédiment pour lutter contre la houle et le vent (Kathiresan and Bingham, 2001).

Les mangroves créent un biotope unique qui abrite un riche assemblage d'espèces (Mumby *et al.*, 2004; Nagelkerken *et al.*, 2008). Le sédiment est habité par une grande variété d'invertébrés épibenthiques et de l'endofaune (Alongi *et al.*, 1989). Les chenaux hébergent des communautés de phytoplancton, de zooplancton et des poissons. Les parties immergées des palétuviers sont des habitats pour les communautés épifauniques, y compris des champignons, des macroalgues et des invertébrés. Insectes, reptiles, amphibiens, oiseaux et mammifères

prospèrent et viennent contribuer au caractère unique de l'écosystème (Kathiresan and Bingham, 2001; Tomlinson, 1986).

De par sa position particulière, la mangrove est essentielle pour la conservation des littoraux tropicaux. Elle sert de barrière contre l'érosion et contre les catastrophes naturelles (Alongi, 2008; Barbier, 2006; Dahdouh-Guebas *et al.*, 2005), de refuge et de nurserie pour de nombreuses espèces faunistiques (Alongi *et al.*, 1989; Mumby *et al.*, 2004). Elle joue aussi un rôle de filtre important entre la terre et la mer, en piégeant les matières en suspension et les contaminants qui la traversent (Kathiresan, 2003; Rivera-Monroy *et al.*, 1999). En outre, la mangrove tient une place socio-économique importante (Mukherjee *et al.*, 2014). Elle fait office de tremplin économique en conditionnant la pêche côtière et en favorisant l'attrait touristique. Elle fournit aux populations locales des ressources naturelles variées, comme par exemple le bois de chauffage, le tanin ou encore des ressources pour la pharmacopée.

Malgré les biens et services assurés, cet écosystème est actuellement un des plus menacés au monde : 30 à 50% de sa surface originelle a déjà disparu dans les deux dernières décennies (Donato *et al.*, 2011) . Son taux de disparition, 1 à 2% par an est égal ou supérieur à celui des récifs coralliens ou de la forêt tropicale humide (Duke *et al.*, 2007). La principale menace qui pèse sur cet écosystème est la croissance démographique dans les pays émergents, qui sont également ceux possédant les plus grandes superficies de mangrove (Asie du Sud Est, Brésil ou encore Mexique). Cette croissance induit le développement d'une urbanisation, la prospection et l'exploitation des ressources naturelles, et un développement industriel intense dont les effluents sont très souvent rejetés dans l'environnement.

La plus récente estimation des surfaces occupées par des mangroves dans le monde date de 2011 et elle est valable pour les années 2000. Elles sont présentes dans 118 pays, et couvrent 137 760 km², soient 0,7% des forêts mondiales (Giri *et al.*, 2011, Figure I-1). Toutefois, il y a de fortes raisons de penser que cette surface a encore diminué dans les 17 dernières années. Leur expansion géographique globale est majoritairement contrôlée par les courants océaniques et limitée par l'isotherme 20°C de l'eau de mer en hiver (Alongi, 2009; Duke, 1992). Cependant, c'est au-delà de l'isotherme 24°C, *i.e.* aux plus faibles latitudes, que l'on trouvera les mangroves les plus diversifiées (Agrawala *et al.*, 2003; Polidoro *et al.*, 2010). Actuellement, elles se distribuent entre 40°S et 30°N de latitude, dont une très grande majorité entre 20°S et 20°N (Giri *et al.*, 2011). À l'échelle locale, la composition spécifique de l'écosystème est

dépendante des exigences de chaque espèce de palétuvier et elle est donc conditionnée par les contraintes biotiques et abiotiques de la zone dont ils vont devoir s'accommoder (Duke *et al.*, 1998).

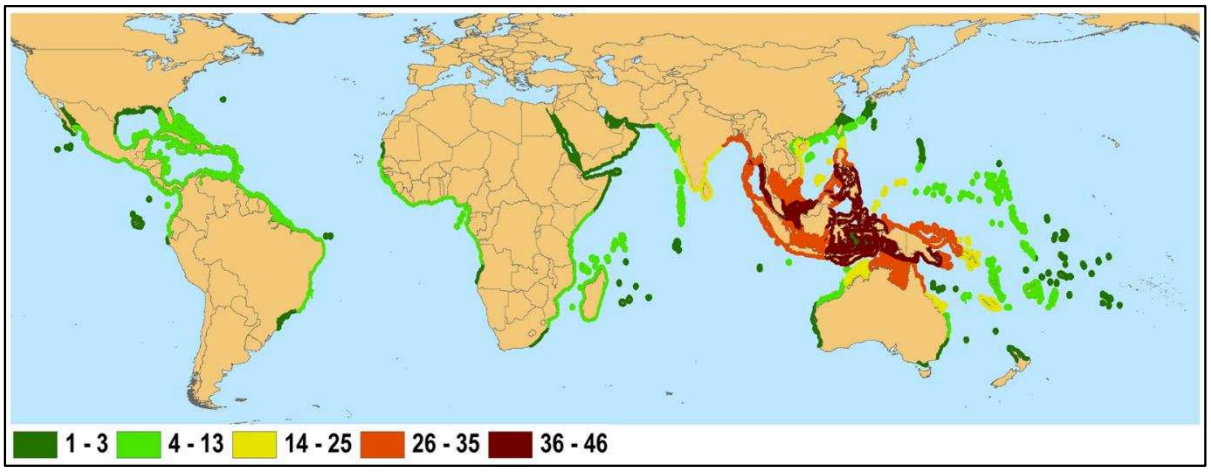

Figure I-1: Répartition mondiale, et richesse spécifique, des forêts de mangroves (Polidoro *et al.*, 2010).

I.1. Spécificités de la Nouvelle-Calédonie

I.1.1. La Nouvelle-Calédonie

I.1.1.1. Géographie

La Nouvelle-Calédonie est un archipel *sui generis* français situé dans le Pacifique Sud, dans la sous-région Mélanésienne (22°16'S 166°27'E). Elle est éloignée d'environ 1400 km à l'est de l'Australie et 2000 km au nord de la Nouvelle-Zélande. L'archipel est composé d'une île principale, appelée Grande Terre, qui s'étend sur plus de 400 km selon un axe nord-ouest sud-est, pour 50 km de large. Elle est bordée à l'est par les Iles Loyauté, ensemble de quatre îles, avec du nord au sud : Ouvéa, Lifou, Tiga et Maré ; au nord par l'archipel des Bélep, et au sud par l'Ile des Pins.

I.1.1.2. Climat

La Nouvelle-Calédonie possède un climat subtropical humide, variant à semi-aride sur les vastes plaines de la côte Ouest. Son climat est fortement influencé par les phénomènes El Niño et La Niña, avec des alizés de direction est, sud-est (Maitrepierre, 2012). L'archipel est marqué par deux saisons contrastées, rythmées par la position de la Zone de Convergence du Pacifique Sud et de la Zone de Convergence Inter Tropicale, intercalées par deux intersaisons. La saison chaude et humide s'étend de mi-novembre à mi-avril, et la saison fraîche et sèche de

mai à septembre. La température annuelle moyenne est variable selon l'altitude et la position à l'intérieur des terres, mais varie entre 27 et 30°C dans les parties basses (Maitrepierre, 2012).

I.1.1.3. Biodiversité

La Nouvelle-Calédonie est caractérisée par une très grande richesse spécifique végétale, avec 3371 espèces vasculaires inventoriées dont plus de 70% sont endémiques au territoire (Morat *et al.*, 2012). De plus, la Nouvelle-Calédonie est bordée par le plus grand lagon au monde, d'une superficie de plus de 24000 km², dont plus de 15000 km² ont été inscrits en 2008 au Patrimoine mondial de l'UNESCO (UNESCO World Heritage Centre, 2009). La diversité des espèces coralliennes et marines ainsi que la grande richesse des différents habitats, mangroves, herbiers et structures récifales en font un sanctuaire parmi les plus exceptionnels du monde. Par conséquent, la Nouvelle-Calédonie est considérée comme un des 25 « hotspots » mondiaux de biodiversité à caractère prioritaire de conservation (Myers *et al.*, 2000).

I.1.2. La mangrove en Nouvelle-Calédonie

I.1.2.1. Présentation générale

L'écosystème mangrove en Nouvelle-Calédonie couvre une superficie de 35 100 hectares dont 88% se situe sur la côte Ouest du fait de vastes plaines plus propices à son installation contrairement aux forts reliefs de la côte Est. La richesse spécifique est de 24 espèces, réparties en 15 genres. À ce jour, une seule variété endémique hybride a été découverte : *Rhizophora samoensis* var. *neocaledonica*, résultat d'un croisement entre *R. samoensis* et *R. selala* (Duke, 2010). Cependant, l'écosystème est fortement dominé par le genre *Rhizophora* qui représente 50% de la surface totale des mangroves néo-calédoniennes, suivi de l'espèce *Avicennia marina*, qui occupe 15% supplémentaires. Finalement, on trouvera un marais salant d'arrière mangrove, localement appelé « tanne », qui occupe 15% supplémentaires de la surface totale de l'écosystème (Virly, 2006).

I.1.2.2. La zonation des espèces

En Nouvelle-Calédonie, l'écosystème mangrove est formé, dans la majorité des cas, d'une zonation à trois niveaux (Figure I-2). Les étages médio et infralittoraux de la zone intertidale sont colonisés par les palétuviers qui se développent en ceintures parallèles à la côte, suivant les tolérances spécifiques aux conditions environnementales de chacune des

espèces. La distribution classiquement observée est une colonisation dominante de la zone aval par *Rhizophora* spp., suivi par *Avicennia marina* en zone médiane (Figure I-2a et b). L'étage supralittoral est occupé par le tanne (Figure I-2c). Les études ont démontré que cette zonation est régie principalement par la distribution de la salinité du sédiment, elle-même dépendante de la durée d'immersion par la marée, et par voie de conséquence, de la topographie de la zone intertidale (Baltzer, 1982; Marchand *et al.*, 2011, 2012).

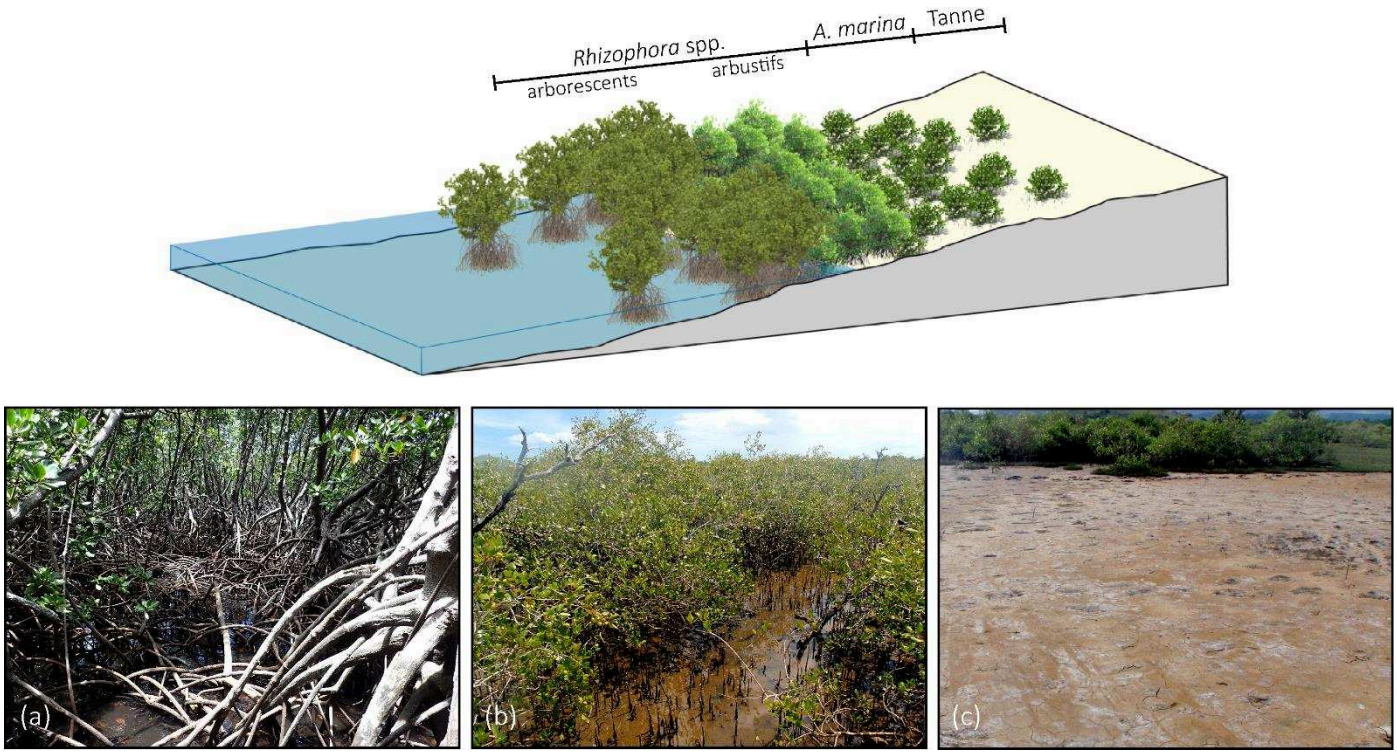

Figure I-2 : Illustration de la zonation classiquement observée dans les mangroves néo-calédoniennes (Bluecham SAS), et photographies des formations à (a) *Rhizophora* spp. (Mangrove de Ouemo-Magenta, Nouméa, 2017) (b) *Avicennia marina* (mangrove de La Foa, 2012), et (c) tanne d'arrière-mangrove (mangrove de La Foa, 2012).

Le genre *Rhizophora* est bien connu par les communautés néo-calédoniennes. Ces palétuviers sont principalement reconnaissables par leurs nombreuses racines aériennes, qui créent un environnement unique et obscur et bien souvent impénétrable (Figure I-2a). Ces racines aériennes – dites « échasses » – en forme d'arceau partent du tronc principal et se ramifient avec la distance, permettant un ancrage optimal dans le sédiment. Elles portent en outre de nombreuses lenticelles qui permettent les échanges gazeux entre l'individu et son environnement. *Rhizophora* spp. possède des feuilles vert foncé, elliptiques, et en position opposées de part et d'autre de la branche. Les fleurs sont composées de quatre sépales jaunes et quatre pétales blancs et poilus, le tout formant une double étoile à quatre branches symétriques (Figure I-3). La graine se développe en une longue propagule pouvant atteindre

Figure I-3 : Illustration de *Rhizophora stylosa* (Deirdre Bean, 2012).

Figure I-4 : Illustration d'*Avicennia marina* var. *eucalyptifolia* (Deirdre Bean, 2014).

plusieurs dizaines de centimètres, qui chute de l'arbre à pleine maturité et peut alors soit se planter directement dans le substrat, soit être dispersée par les marées pour coloniser de nouveaux espaces. La gestion de la salinité chez les palétuviers du genre *Rhizophora* spp. est réalisée par filtration grâce à des membranes osmotiques situées dans le système racinaire. Toutefois, *Rhizophora* spp. se développe de façon optimale à des taux de salinité proche de l'eau de mer (Parida and Jha, 2010), d'où sa présence en partie aval des zones intertidales en Nouvelle-Calédonie.

Avicennia marina, ou « palétuvier gris », est la deuxième espèce de palétuvier emblématique de Nouvelle-Calédonie (Figure I-2b). Il possède des feuilles vert clair, tirant sur le gris, disposées par deux et en opposition sur la tige (Figure I-4). La floraison se fait par bouquets de petites fleurs composées de 4 pétales épais de couleur orange vif qui forment une étoile parfaitement symétrique. Les fruits sont ovoïdes et jaunâtres à maturité. Son système racinaire caractéristique est facilement reconnaissable grâce aux nombreux pneumatophores, recouverts de lenticelles, qui émergent du sédiment (*e.i.* jusqu'à 10 000 par individu adulte, Hogarth, 1999). Ils permettent notamment les apports en oxygène grâce à leur capacité photosynthétique (Kitaya *et al.*, 2002). Cet oxygène est ensuite transféré vers le système racinaire grâce à la présence d'aérenchymes dans les tissus, et peut ensuite être diffusé dans la rhizosphère proximale en cas de forte anoxie, comme c'est le cas lors des submersions tidales (Krauss *et al.*, 2008; McKee, 1996; Scholander *et al.*, 1955). En plus d'un système d'exclusion du sel au niveau des racines (membrane osmotique), *Avicennia marina* possède un double mécanisme d'accumulation-excrétion sous forme de solution saline (Figure I-5) grâce à des glandes spécialisées situées sur les feuilles (Parida and Jha, 2010). Sa tolérance à des niveaux de salinité variables (Patel *et al.*, 2010) en font un arbre pionnier parfaitement adapté à la colonisation de nouveaux espaces dont la partie médiane des zones intertidales, qu'il occupe actuellement en Nouvelle-Calédonie. Cependant, cette position induit une immersion par la marée insuffisante pour l'espèce qui souffre du manque d'eau et de la salinité élevée qui en résulte. Ainsi, le plus souvent, *Avicennia marina* ne dépasse pas le stade buissonnant et sa productivité est réduite en Nouvelle-Calédonie (Leopold *et al.*, 2016).

Figure I-5 : Photographies de la manifestation du phénomène d'excrétion foliaire du sel chez *Avicennia* sp. (2016)

Le tanne constitue la zone d'arrière mangrove (Figure I-2c). Le recouvrement tidal n'y a lieu que lors des marées d'équinoxe, ce qui provoque des processus d'évaporation intenses le reste du temps, causant une salinité très élevée. Il peut être soit nu, soit colonisé, dans sa zone la plus aval, par une plante grasse halophile, *Sarcocornia quinqueflora*, plus connue sous le nom de salicorne. Ce tanne est une zone tampon pouvant être facilement recolonisée par les palétuviers en cas de baisse de la salinité, comme par exemple, lors de modifications hydrologiques, ou climatiques, et notamment, en cas de hausse du niveau marin.

I.1.2.3. Patrimoine naturel

Les mangroves néo-Calédoniennes revêtent des enjeux patrimoniaux importants pour leur intérêt paysager. On peut citer le très célèbre site du « Cœur de Voh » (Figure I-6a). Situé à l'embouchure de la Temala, dans la mangrove de Voh (20°58'18"S 164°39'28"E), cette formation est connue dans le monde entier, notamment grâce à la photographie de Yann Arthus-Bertrand prise en 1990. On peut aussi citer le site de la baie du Carénage situé dans la commune de Prony (22°18'06"S 166°51'39"E). Ce site abrite la seule mangrove du territoire à peuplement dominant de *Bruguiera gymnorhiza.* Son éloignement et sa difficulté d'accès en font un site d'exception encore totalement préservé (Figure I-6b).

I.1.2.1. Utilisation traditionnelle

L'utilisation des mangroves en Nouvelle-Calédonie en termes de ressources est essentiellement axée sur la pêche. S'il est difficile de recenser son utilisation dans la pêche professionnelle, la pêche vivrière pratiquée par les populations locales est bien connue. La mangrove est parcourue en petits canots à fond plat ou à pied. Les principales techniques de pêches pratiquées sont la nasse ou la pêche à pied pour les crabes de palétuviers *Scylla serrata*

et la senne pour les poissons qui sont principalement des mulets noirs *Mugil* spp., des picots rayés *Siganus lineatus* et des poissons lait *Chanos chanos* (Virly, 2006).

Figure I-6 : photographies (a) aérienne du "Coeur de Voh" (© Yann-Arthus Bertrand), (b) de la mangrove à Bruguiera gymnorhiza de la Baie du Carénage (Inès Gayral, 2016), et (c) des tapas colorés avec le tannin de *Rhizophora* spp. (Inès Gayral, 2016)

Le tanin de l'écorce de *Bruguiera gymnorhiza* était utilisé dans la confection de colorants (Rollet, 1975) et permet d'obtenir une teinture ocre. Cette teinture était réservée aux chefs de tribus lors des cérémonies coutumières. Le colorant était alors utilisé pour teinter les manches d'armes, les vêtements en fibre de coco ou de pandanus, ou encore les poils de roussette de la monnaie kanak. Le tanin de *Rhizophora* spp., quant à lui, permet la coloration des tapas, élément essentiel dans le geste coutumier kanak (Figure I-6c). De plus, il servait auparavant à tanner les peaux (Monik Lorfanfant, comm. pers.).

Le fruit du « palétuvier rouge », *Bruguiera gymnorhiza,* est l'ingrédient principal de la confection du gâteau au fruit de palétuvier, *mwata rè nê* en xârâgurè, une des langues de l'aire linguistique xârâcùù (Nonquet, 2005). Le fruit est alors collecté avant sa maturité, macéré dans un trou d'eau saumâtre, et cuit à l'étouffé, roulé dans des feuilles de bananiers. De plus, il était aussi consommé râpé dans du lait de coco. Seulement, cette dernière pratique semble avoir disparu.

Finalement, on peut recenser une utilisation médicinale, même si toutefois cette pratique reste très obscure avec très peu d'informations retransmises. On notera tout de même l'usage de la sève du palétuvier aveuglant, *Excoecaria agallocha*, dans la cicatrisation des plaies (habitante d'une tribu de la Grande Terre, comm. pers.). Ces feuilles peuvent aussi être utilisées, chauffées à la flamme, pour lutter contre les piqûres de raie et de rascasse (Monik Lorfanfant, comm. pers.).

I.1.2.2. Pression anthropique

Comme ailleurs, la mangrove en Nouvelle-Calédonie est sous l'influence des activités anthropiques. Des portions très importantes ont été détruites dans toute la zone urbaine de Nouméa, la capitale de l'archipel. Ce ne sont ainsi pas moins de 380 ha de mangrove qui ont disparu au cours de la seconde moitié du XXIe siècle à cause de l'endiguement et du remblaiement. Un arrêté rendant obligatoire, avant tous travaux, la réalisation d'une étude d'impact sur l'écosystème a été adopté début 2002 (Arrêté n° 2002-1567 du 30 mai 2002 dans la loi de pays n° 2002-017 du 11 janvier 2002). Ces études ont pour vocations de faire envisager les alternatives possibles pour les constructions ou d'imposer des mesures compensatoires proportionnées à l'impact engendré. Toutefois, les mangroves urbaines et péri-urbaines du secteur de Nouméa semblent toujours subir des contraintes d'aménagement côtier importantes, et aucune étude récente ne permet à ce jour d'en constater les effets en termes d'occupation d'espace. De plus, l'aquaculture et l'exploitation minière pèsent aussi fortement sur l'écosystème. Les mines orphelines situées dans les massifs d'altitude et abandonnées depuis de longues années ne font pas toutes l'objet de mesures d'aménagement ni de revégétalisation poussées et subissent une érosion importante. Le matériel latéritique fin, chargé en métaux lourds, issu de l'érosion est facilement transportable par le ruissellement des pluies. À cause de leur grande capacité à piéger les sédiments, ces éléments finissent irrémédiablement dans les mangroves où ils peuvent s'accumuler en grande quantité. Leur toxicité représente ainsi une menace majeure pour la biodiversité (Marchand *et al.*, 2012). Les exploitations récentes adoptent néanmoins des stratégies de piégeage des sédiments plus développées (par exemple des successions de bassins à sédimentation), ce qui limite cette menace sur certains secteurs. Concernant l'activité aquacole, la principale menace réside dans le rejet des effluents à travers les zones de mangrove. Cependant, la gestion adaptée des exploitations, en concertation avec les acteurs locaux de l'environnement, semble être une stratégie payante pour limiter les impacts (Molnar, 2012). Finalement, les évènements naturels majeurs tels que les cyclones et les tempêtes tropicales vont eux-aussi avoir un impact sur l'écosystème. Outre la destruction directe des palétuviers due à la houle et aux vents violents, ils induisent une forte sédimentation, tout particulièrement dans les bassins versants touchés par l'exploitation minière.

I.2. Éléments de généralités sur le cycle du carbone dans les mangroves

I.2.1. Fixation

Le carbone est majoritairement capturé par la productivité primaire des plantes vasculaires (*i.e.* les palétuviers), et représente le carbone acquis durant la photosynthèse, déduit de la perte lors de la respiration, investi dans le maintien ou la croissance des tissus végétaux. Les mangroves sont reconnues comme étant un des écosystèmes forestiers les plus productifs au monde. Leur production primaire nette a été évaluée à 218 ± 72 Tg de carbone par an (Bouillon *et al.*, 2008), mais il semblerait toutefois qu'elle soit sous-estimée. En effet, la productivité primaire est estimée principalement à partir de la production de litière et de bois, des échanges gazeux et de l'atténuation de l'intensité lumineuse (Alongi, 2009), occultant partiellement les processus souterrains (Alongi, 2009; Bouillon *et al.*, 2008; Kristensen *et al.*, 2008). La productivité primaire de l'écosystème varie en fonction des conditions environnementales (*e.g.* intensité lumineuse, type d'espèce, âge de la forêt, disponibilité en eau et en nutriments, salinité ; Clough, 1992), ou encore en fonction de la position latitudinale, avec des valeurs plus élevées aux plus faibles latitudes (*e.g.* Komiyama *et al.*, 2008; Kristensen *et al.*, 2008; Twilley *et al.*, 1992).

La seconde source de carbone provient des différentes communautés algales benthiques et planctoniques. Toutefois, l'apport de ces communautés est généralement considéré comme faible, du fait de la limitation en lumière par la dense canopée formée par les palétuviers, de la turbidité de la colonne d'eau, et de la large proportion en tanin, hautement réfractaire, de la matière organique (Alongi, 1994). Cependant, dans les zones les plus ouvertes, comme par exemple dans les zones d'arrière mangrove (*c.f.* chap. I.1.2.2) , le développement algal de surface peut être à l'origine de près de 90% du carbone organique sédimentaire (Wooller *et al.*, 2003).

Enfin, la troisième source la plus importante concerne l'acquisition de carbone par les apports en matériaux organiques provenant des bassins versants en amont, ou des écosystèmes adjacents. La présence de telles zones à proximité de la mangrove, la forme et la taille des palétuviers, la courantologie du milieu, ou encore la dynamique tidale sont autant de facteurs qui pourront influencer le piégeage de cette source de matière organique.

I.2.2. Minéralisation

La matière organique enfouie au sein des sédiments peut subir d'importantes transformations biogéochimiques qui vont modifier sa composition originelle au cours de la diagénèse précoce. Ce processus est une suite de réactions d'oxydation de la matière organique réalisées par dégradation bactérienne dans un ordre logique dirigé par leur rendement thermodynamique. En outre, de multiples réactions secondaires de réoxydation des composés réduits produits lors de la dégradation primaire ont aussi lieu (voir Van Cappellen and Wang, 1996), le tout donnant lieu à un système biogéochimique extrêmement complexe dont les produits sont, entre autres, des gaz à effet de serre, et notamment du dioxyde de carbone CO_2, du protoxyde d'azote N_2O et du méthane CH_4 (Tableau I-1).

Tableau I-1 : Réactions d'oxydations primaires et secondaires de la matière organique établies selon Froelich *et al.* (1979) dans les sédiments marins. Les équations sont établies suivant la stœchiométrie pour une mole de matière organique proposée par Redfield : C106/N16/P (Redfield *et al.*, 1963).

Equations d'oxydation de la matière organique	Rendement énergétique
Oxydation par l'oxygène $138O_2 + MO + 18HCO_3^- \rightarrow 124CO_2 + 16NO_3^- + 122H_2O + H_3PO_4$ Dénitrification $94,4NO_3 + MO \rightarrow 52,2N_2 + 13,6CO_2 + 84,8H_2O + HPO_4^{2-} + 92,4HCO_3^-$ Oxydation par les oxydes de manganèse $236MnO_2 + MO + 104H_2O + 364CO_2 \rightarrow 236Mn^{2+} + 470HCO_3^- + HPO_4^{2-} + 8N_2$ Oxydation par les oxydes de fer $424FeO_3 + MO + 104H_2O + 740CO_2 \rightarrow 424Fe^{2+} + 846HCO_3^- + 16NH_3 + HPO_4^{2-}$ Oxydation par les sulfates $53SO_4^{2-} + MO \rightarrow 53HS^{2-} + 39CO_2 + 16NH_4^+ + 39H_2O + 67HCO_3^- + HPO_4^{2-}$ Méthanogénèse $MO \rightarrow 53CH_4 + 53CO_2 + 16NH_4^+ + HPO_4^{2-}$	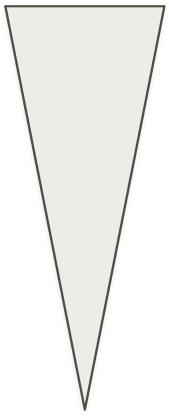

Le CO_2 est produit à la fois par dégradation aérobique et anaérobique (Tableau I-1). Cependant, la dégradation aérobique étant la plus efficace énergétiquement parlant, elle est privilégiée. Toutefois, du fait des immersions régulières des sédiments de mangroves par les marées, l'oxygène libre est très peu présent dans la colonne sédimentaire et l'oxydation aérobique de la matière organique est limitée aux premiers horizons du sédiment, principalement alimentés par la litière et les détritus algaux (Kristensen *et al.*, 2008). Il peut exister néanmoins des micro-zones oxiques plus en profondeur. Celles-ci peuvent être dues à la bioturbation qui crée des conduits favorisant la pénétration d'oxygène, et à la diffusion racinaire d'oxygène par les systèmes racinaires des palétuviers (Alongi, 1998; Kristensen and

Alongi, 2006). Lorsque tout l'oxygène est consommé, la matière organique est oxydée par différentes réactions biogéochimiques utilisant d'autres accepteurs d'électron, toujours selon une hiérarchie dépendante du rendement thermodynamique des réactions (*e.i.* NO^{3-}, Mn^{4+}, Fe^{3+} and SO_4^{2-} ; Tableau I-1). Toutefois, du fait des apports continus de sulfates par les marées, la sulfato-réduction est le processus anaérobique dominant dans les sédiments de mangrove (Alongi *et al.*, 2001; Balk *et al.*, 2016; Kristensen *et al.*, 1994, 2008). La dénitrification et l'oxydation par les oxydes de manganèse et de fer sont, en revanche, considérées comme très peu présentes (Kristensen *et al.*, 1998). Enfin, lorsque tous les autres accepteurs d'électron ont été consommés, le CH_4 est produit par fermentation lors de la méthanogénèse, en utilisant le CO_2 ou d'autres composés méthyl comme substrat (Tableau I-1). Toutefois, des études récentes ont démontré que sulfato-réduction et méthanogénèse pouvaient coexister dans les sédiments de mangrove (Lyimo *et al.*, 2002), complexifiant davantage les processus biogéochimiques qui se déroulent à l'intérieur du sédiment.

Une importante communauté de chercheurs s'est attachée à évaluer les quantités de gaz à effet de serres produits par les forêts de mangroves. Malgré le fait que les processus de décomposition contrôlent la production des gaz dans le sédiment, les émissions à la surface sont dépendantes de nombreux facteurs physiques et biochimiques, comme par exemple, la quantité de carbone dans le sédiment, la quantité de nutriments, la densité du substrat, la salinité, la concentration en oxygène, le taux d'humidité du sol, etc. De plus, les conditions climatiques, et principalement la température, sont très importantes dans la variabilité de ces émissions (Chen *et al.*, 2012). Finalement, à cause de la faible efficacité des processus de dégradation anaérobique, toute la matière organique n'est pas dégradée et une grande partie se retrouve enfouie dans les sédiments.

I.2.3. Stockage

Du fait de leur très forte productivité primaire et des conditions anoxiques des sols qui limitent les processus de décomposition (*c.f.* chap. I §§ I.2.1 et I.2.2), la mangrove a la capacité de stocker des quantités exceptionnelles de carbone relativement aux autres écosystèmes forestiers terrestres (*e.g.* Atwood *et al.*, 2017; Donato *et al.*, 2011; Kauffman *et al.*, 2011; Twilley *et al.*, 1992 ; Figure I-7a). Si la biomasse aérienne représente un stock conséquent, la majeure partie est enfouie dans les sols, qui peuvent contenir jusqu'à 98% du stock total en

carbone organique de l'écosystème (Donato *et al.*, 2011 ; Figure I-7a). À l'échelle mondiale, le stock sédimentaire représenterait 18,4 Tg de carbone par an (Bouillon *et al.*, 2008). Ce stock peut notamment s'accumuler sur plusieurs mètres d'épaisseur et être séquestré pendant plusieurs milliers d'années (*e.g.* Lallier-Verges *et al.*, 1998).

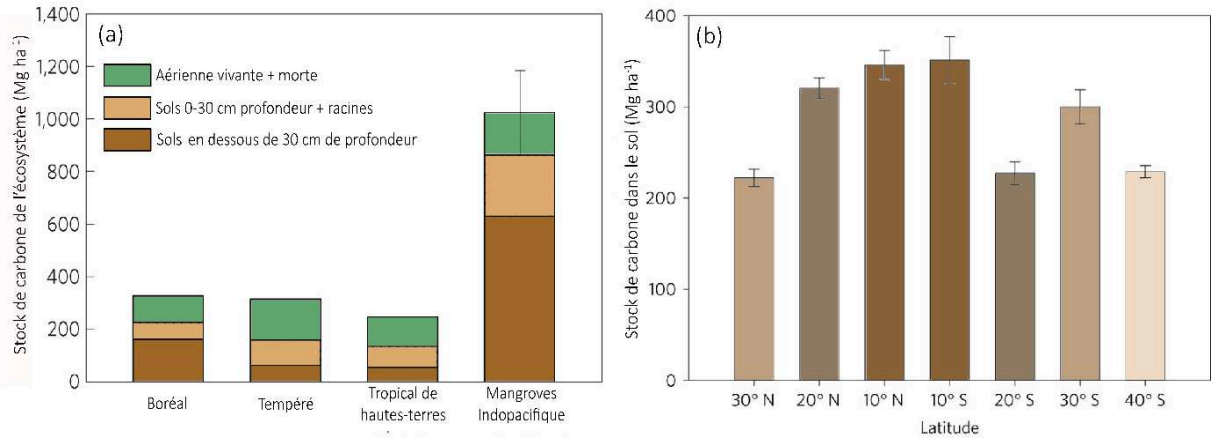

Figure I-7 : (a) Comparaison du stock de carbone avec celui des principaux domaines forestiers mondiaux ; Modifié d'après Donato *et al.*, 2011), (b) stock moyen de carbone dans les sols de mangrove par unité de surface jusqu'à 1 mètre de profondeur en fonction de la latitude. Modifiée d'après Atwood *et al.*, (2017).

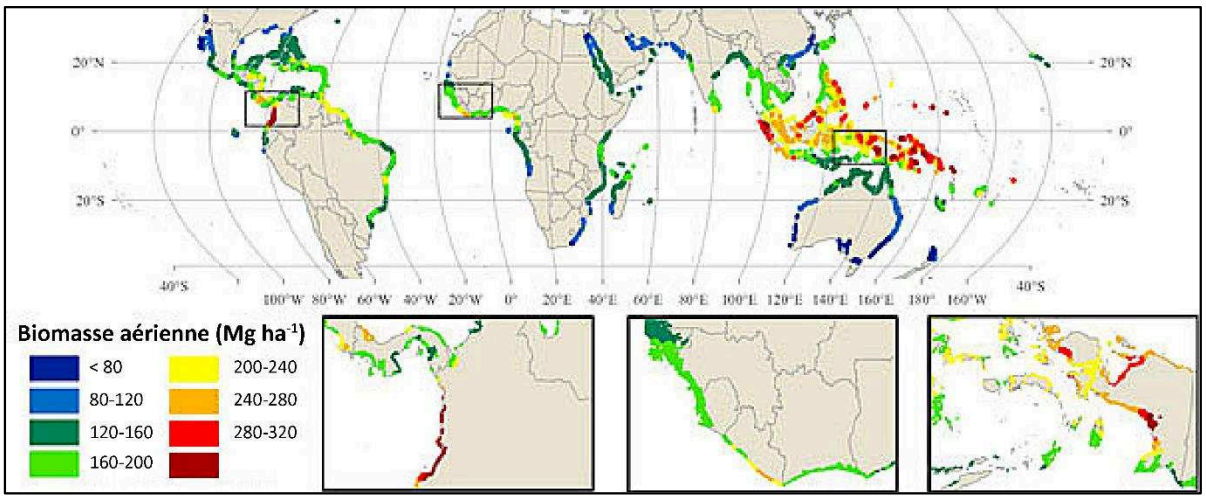

Figure I-8 : Carte mondiale des stocks de carbone par unité de surface liés à la biomasse aérienne. Modifiée d'après Hutchison *et al.* (2014).

Toutefois, les quantités de carbone stockées dans l'écosystème peuvent être très variables et dépendent de nombreux autres paramètres. À l'échelle de l'écosystème, une forte variation peut être trouvée en fonction du type d'espèce rencontré, de la salinité du sol, des apports sédimentaires, ou encore de la disponibilité en nutriments, et par conséquent en fonction de la position de la forêt le long de la zone intertidale (*e.g.* Adame *et al.*, 2013; Alongi *et al.*, 2005; Atwood *et al.*, 2017; Kauffman *et al.*, 2011; Mizanur Rahman *et al.*, 2015; Wang *et al.*, 2013). De plus, l'âge de la forêt est lui-aussi un facteur déterminant dans le stock de

carbone de l'écosystème (Alongi *et al.*, 2004). À une échelle plus large, la quantité de carbone stockée par l'écosystème, tant dans la biomasse aérienne que dans les sols, sera contrôlée par sa productivité, et par conséquent sera dépendante de la latitude, avec une plus importante quantité stockée dans les forêts de basse latitude (*e.g.* Alongi, 2014, 2012; Kristensen *et al.*, 2008; Sanders *et al.*, 2010 ; Figure I-7b et Figure I-8).

I.2.4. Bilan carbone

En 2008, Bouillon *et al.* (2008) proposaient un bilan carbone global pour la mangrove. Dans ce bilan, le devenir de plus de la moitié du carbone capturé par l'écosystème (112 Tg sur 218 capturé) s'est révélé être impossible à expliquer. De nombreuses études ont alors été menées pour tenter de tracer ce carbone manquant, et ainsi combler le manque dans le bilan. Plus récemment, Alongi (2014) propose une réactualisation avec les données nouvellement acquises ces dernières années (Figure I-9). Parmi les manques identifiés, l'export du carbone sous forme inorganique dissoute vers les eaux côtières adjacentes dû au lessivage des sols par les marées s'est montré être primordial (*e.g.* Call *et al.*, 2015; Maher *et al.*, 2013, 2015; Santos *et al.*, 2012; Stieglitz *et al.*, 2013). Parallèlement, de nombreuses études se sont concentrées sur les émissions de gaz à effet de serre depuis les sols (*e.g.* Bulmer *et al.*, 2015; Chanda *et al.*, 2013; Chen *et al.*, 2016a, 2014, 2012, 2010; Grellier *et al.*, 2017; Leopold *et al.*, 2015, 2013; Wang *et al.*, 2016), ou depuis les creeks et les eaux côtières adjacentes (*e.g.* Dutta *et al.*, 2017, 2015, 2013; Nóbrega *et al.*, 2016). Toutefois, ce nouveau bilan est toujours incomplet, manquant, entre autres, de données sur la productivité faunique et pélagique (Alongi, 2014), ainsi que sur la variation des émissions en fonction du climat. De plus, très peu d'informations existent à l'heure actuelle sur la contribution relative des différentes sources de production du CO2 (*e.g.* la respiration racinaire, la décomposition de la litière, la décomposition de la matière organique, la respiration du film algaire de surface) dans les émissions de surface. Finalement, on notera que les émissions de gaz à effet de serres depuis la colonne d'eau vers l'atmosphère, *i.e.* pendant les cycles d'inondation tidaux, ne sont pas prises en compte du fait de l'absence d'études sur le sujet. La position des mangroves dans la zone de balancement des marées implique qu'elles peuvent être immergées une grande partie du temps. Par conséquent, évaluer l'amplitude des émissions depuis la colonne d'eau durant les cycles d'inondation semble être d'une importance certaine dans l'amélioration de notre compréhension du cycle du carbone dans les mangroves.

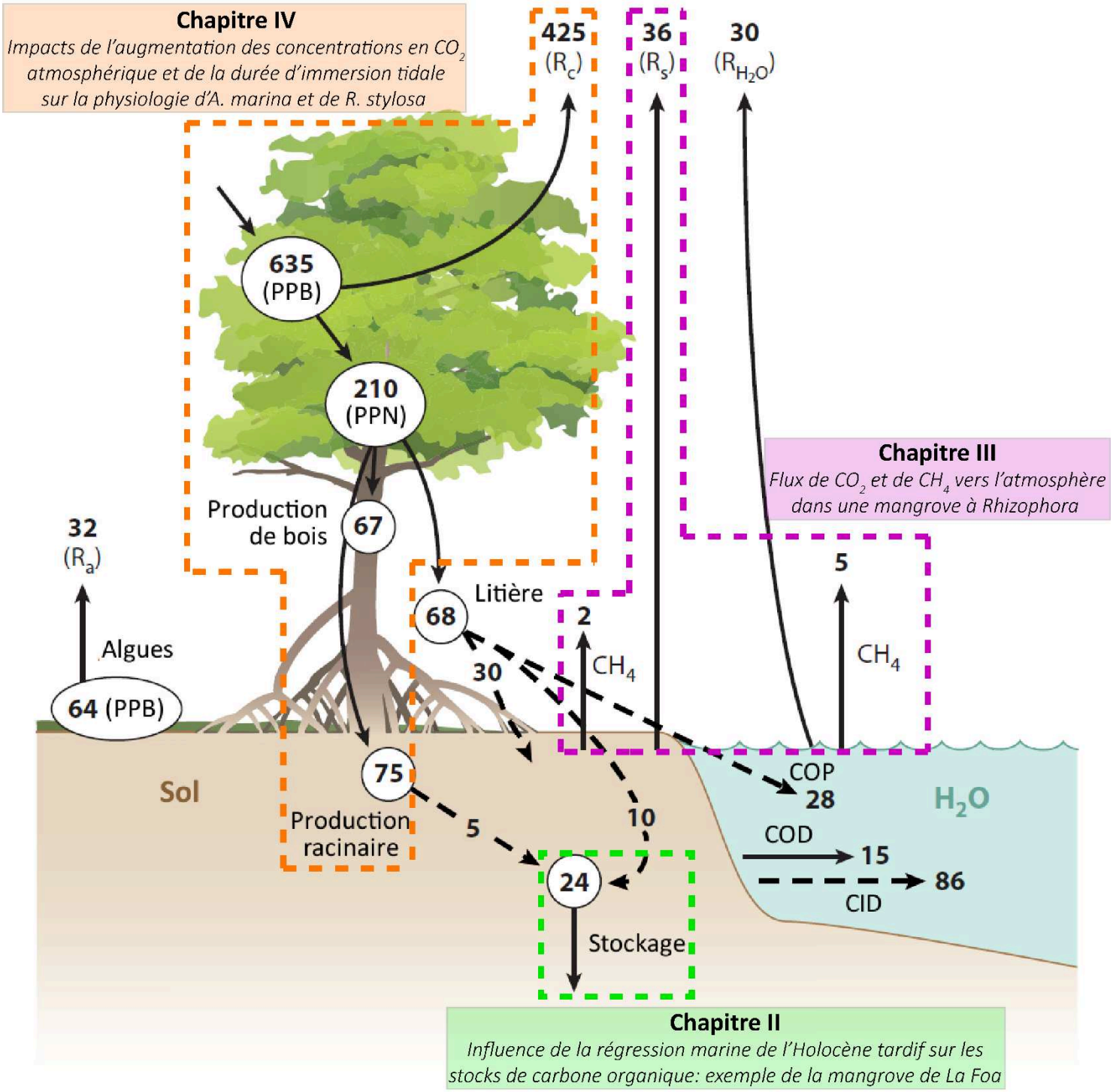

Figure I-9 : Bilan carbone des mangroves du monde modifié d'après Alongi (2014). Les flèches noires représentent des valeurs moyennes basées sur de nombreuses données empiriques. Les flèches pointillées représentent celles estimées indirectement (par différence), ou suggérées à partir de la littérature la plus récente. Toutes les valeurs sont en Tg de carbone par an. Le budget suppose une zone de mangrove globale de 138 000 km² (Giri *et al.*, 2011). Abréviations : CID, carbone inorganique dissous ; COD, carbone organique dissous ; PPB, production primaire brute ; PPN, production primaire nette ; COP, carbone organique particulaire ; R_a, respiration algale ; R_c, respiration de la canopée ; R_s, respiration du sol ; R_{H2O}, respiration par la colonne d'eau. Chaque chapitre du présent travail traite d'une partie de ces processus, tels que mis en évidence dans la figure.

CHAPITRE II Influence de la régression marine de l'Holocène tardif sur les stocks de carbone organique : exemple de la mangrove de La Foa

Présentation

Parmi les écosystèmes à « carbone bleu », les mangroves sont très efficaces pour stocker le carbone dans leurs sols sur des échelles allant du siècle au millénaire (*e.g.* Twilley *et al.*, 1992). Cependant, cette capacité varie en fonction de nombreux paramètres, notamment le climat (*e.g.* Alongi, 2012), et, localement, le type de forêt, son âge et sa position dans la zone intertidale (*e.g.* Adame *et al.*, 2013; Kauffman *et al.*, 2011). En Nouvelle-Calédonie, les mangroves se développent dans des conditions semi-arides, induisant une productivité primaire nette limitée, et une zonation spécifique de l'écosystème (c.f. chap. I § I.1.2.2).

Dans ce contexte, les objectifs de ce chapitre sont multiples. Il s'agit tout d'abord quantifier le stock de carbone organique enfoui dans le sol d'une mangrove qui se développe dans ce contexte spécifique, et de déterminer la variabilité de ce stock en fonction du gradient topographique de la zone intertidale, et donc en fonction de la zonation de surface. Pour cela, il a fallu quantifier la part de carbone stocké lié au développement de la forêt actuelle, et, ensuite, évaluer le stock de carbone de la colonne sédimentaire jusqu'au premier changement de faciès stratigraphique, indicateur d'un milieu de dépôt différent de celui de la mangrove. Nous avons déterminé l'extension maximale du système racinaire des deux faciès majoritaires, *A. marina* et *R. stylosa* grâce au couplage de différents marqueurs, tels que les rapports C/N, des isotopes stables (carbone et azote), et des indicateurs visuels. Les stocks de carbone organique liés au développement de la forêt actuelle sont inférieurs à 100 MgC ha^{-1}. Ceci peut être mis en relation avec la faible productivité primaire de ces forêts soumises à un climat semi-aride. En profondeur, nous avons observé une couche très enrichie en matière organique, avec des rapports C/N élevés (40) et des valeurs de $\delta^{13}C$ très faibles (-26 ‰), sous chacune des trois zones principales de la mangrove. Cette couche s'étend jusqu'à un niveau de sable contenant des débris de coquilles de bivalves et d'huîtres (Figure II-1).

Dans cette couche enfouie, nous avons observé de nombreux débris racinaires rouge ocre, caractéristiques des fibres de *Rhizophora* spp. (Figure II-2). Des analyses carbone 14 ont permis de dater l'installation de la mangrove à la fin de l'Holocène. De plus, les dépôts étant de plus en plus jeunes au fur et à mesure que l'on descend sur la zone intertidale, nous en avons déduit que la mangrove a progressé vers l'aval en suivant la régression marine qui caractérise la fin de l'Holocène dans cette région du Pacifique Sud.

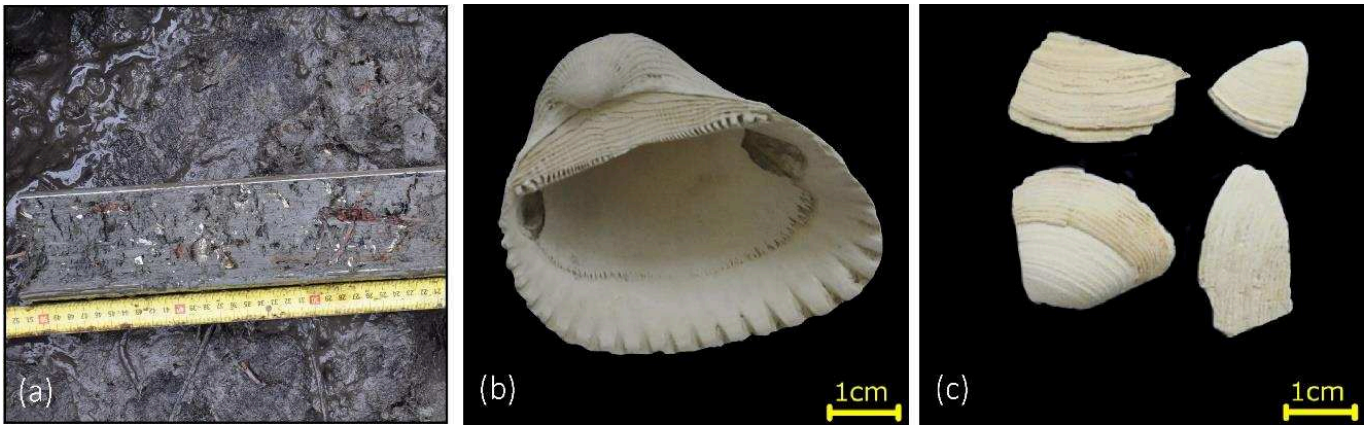

Figure II-1: Photographies : (a) du bas de la carotte prélevée sous *R.* spp. montrant la présence des débris coquilliers, (b et c) des débris de coquilles retrouvés en profondeur sous les actuelles zones de tannes, d'*A. marina* et de *R. stylosa*, à la limite entre le lit sableux déposé à l'Holocène tardif et les premiers sols de mangroves.

Dans ces couches plus profondes, le stock de carbone atteignait 550 MgC ha^{-1}, 245 MgC ha^{-1} et 300 MgC ha^{-1} pour la zone de tanne, le peuplement d'*A. marina* et de *Rhizophora.* spp., respectivement. Le stock élevé en carbone sous le tanne est probablement lié à une période de stabilité du niveau de la mer qui aurait duré près de 3000 ans, contrairement aux autres zones, dans lesquelles la mangrove s'est développée avec la régression marine. Finalement, grâce à la datation des zones de transition entre la couche enfouie et les couches supérieures, nous avons pu retracer l'évolution de cette mangrove depuis sa mise en.

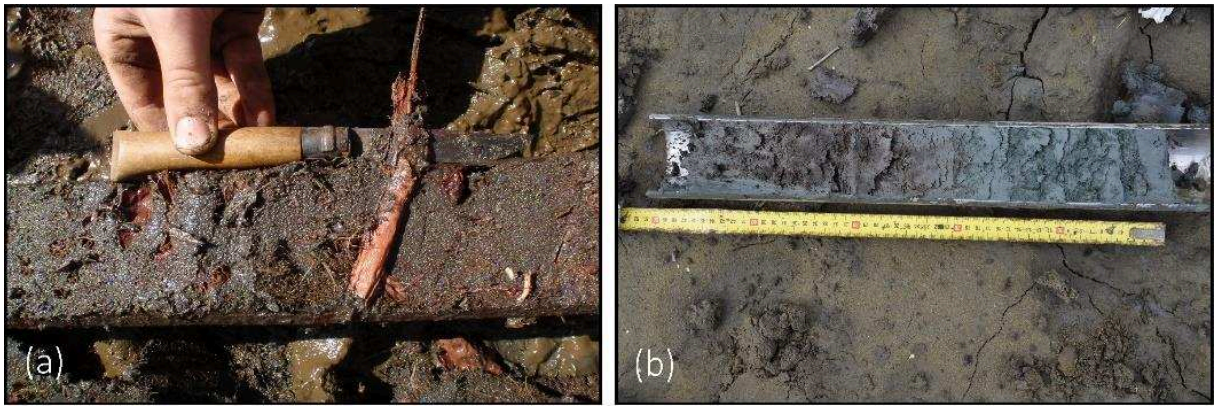

Figure II-2: Photographies (a) des fibres rouges caractéristiques de *R.* spp., et (b) de la limite visuelle entre la couche supérieure et la couche enfouie dans la carotte prélevée sous le tanne.

En conclusion, les variations eustatiques, et en particulier la hausse actuelle du niveau marin dû au changement climatique, peuvent fortement influencer la capacité des mangroves à stocker du carbone et ce, en raison de leur migration le long du gradient d'élévation intertidal afin de maintenir les conditions biotiques nécessaires à leur développement.

Mangrove soil carbon stocks along an intertidal elevation gradient: influence of the late Holocene marine regression (New Caledonia)

Adrien Jacotot, Cyril Marchand, Brad E. Rosenheim, Eugene Domack, Michel Allenbach

Abstract

Among blue carbon ecosystems, mangroves are very efficient in storing carbon in their soils over century to millennial time scales. However, this ability varies with numerous parameters, including climate and sea-level variations. In New Caledonia, mangrove ecosystems develop in semi-arid conditions with a typical zonation: *Rhizophora* spp. colonize the seaward side of the intertidal area, while *Avicennia marina* develops at higher elevations, just below the salt-flat.

Within this context, we determined both the quantity (TOC and stocks) and the quality (C/N ratios, stable carbon and nitrogen isotopes, radiocarbon age) of the organic matter stored beneath each mangrove stands. Carbon stocks were determined down to different limits with depth: approximate extension of the root systems, one-meter depth, and the hard substrate. Within the extension of the root systems, the soil carbon stock was lower than 100 MgC ha^{-1} regardless of the mangrove species. This low value resulted directly from the semi-arid climate that limits mangrove productivity. At depth beneath every zone, a buried layer enriched in mangrove-derived OM, with C/N values around 40 and $\delta^{13}C$ values around -26 ‰ was observed. This layer likely resulted from the late Holocene marine regression that induced a seaward migration of the mangrove. In this buried layer, the carbon stock was higher than in the upper sediment and reached up to 665, 255 and 300 MgC ha^{-1} in the salt-flat zone, the *A. marina* stand and the *R.* spp. stand, respectively. The highest stock, determined beneath the salt-flat, was suggested to be related to a period of sea-level stability that lasted ~3,000 years, whereas beneath the other zones, which are at lower elevations, mangrove colonization was more recent and the sea-level was continuously decreasing till recently. Sea-level variations, and, specifically current sea-level rise, may strongly influence mangrove ability to store carbon due to their migration along the tidal elevation gradient to maintain the biotic conditions needed for their development.

Keywords: Mangrove; Carbon stocks; Sea-level; Holocene; Stable isotopes; Radiocarbon

II.1. Introduction

Mangroves are considered as major ecosystems in the carbon cycle along tropical and subtropical coastlines, being among the most efficient blue carbon sinks (Kauffman *et al.*, 2011). This specificity results from a combination of different parameters including i) their high primary productivity (average of 218 ± 72 Tg C yr^{-1}) (Bouillon *et al.*, 2008), ii) their high storage capacity, with up to 15% of mangrove productivity being buried in mangrove soils (Breithaupt *et al.*, 2012), iii) the anoxic character of their soil resulting from waterlogging and limiting organic matter (OM) decay processes (Kristensen *et al.*, 2008). As a result, potentially up to 98% of their carbon content is stored in their substrate (Donato *et al.*, 2011), and organic carbon can accumulate over several meters depth on centennial to millennial time scales (Dittmar and Lara, 2001; Lallier-Vergès *et al.*, 2008; Twilley *et al.*, 1992). This contrasts with other blue carbon sinks in which the labile OM produced can be rapidly decomposed. However, soil carbon stocks in mangrove soils can be highly variable. On a local scale, they depend notably on tree species, soil salinity, nutrient availability, and, thus, on the forest's position in the tidal zone (Kauffman *et al.*, 2011; Adame *et al.*, 2013; Mizanur Rahman *et al.*, 2015; Wang *et al.*, 2013). On a global scale, climatic conditions have been found to be an important driver controlling mangrove soil carbon stocks. A strong relationship between the latitudinal position of the mangrove and the organic carbon stored in its soil can be established such that mangrove productivity is higher at low latitudes (Kristensen *et al.*, 2008; Sanders *et al.*, 2010; Alongi, 2012). Yet, most studies have been conducted in tropical and subtropical regions, and more data from temperate and arid regions are needed to ascertain the global mangrove carbon budget (Alongi, 2012; Sanders *et al.*, 2016). In addition, the integration with depth is a major challenge when assessing carbon stocks in mangrove ecosystems and should be carefully taken into consideration (Lunstrum and Chen, 2014; Marchand, 2017). Determining the depth reached by the organic matter produced by the above forest is crucial if the objective is to assess the recent carbon stock (Ha *et al.*, 2017; Marchand, 2017). Conversely, if the objective is to determine the total carbon stock of the ecosystem, the entire soil profile, down to a hard substrate, should be sampled. However, mangrove ecosystems can migrate landward or seaward as sea-level rises or falls (Gilman *et al.*, 2008), and, as a result, integrating the whole soil profile results in adding the stock of different mangrove forests that developed at different sea-level. Some paleo-environmental studies have been developed to reconstruct the

ecosystem dynamics and to investigate the Holocene sea-level and climate fluctuations (see review by Ellison (2008)). However, few were interested in the influence of sea-level variations on carbon stocks in mangrove soils.

In New Caledonia, mangrove forests cover over 35,000 ha, fringing on about 80% and 15% along the western and the eastern coastline of the island, respectively (Virly, 2006). These forests exhibit a typical mangrove zonation in semi-arid climate, which includes: (i) a back-side salt-flat, a highly saline zone, only submerged during high spring tides, and sometimes covered by a halophile herb, *Sarcocornia quinqueflora*; (ii) a second, downstream stand of vegetation, occupied by *Avicennia marina*; (iii) finally, the seaward edge is occupied by *Rhizophora* spp., which is periodically submerged at each tide. Previous studies (Marchand *et al.*, 2011a, 2012) suggested that the main factor controlling the distribution of mangrove species in New Caledonia was soil salinity, which in turn was controlled by the duration of tidal inundation and thus by the soil elevation. Consequently, the upper soil layers within the mangrove demonstrate gradients in water, salinity, and organic carbon contents, from the landward side to the seaward side (Deborde *et al.*, 2015).

Within such considerations of gradient, the main objectives of our study were: i) to determine the soil carbon stock related to the development of the current zoned forest, ii) to determine the soil carbon stock down to the bedrock, and iii) to identify the possible influence of sea-level variations on the carbon stock. We hypothesized that carbon stocks will decrease from the sea side to the land side of the forest as a result of this specific zonation related to soil salinity and elevation. We further suggested that sea-level variations may have allowed for the burial of former mangrove soils. To test these ideas, we conducted the following activities: cores were collected in the different stands down to a hard substrate, the elevations of sampled soils at depth were noted to a common reference elevation, the organic matter quality along depth in each core was assessed using C/N ratios and stable isotope analyses ($\delta^{13}C$ and $\delta^{15}N$), and carbon stocks were determined combining bulk density and total organic carbon content. Finally, radiocarbon measurements were performed to date core bottom and some other important strata for testing our hypothesis about sea-level variations.

II.2. Material and methods

II.2.1. Study site, climate and geology

The study was conducted in the Amboa Swamp of New Caledonia (Fig. II-3), which is in the upstream part of the estuarine mangrove forest of La Foa, on the west coast of the main island of this French overseas archipelago (Fig. II-3). This mangrove forest, part of the UNESCO World Heritage since 2008, is one of the most extensive on the archipelago covering more than 1,000 hectares. The mangrove ecotone is formed by a belt of *Rhizophora.* spp. in the external side, followed by a monospecific belt of *Avicennia marina* in the internal side. The upper wetland is composed by a salt-flat zone, without vegetation (Fig. II-3 and 2).

Climate in the region is semi-arid. It is strongly influenced by the inter-tropical convergence zone and by the El Niño Southern Oscillation (ENSO). Mean annual rainfall and air temperature in La Foa for the last 4 years are 1,040 mm and 22.8°C, respectively (data from meteofrance.com). The La Foa River drains a catchment area of 413 km², with a population density of 7.6 people km^{-2}. Outcrop rocks are mainly from volcanoclastic and volcano-sedimentary origin, Jurassic to Permian age. The entire basin is devoid of major anthropogenic activities, resulting in a low sediment discharge by the river through the mangrove.

II.2.1. Sampling and analytical processes

II.2.1.1. Field work and sampling

Three sediment cores per stand were collected using an Eijkelkamp gouge auger (1-meter-long, 8 cm diameter) (Fig. II-3). For each zone, two of the three sediment cores were collected down to 50 cm depth to determine organic matter quality and quantity related to the development of the above forest. The third core was collected down to the first hard substrate to determine possible evolution of the ecosystem induced by past sea-level variations. These three long cores were named: LF1 in the salt-flat, LF2 in the *Avicennia marina* stand, and LF3 in the *Rhizophora* spp. stand (Fig. II-3). Taking into account the low variability between the triplicate cores for the upper 50 cm, we feel confident that our results below this depth are representative of the system, even if we were able to collect just one long core per zone due to logistical difficulties.

To determine the vegetation characteristics, three areas of 10 m x 10 m were delimited in both *A. marina* and *R. stylosa* stands, close to the core positions. The number of trees were counted, and their respective height were measured. Additionally, twenty fresh and mature leaves were randomly sampled on trees surrounding the core positions. Similarly, fresh wood and roots were sampled.

Altitudinal heights, reported to the mean sea-level (MSL), of the three cores, and the vertical limits of the vegetation along the intertidal zone were obtained using a differential GPS (Trimble R4 GNSS).

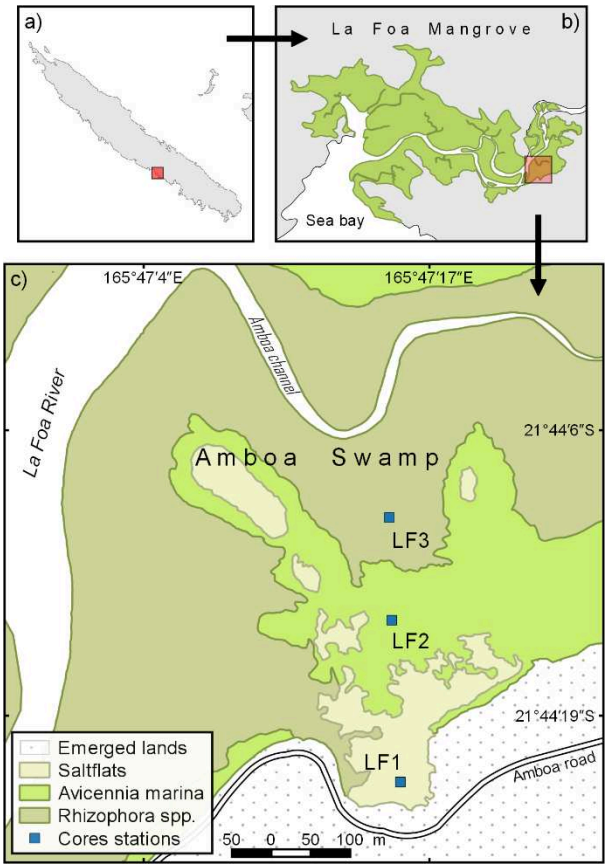

Fig. II-3: Location of the Amboa Swamp study area in New Caledonia (a) and in the La Foa estuary system (b). Representation of the species zonation, and cores stations (c).

II.2.1.2. Radiocarbon dating

Samples of wood debris were selected from the bottom of each core for radiocarbon dating. Two additional samples were taken, one in the interval 65-70 cm depth in the salt-flat, and one in the interval 30-35 cm depth in the *Avicennia* stand, as these intervals presented clear stratigraphic evolution along these two cores. All wood samples were acid-base-acid treated and combusted at 900°C over copper oxide *in vacuo* at the College of Marine Science,

University of South Florida. Samples of CO_2 gas were subsequently submitted for radiocarbon analysis at the National Ocean Sciences Accelerator Mass Spectrometry Facility (NOSAMS) at Woods Hole Oceanographic Institution (WHOI). Calibration of radiocarbon ages to calendar ages was done using OxCal version 4.3 (Bronk Ramsey, 2009) with the SHCal13 curve (Hogg *et al.*, 2013).

II.2.1.3. Samples preparation

The cores were separated into 5cm intervals. For each interval, a subsample of a known volume was taken. Subsamples were dried by freeze-drying until a constant weight was achieved. The dried bulk density (DBD) of each sample was obtained by dividing the dry mass by the fresh volume. Vegetation samples were rinsed with dezionized water to remove sediment and salt, and then dried at 55°C for 72h.

II.2.1.4. TOC, TIC, and stable isotopes ($\delta^{13}C$ and $\delta^{15}N$) analysis

Total organic carbon (TOC) and total inorganic carbon (TIC) contents were determined using a Total Organic Carbon Analyzer coupled to a SSM-5000A Solid Sample Module (TOC-LCPH-SSM500A, Shimadzu Corporation, Japan). The analytical precision was checked using glucose standard (Sigma Aldrich) and was less than 1% and 1.5% for TOC and TIC, respectively. Stable isotopes $\delta^{13}C$ and $\delta^{15}N$ were analyzed using an elemental analyzer coupled to an isotope ratio mass spectrometer (Integra2, Sercon, UK). Stable isotopes values ($\delta^{13}C$ and $\delta^{15}N$) are reported in per mille (‰) deviations from Pee Dee Belemnite (PDB) for $\delta^{13}C$ and atmospheric N for $\delta^{15}N$. All the analyses were performed at the French Institute for the Sustainable Development (IRD) of Noumea, New Caledonia. The analytical precision was checked using IAEA-600 caffeine standard (IAEA Nucleus) and was 0.3% for C and 0.15% for N.

II.2.1.5. Determination of the carbon stocks

The carbon density (CD) of each sample was calculated using DBD and TOC values. Then, the organic carbon stock (OCS) in the different sediment layers was calculated using the following equation:

Organic Carbon Stock ($MgC\ ha^{-1}$) = DBD ($g\ cm^{-3}$) * TOC (%) * depth interval (cm)

II.2.1.6. Determination of the limit reached by the OM due to the actual forest

To evaluate the depth reached by the organic matter derived from the above forest, we used a combination of parameters: (i) the sedimentological aspects of the cores (Fig. II-4), and (ii) the vertical distribution of C/N ratios and stable isotopes $\delta^{13}C$ and $\delta^{15}N$ (Fig. II-6).

II.2.1.7. Statistical analysis

Student's T-Tests were used to compare the characteristics of the vegetation, different parameters of the OM within each stand and between stands. A Multivariate Analysis of Variance (MANOVA) was used to determine the limits reached by the actual vegetation in each stand. All statistical analysis were performed under R software version 3.3.1 (R Development Core Team, 2008).

II.3. Results

II.3.1. Vegetation characteristics

The *A. marina* stand was the densest vegetated stand, with 7,167 ± 815 trees per hectare, whereas the *R.* spp. stand was twice less dense, with 3,667 ± 1,172 trees per hectare. However, *R.* spp. trees were taller than *A. marina* trees with a mean height of 263 ± 42 cm in comparison to 79 ± 55 cm for *A. marina* trees (Table II-1).

The mean $\delta^{13}C$ values and C/N ratios of the fresh mangrove tissues were significantly different between species (two-sample t-test, $p<0.05$). An enriched $\delta^{13}C$ value (-27.18 ± 1.15‰ vs. -29.60 ± 2.12‰) and a lower C/N ratio (41.16 ± 14.63 vs. 94.85 ± 46.05) were obtained for *A. marina* in comparison to *R.* spp.. The $\delta^{13}C$ and C/N values of leaves, roots and wood were significantly lower for *R.* spp. than for *A. marina* (two-sample t-test, $p<0.01$, Table II-1). For both species, the C/N ratio of leaves was lower than the one of roots and wood (Table II-1). However, no significant differences in the $\delta^{15}N$ value were determined between the two species (two-sample t-test, $p>0.05$).

II.3.1. Repartition of *A. marina* and *R.* spp. along the intertidal gradient

The salt-flat extended in the upper position, from 0.66 to 1.12 m above MSL. *A. marina* developed in the middle position, from 0.52 to 0.69 m above the sea-edge. *R.* spp. developed in the lowest part of the intertidal gradient, from -0.24 to 0.57 m above MSL. Stations LF1, LF2,

and LF3 were situated at an altitude of 0.80 ± 0.01, 0.65 ± 0.02 and 0.59 ± 0.01 m above MSL, respectively.

Table. II-1. Vegetation characteristics of *A. marina* and *R.* spp. in the studied mangrove swamp: tree density (stem ha^{-1}), tree height (cm), $\delta^{13}C$ and $\delta^{15}N$ (‰) signatures and C/N ratios.

Source	*A. marina*	*R.* spp.
Stem density (NB ha^{-1})	7,167 ± 815	3,667 ± 1,172
Tree height (cm)	79 ± 55 *(n=215)*	263 ± 42 *(n=110)*
$\delta^{13}C$ (‰)		
Leaves *(n=3)*	-28.36 ± 0.55	-30.46 ± 0.30
Roots *(n=3)*	-27.14 ± 0.69	-31.16 ± 0.84
Wood *(n=3)*	-26.06 ± 0.26	-27.19 ± 0.38
$\delta^{15}N$ (‰)		
Leaves *(n=3)*	2.77 ± 0.18	3.71 ± 1.85
Roots *(n=3)*	3.89 ± 0.25	4.37 ± 1.79
Wood *(n=3)*	5.30 ± 0.88	4.74 ± 0.41
C/N		
Leaves *(n=3)*	25.48 ± 1.05	66.22 ± 0.44
Roots *(n=3)*	43.57 ± 1.20	70.35 ± 3.81
Wood *(n=3)*	54.44 ± 7.11	147.96 ± 1.71

II.3.2. Stratigraphic description

In the salt-flat, the hard substrate was reached at 265 cm, it was composed of sand and shells, some of them were fully preserved but most were debris. The upper 70 cm of the sedimentary column was constituted of undifferentiated clays. Between 70 and 265 cm depth, core was characterized by dark brown muddy sediments enriched in red woody debris (Fig. II-4).

In the *A. marina* stand, the hard substrate was reached at 140 cm, with a similar composition as in the salt-flat. The upper 35 cm was constituted of brown sediments. Between 35 and 140 cm depth, core was characterized by dark-brown muddy sediments enriched in red woody debris (Fig. II-4).

In the *R.* spp. stand, the hard substrate was reached at 125 cm. Its composition was similar than for the two others stands, with sand and shells debris. Only one facies was found in the sedimentary column, from the surface to the depth of 125 cm. It was composed of a muddy dark-brown sediment, enriched in red woody debris (Fig. II-4).

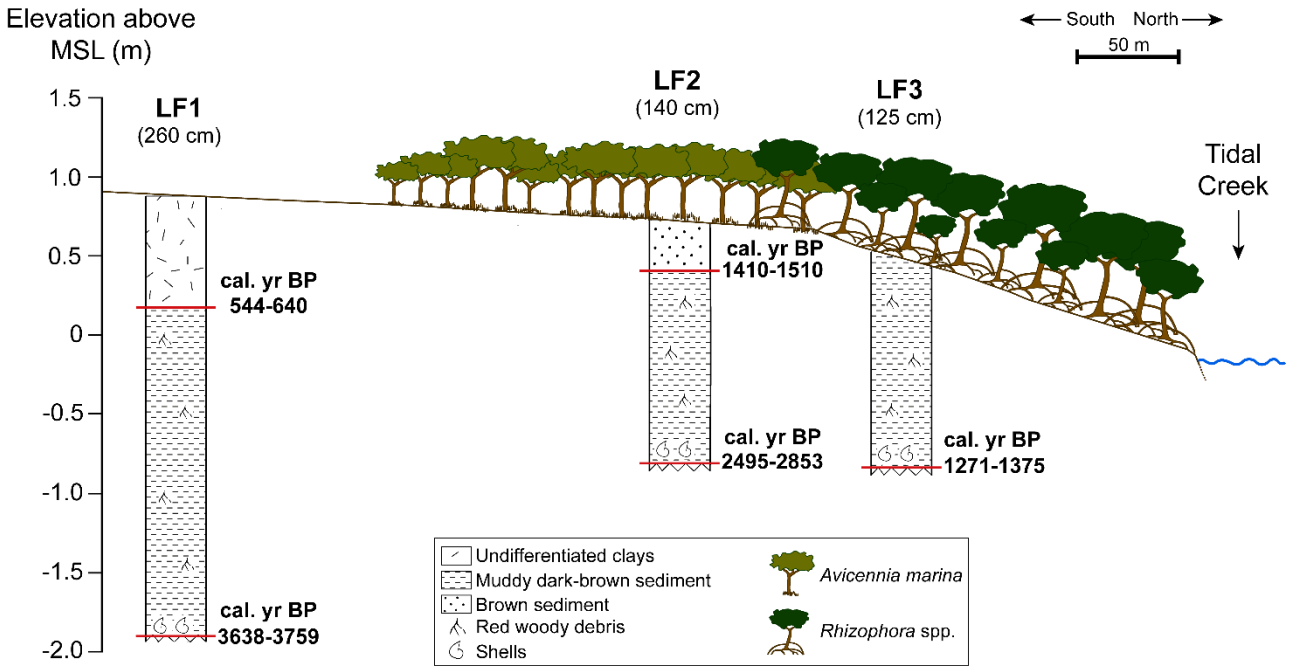

Fig. II-4: Stratigraphic profiles of cores LF1, LF2 and LF3, and mangroves species distribution along a South-North transect. MSL: Mean Sea Level.

II.3.3. Radiocarbon dating

For station LF1, in the salt-flat area, the bottom of the core (260-265 cm depth) was dated at *ca.* 3,699 cal. yrs BP, and the intermediate limit between the brown muddy sediment and the clays, at 65-70 cm, (Fig. II-4) was dated at *ca.* 592 cal. yrs BP (Table II-2). In station LF2, in the *A. marina* stand, the limit between the sedimentary column and the hard substrate, at 135-140 cm depth, was date at *ca.* 2,674 cal. yrs BP. The limit between the muddy brown sediment and the brown sediment (depth 30-35 cm) was dated at *ca.* 1,460 cal. yrs BP (Table II-2). Due to the apparent homogeneous sedimentary column (Fig. II-4), no intermediate date was measured in station LF3, in the *R.* spp. stand, and only the limit with the hard substrate, at depth 120-125 cm was dated, with a result around 1,323 cal. yrs BP (Table II-2).

Table. II-2: List of CFAMS radiocarbon dates and calibrated dates (2σ) using using OxCal version 4.3 (Bronk Ramsey, 2009) with the SHCal13 curve (Hogg *et al.*, 2013).

Core	Depth (cm)	^{14}C age (yrs BP)	Cal. Range (cal. yrs BP)	Median age (cal. yrs BP)	NOSAMS number
LF1	65-70	1,520 ± 25	544-640	592	OS-130664
	260-265	4,940 ± 20	3,638-3,759	3,699	OS-130665
LF2	30-35	3,230 ± 20	1,410-1,510	1,460	OS-132455
	135-140	4,120 ± 15	2,495-2,853	2,674	OS-132454
LF3	120-125	755 ± 15	1,271-1,375	1,323	OS-130690

II.3.4. Carbon content of the sediments

For the salt-flat zone, profiles of TOC, DBD and CD are characterized by two modes from the surface to the bottom of the sediment core with relatively invariant values within each mode. From the top to 70 cm in depth, mean values of 1.54 ± 0.56 %, 0.69 ± 0.09 g cm^{-3} and 1.09 ± 0.49 gC cm^{-3} were measured for TOC, DBD, and CD, respectively. From 100 cm to 265 cm in depth, mean values of TOC and CD were higher for TOC ($t_{(8.97)}$=-3.05, p<0.05) and CD with mean values of 9.81 ± 1.12 % and 0.30 ± 0.03 g cm^{-3}, respectively, and lower for DBD ($t_{(8.68)}$=4.75, p<0.01), with a mean value of 3.04 ± 0.57 gC cm^{-3} (Fig. II-5a, c, d).

For the *A. marina* stand, TOC had a mean value of 6.25 ± 1.92 % from the surface to 35 cm in depth, and then increased to 11.27 % at 62.5 cm. Then, TOC decreased to around 5.68 % towards the bottom of the core (Fig. II-5a). DBD was significantly higher from 0 to 35 cm than from 35 cm to 140 cm, with mean values of 0.40 ± 0.04 and 0.31 ± 0.05 g cm^{-3}, respectively ($t_{(10.96)}$=3.66, p<0.01, Fig. II-5c)

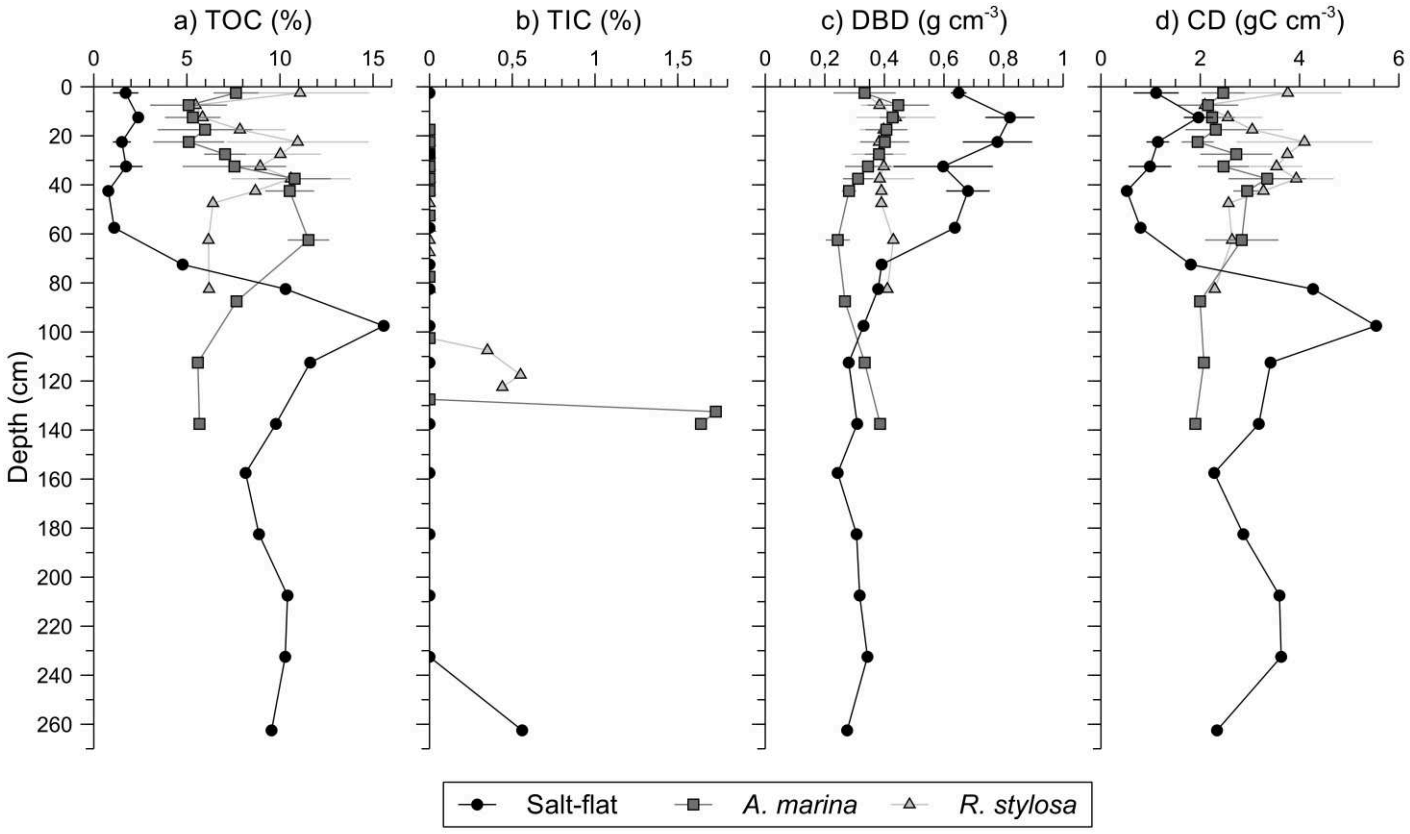

Fig. II-5: Vertical profiles of TOC (%), TIC (%), DBD (g cm^{-3}) and CD (gC cm^{-3}). The black line with the circle markers represents the salt-flat zone; the dark grey line with the square markers the *A. marina* stand; and the grey line with the triangle markers the the *A. marina* stand; and the grey line with the triangle markers the *R.* spp. stand.

For the *R.* spp. stand, TOC and CD rapidly decreased in the upper 15 cm, from 11.08 % to 5.47 % and from 3.76 to 2.09 gC cm^{-3}, respectively. TOC and CD then peaked to 10.95 % and 4.09 at 22.5 cm in depth. TOC and CD values then gradually decreased to 82.5 cm in depth, and thereafter remained relatively invariant to the bottom of the core, with mean values of 6.25 ± 0.13 % and 2.50 ± 0.18 gC cm^{-3}, respectively (Fig. II-5a, d). Mean value of DBD throughout the core was 0.40 ± 0.03 g cm^{-3} (Fig. II-5c).

For the three cores, TIC was different from zero only at depths 260 to 265, 130 to 140, and 105 to 125 cm for the salt-flat zone, the *A. marina* stand, and the *R.* spp. stand, respectively (Fig. II-5b).

II.3.5. OM in the sediment column

The characteristics of the OM in the sediment column for the salt-flat zone, the *A. marina* stand, and the *R.* spp. stand, were plotted in two scatter plots: $\delta^{13}C$ vs. C/N and $\delta^{15}N$ vs. C/N (Fig. II-6). For each stand, two groups were distinguished with the scatter plots, indicating a difference in the origin of the OM: one group for the top of the sediment column (group 1), and one group at the bottom (group 2). A MANOVA analysis, with $\delta^{13}C$, $\delta^{15}N$ and C/N as variables, showed that the two groups were significantly different for each stand ($p<0.01$).

For the salt-flat zone, the first group (a1) corresponded to depth interval 0-70 cm, and the second group (a2) to depth interval 70 – 265 cm. For group a1, mean values of C/N ratios, $\delta^{13}C$ and $\delta^{15}N$ were 16.12 ± 4.49, -24.76 ± 1.29 ‰ and 8.16 ± 1.36 ‰, respectively. Group a2 showed significantly higher values of C/N ratio ($t_{(4.96)}$=-9.69, $p<0.001$) and lower values of $\delta^{13}C$ and $\delta^{15}N$. Mean values of C/N ratio, $\delta^{13}C$ and $\delta^{15}N$ were 40.99 ± 3.74, -25.71 ± 0.58 ‰ and 3.96 ± 0.71 ‰, respectively (Fig. II-6a).

For the *A. marina* stand, group b1 was representative of the depth interval 0-35 cm, with mean values of C/N ratio, $\delta^{13}C$ and $\delta^{15}N$ of 20.74 ± 8.31, -25.69 ± 0.37 ‰ and 2.47 ± 0.58‰, respectively. The group b2 regrouped the depth interval 35-140 cm. Mean values of C/N ratio, $\delta^{13}C$ and $\delta^{15}N$ were significantly different than for group b1, with 44.28 ± 6.31, -26.30 ± 0.34 ‰ and 4.41 ± 0.28‰, respectively (C/N: $t_{(7.98)}$=-5.29, $p<0.001$; $\delta^{13}C$: $t_{(6.83)}$=2.91, $p<0.05$; $\delta^{15}N$: $t_{(8.92)}$=-7.43, $p<0.001$, Fig. II-6b).

For the *R.* spp. stand, group c1 was integrated from 0 to 25 cm of depth, and group c2 from 25 to 125 cm. Mean C/N ratio were significantly lower for group c1 than for group c2 with mean values of 29.16 ± 3.14 and 43.43 ± 1.43, respectively ($t_{(4.94)}$=-9.63, p<0.001). However, no significant difference of $\delta^{13}C$ and $\delta^{15}N$ were observed between group c1 and group c2 ($\delta^{13}C$: $t_{(6.28)}$=1.60, p>0.05 ; $\delta^{15}N$: $t_{(5.91)}$=-0.70, p>0.05). Mean values for group c1 and group c2 were respectively -25.77 ± 0.58 and -26.24 ± 0.41 ‰ for $\delta^{13}C$, and 3.39 ± 0.65 and 3.62 ± 0.42 ‰ for $\delta^{15}N$, Fig. II-6c).

Considering groups 2 in the three cores (a2, salt-flat zone, 80 – 265 cm depth; b2, *A. marina* stand, 40 – 140 cm depth; c2, *R.* spp. stand, 25 – 125 cm depth), no significant differences of C/N ratios, $\delta^{13}C$ and $\delta^{15}N$ were observed (ANOVA, $F_{(2,19)}$=1.57, p>0.05).

Attributing groups 1 and 2 allowed to determine some limits between an upper layer, under the influence of the development of the current living forest, and a buried layer related to the development of a former mangrove forest. In the salt-flat zone, there was no forest at the surface of the sediment, therefore only the deep layer was considered, from 70 – 265 cm depth. For *A. marina* and *R.* spp. stands, the limits were fixed at 35 and 25 cm, respectively.

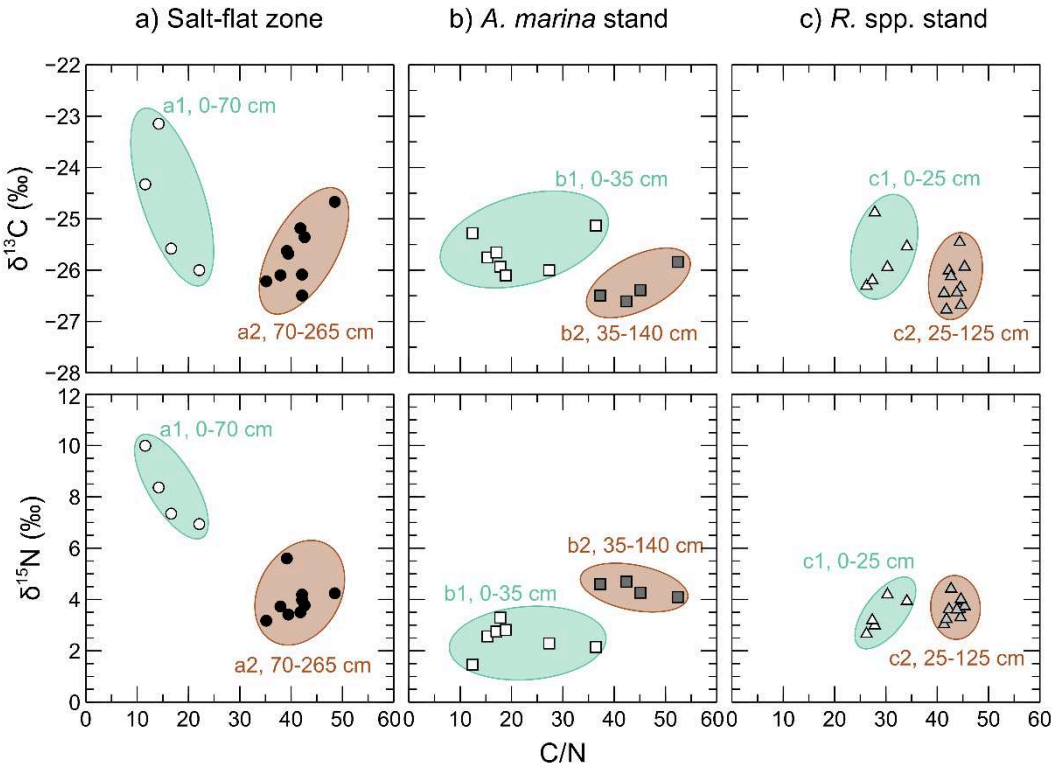

Fig. II-6: Scatter plots of δ13C vs. C/N and $\delta^{15}N$ vs. C/N. (a) in the salt-flat zone, with groups a1 for depth 0 - 80 cm and a2 for depth 80 - 265 cm; (b) in the *A. marina* stand, with groups b1 for depth 0 - 40 and b2 for depth 40 - 140 cm; (c): in the *R.* spp. stand, with groups c1 for depth 0 – 25 cm and c2 for depth 25 – 125 cm.

II.3.6. Soil carbon stocks

Integrating down to the hard substrate, the soil carbon stocks were 747.33 MgC ha^{-1}, 344.64 MgC ha^{-1} and 378.91 MgC ha^{-1} for the salt-flat zone, the *A. marina* stand and the *R.* spp. stand, respectively (Fig. II-7). Then, integrating the top meter of sediment under the living forest, the soil carbon stocks were 255.48 and 314.57 MgC ha^{-1} for *A. marina* and *R.* spp., respectively (Fig. II-7). When considering the limit reached by the organic matter of the current forest, determined using the preceding results, the soil carbon stocks were integrated from the top of the sediment column to 35 cm depth in the *A. marina* stand and to 25 cm depth in the *R.* spp. stand. Therefore, the soil carbon stocks in the layer under the influence of the current forest were 81.02 MgC ha^{-1} and 77.79 MgC ha^{-1} for *A. marina* and *R.* spp., respectively (Fig. II-7). Regarding the buried layer, the soil carbon stocks were 665.36 MgC ha^{-1}, 256.12 MgC ha^{-1} and 301.12 MgC ha^{-1} for the salt-flat zone, the *A. marina* stand and the *R.* spp. stand, respectively (Fig. II-7). Consequently, the buried layer represented 89.03%, 74.32% and 79.47% of total stock for the salt-flat, *A. marina* stand and *R.* spp. stand, respectively.

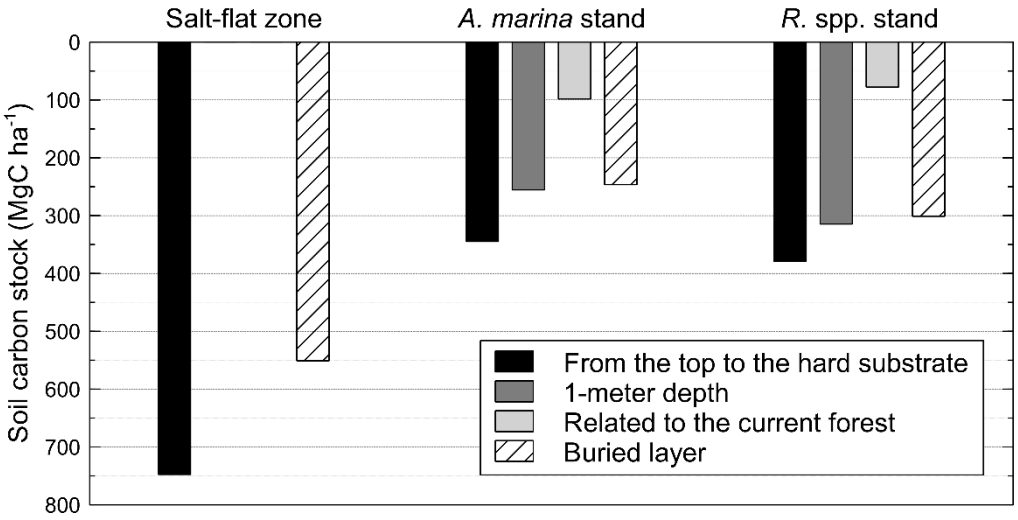

Fig. II-7: Figure 5: Representation of the soil carbon stocks (MgC ha^{-1}) for different sediment layers at the three zones: salt-flat, *A. marina* stand, and *R.* spp. stand. Concerning the stocks related to the current forest, carbon stocks were integrated from 0 to 35 cm and from 0 to 25 cm under *A. marina* and *R.* spp., respectively. Regarding the buried layer, carbon stocks were integrated from 70 cm to 265 cm in the salt-flat zone, from 35 to 140 cm in the *A. marina* stand, and from 25 to 125 cm in the *R.* spp. stand.

II.4. Discussion

II.4.1. OM characterization with depth and along the intertidal elevation gradient

In mangrove sediments, OM may derive from various sources; mangrove leaves, roots and microphytobenthos are the main contributors, but allochthonous sources of marine or terrestrial origin may also contribute to the organic carbon pool to a lesser extent (Kristensen *et al.*, 2008). To characterize OM in a complex mixture like mangrove sediments, a combination of biomarkers is required. In the present study, the depth distribution of C/N ratios and stable isotopes ($\delta^{13}C$ and $\delta^{15}N$) showed two distinct strata characterized by specific OM quantity and quality (Fig. II-6). The limit between the two layers decreased seaward, being reached at 70, 35 and 25 cm depth for the salt-flat, the *Avicennia* stand and the *Rhizophora* stand, respectively.

In the upper layers, C/N ratios and $\delta^{13}C$ ranged between 10 to 40 and between -24 to -27 ‰, respectively, being consistent with those previously reported in mangrove sediments (Bouillon *et al.*, 2003; Prasad *et al.*, 2017). OM quality differed between the *Avicennia* and the *Rhizophora* stands, with notably higher C/N ratios under *R.* spp. than under *A. marina* stand. This C/N depletion under *A. marina* may result from different causes. First, the fresh tissues of *A. marina* typically had lower C/N ratios than *R.* spp. (Table II-1). Then, due to its intermediate position in the intertidal zone, *A. marina* is less submitted to tidal flushing and thus might accumulate more leaf litter, characterized by low C/N ratios, while *R.* spp. might accumulate more woody tissues with higher C/N ratios (Table II-1), the leaf litter being flushed away. In addition, surface sediments of *A. marina* may shelter a larger amount of microphytobenthos, having typical values of C/N <10 (Lamb *et al.*, 2006), due to an open canopy that allows light to reach the sediment surface, and less immerged conditions (Leopold *et al.*, 2013). Eventually, sediments beneath *Rhizophora* are more anoxic with long periods of immersion, which limit OM decay processes, while upper sediments beneath *Avicennia* are usually oxic to suboxic due to air diffusion from the atmosphere into the soil during the long emerged periods, and due to air diffusion from the specific root system (Alongi *et al.*, 2000; Andersen and Kristensen, 1988; Marchand *et al.*, 2004). The suboxic conditions beneath *Avicennia* stand may favor OM decomposition and thus C/N decrease. Consequently, we suggest that the position of the stand

may have an influence on OM quantity and quality, either because it drives the zonation, or because tidal flushing and decay processes differ due to different tidal immersion.

Whatever the stand, the deep layer was enriched in OM compared to the upper layer, with TOC concentrations up to 15%, and was characterized by high C/N ratios and low $\delta^{13}C$ values, both typical of higher plant debris (Meyers and Lallier-Vergès, 1999). However, this layer extends down to the hard substrate, which was deeper than one meter beneath the forested stands, and thus the accumulated OM in this layer cannot originate from the above forest. In mangroves, root systems usually develop between 20 and 60 cm depth, and never deeper than one meter (Castañeda-Moya *et al.*, 2011; Claus and George, 2005; Ferreira *et al.*, 2007; Gill and Tomlinson, 1977; Komiyama *et al.*, 2000; Ong *et al.*, 2004; Tamooh *et al.*, 2008). In addition, this organic-rich layer was also observed in the salt-flat, without any vegetation cover, and extends down to 260 cm depth. In fact, no matter the stand, this layer was visually enriched in red woody tissues, characteristic of *Rhizophora* trees. Consequently, we suggest that the current living forest develops on sediments that were previously colonized by a *Rhizophora* forest. However, it was surprising to observe that OM in the buried layer was more preserved than in the upper layer beneath the *Rhizophora* stand, with $\delta^{13}C$ values and C/N ratios closed to the one of fresh root tissues (Table II-1). In addition, the OM quantity was much higher. These two results may indicate that either the productivity of the former forest was higher, or that the conditions were more favorable to OM accumulation, *eg* more anoxic conditions (longer immersion time) or higher sedimentation rates. This buried organic-rich layer was already observed in different mangroves of the west coast of New Caledonia (Deborde *et al.*, 2015; Marchand *et al.*, 2011; Marchand *et al.*, 2012), indicating that the cause may not be local but rather related to sea-level evolution in this region. From the landside to the seaside, both the bedrock and the limit between the two layers tend to decrease in depth, suggesting a sea-level drop rather than sea-level rise.

II.4.2. Migration of the mangrove ecosystem down the intertidal zone

The hard substrate reached beneath every stands stand was sandy, characterized by broken or fully preserved shells, and increased quantity of inorganic carbon (Fig. II-5), which was null above. The presence of *Rhizophora* red woody tissues above these shells indicates a transition from a marine dominated system to a mangrove dominated ecosystem. The red

woody debris collected just above the hard substrate in the three stands were dated at *ca.* 3,700, 2,700 and 1,300 cal. yrs BP beneath the current salt-flat, *A. marina* and *R.* spp. stands, respectively. These results confirm a seaward migration of the mangrove (Fig. II-8a, b and c). Our observations show that *Rhizophora* trees developed preferentially in the low intertidal zone, until 0.57 cm above MSL, whereas *A. marina* developed in the middle intertidal zone, between 0.52 to 0.69 m above MSL. Soil salinity was recognized as the main factor controlling this distribution (Deborde et al., 2015; Marchand et al., 2012, 2011a), which is, in turn, directly linked to the soil inundation and elevation, and thus to the current mean sea-level. The progressive colonization of *Rhizophora* downward the intertidal zone might be linked to a regular retreat in mean sea-level, starting before 3,700 cal. yrs BP. The marine regression created new accommodation spaces at the mangrove front, allowing *Rhizophora* to colonize, leaving the less attractive upper intertidal zone, due to an increase in salt concentrations, to the benefit of *A. marina*. This pattern was observed in site LF2, where the *Rhizophora* forest lasted around 1,200 cal. yrs before being colonized by *A. marina ca.* 1,450 cal. yrs BP, which is still present at this position (Fig. II-8c and d). This hypothesis of a regular marine regression in New Caledonia is consistent with the theory developed by Cabioch *et al.* (1989), later reinvested by Mitrovica and Peltier (1991), or more recently by Yamano *et al.* (2014) and Nunn and Carson (2015). They notably showed that the sea-level was ~1.1 m higher around 4,500 cal yr BP, and that the sea-level fall at the latest since 2,800 cal yr BP.

Site LF1 suggests that a *Rhizophora* mangrove forest was stable during more than 3,000 years, before being replaced around 590 cal. yrs BP by the actual salt-flat (Fig. II-8d). This last establishment was due to a low sea-level that has induced low period of immersion resulting in elevated evaporation processes and, thus, too much salt in the soil for mangrove development. No evidence of an establishment of *A. marina* forest was observed between the *Rhizophora* forest and the salt-flat, neither in the stratigraphic observations (Fig. II-4), nor in the geochemical results (Fig. II-6). Therefore, two hypotheses may be developed. First, a sharp sea-level drawdown around 590 cal. yrs BP, might have prevented the establishment of *A. marina*. This sea-level drawdown was described by Cabioch *et al.* (1989) and more recently by Wirrmann *et al.* (2011). However, the presence of *A. marina* in site LF2 since *ca.* 1,450 cal. yrs BP, suggests that this hypothesis cannot explain the absence of *A. marina* debris between the salt-flat soil and the buried layer. As explained earlier, *Avicennia* soils may favor OM

decomposition due to their higher position and the oxygen released from their root system. In addition, *Avicennia* debris are less refractory to decomposition than *Rhizophora* ones, which contain abundant tannins (Kristensen *et al.*, 2008). Therefore, we consider that *Avicennia*-derived OM may have been decomposed, and that other biomarkers (*eg* lignin-derived phenols or pollen) should be used to determine their presence. The continuous sea-level drop, and the fact that LF1 was the highest intertidal position, may have led to a short period of development of the *Avicennia* forest at this position, which has resulted in low organic enrichment of the soil, not visible with the parameters studied herein.

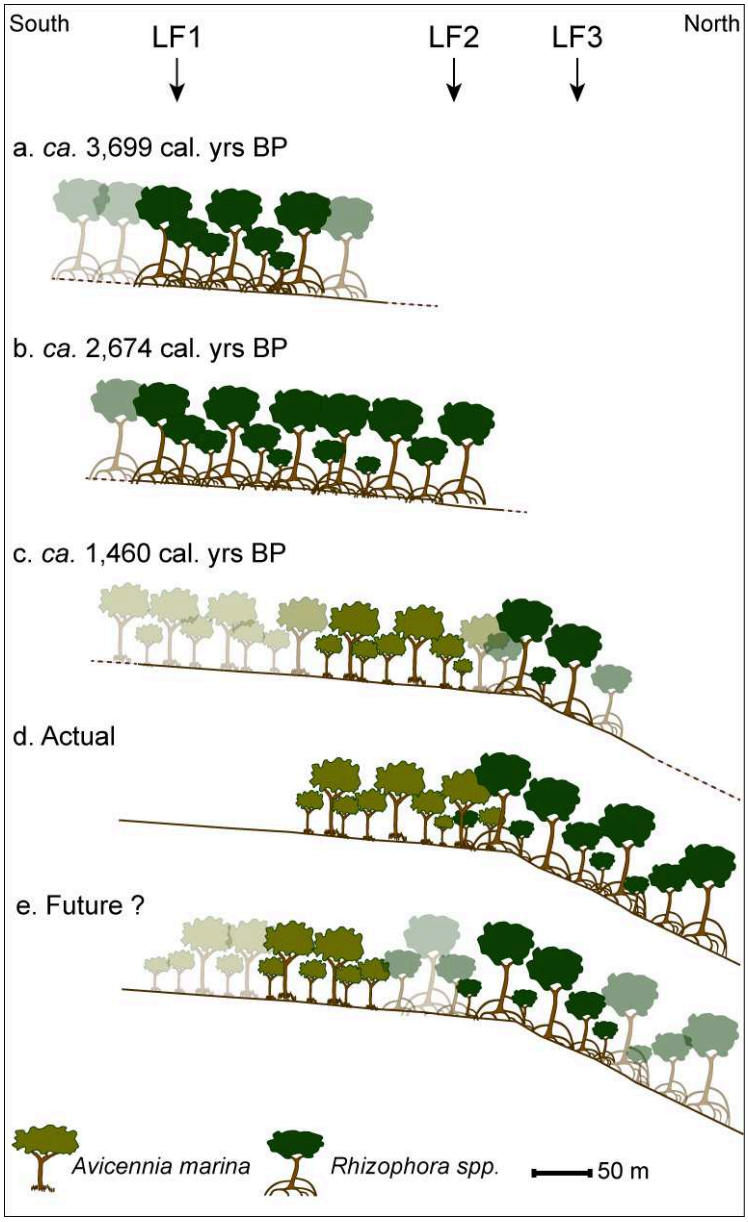

Fig. II-8: Simplified illustration of the colonization phases of the actual mangrove swamp during the last 4,000 years, and possible future evolution of the ecosystem.

We are aware that the organic carbon dating in mangrove sediments can be quite difficult due to roots extension and fauna bioturbation (Woodroffe *et al.*, 2016, 2015). However, as the woody debris collected in the present study were of pluri-centimetric size and in a horizontal position, we are confident with the results reported here, and with the evolution model presented above, which fits well with the sea-level evolution in New Caledonia described by the authors cited above. We, thus, suggest that the late Holocene marine regression induced a seaward migration of the mangrove forest, and was responsible of a buried layer enriched in *Rhizophora* tissues beneath every stand.

II.4.3. Influence of mangrove seaward migration on soil carbon stocks

To determine soil carbon stocks in mangrove, depth integration should be clearly discussed, as suggested by Lunstrum and Chen (2014). Thus, it is recommended to sample the soil down to the bedrock, but, most of the time, the stocks are determined down to one meter deep. In the studied mangrove, integrating the top meter of sediment beneath *A. marina* and *R.* spp. stands resulted in a soil carbon stock of 255 and 315 MgC ha^{-1}, respectively, which is lower than the reported values for tropical mangroves, ranging from 337 to 640 MgC ha^{-1} (Adame *et al.*, 2013; Castillo *et al.*, 2017; DelVecchia *et al.*, 2014; Hossain, 2014; Kauffman *et al.*, 2011). Different climatic conditions may be the major explanation of this difference, as tropical mangroves are typically more productive than higher latitudinal mangroves (Alongi, 2012; Kristensen *et al.*, 2008; Sanders *et al.*, 2010). In New Caledonia, the climate is semi-arid, and mangrove trees are most of the time dwarf (Table II-1). They suffer from the lack of water and have a limited productivity (Leopold *et al.*, 2016), which may induce the lower soil carbon stock values in comparison to tropical mangrove forests.

However, the visual observations of the cores, the C/N and isotopic results showed that the root system mainly developed in the upper 40 cm. Consequently, the stock down to one meter is not only related to the development of the current forest, but also takes into account part of the buried layer enriched in *Rhizophora* debris, induced by the sea-level drop in the region. Therefore, comparing soil carbon stocks integrated down to one meter may not be relevant since it implies to sum stocks of different forests that developed when the mean sea-level was different. This result highlights the necessity to precisely define the objectives of the study before measuring soil carbon stocks in highly dynamic ecosystems such as mangroves, and, if

the objectives are to evaluate the effect of the current living forest on soil carbon stocks, the vertical limit of the root system must be determined (Lunstrum and Chen, 2014; Marchand, 2017). Our results suggest that the upper soil carbon stock is directly related to the living forest at the time of deposit, which is, in turn, related to the mean sea-level.

Taking into account the limits determined using C/N ratios and isotopic values, the development of the current forest induced a slightly higher carbon stock under *A. marina* than *R.* spp., with about 81 and 78 MgC ha^{-1}, respectively. However, comparing carbon stocks between these two layers may be biased as the integration depth under *A. marina* was higher than under *R. stylosa*. When comparing mean carbon density, we found higher values under *R. stylosa* (3.11 ± 0.83 gC cm^{-3}) than under *A. marina* (2.46 ± 0.43 gC cm^{-3}, due to the higher productivity of *Rhizophora* trees in comparison to *Avicennia* trees (Komiyama *et al.*, 2008), and the more oxic conditions of the soil under *Avicennia*, as discussed earlier, enhancing the rate of OM decomposition.

Due to the integration of buried layers, resulting from mangrove development at different sea-level, soil carbon stocks down to the bedrock were 3.5 and 4.8-fold higher than for the upper layer under *A. marina* and *R.* spp., respectively. Specifically, the soil carbon stock in the buried layer beneath the salt-flat was higher than 665 MgC ha^{-1}, and was more than twice the ones beneath *A. marina* and *R.* spp.. In fact, the thickness of the buried layer beneath the salt-flat was almost 2 m, which were deposited during more than 3,000 years, during the relatively stable sea-level highstand before the drop. Beneath the *Avicennia* and the *Rhizophora* stands, the thicknesses of the buried layers were smaller, and OM accumulated during shorter periods, due to later mangrove colonization and continuous sea-level drop. Consequently, we suggest that periods of sea-level stability may result in high accumulation of organic peat in mangrove ecosystems. Considering another time scale, it is possible that mangrove ecosystems may have been at the origin of source rocks for oil and gas.

Understanding the evolution of mangroves with sea-level variations and its implication on soil carbon stocks is of major concern considering the prime importance of mangrove ecosystems in carbon storage (Donato *et al.*, 2011). Global sea-level increased over recent decades and is predicted to increase from 0.26 to 0.98 m by the end of the 21st century (Church *et al.*, 2013). The most probable evolution of the studied mangrove, if it cannot keep pace with sea-level rise, is a landward migration to the upper intertidal area, resulting in the installation

of *Avicennia* and *Rhizophora* stands on the current salt-flat and *A. marina* stands, respectively (Fig. II-8e). However, whilst this inland migration of the mangrove may be possible in New Caledonia, due to high spaces availability at the back of mangroves, this retreat may be more difficult in other locations as in developing countries, where coastal squeeze may be important due to strong urban development. In the latter case, other scenarios have to be considered for these mangroves that will be directly affected by the increase in sea-level.

II.5. Conclusion

- The present study aimed to evaluate soil carbon stocks along an intertidal gradient in a zoned mangrove growing under the semi-arid climate of New Caledonia and to identify a possible influence of sea-level evolution during the Holocene on these stocks. Our main results can be summarized as follow:
- The sediment under the three studied mangrove stands could be separated in two different layers, according to depth. The top layer extended from the surface to 70, 35 and 25 cm in the salt-flat, the Avicennia and the Rhizophora stands, respectively, while the bottom part extended down to the hard-sandy substrate, at 265, 140 and 125 cm depths, respectively.
- The limits between these layers were identified using a combination of different markers as stratigraphic observations, and the distribution of C/N ratio and stable isotopes δ13C and δ15N. The large proportion of red woody tissues found in the deep layers suggests that these horizons result from the development of a Rhizophora forest, now disappeared.
- The organic material collected just above the hard substrate revealed younger ages when progressing downward the intertidal zone. We suggested that the marine regression of the late Holocene leaded to a downward colonization of the intertidal zone by the mangrove. Rhizophora colonized firstly, later followed by Avicennia when the sea-level was too low for Rhizophora to develop.
- This evolution of the mangrove with sea-level fall influenced mainly the evaluation of soil carbon stocks. Integrating down from the surface to the hard substrate leaded to take into account the former mangrove, and thus, considerably increased the soil carbon stocks. Integrating only the top meter of sediment, as it is commonly observed in other studies, led to an under-estimation of the stocks. On the contrary, over-

estimation of the stocks can occur when integrating the top meter to evaluate the effect of the development of the current forest. In this case, we suggest that the vertical limit of the root system of the surface vegetation has to be precisely defined before determining the carbon stocks.

- Future research will be now needed to evaluate the evolution of the mangrove during the mid-Holocene marine transgression, and its effect on soil carbon stocks. As sea-level rose during mid-Holocene, a carbon rich sediment probably formed, now buried under the hard substrate found in this study. This future study could help to understand how past sea-level rise influenced the evolution of the mangrove, and thus, the soil carbon stocks, and therefore help to understand the future evolution of the mangrove with projected sea-level rise.

Acknowledgments

The authors are very grateful to the Southern Province of New Caledonia, the City of Mont Dore, KNS Koniambo Nickel SAS and Vale NC for funding the study. We gratefully thank Ryan Venturelli for handled the radiocarbon analysis.

CHAPITRE III Flux de CO_2 et de CH_4 vers l'atmosphère dans une mangrove à *Rhizophora*

Présentation

Nous avons vu dans le chapitre précédent que les mangroves pouvaient stocker des quantités importantes de matière organique dans leur sol, et que ce stock est dépendant de la forêt qui se développe en surface et des variations du niveau marin. Toutefois dans les sols, la matière organique accumulée, et qui provient principalement de la litière des palétuviers, peut-être dégradée par les micro-organismes, produisant des gaz à effet de serres (GES) qui sont ensuite réémis vers l'atmosphère. En effet, en raison de la richesse en matière organique de leurs sols, les mangroves se sont révélées être une source nette de GES vers l'atmosphère (Chen *et al.*, 2014), même si les émissions de GES sont plus faibles que pour d'autres écosystèmes, notamment du fait l'engorgement hydrique des sols qui induit la dominance de processus anoxiques de décomposition de la MO. Cependant, ces émissions sont fonction de nombreux paramètres environnementaux qui ne sont pas encore tous maitrisés. En particulier, les émissions depuis la surface de la colonne d'eau lorsque la forêt est inondée par la marée haute n'ont, à ce jour, pas fait l'objet d'études spécifiques.

Dans ce contexte, nous avons étudié les variations saisonnières des flux de CO_2 et de CH_4, depuis les sols et la colonne d'eau, dans une forêt de mangrove de *Rhizophora*. Durant les périodes de marée basse, les flux ont été mesurés à l'aide de chambres d'incubation transparentes et opaques (Figure III-1a). Les mesures ont été réalisées à la lumière, à l'obscurité et à l'obscurité après avoir enlevé les 1-2 mm de sol considérés comme contenant du biofilm constitué de microphytobenthos. En effet, plusieurs études ont montré son implication dans les émissions de GES depuis les sols de mangrove (Bulmer *et al.*, 2015; Leopold *et al.*, 2015, 2013). Durant la marée haute, les émissions ont été mesurées grâce à une chambre flottante complètement opaque (Fig. III-3b). En outre, les chambres ont toutes été reliées à un spectromètre de masse de terrain (CRDS, Figure III-1c) qui permet l'analyse simultanée du CO_2, du CH_4 et de la valeur isotopique du CO_2 émis ($\delta^{13}C\text{-}CO_2$). Durant la période de mesure, les flux de CO_2 et de CH_4 à marée basse ont varié de 31,34 à 187,48 mmol m^{-2} j^{-1} et de 39,36 à 428,09 µmol m^{-2} j^{-1}, respectivement. Ces émissions ont montré une forte variabilité saisonnière avec des flux plus élevés mesurés pendant la saison chaude, principalement dû à son effet stimulant sur les processus de décomposition de la matière organique, et par conséquent sur la production de gaz à effet de serre. De plus, les flux de CO_2 et de CH_4 se sont révélés plus élevés à l'obscurité qu'à la lumière, soulignant le rôle du biofilm de surface dans

la régulation de ces émissions. La valeur moyenne du $\delta^{13}C$-CO_2 était de -19,76 ± 1,19‰, sensiblement enrichie par rapport à celle obtenue pour le CO_2 émis par la respiration racinaire (-22,32 ± 1,06‰), la décomposition de la litière (-21,43 ± 1,89‰) et la dégradation de la matière organique (-22,33 ± 1,82‰). Ce résultat a mis en évidence l'utilisation du CO_2 produit dans le sol par le biofilm qui se développe à sa surface. Après avoir enlevé les 1 à 2 mm supérieurs du sol, les flux de CO_2 et de CH_4 ont été améliorés, mais le $\delta_{13}C$-CO_2 s'est enrichi, suggérant que l'intégralité du biofilm n'a pas été éliminée et que la partie restante a été détériorée, ce qui a conduit à sa décomposition et donc à des flux de CO_2 plus élevés dans l'atmosphère.

Figure III-1: Photographies (a) d'une chambre d'incubation opaque utilisée à marée basse, (b) d'une chambre d'incubation flottante utilisée à marée haute, et (c) de l'analyseur CRDS utilisé pour mesurer les émissions.

Lors de la marée haute, les émissions de CO_2 et de CH_4 ont varié de 3,00 à 441,75 mmolC m^{-2} j^{-1} et de 4,32 à 4129.75 µmolC m^{-2} j^{-1}, respectivement. Le type de marée et l'amplitude de la marée se sont avérés êtres les principaux paramètres contrôlant les flux de GES vers l'atmosphère. En effet, une forte relation inverse entre l'amplitude des émissions et l'épaisseur de la colonne d'eau au-dessus du sol a pu être observée. En considérant la gamme des valeurs de $\delta_{13}C$-CO_2, entre -26,88 ‰ et -8,6 ‰, nous avons déduit que le CO_2 émis depuis le sol était fortement dilué par l'eau estuarienne. De plus, les émissions de CO_2 et de CH_4 étaient plus importantes en marée descendante, du fait de l'enrichissement progressif de la colonne d'eau par la diffusion du gaz depuis les sols avec l'augmentation de son temps de résidence. Finalement, les marées de vives eaux émettent plus de CO_2 et de CH_4 vers l'atmosphère. Ceci

est dû à une plus grande épaisseur de la colonne d'eau qui, dès lors, couvre une étendue plus importante sur la zone intertidale, augmentant ainsi la surface d'échange avec le sol.

Cette étude fournit des informations importantes sur la variabilité des flux de CO_2 et de CH_4 depuis les mangroves vers l'atmosphère, et aide à affiner le bilan carbone de l'écosystème et donc de mieux comprendre l'implication de ces dernières dans l'atténuation du changement climatique. Elle permet également de donner des premières estimations quant à l'amplitude des émissions de CO_2 et de CH_4 vers l'atmosphère lorsque la forêt est inondée par la marée.

Partie 1.

Seasonal variability of CO_2 and CH_4 emissions from a *Rhizophora* mangrove soil (New Caledonia)

Adrien Jacotot, Cyril Marchand, Michel Allenbach

Abstract

Mangroves are intertidal ecosystems developing along tropical and subtropical coastlines. Due to their richness in organic matter, mangrove soils have been shown to be net sources of greenhouse gases to the atmosphere. However, biotic and abiotic factors driving these emissions remains poorly characterized. Within this context, we investigated the seasonal variations of CO_2 and CH_4 fluxes in a *Rhizophora* mangrove forest that develops under a semi-arid climate, in New Caledonia. Fluxes were measured using closed incubation chambers connected to a CRDS analyzer. They were performed during low tide at light, in the dark, and in the dark after having removed the top 1-2 mm of soil, which may contain biofilm. CO_2 and CH_4 fluxes ranged from 31.34 to 187.48 mmol m^{-2} d^{-1} and from 39.36 to 428.09 µmol m^{-2} d^{-1}, respectively. Both CO_2 and CH_4 emissions showed a strong seasonal variability with higher fluxes measured during the warm season, increased temperatures induced enhanced GHG production within the soil. Furthermore, CO_2 fluxes were higher in the dark than at light, evidencing photosynthetic processes at sediment surface and thus the role of biofilm in the regulation of greenhouse gas emissions from mangrove soils. The mean $\delta^{13}C$-CO_2 value of the CO_2 fluxes measured was -19.76 ± 1.19 ‰, which was depleted compared to the one emitted by root respiration (-22.32 ± 1.06 ‰), leaf litter decomposition (-21.43 ± 1.89 ‰) and organic matter degradation (-22.33 ± 1.82 ‰). This result confirmed the use of the CO_2 produced within the soil by the biofilm developing at its surface. After removing the top 1-2 mm of soil, both CO_2 and CH_4 fluxes increased. The fact that CH_4 fluxes were enhanced also suggest that the biofilm may act as a physical barrier for the transfer of GHG produced with the soil to the atmosphere. However, the $\delta^{13}C$-CO_2 became more enriched, evidencing that the biofilm was not integrally removed, and that its partial removal resulted in physical disturbance that stimulated CO_2 production. Therefore, this study provides useful information about some biotic and abiotic factors that control GHG emissions from mangrove soils, and thus help to understand their global implication in climate change mitigation.

Keywords: Soil fluxes, Greenhouse gas, Carbon stable isotopes, Biofilm, Mangrove, New Caledonia

III.1.1. Introduction

Anthropogenic emissions of greenhouse gases to the atmosphere increased significantly since preindustrial times to the point that current emissions have reached their highest rates for the last 66 million years (Zeebe *et al.*, 2016). As a result, atmospheric CO_2 concentrations are now at their highest level for the last 800,000 years (Lüthi *et al.*, 2008). Despite the development of alternative energies to fossil fuels, the different projections for the end of the century do not show any decrease of the emissions. Therefore, there are urgent needs to evaluate the ability of natural ecosystems to fix and store carbon, which also includes the greenhouse gas emissions from these ecosystems, in order to adopt appropriate climate change mitigation programs such as ecosystems conservation and restauration strategies.

Mangroves are forested ecosystems that develop along tropical and subtropical coastlines, providing numerous ecosystems services (Barbier *et al.*, 2011; Lee *et al.*, 2014). Due to their high primary productivity, estimated to 218 ± 72 Tg C yr^{-1} (Bouillon *et al.*, 2008), and their high carbon storage capacity, with up to 15% of their productivity being buried in their soils (Breithaupt *et al.*, 2012), mangroves notably play a critical role in the coastal carbon cycle and were thus recently named "blue carbon" sinks (Mcleod *et al.*, 2011). Mangrove soils are mainly anoxic, limiting organic matter (OM) decay processes and thus greenhouse gas (GHG) production. However, due to their position between land and sea, mangroves are regularly flooded by tides, and their soils may alternate between suboxic and anoxic conditions, modifying GHG production and emissions (Allen *et al.*, 2007; Chauhan *et al.*, 2015; Chen *et al.*, 2016b; Oertel *et al.*, 2016; Chen *et al.*, 2016a). In mangrove soils, the CO_2 produced derives mainly from biofilm respiration, roots respiration, leaf litter degradation, and organic matter decomposition (Kristensen *et al.*, 2008). In contrast to CO_2 production, methanogenesis is a strictly anaerobic process that only occurs when all electron acceptors have been exhausted. Considering the inputs of sulfate during each tide, CH_4 emissions from mangrove forests may be low or non-existent (Alongi *et al.*, 2001; Alongi *et al.*, 2004). However, recent studies demonstrated that sulfate reduction and methanogenesis can coexist in mangrove soils due to the utilization of other non-competitive substrates by methanogens (Lyimo *et al.*, 2002), and thus it was suggested that these CH_4 emissions may have been underestimated (Lyimo *et al.*,

2002; Chauhan *et al.*, 2015). CH_4 may notably be of major concern due to its global warming potential, 25 times higher than CO_2 over a 100 year time frame (Myhre *et al.*, 2013). Nevertheless, there is still a paucity of research in this area, and the variability of greenhouse gas emissions from mangrove soils remains poorly understood, notably due to the number of parameters that have to be taken into account (*e.g.* mangrove species, latitude, anthropic pressure, etc.).

For a specific area, several environmental factors have been shown to influence the emissions of greenhouse gases to the atmosphere from mangrove soils, such as soil water content, organic matter content, or even salinity (Kirui *et al.*, 2009; Poungparn *et al.*, 2009; Livesley and Andrusiak, 2012; Chen *et al.*, 2012; Chanda *et al.*, 2013; Leopold *et al.*, 2013; Chen *et al.*, 2014; Leopold *et al.*, 2015; Bulmer *et al.*, 2015; Chen *et al.*, 2016b). Seasonal evolution of temperature is also an important parameter involved in the variability of greenhouse gas emissions, affecting the rates of soil organic matter decay, and thus GHG production and emissions (Mackey and Smail, 1996; Fang and Moncrieff, 2001; Fierer *et al.*, 2005; Davidson and Janssens, 2006; Conant *et al.*, 2011; Barroso-Matos *et al.*, 2012). In addition, the development of biofilm at the sediment surface has been shown to be a another major driving factor of GHG emissions from mangroves soils (Leopold *et al.*, 2013; Leopold *et al.*, 2015; Bulmer *et al.*, 2015).

Furthermore, recent development of advanced technologies such as cavity ring-down spectroscopy (CRDS) allows high resolution in situ simultaneous measurements of both CO_2 and CH_4 fluxes, and also of $\delta^{13}C\text{-}CO_2$. These new analytical means could help to identify the origins of the CO_2 emitted from mangrove soils.

With this context, our main objectives were to: (i) quantify the CO_2 and CH_4 fluxes from the soil to the atmosphere, in the light and in the dark, during low tide within a *Rhizophora* spp. mangrove forest developing under semi-arid climate, (ii) evaluate the seasonal variability of the emissions, and (iii) identify the origin of the CO_2 fluxes measured. We hypothesized that fluxes will be higher during the warm season as a result of higher temperatures. Then, we further suggested that CO_2 fluxes will be lower in the light due to biofilm photosynthetic activity, which may consume CO_2. To reach our goals, we performed a one-year survey, with measurements every month, using incubation chambers connected to a CRDS analyzer. CO_2 and CH_4 fluxes were measured (i) at light with a transparent chamber, (ii), in the dark, with an

opaque chamber, and (iii) in the dark after having removed the upper 1-2 mm of soil that may contain the biofilm. The CO_2-emitted isotopic value ($\delta^{13}C$-CO_2) was measured for each incubation, and the gases concentrations as well as the physicochemical parameters within the soil were also measured.

III.1.2. Materials and Methods

III.1.2.1. Site description

The study was conducted in New Caledonia, a French overseas archipelago located in the South Pacific, in the Melanesia sub region (21°21'S, 165°27'E). The archipelago sheltered 35,100 ha of mangroves, composed of 24 different species (Virly, 2006). Climate in the region is semi-arid, with two contrasting seasons: a warm season from November to April, and a cool season from June to October. During the studied period, from October 2016 to September 2017, temperatures ranged from 20.4 to 26.85°C, and cumulative rainfall was 857 mm (data from meteofrance.com).

Field work were performed in the mangrove of Ouemo, located in the South Province of New Caledonia (22°16'50"S, 166°28'16"E). The studied mangrove was dominated by three *Rhizophora* mangrove species: *R. stylosa*, *R. samoensis* and *R. selala*. The tidal regime in the region is semi-diurnal, with a tidal range ranging from 1.10 to 1.70 m. All measurements were realized between 2 hours prior and after low tide.

III.1.2.2. Soil CO_2 and CH_4 emissions, and $\delta^{13}C$-CO_2

Soil CO_2, $\delta^{13}C$-CO_2 and CH_4 emissions were measured using closed incubation chambers connected to a G2131-*i* CRDS analyzer (Picarro Inc., Santa Clara, CA, USA). Firstly, triplicate incubations (6 min each) were realized at light, using a transparent acrylic chamber (459.9 cm^2; 5,122 cm^3). Then, after 15 min of soil shading, measurements were performed in the dark, using an opaque acrylic chamber (317.8 cm^2; 4,843 cm^3). Finally, the top 1-2 mm of soil that may contain the biofilm was carefully removed and stored for chlorophyll-*a* analyses, and three supplementary dark incubations were performed (Leopold *et al.*, 2015; Bulmer *et al.*, 2015). The entire procedure was repeated three times during each campaign of measurement. Accuracy of the CRDS analyzer was periodically checked using certified N_2 (0 ppm CO_2 and CH_4), CO_2 (503 ppm) and CH_4 (100 ppm) gas standard samples (Calgaz, Air Liquide, USA).

To characterize the isotopic value of the CO_2 sources, additional incubations on intact roots and leaf litter were also realized, thanks to cylindrical specific opaque incubation chambers made with PVC pipe (203,97 cm^3). Measurements of roots and leaf litter isotopic values were realized in triplicate.

III.1.2.3. Flux calculations

CO_2 and CH_4 fluxes were calculated from the linear regression of the concentrations within the chamber over time, using the following equation:

$$F_{(CO2, CH4)} = (d(CO_2, CH_4) / dt) * V / (R * S * T) * 86.4$$

where F is the fluxes of CO_2 or CH_4 ($\mu molC \cdot m^{-2} \cdot d^{-1}$); $d(CO_2, CH_4) / dt$ is the variation in CO_2 or CH_4 as a function of time (ppm s^{-1}); V is the total volume of the system (m^3); R is the ideal gas constant of 8.205746 10^{-5} ($atm \cdot m^3 \cdot K^{-1} \cdot mol^{-1}$); T is the absolute air temperature (K); and S is the area of the bottom of the incubation chamber (m^2).

III.1.2.4. Isotopic CO_2 characterization

A Keeling plot approach was used to measure the isotopic value of the CO_2 ($\delta^{13}C$-CO_2) released from the soil, roots respiration and leaf litter decomposition (Keeling, 1958, 1961; Pataki *et al.*, 2003).

III.1.2.5. Soil CO_2 and CH_4 concentrations

Three 60 cm deep cores were collected during each campaign of fluxes measurements using a Eijkelkamp gouge auger (1 m long, 8 cm diameter). Cores were separated in 6 subsections of 10 cm length, and pore-water was extracted from each section using Rhizon micro sampler (10 cm long, 2.5 mm diameter, Rhizosphere Research products, Wageningen, Netherlands). Pore-water samples were then gently transferred to 7.5 ml vials until overflow, and capped with 10 mm butyl rubber stoppers (Apodan Nordic, Denmark) with an aluminum crimp seal (Bastviken *et al.*, 2010).

Back to the laboratory, 5 ml of pore-water samples were withdrawn from the vials thanks to a glass syringe. Then, an air space was created in the syringe by adding 5 ml of pure nitrogen (Calgaz, Air Liquide, USA). The syringe was then vigorously agitated to equilibrate the gases between the two phases, and, after one minute, 1 ml of the air space sample was injected into a G2131-*i* CRDS analyzer operating in continuous flow mode with pure nitrogen (Calgaz,

Air Liquide, USA) as carrier gas. Peak areas were then integrated and reported to a standard calibration curve created with pure nitrogen as a zero for both CO_2 and CH_4, and gas standard of 503 ppm for CO_2, and 100 ppm for CH_4 (Calgaz, Air Liquide, USA). All pore-water analyses were realized within 4 hours after sampling. All calculations were realized following Bastviken *et al.* (2010, 2008, 2004).

III.1.2.6. Physicochemical characteristics of the sedimentary column

Additional triplicate cores were collected two times during the year for physicochemical analyses. Cores collection were done in January and in June 2017, representing respectively the warm and the cool season. Cores were then separated in six subsections of 10 cm. Redox potentials were measured using a combined Pt-Ag/Ag-Cl (reference) electrode connected to a WTW pH/mV/T meter. Redox data are reported relative to a standard hydrogen electrode, *i.e.*, after adding 202 mV to the original values obtained with an Ag/AgCl reference electrode at 25°C (Marchand *et al.*, 2011). pH was measured using a glass electrode and a WTW pH meter. The pH electrode was calibrated prior utilization using three standards solutions of pH 4, 7 and 9 at 25°C (National Institute of Standards and Technology, USA). Pore-water salinity was measured using an Atago hand refractometer.

Total organic carbon (TOC) content and $\delta^{13}C$ were determined for each sampling period. TOC was analysed using a Total Organic Carbon Analyzer equipped with a SSM-5000A Solid Sample Module (TOC-LCPH-SSM500A, Shimadzu Corporation, Japan). $\delta^{13}C$ was measured using an elemental analyzer coupled to an isotope ratio mass spectrometer (Integra2, Sercon, UK). $\delta^{13}C$ values are reported in per mill (‰) deviations from a Pee Dee Belemnite (PDB) limestone carbonate for reference. Analytical precisions were check using IAEA-600 caffeine standard (IAEA Nucleus) and were less than 1% for TOC, and 0.3% for $\delta^{13}C$. All analyses were performed at the French Institute for the Sustainable Development (IRD) of Noumea, New Caledonia. Additional samples of roots, leaves, and surface sediment, the latest used as a proxy for biofilm isotopic value, were also analysed for $\delta^{13}C$.

III.1.2.7. Air temperature and chlorophyll-*a*

Air temperature was recorded before each measurement thanks to a handheld thermometer. The relationships between CO_2 and CH_4 fluxes and temperature were estimated on an exponential basis (Lloyd and Taylor, 1994), and then, Q_{10} ratios, which represent the

factor to be multiplied to the fluxes for a 10°C rise, were calculated using the equation described by Xu and Qi (2001) and Chanda *et al.* (2013).

Soil surface chlorophyll-*a* (chl-*a*) was analysed for each point of measurement. Samples for chlorophyll-*a* were firstly freeze-dried, and then a subsample of ~200 mg was weighted for extraction. Chl-*a* was extracted in the dark, at ambient temperature, in 8 ml of 93% methanol during 30 min. Concentrations were then determined using a fluorimeter (Yentsch and Menzel, 1963).

III.1.2.8. Statistical analyzes

Student's T-Tests were used to test the significant differences ($p<0.05$) between seasons and between soil physicochemical parameters. The differences in seasonal, and light/dark CO_2 and CH_4 emissions, as well as the differences in soil $\delta^{13}C$-CO_2 values in light, dark, and dark after biofilm removal were tested using a two-way analysis of variance (ANOVA), followed by a Scheffe post-hoc test. The relationship between dark and light fluxes and the different parameters, were determined by simple linear regression analyzes. All statistical analyzes were performed under R software version 3.3.1 (R Development Core Team, 2008).

III.1.3. Results

III.1.3.1. Soil physicochemical characteristics

No significant variations with seasons of the physicochemical parameters studied were observed (two-sample t-tests, $p>0.05$) (Fig. III-2). TOC decreased from 22.23 ± 2.29 % at the surface to 19.11 ± 0.61 % at 25 cm depth, and then, increased with depth until 21.43 ± 1.29 % at 55 cm depth, with a mean value 20.93 ± 2.14% (Fig. III-2a). Mean value of dry bulk density (DBD) was 0.25 ± 0.06 g cm^{-3} (Fig. III-2b). Redox potentials rapidly decreased from -130.43 ± 47.02 mV at the surface to -191.12 ± 10.99 mV at 15 cm depth, and then remained stable to the bottom of the core (Fig. III-2c). pH and soil water content were almost invariable along the core profile, with mean values of 6.70 ± 0.14 and 70.29 ± 4.64 %, respectively (Fig. III-2d and e). Soil salinity increased from 37.83 ± 2.64 at the surface to 41.33 ± 1.97 at 15 cm depth, and remained stable until 55 cm depth (Fig. III-2f).

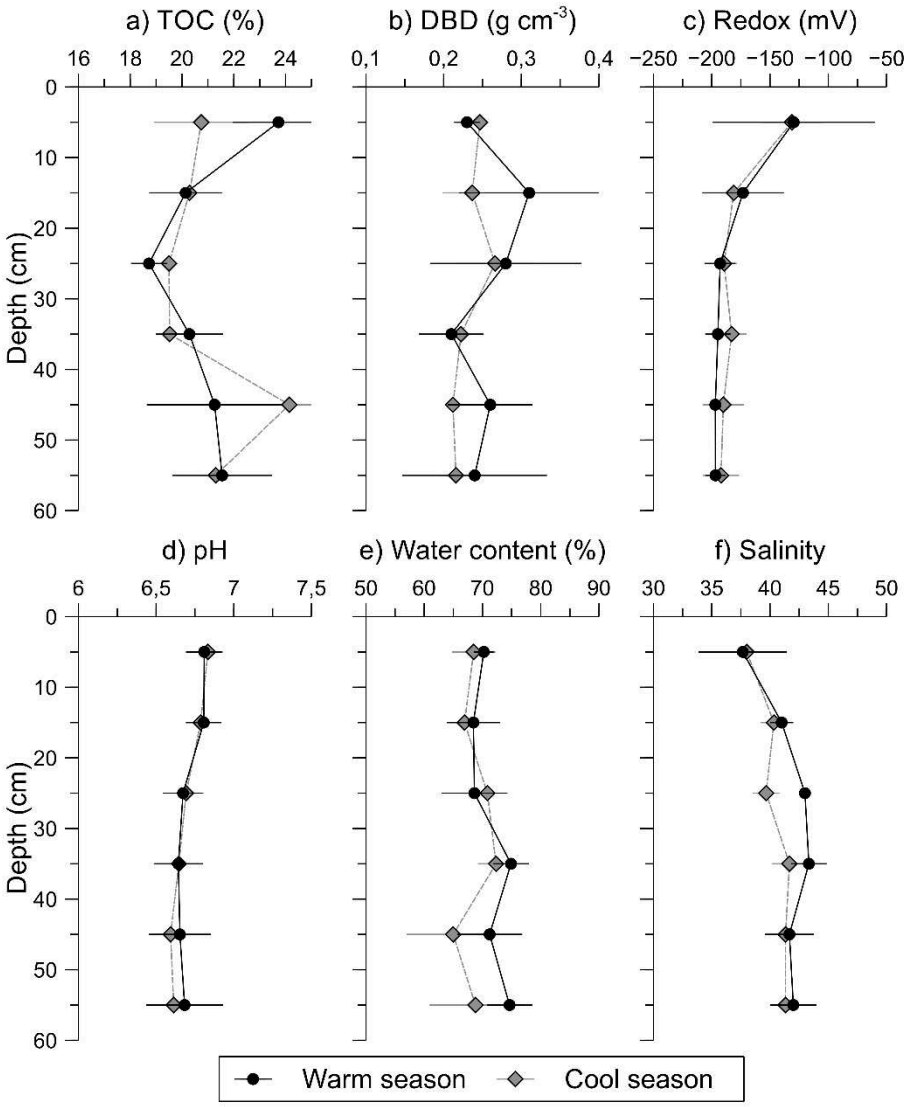

Fig. III-2: Physicochemical profiles measured in January (black lines) and in June (grey dotted lines) 2017. Each point is the mean of three replicates ± SD.

III.1.3.1. CO_2 and CH_4 emissions

Considering the whole studied period, CO_2 and CH_4 emissions from the soil to the atmosphere ranged from 31.34 to 187.48 mmol m^{-2} d^{-1} and from 39.36 to 428.09 µmol m^{-2} d^{-1}, respectively. Seasons had significant effects on both dark and light CO_2 and CH_4 fluxes (Table III-1), which were higher during the warm season (Table III-2). Significant differences were also observed between dark and light CO_2 fluxes (Table III-1), either for the warm and the cool season, with higher emissions in the dark. In addition, CO_2 emissions in the dark, after having removed the upper 1-2 mm of soil, ranged from 145.22 to 282.30 mmol m^{-2} d^{-1}, which was significantly higher than on intact soil surface (ranging from 57.64 to 187.48 mmol m^{-2} d^{-1}; two-

sample t-test, $t_{(-5.31)}$=59.99, p<0.001). Moreover, CO_2 and CH_4 fluxes, measured in the dark, were positively correlated to fluxes measured at light (Fig. III-3a and b; Table III-3 eq. 1 and 2).

Table. III-1: Mean seasonal emissions (n=101 ± SD) of CO_2 (mmol m^{-2} d^{-1}) and CH_4 (µmol m^{-2} d^{-1}), in the light and in the dark. Different letters indicate significant differences (Scheffe post-hoc test, p<0.05).

Parameters	Dark		Light	
Season	Warm	Cool	Warm	Cool
CO_2	126.97 (59.12)^{a}	98.96 (44.22)^{b}	77.16 (33.09)^{bc}	54.79 (28.57)^{c}
CH_4	146.30 (115.80)^{a}	69.79 (37.78)^{b}	97.41 (75.43)^{bc}	54.12 (17.02)^{c}

Table. III-2: F values of two-way ANOVA tests showing the seasonal and dark/light effects on CO_2 and CH_4 emissions.

Parameters	Sources of variation		
	Season	Dark/Light	Interaction
CO_2	13.833***	56.848***	0.187^{NS}
CH_4	26.715***	15.422***	3.423^{NS}

*** indicates significant effects at p<0.001, *NS*: non-significant

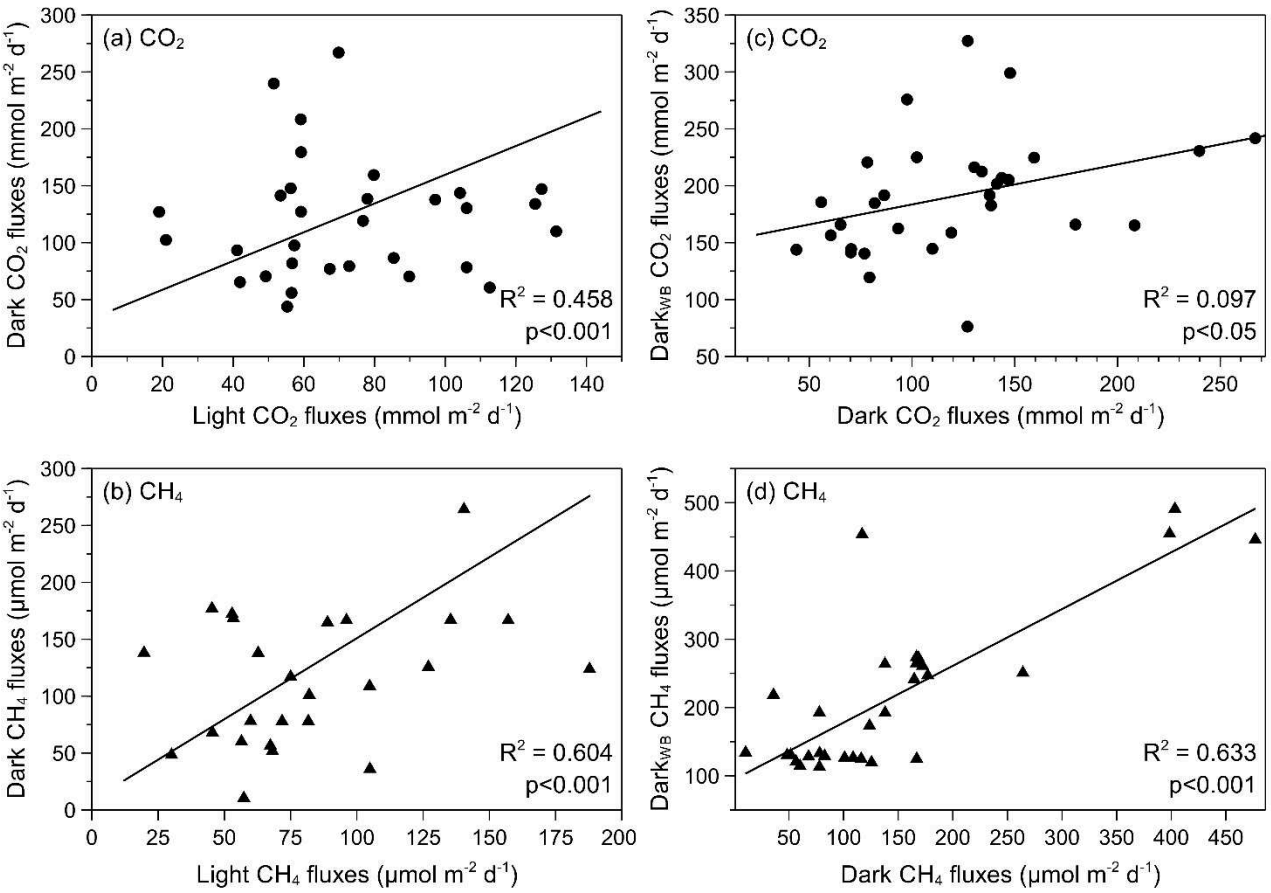

Fig. III-3 : (a) and (b): Relationship between light and dark fluxes of CO_2 (mmol m^{-2} d^{-1}) and CH_4 (µmol m^{-2} d^{-1}); (c) and (d): Relationship between dark fluxes without the upper 1-2 mm of soil ($Dark_{WB}$) and dark fluxes of CO_2 (mmol m^{-2} d^{-1}) and CH_4 (µmol m^{-2} d^{-1}); *n*=35, each point is the mean of three replicates.

III.1.3.2. Relationships between CO_2 and CH_4 fluxes and temperature, soil gas concentrations and chlorophyll-*a*

Dark CO_2 and CH_4 fluxes were correlated to temperature in positive relationships (Fig. III-4a and b; Table III-3 eq. 5 and 6). Dark emissions without the upper 1-2 mm of soil were correlated to the dark emissions before removal (Fig. III-4c and d; Table III-3 eq. 3 and 4). In addition, positive correlations were also determined between dark and light CO_2 (Fig. III-4c; Table III-3 eq. 7 and 8) and CH_4 (Fig. III-4d; Table III-3 eq. 9 and 10) emissions and their respective soil concentrations. The slopes of these two last relationships were higher for dark incubation compared to light ones. Eventually, the difference between dark and light fluxes was related to the soil surface chlorophyll-*a* concentrations (Fig. III-5; Table III-3 eq. 11).

Table. III-3: List of the different equations of regression, the R^2 (coefficient of determination) and the corresponding p-values.

Equations of regression		R^2	*p*-values	Fig.s
Dark CO_2 fluxes = 33.3227 * Light CO_2 fluxes + 1.2632	(1)	0.458	<0.001	Fig. III-3a
Dark CH_4 fluxes = 8.5342 * Light CH_4 fluxes + 1.4237	(2)	0.604	<0.001	Fig. III-3b
$Dark_{WB}$ CO_2 fluxes = 148.3216 * Dark CO_2 fluxes + 0.3521	(3)	0.097	<0.05	Fig. III-3c
$Dark_{WB}$ CH_4 fluxes = 94.6615 * Dark CH_4 fluxes + 0.8317	(4)	0.633	<0.001	Fig. III-3d
Dark CO_2 fluxes = 17.85113 * exp^(0.08698 * Temperature)	(5)	0.366	<0.05	Fig. III-4a
Dark CH_4 fluxes = 0.5 * exp^(0.2029 * Temperature)	(6)	0.244	<0.05	Fig. III-4b
Dark CO_2 fluxes = 158.494 * soil CO_2 concentrations + 9.105	(7)	0.763	<0.01	Fig. III-4c
Light CO_2 fluxes = 58.9 * soil CO_2 concentrations + 24.63	(8)	0.441	<0.05	Fig. III-4c
Dark CH_4 fluxes = 358.27 * soil CH_4 concentrations - 151.29	(9)	0.952	<0.001	Fig. III-4d
Light CH_4 fluxes = 171.38 * soil CH_4 concentrations - 42.95	(10)	0.768	<0.01	Fig. III-4d
Dark-light CO_2 fluxes = 1.258 * soil chl-*a* – 12.828	(11)	0.323	<0.05	Fig. III-5
Dark-Light fluxes = 61.222 * Dark-Light $\delta^{13}C$-CO_2 - 11.819	(12)	0.291	<0.01	Fig. III-6

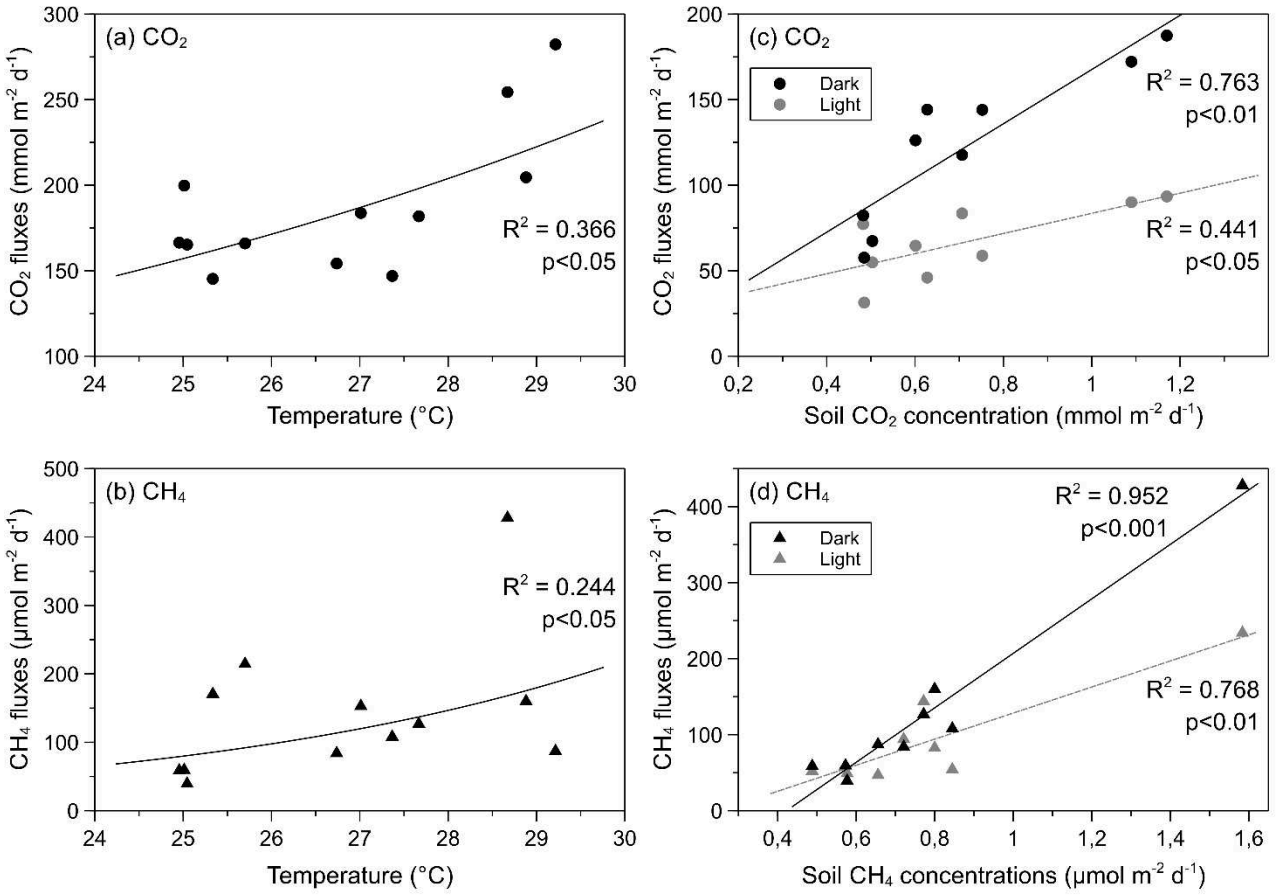

Fig. III-4: (a) and (b): Relationship between CO_2 (mmol m^{-2} d^{-1}) and CH_4 (µmol m^{-2} d^{-1}) fluxes and temperature (°C); *n*=12, each point is the mean of 9 replicates. (c) and (d): Relationship between CO_2 (mmol m^{-2} d^{-1}) and CH_4 (µmol m^{-2} d^{-1}) fluxes and soil CO_2 (mmol m^{-2} d^{-1}) and CH_4 (µmol m^{-2} d^{-1}) concentrations, in the dark (dark points) and at light (grey points); *n*=10; each point is the mean of 3 replicates.

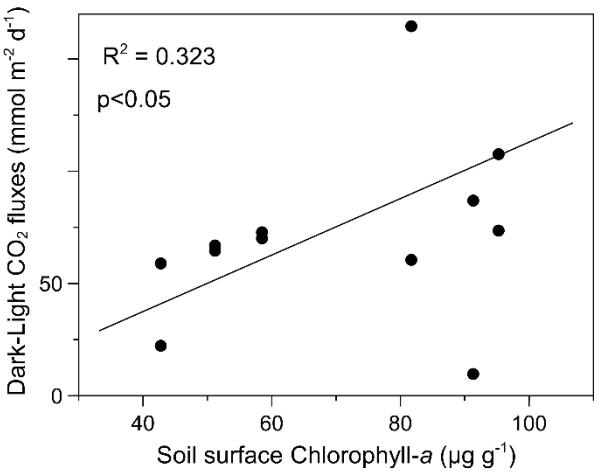

Fig. III-5: Relationship between the difference in Dark and Light CO_2 fluxes (mmol m^{-2} d^{-1}) and chlorophyll-*a* soil surface concentration (µg g^{-1}). *n*=12, each point is the mean of three replicates.

III.1.3.3. $\delta^{13}C$ and $\delta^{13}C$-CO_2

Mean $\delta^{13}C$-CO_2 values of the CO_2-emitted during soil incubations at light, in the dark and in the dark after having removed the upper 1-2 mm of soil were -19.75 ± 2.88 ‰, -20.17 ± 2.38 ‰ and -15.92 ± 2.44 ‰, respectively. Consequently, dark $\delta^{13}C$-CO_2 values were thus the more depleted, however the difference between light and dark fluxes were not significant (p>0.05). In addition, the difference of dark and light $\delta^{13}C$-CO_2 values was correlated to the difference of dark and light CO_2 fluxes in a negative relationship (Fig. III-6; Table III-3 eq. 12). Furthermore, the $\delta^{13}C$-CO_2 value of the CO_2 emitted in the dark after removal of the upper 1-2 mm of soil was significantly higher than at light and in the dark (two-way ANOVA, $F_{(1,278)}$=75.51; p<0.001).

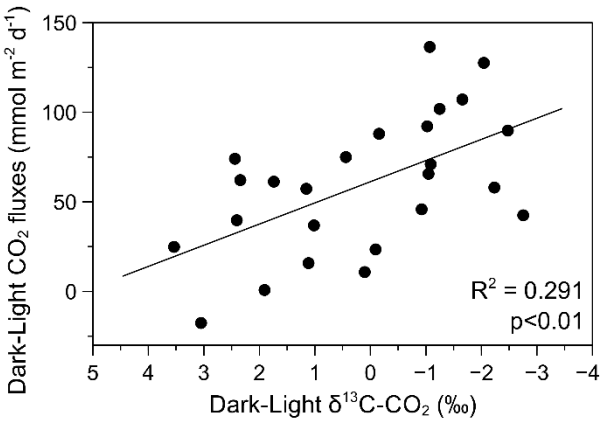

Fig. III-6: Difference in dark and light fluxes (mmol m^{-2} d^{-1}) as a function of the difference between dark and light $\delta^{13}C$-CO_2 (‰). *n*=25, each point representing the mean of three replicates.

The $\delta^{13}C$ values of roots, leaves, soil surface and soil column, as well as the $\delta^{13}C$-CO_2 signatures of the CO_2-emitted by root respiration and leaf litter decomposition are presented in Table III-4.

Table. III-4: $\delta^{13}C$ (‰ (SD)) values for roots, leaves, soil surface (1-2mm depth) and for the soil column (0-50cm cm depth, *n*=6); and $\delta^{13}C$-CO_2 (‰ (SD)) emitted by roots respiration (*n*=3) and leaf litter decomposition (*n*=3).

Parameters	Roots	Leaf litter	Soil surface (1-2mm)	Soil column (0-50 cm)
$\delta^{13}C$ (‰)	-25.88	-23.86	-18.67	-22.33 (1.82)
$\delta^{13}C$-CO_2 (‰)	-22.32 (1.06)	-21.43 (1.89)		Na

III.1.4. Discussion

III.1.4.1. Mangroves as a net source of CO_2 and CH_4 to the atmosphere

Soil CO_2 and CH_4 emissions to the atmosphere in the studied mangrove forest were elevated throughout the year. Mean CO_2 emissions ranged from 31.35 to 282.30 mmol m^{-2} d^{-1}, and therefore confirmed those measured previously in another *Rhizophora* mangrove forest in New Caledonia by Leopold *et al.* (2013 and 2015), for which CO_2 fluxes ranged from 14.5 to 262.8 mmol m^{-2} d^{-1}. Furthermore, in a broader study of eleven mangrove swamps in the Caribbean, in Australia and in New Zealand, Lovelock (2008) evaluated the soil CO_2 fluxes to range from -21.6 to 256.6 mmol m^{-2} d^{-1}. Later, Bulmer *et al.* (2015) measured mean CO_2 emissions of 168.5 ± 45.8 mmol m^{-2} d^{-1} in a mangrove developing at higher latitudes (New

Zealand). Only mangroves subjected to strong eutrophication were reported to have high CO_2 emissions, and for example up to 749.34 mmol m^{-2} d^{-1} in Hong Kong (Chen *et al.*, 2012). Eventually, CO_2 fluxes measured in the present study were higher than the compilation from 140 study sites made by Alongi (2014), who reported mean CO_2 emissions of 69 ± 8 mmol m^{-2} d^{-1}. Regarding CH_4, fluxes measured in the present study ranged from 39.36 to 466.33 µmol m^{-2} d^{-1}. When converted into CO_2-equivalent, considering its 100-year global warming potential (Myhre *et al.*, 2013), CH_4 represented 1% of the total emissions measured (CO_2 + CH_4). CH_4 emissions were in the same range than those measured in previous studies, as for instance in the Sundarbans, where CH_4 fluxes ranged from 1.97 to 567.12 µmol m^{-2} d^{-1} (Biswas *et al.*, 2007; Chanda *et al.*, 2013), or in Australia, where CH_4 fluxes ranged from 30 to 520 µmol m^{-2} d^{-1} (Kreuzwieser *et al.*, 2003). Eventually, CH_4 emissions were also in the same range than those reported by (Chen *et al.*, 2014) in Indonesia (-145.2 to 315.36 µmol m^{-2} d^{-1}).

However, when compared to other ecosystems, CO_2 and CH_4 emissions from the studied mangrove soil were much lower (Oertel *et al.*, 2016). For example, CO_2 emissions in the present study were twice lower than the CO_2 emissions in some tropical rainforests from Malaysia, Hawaii and Brazil, which were evaluated to range from 295.7 to 598.4 mmol m^{-2} d^{-1} (Metcalfe *et al.*, 2007; Katayama *et al.*, 2009; Litton *et al.*, 2011). Similar observations can be made regarding CH_4, which may be emitted in very large quantities from interior tropical wetlands (Sjögersten *et al.*, 2014). Therefore, even if mangroves are among the carbon-richest forests in the world (Donato *et al.*, 2011), they emit low quantities of greenhouse gas. This particularity mainly derives from the waterlogging conditions of their soils, which favor anaerobic organic matter decomposition, which is less efficient than aerobic decay processes. However, even if GHG emissions from mangrove soils are low, they are highly variable, and depend notably on season, or on the development of biofilm at the soil surface, which may sometimes induce negative fluxes (*e.g.* Chen *et al.*, 2014; Bulmer *et al.*, 2015; Wang *et al.*, 2016).

III.1.4.2. Variability of CO_2 and CH_4 emissions

Seasonal differences in CO_2 and CH_4 emissions were evidenced in the present study, with higher values during the warm season (Table III-2). Several environmental factors may influence GHG emissions to the atmosphere, including notably the physicochemical properties of the soil and its water content (Kirui *et al.*, 2009; Poungparn *et al.*, 2009; Livesley and

Andrusiak, 2012; Chanda *et al.*, 2013; Leopold *et al.*, 2013; Leopold *et al.*, 2015; Bulmer *et al.*, 2015). Herein, fluxes measurements were performed between 2h prior and after the low tide, when the soil was the most unsaturated in water. Consequently, we are confident that variations in soil water content due to the tidal cycle was not involved in the variability of the fluxes. In addition, no significant variations between the two seasons were observed for the physicochemical parameters (Fig. III-2), suggesting that these parameters were not involved in the seasonal difference of CO_2 and CH_4 fluxes. This absence of variability in the physicochemical parameters studied may be surprising but is suggested to result from the position of the study site, in the lowest intertidal zone, in which tides are coming twice a day, possibly buffering redox, pH and salinity variations.

Higher CO_2 fluxes to the atmosphere with warmer temperatures was consistent with other studies in terrestrial ecosystems (Raich and Schlesinger, 1992; Lou *et al.*, 2003; Parkin and Kaspar, 2003), including mangroves (Allen *et al.*, 2011; Chen *et al.*, 2012; Leopold *et al.*, 2015). Similarly, several studies showed that temperature is a major factor driving CH_4 emissions to the atmosphere in terrestrial wetlands (Crill *et al.*, 1988; Moore and Knowles, 1990; Bubier *et al.*, 1995; Turetsky *et al.*, 2008; Trudeau *et al.*, 2013) or in tidal wetlands (Sun *et al.*, 2013; Wang *et al.*, 2015). Estimated Q_{10} value for CO_2 emissions in the studied mangrove was 2.39, which was in complete accordance with other values reported for mangrove ecosystems (Lovelock, 2008; Leopold *et al.*, 2015) or even for terrestrial ecosystems (Raich and Schlesinger, 1992). Concerning CH_4, Q_{10} value in this study was 7.61, and thus was higher than for CO_2, suggesting that CH_4 production was more sensible to temperature variations. Q_{10} values of methane production in oligotrophic wetlands environments, such as mangroves, are described as having a wide range of variation, from 1.7 to 28 (Segers, 1998), which is thus consistent with our findings. The temperature sensitivity of biogeochemical processes, such as soil organic matter decomposition by respiration and methanogenesis, have been widely described in the literature for different ecosystems (Segers, 1998; Fang and Moncrieff, 2001; Fierer *et al.*, 2005; Davidson and Janssens, 2006; Conant *et al.*, 2011; Inglett *et al.*, 2012), including mangroves (Mackey and Smail, 1996; Barroso-Matos *et al.*, 2012). Consequently, soil gases production, and thus, their emissions at the soil-air interface, may increase with temperature. In fact, higher average soil CO_2 and CH_4 concentrations were measured in this

study during the warm season in comparison to the cool season, therefore adding to the hypothesis of a temperature control on soil greenhouse gas production.

In addition, strong relationships were found between soil CO_2 and CH_4 concentrations and their respective emissions at the soil-air interface (Fig. III-4c and d), therefore confirming that soil greenhouse gas concentrations are another primary factor in greenhouse gas emissions to the atmosphere. However, our result showed that for the same soil gas concentrations, fluxes were lower when measurements where performed at light (Fig. III-4c and d), suggesting that other constraining factors were involved during light incubations, like, possibly, biofilm, as demonstrated in other studies (*e.g.* Bulmer *et al.*, 2015; Leopold *et al.*, 2013, 2015).

III.1.4.3. Evidences of microphytobenthos control on greenhouse gas emissions

CO_2 emitted at the surface of mangrove soils derives from various sources such as: roots respiration, leaf litter decomposition, organic-matter degradation, as well as biofilm respiration and degradation. The $\delta^{13}C$-CO_2 value of the emitted CO_2 is therefore a mixture of the specific values of the CO_2 produced by these different sources. In the present study, the $\delta^{13}C$-CO_2 value of the CO_2 emitted by roots respiration was -22.32 ± 1.06 ‰, while it was -21.43 ± 1.89 ‰ for leaf litter decomposition (Table III-4). Although the isotopic value of the CO_2 produced by organic matter decomposition within the soil was not measured in this study, some authors reported low fractionation during organic matter decomposition, and, consequently, a low difference between the $\delta^{13}C$ value of the source and the $\delta^{13}C$-CO_2 value of the produced CO_2 (Lin and Ehleringer, 1997; Maher *et al.*, 2015). Therefore, we used the mean $\delta^{13}C$ value of the organic matter in the soil, -22.33 ± 1.82 ‰, as a proxy of the $\delta^{13}C$ value of the CO_2 produced by its decomposition. Consequently, these three sources all had $\delta^{13}C$-CO_2 values lower than -21.43 ‰, whereas the mean $\delta^{13}C$ value of the CO_2 emitted at the soil-air interface was -19.76 ± 1.19 ‰, therefore suggesting that another source must be involved in the emissions. Biofilm is mainly composed by an assemblage of heterotrophic bacteria and autotrophic eukaryotes (Decho, 2000; Bouchez *et al.*, 2013) that are $\delta^{13}C$ enriched comparatively to mangrove organic matter (Coffin *et al.*, 1989; Bouillon *et al.*, 2002; Lamb *et al.*, 2006; Khan *et al.*, 2015). We, thus, suggest that the $\delta^{13}C$ value of the CO_2 fluxes demonstrated that biofilm respiration/photosynthesis and/or its decomposition contributed to GHG emissions along with the roots respiration, and soil organic matter decomposition.

Apart from few measurements, CO_2 emissions at the soil surface were always higher in the dark than at light. This result suggests that, at light, CO_2 diffusing from mangrove soils may be consumed by the primary producers composing the biofilm during photosynthesis processes, as suggested in previous studies (Chen *et al.*, 2014; Bulmer *et al.*, 2015; Wang *et al.*, 2016). This process was also evidenced by a positive relationship between the difference in dark and light CO_2 fluxes and the soil surface chlorophyll-*a* (Fig. III-6). More biofilm implies more consumption of the CO_2 during photosynthesis, and therefore higher difference between dark and light fluxes. In addition, due to carbon fractionation during photosynthesis, which uses ^{12}C preferentially to ^{13}C (O'Leary, 1988; Farquhar *et al.*, 1989), the $\delta^{13}C\text{-}CO_2$ measured during light incubations should have an enriched value, relatively to the one measured during dark incubations. Consequently, as the rate of photosynthesis increases, the difference between dark $\delta^{13}C\text{-}CO_2$ and light $\delta^{13}C\text{-}CO_2$ may decrease. Such a variation was observed in this study (Fig. III-6), therefore confirming that photosynthetic activity was involved in the reduction of the CO_2 emissions at the soil surface.

Higher CH_4 fluxes were also observed during dark incubations relatively to light incubations (Fig. III-3b). However, the absence of correlation between dark and light emissions and the soil surface chlorophyll-*a* indicates that biofilm was not involved in these reductions. We suggest that the lower emissions at light may result from CH_4 photo-oxidation processes, as evidenced in others studies (Johnston and Kinnison, 1998; Dutta *et al.*, 2017). Consequently, strong differences between light and dark CO_2 and CH_4 fluxes were measured. Considering that mangroves are subject to the daily cycle of light, we suggest that these differences should be taken into account in future carbon budgets, since light and dark fluxes each account for only half of the daily emissions.

Previous studies suggested another role of the microphytobenthos in GHG emissions, reducing them by forming a physical barrier at the soil surface (Leopold *et al.*, 2013; Leopold *et al.*, 2015; Bulmer *et al.*, 2015). In our study, removing the upper 1-2 mm of soil also lead to an enhancement of the CO_2 emissions that were multiplied by a factor of 1.75, which is consistent with the 2.2 factor reported by (Leopold *et al.*, 2015) in another *Rhizophora* mangrove forest in New Caledonia. However, after removal, significant enriched values of $\delta^{13}C\text{-}CO_2$ (mean of -16.70 ± 2.70 ‰) were measured compared to the ones obtained before removal (mean of -19.76 ± 1.19 ‰). Such a result was surprising as we expected a greater contribution

of the CO_2 produced within the soil, characterized by $\delta^{13}C$ values lower than -21.59 ‰. Consequently, we suggest that removing the upper 1-2 mm of soil resulted in a partial removal of the biofilm but also and mainly to its deterioration, inducing higher CO_2 emissions and depleted $\delta^{13}C$-CO_2 values. However, the strong positive relationship between dark CH_4 emissions before and after biofilm removal supports the hypothesis that the biofilm acts as a physical barrier preventing GHG emissions (Fig. III-3d). Methanogenesis is a strictly anaerobic process that only occurs in the deep anoxic sediment layers (Dutta *et al.*, 2013; Dutta *et al.*, 2015), and is suggested not to be enhanced by biofilm removal. Similar relationship was also observed for CO_2 (Fig. III-3c), therefore adding to the previous finding, however, the relationship was weaker than for CH_4, suggesting that both biodegradation and absence of physical barriers properties were involved in the higher CO_2 emissions after the removal of the upper 1-2 mm of soil.

III.1.5. Conclusion

CO_2 and CH_4 emissions from a *Rhizophora* mangrove soil were relatively low throughout the year, with CH_4 representing only 1% of the combined CO_2 and CH_4 emissions. Nevertheless, GHG fluxes showed a high seasonal variability, with higher values measured during the warm season. We suggest that these enhanced emissions mainly derived from increased organic matter decomposition rates due to elevated temperature, higher CO_2 and CH_4 concentrations were measured within the soil. In addition, CO_2 and CH_4 emissions were controlled by biofilm development at the soil surface. First, biofilm may act as a physical barrier preventing the gases to reach the atmosphere. In addition, thanks to the measurements of the $\delta^{13}C$-CO_2 values of the CO_2 emitted in the dark and at light, we were able to confirm the reduction of CO_2 emissions by its consumption during photosynthesis processes at sediment surface. However, we were not able to evaluate the respective contribution of each CO_2 source within the soil due to their too close $\delta^{13}C$-CO_2 values. Eventually, we observed *that removing* the upper 1-2 mm of soil resulted only in a partial removal of the biofilm but also and mainly to its deterioration, inducing higher CO_2 emissions and depleted $\delta^{13}C$-CO_2 values.

Although some forcing factors remain unidentified, major advances have been made during the last few years in the evaluation of the greenhouse gas emissions from mangrove soils. However, all the studies focused on fluxes during emersion periods, consequently occulting inundation periods. Due to their position, mangroves are regularly flooded, and up

to half of the time for some regions, which may severely contribute to the emissions of greenhouse gas. Consequently, we suggest that further studies may focus on these potential emissions.

Acknowledgments

This work was funded by the Province Sud of New Caledonia, the City of Mont Dore, KNS Koniambo Nickel SAS, Vale NC, and the GOPS. The authors thank the Air Liquide Foundation for funding the CRDS analyzer. The authors are grateful to Inès Gayral for her support in field work.

Partie 2.

Tidal variability of CO_2 and CH_4 emissions from the water column within a *Rhizophora* mangrove forest (New Caledonia)

Adrien Jacotot, Cyril Marchand, Michel Allenbach

Abstract

We performed a preliminary study to quantify CO_2 and CH_4 emissions from the water column within a *Rhizophora* spp. mangrove forest. Mean CO_2 and CH_4 emissions during the studied period were 3.35 ± 3.62 mmolC m^{-2} h^{-1} and 18.30 ± 27.72 µmolC m^{-2} h^{-1}, respectively. CO_2 and CH_4 emissions were highly variable and mainly driven by tides (flow/ebb, water column thickness, neap/spring). Indeed, an inverse relationship between the magnitude of the emissions and the thickness of the water column above the mangrove soil was observed. $\delta^{13}CO_2$ values ranged from -26.88‰ to -8.6‰, suggesting a mixing between CO_2-enriched pore waters and lagoon incoming waters. In addition, CO_2 and CH_4 emissions were significantly higher during ebb tides, mainly due to the progressive enrichment of the water column by diffusive fluxes as its residence time over the forest floor increased. Eventually, we observed higher CO_2 and CH_4 emissions during spring tides than during neap tides, combined to depleted $\delta^{13}CO_2$ values, suggesting a higher contribution of soil-produced gases to the emissions. These higher emissions may result from higher renewable of the electron acceptor and enhanced exchange surface between the soil and the water column. This study shows that CO_2 and CH_4 emissions from the water column were not negligible and must be considered in future carbon budgets in mangroves.

Keywords: Mangrove ; Carbon Dioxide ; Methane ; Carbon isotope; Tidal cycles ; New Caledonia

III.2.1. Introduction

Mangroves are considered as major ecosystems in the carbon cycle along tropical and subtropical coastlines, being among the most efficient blue carbon sinks (Kauffman *et al.*, 2011). Due to their high primary productivity, estimated at 218 ± 72 TgC yr^{-1} (Bouillon *et al.*, 2008), and their long-term carbon storage capacities (Donato *et al.*, 2011), mangroves have

been recognized as having a key role in climate change mitigation (Howard *et al.*, 2017; Mcleod *et al.*, 2011). However, part of mangroves primary productivity is mineralized in their soils, producing greenhouse gas (GHG) that can be subsequently emitted towards the atmosphere (Chen *et al.*, 2014). Among GHG, methane may be of major concern due to its global warming potential, 34 times higher than CO_2 using a 100 year time frame and climate-carbon feedback (Stocker *et al.*, 2013). In anoxic mangrove soils, when electron acceptors such free oxygen, metal oxides, nitrates, and sulfates have been exhausted, methanogenesis can occur. Recently, it was demonstrated that sulfate reducing and methanogens microorganisms can coexist in mangrove soils and it was thus suggested that methane emissions have been underestimated (Chauhan *et al.*, 2015; Lyimo *et al.*, 2009).

In mangrove soils, organic matter (OM) decay processes depend on numerous factors, including waterlogging (Kristensen *et al.*, 2008a). In fact, mangroves are subjected to tidal cycles that influence the redox characteristics of their soils, modifying the rate of GHG production. In addition, tides can also influence GHG emissions towards the atmosphere since gas diffusion differs when the soil is immerged or unsaturated. Recently, many studies focused on CO_2 or CH_4 emissions at the soil-air interface at low tide (Bulmer *et al.*, 2015; Chanda *et al.*, 2014; Chauhan *et al.*, 2015; Chen *et al.*, 2016, 2010, Leopold *et al.*, 2013, 2015; Livesley and Andrusiak, 2012; Wang *et al.*, 2016), or at the water-air interface in adjacent tidal creeks (Borges *et al.*, 2003; Bouillon *et al.*, 2003b; Call *et al.*, 2015; Maher *et al.*, 2015). However, to our knowledge, no study focused on water to atmosphere GHG emissions when the forest is inundated, which may frequently occur, depending on the tidal range and the position of the forest in the intertidal zone.

Stable isotope of carbon ($\delta^{13}C$) is a widely used tool for studying carbon dynamic in natural environments (Gonneea *et al.*, 2004; Graham *et al.*, 2001; Lu *et al.*, 2016; Yamamuro, 2000), including the partitioning of the different sources (Midwood and Millard, 2011; Millard *et al.*, 2010; Paterson *et al.*, 2009). In mangrove ecosystems, mangrove litter, benthic microalgae, phytoplankton and seagrass detritus are the main OM sources (Kristensen *et al.* 2008), and the latter may be distinguishable thanks to their specific $\delta^{13}C$ values. Marine OM has typical value of $\delta^{13}C$ ranging from -30 to -16‰, whereas mangroves plants are C3 photosynthetic pathways, and therefore produce OM that have a $\delta^{13}C$ value ranging from -32 to -21‰ (Lamb *et al.*, 2006). In addition, due to a low carbon fractionation during respiration

processes (Lin and Ehleringer, 1997; Maher *et al.*, 2015), the $\delta^{13}C$ of the CO_2 is close to the $\delta^{13}C$ value of its source. Recent development of advanced technologies such as cavity ring-down spectroscopy (CRDS) allows high resolution *in situ* measurements of $\delta^{13}CO_2$. Therefore, these new analytical means could help to identify the origins of the CO_2 emitted from mangrove ecosystems.

Within this context, the present study aimed to (i) quantify the CO_2 and CH_4 emissions at the water-air interface within a *Rhizophora* spp. mangrove forest, and (ii) evaluate the variability of these emissions along tidal cycles, and (iii) identify the origin of the CO_2 fluxes measured. To reach our goals, we measured CO_2 and CH_4 fluxes, as well as $\delta^{13}CO_2$ values, in the field, using a dark floating chamber connected to a cavity ring-down spectrometer analyzer (CRDS), along different tidal cycles from neap to spring tides.

III.2.2. Material and methods

III.2.2.1. Study site

The present study was conducted in the mangrove of Ouemo (22°16'50"S, 166°28'16"E), in New Caledonia, a French overseas archipelago located in the South Pacific (21°21'S, 165°27'E). The studied mangrove was dominated by three *Rhizophora* mangrove species: *R. stylosa*, *R. samoensis* and *R. selala*. Climate in the region is semi-arid and strongly influenced by the inter-tropical convergence zone and by the El Niño Southern Oscillation (ENSO). Average air temperature varied between 20.5 to 26.6 °C, with a mean annual precipitation of 1,070 mm (data from meteofrance.com). The tidal regime is semi-diurnal, with a tidal range ranging from 1.10 to 1.70 m.

III.2.2.2. Gas fluxes measurements

CO_2, $\delta^{13}CO_2$ and CH_4 measurements were performed using a dark custom-built floating chamber (466 cm^2; 5,050 cm^3) connected to a G2131-*i* CRDS analyzer (Picarro Inc., Santa Clara, CA, USA) that measures gas concentrations at a frequency of 1 Hz. Guaranteed precision of the analyzer are 200 ppb + 0.05% of reading, 50 ppb +0.05% of reading and 0.1 ‰, for CO_2 and CH_4, and $\delta^{13}CO_2$, respectively. Accuracy of the CRDS analyzer was periodically checked using certified N_2 (0 ppm CO_2 and CH_4), CO_2 (503 ppm) and CH_4 (100 ppm) gas standard samples (Calgaz, Air Liquide, USA).

We are aware that floating chambers may induce a bias in flux measurements during windy conditions or with high current velocity that induce artificial turbulences and, as a result, increase fluxes (Kremer *et al.*, 2003; Yang *et al.*, 2014). However, in low turbulence environment, like inside the mangrove forest where the wind is almost null, and the water flow is slow, the floating chamber technique can be a powerful method (Lorke *et al.*, 2015; Vachon *et al.*, 2010). Thus, we feel confident about the validity of our measurements. In addition, floating chambers have the capability to capture ebullition events that may account for a large proportion of the gas transferred to the atmosphere, particularly CH_4 (Chuang *et al.*, 2017).

Measurements were performed every three weeks, from December 2016 to September 2017, at a single sampling station. Measurements were done during sunny days, with the slack high tide around noon, and included different tidal regimes. During neap tides, the tidal range varied from 1.10 to 1.25 m, which corresponded to a water column thickness above the mangrove sediment of 15 to 30 cm at the maximum of the high tide. During spring tides, the tidal range varied from 1.25 to 1.55 m, and, therefore, the water column thickness at the maximum of the high tide ranged from 30 cm to 60 cm. Measurements were performed all along the high tide, from the beginning of the flow to the end of the ebb. For each incubation, an integrating period of 3 to 6 minutes was chosen, depending on the linearity of the signal. Therefore, 19 to 40 measurements were performed during each campaign, resulting in a total of 284 flux measurements.

In addition, before each incubation, water level was measured thanks to a water gauge, and air temperature was recorded thanks to a handheld Skymate SM-19 thermometer.

III.2.2.3. Flux calculation

Water to atmosphere fluxes of CO_2 and CH_4 were integrated as a function of time, and calculated using the following formula:

$$F_{(CO2,\ CH4)} = (d(CO_2, CH_4) / dt) * V / (R * S * T) * 3.6$$

where F is the water to atmosphere fluxes of CO_2 or CH_4 ($mmolC \cdot m^{-2} \cdot h^{-1}$); $d(CO_2, CH_4) / dt$ is the variation in CO_2 or CH_4 as a function of time ($ppm\ s^{-1}$); V is the total volume of the system (m^3); R is the ideal gas constant of $8.205746\ 10^{-5}$ ($atm \cdot m^3 \cdot K^{-1} \cdot mol^{-1}$); T is the absolute air temperature (K); and S is the area of the bottom of the incubation chamber (m^2).

III.2.2.4. $\delta^{13}C$-CO_2

To measure the isotopic value of the CO_2 ($\delta^{13}CO_2$) released from the water column, we used a Keeling plot approach (Keeling, 1958, 1961; Pataki *et al.*, 2003). By plotting the $\delta^{13}CO_2$ value CO_2 as a function of the inverse of the CO_2 concentration ($\delta^{13}CO_2$=*f*(1/CO_2)) during each incubation, the intercept of a linear regression with the y-axis is equivalent to the $\delta^{13}CO_2$ value of the flux.

In addition, three supplementary incubations were realized at high tide outside the mangrove forest to evaluate the $\delta^{13}CO_2$ value of the CO_2 produced within the water column in the lagoon.

III.2.3. Results and Discussion

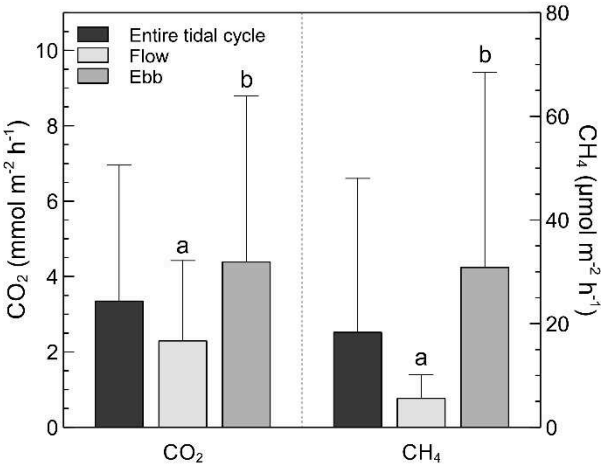

Fig. III-7: Mean CO_2 (mmolC m^{-2} h^{-1}) and CH_4 (µmolC m^{-2} h^{-1}) (+SD) emissions during the complete tidal cycles (*n*=284), the flow tides (*n*=141) and the ebb tides (*n*=143) in the mangrove of Ouemo for the period December 2016 to September 2017. Different letters indicate significant differences (two-samples t-test, CO_2: $t_{(205.66)}$=5.11, p<.001, CH_4: $t_{(146.3)}$=7.96, p<.001).

CO_2 and CH_4 emissions from the water column to the atmosphere varied from 0.13 to 18.41 mmolC m^{-2} h^{-1} and from 0.18 to 172.07 µmolC m^{-2} h^{-1}, respectively (Fig. III-7). Thus, when converted into CO_2-equivalent and considering its 100-year global warming potential (Stocker *et al.*, 2013), methane represented 18% of the total emissions measured (CO_2 + CH_4). Gas transfer to the atmosphere may occur by upward molecular diffusion (Kristensen *et al.*, 2008b) but also through gas bubble ebullition, mainly for methane due to its lower solubility (Barnes *et al.*, 2006; Komiya *et al.*, 2015; Stamp *et al.*, 2013). However, in the present study, considering

the linear evolution of CO_2 and CH_4 concentrations with time during each flux measurement, we suggest that only the diffusive fluxes were measured. As a consequence, the emissions reported herein may have been under-estimated, particularly methane.

To our knowledge, this study was the first one interested in measuring GHG emissions at the water-air interface within a mangrove forest. Therefore, we decided to compare our results with fluxes from other interfaces (*i.e.* from mangrove soils and creek waters to the atmosphere). CO_2 emissions were in the same order of magnitude and even higher than from mangrove soils at low tide or from mangrove tidal creeks (Table III-5). It was demonstrated that soil surface biofilm may limit GHG emissions from mangrove soils, notably by acting as a physical barrier but also by using the CO_2 for primary production through photosynthesis (Bulmer *et al.*, 2015; Leopold *et al.*, 2015, 2013). As a result, some authors reported negative fluxes at the soil surface (*e.g.* Chen *et al.*, 2014; Leopold *et al.*, 2015), which was never the case from the water column in the studied *Rhizophora* forest. Closed canopy and elevated water turbidity probably limited the development of microalgae that might have used the CO_2 produced in the soil. In addition, low tide fluxes measurements are strictly representative of the surface that is covered by the incubation chamber, and, usually, roots and crab burrows are excluded to avoid overestimations of the fluxes. At the opposite, water-air fluxes integrate the entire soil surface that is flooded by the water, and, therefore, roots and burrows are an important factor to take into account as they represent preferential diffusion pathways for the gases to escape from the sediment. The density of *Rhizophora* roots and crab burrows could not be measured in our study site, however, the density of crab burrows was reported for other mangrove in New Caledonia and was evaluated to 83 burrows m^{-2} for the fiddler crab *Uca* spp. (Nielsen *et al.*, 2003), and from 8.9 to 29.1 crabs ha^{-1} for the mud crab *Scylla serrata* (Dumas *et al.*, 2012).

However, regarding CH_4, some studies reported much higher values from mangrove soils but lower from tidal creeks (Table III-5). When CH_4 diffuses from anoxic mangrove soils into oxic lagoon water, it may be subject to aerobic oxidation by methane-oxidizing bacteria or to photo-oxidation (Morana *et al.*, 2015; Smith *et al.*, 2003), therefore limiting emissions at the water-air interface both in mangrove forests and in tidal creeks. We thus suggest that further measurements of GHG emissions must be performed in mangroves at high tide with different

physiographic conditions. We also suggest including these results in future mangrove carbon budgets to make them more accurate, this ecosystem being flooded part of the time.

Table. III-5: Various dark CO_2 CO_2 (mmolC m^{-2} h^{-1}) and CH_4 (µmolC m^{-2} h^{-1}) emissions from mangrove forests during emersion periods, and from mangrove creeks and estuaries.

Location	Climate	CO_2 (mmolC m^{-2} h^{-1})	CH_4 (µmolC m^{-2} h^{-1})	Reference
Mangrove waters				
New Caledonia	Semi-arid	0.13 to 18.41	0.18 to 172.07	This study
Mangrove soils				
New Zealand	Temperate	7.02 ± 1.91	-	Bulmer *et al.* (2015)
New Caledonia	Semi-arid	-0.71 to 2.41	-	Leopold *et al.* (2015)
China	Subtropical	6.92 to 20.56	34.24 to 5,168.60	Chen *et al.* (2010)
China	Subtropical	-0.19 to 4.62	21.56 to 1,919.68	Wang *et al.* (2016)
Indonesia	Tropical	-1.34 to 3.88	-6.05 to 13.14	Chen *et al.* (2014)
Tanzania	Tropical	1.50 to 3.67	0 to 3.65	Kristensen *et al.* (2008b)
Mangrove creeks and estuaries				
Brazil	Semi-arid	0.62 ± 0.30	0.0000093	Nóbrega *et al.* (2016)
Australia	Subtropical	0.38 to 26.21	0.54 to 26.38	Call *et al.* (2015)
Florida	Subtropical	-	-2.60 to 9.61	Cabezas *et al.* (2017)
Australia	Subtropical	0.79 to 2.92	0.29 to 2.13	Maher *et al.* (2015)
India	Tropical	-	0.08 to 5.61	Biswas *et al.* (2007)
India	Tropical	-	0.37	Dutta *et al.* (2015)

Our results demonstrate that CO_2 and CH_4 fluxes were highly variable with tides. As the thickness of the water column above the mangrove soil increased, CO_2 and CH_4 emissions decreased (Fig. III-8a, b, c and d). The $\delta^{13}CO_2$ value of the CO_2 fluxes measured at the lowest tidal level was -26.88‰ (Fig. III-8e), which was closed to the $\delta^{13}C$ values of *Rhizophora* roots, ranging from -32 to -25‰ (Weiss *et al.*, 2016), and organic matter, ranging from -30 to -20‰ (Bouillon *et al.*, 2003a; Saintilan *et al.*, 2013; Weiss *et al.*, 2016). Oppositely, the $\delta^{13}CO_2$ value measured at the highest tidal level that was -8.6‰ (Fig. III-8e and f), which was similar to the values of $\delta^{13}CO_2$ measured in the lagoon outside the mangrove. Consequently, we suggest that (i) the variability of the CO_2 fluxes measured resulted from a mixing between these two sources, *i.e.* the CO_2-produced within the soil and the one produced within the water column, and that (ii) emissions decreases with the increasing water column thickness resulted from the dilution of pore waters, enriched in CO_2, by lagoon waters. We also suggest that few biogeochemical processes affected CO_2 dynamic within the water column due to (i) its low thickness that implied a low residence time of the gas, and (ii) limited photosynthetic processes resulting from dense canopy and water turbidity, as explained earlier. Regarding CH_4, water

mixing and aerobic oxidation, within the water column, as it was observed in other studies (Abril *et al.*, 2007; Bouillon *et al.*, 2007; Dutta and Mukhopadhyay, 2016) may partly explain the results obtained. However, measurements of both $\delta^{13}CH_4$ and dissolved oxygen are needed to comfort these hypotheses.

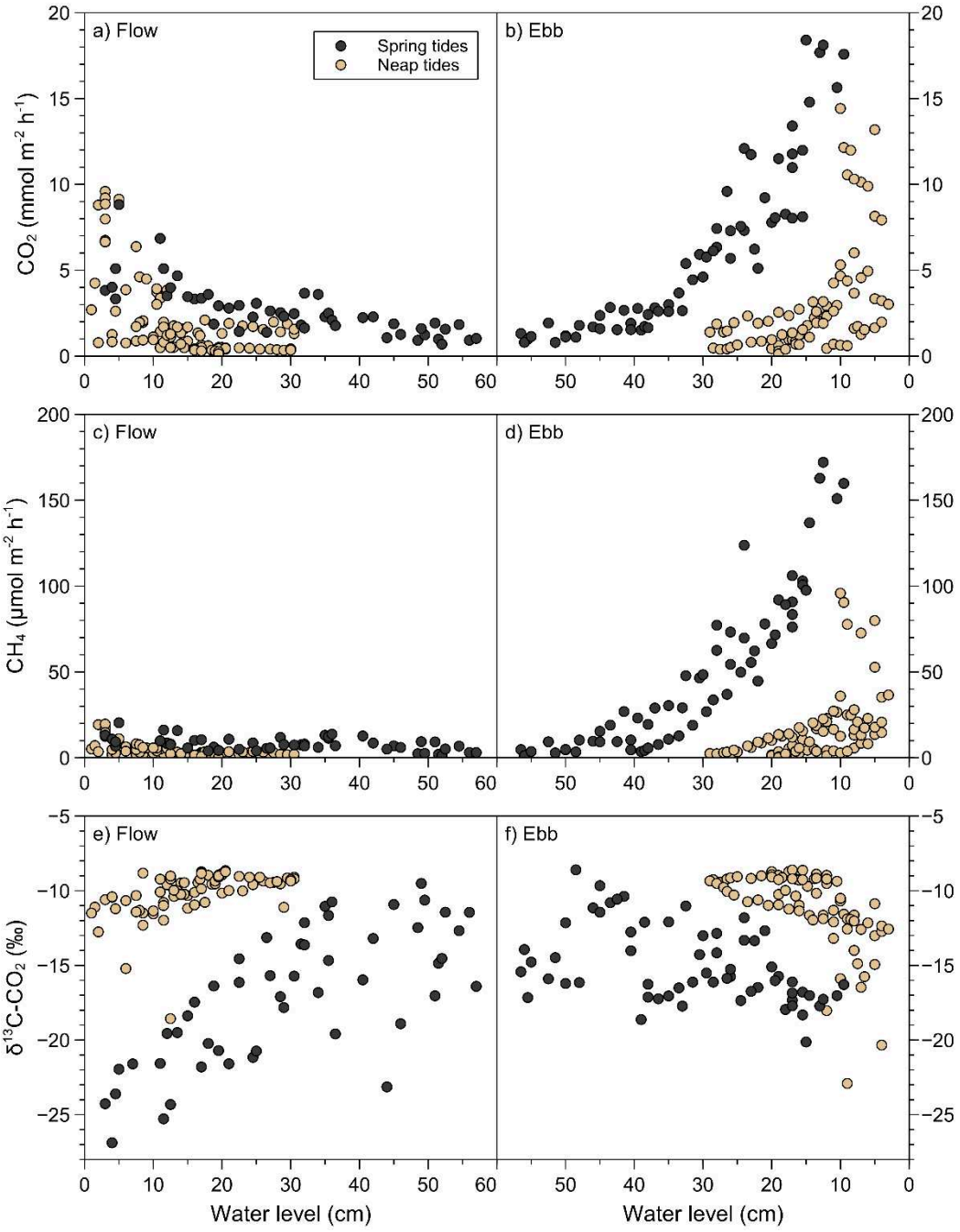

Fig. III-8: Emissions of CO_2 and CH_4 fluxes, and $\delta^{13}C$-CO_2 values (‰) as a function of the water level above the sediment: (a, c and e) during flow tides, and (e, d and f) during the ebb tides.

In addition, significant higher emissions were measured during the ebb than during the flow (two-samples t-test, CO_2: $t_{(205.66)}$=5.11, p<.001, CH_4: $t_{(146.3)}$=7.96, p<.001), but also during spring tides than during neap tides (CO_2, $t_{(180.56)}$=-4.60, p<.001, and CH_4, $t_{(134.1)}$=-5.32, p<.001) (Fig. III-8a, b, c and d). We suggest that these differences may result from a combination of different factors including: residence times of the water in the soil, volume of lagoon water entering the mangrove, area of submerged mangrove, and electron acceptor renewal.

During neap tides, CO_2 emissions reached up to 9.59 mmolC m^{-2} h^{-1} at the beginning of the rising tide, and up to 14.42 mmolC m^{-2} h^{-1} at the end of the ebb tide (Fig. III-8a and b). Meanwhile, as water thickness decreased during ebb, the $\delta^{13}CO_2$ values showed clearly an increased contribution of the CO_2 originated from mangrove soils, with more depleted values at the end of the ebb tides (Fig. III-8e and f). Several forcing factors may enhance the exchanges of gaseous compounds between the soil and the overlying water, including: (i) flushing of the upper centimeters of soil driven by bottom currents inducing pressure gradients at the soil surface, concept of "skin circulation" introduced by Billerbeck *et al.* (2006); (ii) macrofaunal burrowing activities during inundation, causing an increase in soil permeability (Santos *et al.*, 2012); (iii) flushing of crab burrows, the later significantly enhancing the effective surface area of mangrove soils (up to 7-fold), therefore increasing the diffusive fluxes towards the water column (Stieglitz *et al.*, 2000, 2013; Heron and Ridd, 2008). We suggest that the increased residence time of the water during inundation resulted in enhanced exchanges across the soil-water interface due to the different processes listed above, inducing its enrichment in gaseous compounds, and explaining thus the higher emissions measured during the ebb than during the flow. Additional processes may be involved for CH_4 since the difference between the beginning of the flow and the end of the ebb was much higher than for CO_2 (Fig. III-8); CH_4 concentrations was less than 21 µmolC m^{-2} h^{-1} during the flow and reached more than 170 µmolC m^{-2} h^{-1} during the ebb when the water levels were minimum (Fig. III-8c and d). During low tide, atmospheric air can penetrate deeper in the soil, limiting its anoxic character and thus CH_4 production (Kristensen *et al.*, 2008a). However, although its production can occur deeper in the soil, CH_4 may be oxidized during its transit to the atmosphere within the soil, resulting in the low emissions measured at the beginning of the flow. Conversely,

at the end of the ebb, most of electron acceptors may have been exhausted due to the installation of an anoxic environment during the high tide, and thus, methanogenesis may occur, resulting in higher CH_4 emissions.

During spring tides, emissions intensity differed from neap tides. If fluxes were not significantly higher during the flow, they were during the ebb, with CO_2 and CH_4 emissions reaching up to 18.41 mmolC m^{-2} h^{-1} and 172.07 µmolC m^{-2} h^{-1}, respectively (Fig. III-7 and Fig. III-8a, b, c and d). One possible explanation is a higher renewable of the electron acceptors pool within the soil during spring tide, which enhanced the microbial activity and consequently greenhouse gas production. Then, at low tide, the water level within the soil may be lower during spring tide, resulting in higher contribution of the soil deep layers to CH_4 emissions, as gas diffusion is higher in air than in water. Additionally, higher water level during spring tides may have flooded the upper intertidal zones within the mangrove forest, increasing therefore the exchanges between the surface pore waters and the overlying water column. The flushing of surface pore waters and burrows of this upper intertidal zone, due to changes in hydrostatic pressure along the topographic gradient during ebb, may be involved in the enhancement of the emissions, analogically to the concept of "mangrove tidal pumping", which has been described to significantly enrich tidal creeks in nutrients, gaseous and dissolved compounds (Call *et al.*, 2015; Dittmar and Lara, 2001; Maher *et al.*, 2013, 2015). In addition, the more depleted $\delta^{13}CO_2$ values during ebb of spring tides, in comparison to ebb of neap tides (Fig. III-8f), and except at the lowest water column thickness, support the hypothesis of a higher contribution of CO_2 produced within mangrove soils to the water column. Surprisingly, the lowest $\delta^{13}CO_2$ values were measured at the beginning of the flow (Fig. III-8e), which were close to the $\delta^{13}C$ values of mangrove soil organic matter or mangrove roots as explain earlier in this study, suggesting than mangrove pore waters strongly dominated the water column composition at this period of the tide, which is clearly different from neap tides (Fig. III-8e). This result may be related to the tidal wave spread when entering the mangrove, inducing higher pore water advection during the spring tides notably through crab burrows. However, although higher mean CO_2 and CH_4 emissions were observed for the flow during spring tides, the maximal value reached by the emissions was not higher than during neap tides (Fig. III-8a). One possible explanation is that CO_2 and CH_4 did not accumulate within the soil at low tide due to the more efficient diffusion of GHG in air than in water, and thus were rapidly emitted to

the atmosphere. When the tide increased, the deep soil pore waters, depleted in $\delta^{13}CO_2$, were transported to the surface, resulting in low $\delta^{13}CO_2$ values emitted at the water surface. This study thus highlighted that tides (flow/ebb, water column thickness, neap/spring) is a key factor controlling CO_2 and CH_4 emissions from the water column during mangrove forests immersion periods. In a future research effort, the influence of other environmental parameters such as seasonal temperature variations should be studied. Although the sampling period in this study encompassed the two main seasons in New Caledonia, they were not entirely covered, and considering the high tidal variability, our data set did not allow us to conclude on a possible seasonal effect.

III.2.4. Conclusion

This preliminary study demonstrates that tide characteristics (flow/ebb, water column thickness, neap/spring) drove CO_2 and CH_4 emissions at the water-air interface within the studied *Rhizophora* spp. mangrove forest. Simultaneous measurements of CO_2, CH_4 and $\delta^{13}CO_2$ values highlighted that:

- the water column above the forest floor was a mix between soil pore waters, enriched in gaseous compounds originated from OM decomposition and root respiration, and incoming lagoon water, poor in CO_2 and CH_4 and characterized by enriched $\delta^{13}C$ values, resulting in lower fluxes when the water column thickness increased,

- the progressive enrichment of the water column in CO_2 and CH_4 by diffusive fluxes, as its residence time over the forest floor increased, induced higher fluxes during the ebb tide than during the flow,

- CO_2 and CH_4 emissions were higher during spring tides than during neap tides possibly due to (i) higher renewable of the electron acceptor pool within the soil that enhanced microorganism's activity, and (ii) flooding of the upper intertidal zones that induced a higher exchange surface between the soil and the water column.

These results also showed that CO_2 and CH_4 emissions were not negligible and therefore, we suggest that these fluxes should be integrated in future carbon budget to make them more accurate. Further studies should now examine the variability of these emissions across mangroves that differ by their physiographic conditions to assess their spatial variability.

Acknowledgments

This work was supported by the Province Sud of New Caledonia, the City of Mont Dore, KNS Koniambo Nickel SAS, Vale NC, and the GOPS. We thank the Air Liquide Foundation for funding the CRDS analyzer. We are grateful to Inès Gayral for her support in field work.

CHAPITRE IV Impacts de l'augmentation des concentrations en CO_2 atmosphérique et de la durée d'immersion tidale sur la physiologie d'*A. marina* et de *R. stylosa*

Présentation

Dans les deux chapitres précédents, nous avons abordé l'impact des variations passées du niveau marin sur les stocks en carbone organique enfouis dans les sols de mangrove (c.f. CHAPITRE II), ainsi que la variabilité des émissions de CO_2 et de CH_4 depuis les sols et la colonne d'eau vers l'atmosphère dans les forêts de mangrove en fonction des saisons ou de la marée (c.f. CHAPITRE III).

Dans ce dernier chapitre, la réponse des mangroves face aux changements climatiques, et particulièrement, face aux augmentations des concentrations en CO_2 atmosphérique et de la durée d'immersion par les marées, est abordée. Ces différents paramètres pourraient induire des effets très complexes et doivent être étudiés conjointement pour comprendre leurs impacts sur l'écosystème. L'élévation du niveau marin pourrait provoquer un stress supplémentaire à l'écosystème qui souffre déjà des spécificités de son environnement : sol anoxique, salinité élevée, et instabilité du substrat. En revanche, les augmentations en CO_2 atmosphérique pourraient favoriser le développement des palétuviers, notamment en stimulant leur activité photosynthétique, et par conséquent, leur croissance. Toutefois, très peu d'informations sont disponibles sur la façon dont les futurs changements vont affecter le fonctionnement des écosystèmes à mangrove, tels que leur productivité et leur capacité de séquestration en carbone, ou même leur capacité d'expansion et de conquête de nouveaux territoires.

Dans ce contexte, les objectifs de ce chapitre ont été de tester la réponse de jeunes plantules d'*A. marina* et de *R. stylosa* face à une augmentation des concentrations en CO_2 atmosphérique et de la durée d'immersion par la marée. Les concentrations en CO_2 atmosphérique ont été fixées à 800 ppm, soit le double des concentrations actuelles (400 ppm) afin de simuler celles que les différents modèles de projection climatique prévoient pour la fin du XXI^{e} siècle (Collins *et al.*, 2014). La durée d'immersion par la marée a, elle, été augmentée de 1h45 relativement à celle expérimentée à l'heure actuelle par chacune des deux espèces en Nouvelle-Calédonie. Cette expérience a été réalisée sous des serres (Figure IV-1a et b) qui permettent, d'une part, de contrôler les concentrations en CO_2 atmosphérique, grâce à des mésocosmes étanches, et d'autre part, de faire varier la durée d'immersion tidale, grâce à un système de simulation des marées entièrement personnalisé (Figure IV-1b et c).

L'expérimentation a duré une année, et plus de 700 *R. stylosa* et 400 *A. marina* ont été suivis. Les différents paramètres d'échanges gazeux au niveau des feuilles (*i.e.* la photosynthèse, le taux de respiration, le taux de transpiration, et la conductance stomatique) ont été mesurés chaque mois.

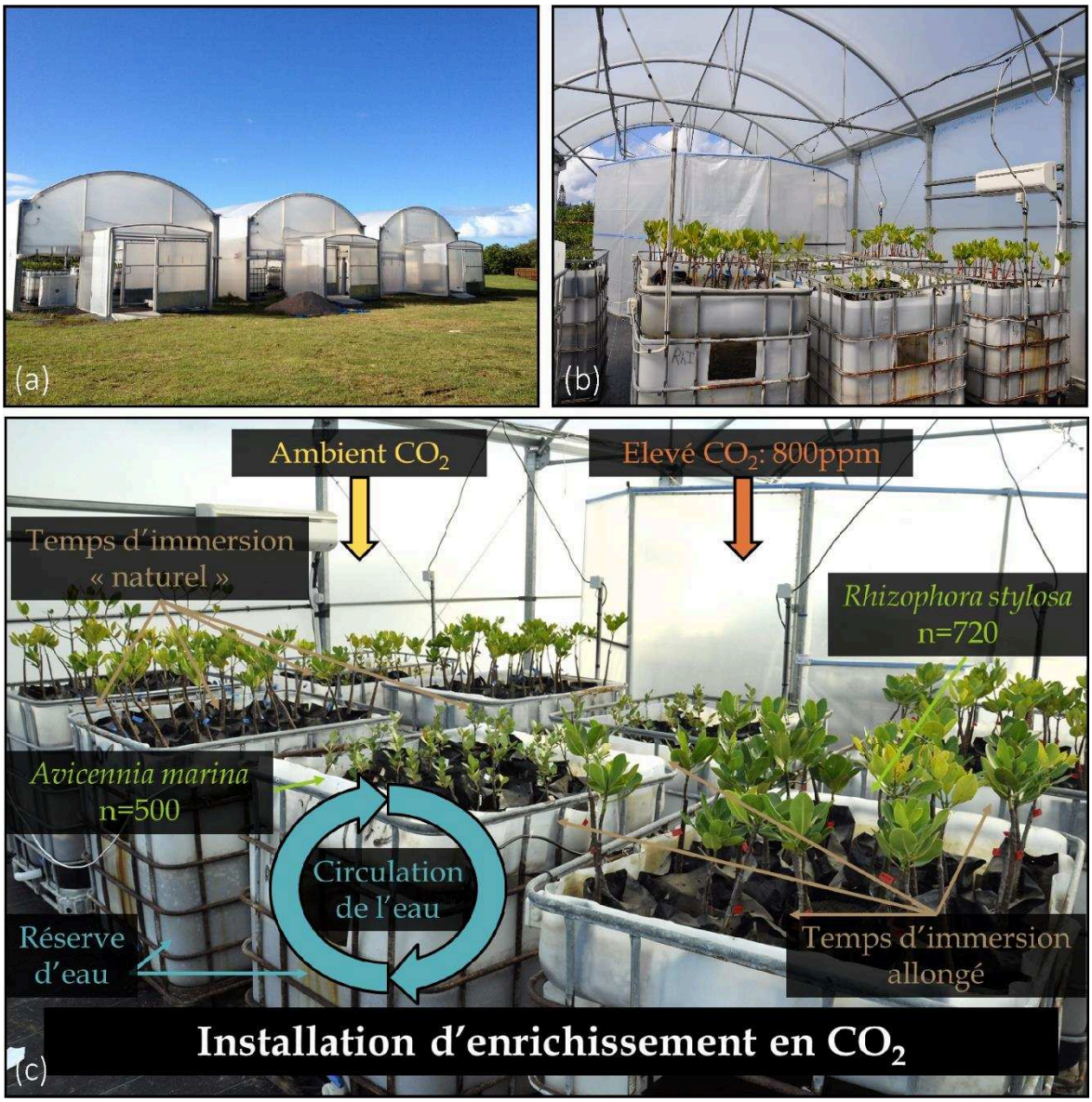

Figure IV-1: Photographies de (a) la face extérieure des serres à atmosphère contrôlée, et (b) de l'intérieur d'une serre, avec, au premier plan, les tables à marée, et, au second plan, le mésocosme qui permet le contrôle des concentrations en CO_2 atmosphérique, et (c) illustration du fonctionnement des serres (2016)

En outre, toutes les plantules ont été étiquetées et numérotées dès le début de l'expérience (Figure IV-2), ce qui nous a permis de suivre régulièrement leur croissance tout au long de l'expérience. À la fin de l'année d'enrichissement, 30 palétuviers par espèce et par traitement ont été prélevés afin de déterminer différents paramètres, tels que la biomasse

aérienne et souterraine, la surface foliaire, la densité de stomates, ou encore le contenu en carbone et en azote dans les racines, la tige principale et dans les feuilles.

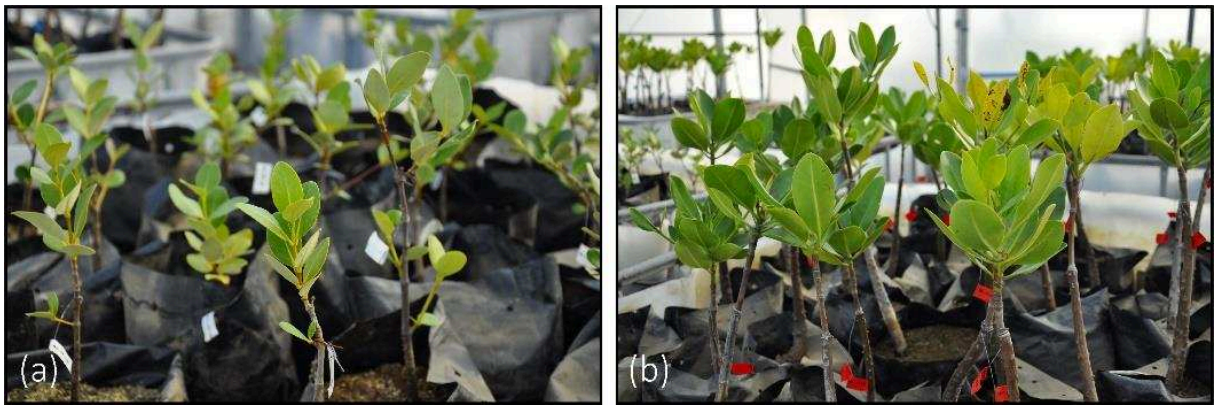

Figure IV-2: Photographies de (a) *A. marina*, et (b) *R. stylosa*, placés dans les tables à marées (2017)

L'augmentation des concentrations en CO_2 atmosphérique ont fortement stimulé l'activité photosynthétique des deux espèces, qui a augmenté de 37% pour *A. marina* et de 45% pour *R. stylosa*. Cette augmentation de l'activité photosynthétique s'est accompagnée d'un accroissement de la biomasse totale, de 46% et de 32% pour *A. marina* et *R. stylosa*, respectivement. De plus, les taux de transpiration ont fortement diminué, résultant d'une augmentation de 76% et 98% de la gestion de l'eau chez *A. marina* et *R. stylosa*. Toutefois, ces réponses à l'augmentation des concentrations en CO_2 atmosphérique ont été légèrement diminuées avec l'augmentation de la durée d'immersion par la marée. Finalement, nous avons pu constater une augmentation du rapport carbone/azote dans tous les différents compartiments des plantules des deux espèces. Ces résultats fournissent des informations importantes pouvant aider à comprendre le futur fonctionnement de l'écosystème face aux changements climatiques. Ils suggèrent que les futures augmentations des concentrations en CO_2 atmosphérique vont avoir des répercussions importantes, notamment en augmentant la quantité de carbone stocké dans la biomasse aérienne. Nos résultats indiquent de plus que l'augmentation de la durée d'immersion par les marées ne modifie pas les effets bénéfiques de l'élévation des concentrations en CO_2. De plus, grâce au développement accru du réseau racinaire, élément indispensable à la survie des plantules sur les zones intertidales, avec l'élévation en CO_2 atmosphérique, les capacités futures de l'écosystème à coloniser de nouvelles zones de développement seront accrues. En effet, l'élévation du niveau provoquera la migration de l'écosystème vers l'intérieur des terres, afin que les palétuviers maintiennent les conditions biotiques nécessaires à leur développement.

Partie 1.

Effects of elevated atmospheric CO_2 and increased tidal flooding on leaf gas-exchange parameters of two common mangrove species: *Avicennia marina* and *Rhizophora stylosa*

Adrien Jacotot, Cyril Marchand, Simon Gensous, Michel Allenbach

Abstract

In this study, we examined interactive effects of elevated atmospheric CO_2 concentrations and increased tidal flooding on two mangroves species, *Avicennia marina* and *Rhizophora stylosa*. Leaf gas exchange parameters (photosynthesis, transpiration rates, water-use efficiency, stomatal conductance and dark respiration rates) were measured monthly on more than 1,000 two-year-old seedlings grown in greenhouses for one year. In addition, stomatal density and light curve responses were determined at the end of the experiment. Under elevated CO_2 concentrations (800 ppm), the net photosynthetic rates were enhanced by more than 37% for *A. marina* and 45% for *R. stylosa*. This effect was more pronounced during the warm season, suggesting that an increase in global temperatures would further enhance the photosynthetic response of the considered species. Transpiration rates decreased by more than 15 and 8% for *A. marina* and *R. stylosa*, respectively. Consequently, water-use efficiency increased by 76% and 98% for *A. marina* and *R. stylosa*, respectively, for both species, which will improve drought resistance. These responses to elevated CO_2 were minimized (by 5%) with longer flooding duration. Consequently, future increases of atmospheric CO_2 may have a strong and positive effect on juveniles of *A. marina* and *R. stylosa* during the next century, which may not be suppressed by the augmentation of tidal flooding duration induced by sea-level rise. It is possible that this effect will enhance seedling dynamic by increasing photosynthesis, and therefore will facilitate their settlements in new area, extending the role of mangrove ecosystems in carbon sequestration and climate change mitigation.

Keywords: Mangrove; Elevated CO_2; Photosynthetic activity; Climate change; Sea level Rise

IV.1.1. Introduction

Mangroves are considered to be major ecosystems involved in the carbon cycle along tropical and subtropical coastlines. Due to their high ability to fix and store CO_2 (Donato *et al.* 2011; Alongi 2014), they are among the most efficient blue carbon sinks (Kauffman *et al.* 2011). Besides providing many ecosystem services (Lee *et al.* 2014), mangroves are characterized by a limited number of plant species because of a stressful environment (*e.g.* salinity, anoxia, soil instability). Little is known on how future climate change will affect the functioning of mangroves ecosystems, such as their productivity and carbon sequestration capacities, or even their ability to conquer new available spaces. Sea-level rise will probably induce an even more stressful environment for mangrove plants, while temperature and atmospheric CO_2 increases would favor their growth.

Atmospheric CO_2 concentrations have been rising continuously from 280 ppm at the preindustrial age to more than 400 ppm currently (Betts *et al.* 2016). By the end of the 21st century, atmospheric CO_2 concentrations could range from 794 to 1,150 ppm, depending on simulation models (Collins *et al.* 2014). The effects of elevated atmospheric CO_2 concentrations on temperate plant species is well documented, usually an enhancement of photosynthesis and water-use efficiency is observed (Urban 2003; Karnosky 2003; Ainsworth and Long 2005). Photosynthesis responses of tropical plants, especially mangroves, are less well studied, although stimulation of photosynthesis and net primary productivity has been reported (Farnsworth *et al.* 1996; Reef *et al.* 2015).

Climate change is not a single parameter but a combination of numerous ones, which may have opposing effects on mangrove plants. Sea-level rise is considered to be the major climate change threat to mangrove ecosystems because of their development in the intertidal areas (Ellison 2015). Global mean sea-level increased over recent decades and is predicted to increase from 0.26 to 0.98 m by 2100 (Church *et al.* 2013). All mangroves may not be able to keep pace with sea-level and will have to migrate landward to maintain their preferred hydroperiod (Gilman *et al.* 2008). However, both natural and artificial barriers will strongly limit the inland migration of mangroves (Mcleod *et al.* 2011; Lovelock *et al.* 2015). If mangroves cannot migrate or keep pace with sea-level rise, they will be subjected to greater depth and duration of tidal flooding. When grown outside their optimum flood duration, mangrove trees

respond by a decrease in photosynthetic activity and in net primary productivity (Krauss *et al.* 2008).

Major advances in the comprehension of the evolution of the ecosystem have been made recently by studying the effects of elevated atmospheric CO_2 in combination with other environmental parameters such as salinity (Reef *et al.* 2015), nutrient availability (McKee and Rooth 2008; Reef *et al.* 2016) or species competition (McKee and Rooth 2008). However, the available literature is still limited, and restricted to some species. In addition, although the interactive effect of elevated CO_2 and tidal flooding duration was tested on brackish marshes (*e.g.* Cherry *et al.* 2009), to our knowledge, no study tested these effects on mangrove physiology and specifically on photosynthesis.

Within this context, the main objective of this study was to evaluate the long-term effects of elevated CO_2 and tidal flooding duration on the leaf gas-exchange parameters (assimilation, transpiration, dark respiration, stomatal conductance, water-use efficiency) of seedlings of *Avicennia marina* and *Rhizophora stylosa*, the most widespread mangrove species throughout the Indo-Pacific region (Buchmann *et al.* 2008; Ellison *et al.* 2008). We were also interested in the seasonal variations of leaf net photosynthetic rates. Our main hypotheses were: (i) atmospheric CO_2 enrichment will lead to a stimulation of photosynthetic activity, (ii) tidal flooding duration will reduce the photosynthesis response due to waterlogging stress. To reach our goals, we used a closed chamber experiment, where more than 1,000 two-year-old mangrove seedlings were grown at two CO_2 concentrations (400 vs 800 ppm), over two semi-diurnal tidal flooding durations (3h15 vs 4h45 for *A. marina*, 6h00 vs 7h45 for *R. stylosa*), during one complete year. Leaf-gas exchange parameters were measured monthly during the whole year of experiment, and chlorophyll fluorescence was determined only for the last 6 months. Light curve responses, stomatal density and specific leaf area were assessed at the end of the experiment.

IV.1.2. Materials and Methods

IV.1.2.1. Description of the facility

The experiment was conducted in the City of Mont-Dore in New Caledonia (22°13'49"S, 166°31'09"E) from June 2016 to May 2017. The facility consists of three semi-open greenhouses of 72 m² each (12 m x 6 m, 6 m height). Inside each greenhouse, a circular closed

chamber of 36 m² (2.4 m height) was built to maintain elevated atmospheric CO_2 concentrations. The atmospheric CO_2 concentrations in each of the three closed chambers were continuously monitored during the experiment using CO_2 probes connected to a CO_2 central unit, which controlled the entire system (MAXICLIM NG 08/3Z, Anjou Automation). Pure CO_2 gas was supplied from 5:00 am to 7:00 pm at the top of the chambers by brief pulses from a high-pressure cylinder.

HOBO temperature and humidity sensors (Onset, Cape Cod, Massachusetts, USA) were installed inside the greenhouse and the closed chamber. Air temperature and humidity were recorded every 5 min. Temperature and humidity were allowed to fluctuate naturally inside the greenhouses, however air cooling units were installed in the closed chambers to prevent high variations of temperatures. Mean temperatures and relative humidity for the experiment period are given in Table IV-1.

Table. IV-1. Mean annual and seasonal temperatures (°C) and relative humidity (%) ± standard deviations (SD) inside the greenhouses and the closed chamber.

Parameters (Means ± SD)	Annual	Cool season (June - November)	Warm season (December - May)
Greenhouse temperature (°C)	25.14 ± 2.93	23.14 ± 2.59	26.39 ± 3.15
Chamber temperature (°C)	25.00 ± 3.31	22.30 ± 3.03	26.68 ± 3.49
Greenhouse relative humidity (%)	82.62 ± 13.56	85.78 ± 12.55	80.65 ± 14.19
Chamber relative humidity (%)	79.91 ± 12.55	78.43 ± 12.16	80.83 ± 12.78

Mangrove seedlings were placed on custom-build tidal tables. The latter are made of a 700-liters polypropylene water reserve (1 m² area over 0.7 m height), surmounted by a 300-liters planting tray (1 m² area over 0.3 m height). Each tidal table works as an individual unit. Fresh seawater was pumped from the adjacent sea (20 m) and stored in the water reserves, which was replaced twice a month during the entire study. To simulate high tide periods, an aquarium pump, placed in each water reserve, sent the water to the planting tray. A siphon pipe allowed the planting tray to drain the water back to the reserve to reproduce low tide periods. To control the tidal treatment attributed to each tank, the aquarium pumps were connected to three open-source Arduino Uno cards (one per greenhouse) coupled to currents relays, which were programmed according to the needs of the experiment. Water quality (pH, salinity, DO) in the reservoir was checked periodically using YSI probes.

IV.1.2.2. Plant material

Mature propagules of *Avicennia marina* and *Rhizophora stylosa* were collected from the natural mangrove of Oundjo, in New Caledonia (21°4'8"S, 164°42'51"E). The propagules were collected from February to March 2014, during the optimum fruiting period and were then planted in 2.5-liter polyethylene bags in a 1:1 hand mixed mangrove peat and sand. During the two years preceding the experiment, the seedling mortality was high, resulting in a different number of seedlings used for the experiment. A total of 720 and 400 two-years old *R. stylosa* and *A. marina*, respectively, were followed for this study. During the year of experiment, the mortality dropped to less than 1%. Prior to the experiment, mean heights were 172.4 ± 40.17 and 90.91 ± 23.33 mm, and mean basal diameters 4.81 ± 0.98 mm and 5.54 ± 0.65 mm for *A. marina* and *R. stylosa*, respectively. For all seedlings, height measurements were made along the main axis, from the soil for *A. marina*, and from the seed to the apex for *R. stylosa*.

IV.1.2.3. Experimental design

The experiment was setup as a split-plot design with CO_2 atmospheric concentrations as the whole-plot (Ambient, 400 ppm vs. Elevated, 800 ppm) and tidal flooding duration (TFD) as the split-plot nested within CO_2 (Natural vs. Longer). Elevated atmospheric CO_2 concentrations were maintained between 780 and 820 ppm CO_2. Natural TFD were set-up according to the average flooding duration observed in New Caledonian mangroves for both species (unpublished data). In New Caledonia, mangroves develop in semi-arid conditions with a specific zonation of the ecosystem: *Rhizophora* spp. colonizes the seaward side, while *Avicennia marina* develops at higher elevations. Previous studies suggested that the main factor controlling the distribution of mangrove species in New Caledonia was soil salinity, which in turn was controlled by the duration of tidal inundation and thus by the soil elevation (Marchand *et al.* 2011, 2012). As a result, the flooding duration for *Rhizophora* trees is higher than for *Avicennia*. Consequently, in the experiment, natural TFD were 3h15 for *A. marina* and 6h00 for *R. stylosa* for each high tide. Simulated tidal cycles were semi-diurnal, meaning that there were two high tides and two low tides each day. We hypothesized that an increase in mean sea-level will similarly affect the flooding duration of both species; thus, in the experiment, longer TFD was simulated by increasing the natural times by 1h45. This increase in flooding duration has been randomly defined, but however remains realistic given the

expected sea-level rise at the end of the century. Nevertheless, an increase of 1h45 of tidal duration will have different implication for both species, as it corresponds to an increase of 45% of the natural tidal duration of *A. marina*, whereas it is only to 25% for *R. stylosa*. During high tide, the water level in the planting trays was identical for all tidal tables, 5 cm above sediment surface.

The mangrove seedlings were allocated randomly between the tidal tables, with 25 *A. marina* or 30 *R. stylosa* on each tidal table, resulting in 100 *A. marina* (4 tidal tables) and 180 *R. stylosa* (6 tidal tables) for each of the four treatments. The tidal tables were then distributed between the three greenhouses and the three closed chambers, according to their CO_2 treatment. During the experiment, the mangrove seedlings were regularly rotated within each tidal table, and were rotated three times between the greenhouses to minimize the greenhouse effect.

IV.1.2.4. Leaf gas-exchange measurements

Gas-exchange parameters were performed using a semi-open gas-exchange analyzer (CO-650, Qubit Systems, Canada). Assimilation (P_n) and transpiration (T) rates, as well as the stomatal conductance (g_s), were determined every month from June 2016 to May 2017. Measurements were performed in the morning (8:00-12:00 am), on 30 different fully expended leaves for the two species and the four treatments with a photon flux density (PPFD) of 1,200 µmol m^{-2} s^{-1}. The instantaneous water use efficiency (WUE) was then calculated as $WUE=P_n/T$. Dark respiration (D_r) measurements were made at night (8:00-10:00 pm) on three different seedlings for each species and treatment. No dark respiration measurements were made in July and September 2016.

Light-curve responses ($P_n/PPFD$ curves) were generated at the end of the experiment on three leaves per species and per treatment. Eight PPFD intensities of 1200, 800, 400, 200, 100, 50, 25, and 0 µmol m^{-2} s^{-1} were chosen. Transitions between PPFD levels were made once photosynthesis was stable, and lasted between four to ten minutes. Curve fitting was resolved using the solver function of *Microsoft Excel* (Lobo *et al.* 2013, 2014), and the best fitting was chosen according to the lower sum of the squares of the errors. The model, which best fitted with our results, was the rectangular hyperbola Michaelis-Menten based model (Kaipiainen 2009).

IV.1.2.5. Specific leaf area

At the end of the experiment, 30 mature and fully expanded leaves per species and treatment were scanned and analyzed for leaf area (SLA) using ImageJ (Schneider *et al.* 2012). Then, all leaves were dried at 60°C for 72 hours before being weighed for dry mass (g). SLA ($cm^2\ g^{-1}$) was calculated as the ratio of leaf area to the corresponding leaf dried mass.

IV.1.2.6. Chlorophyll fluorescence measurements

Chlorophyll fluorescence was measured using a portable chlorophyll fluorometer (FluorPen FP 100, Photon Systems Instruments, Czech Republic). The maximum quantum efficiency of PSII photochemistry (F_v/F_m) was measured on the abaxial leaf surface at night from 8:00 pm to 10:00 pm, using a PPFD of 3,000 µmol $m^{-2}\ s^{-1}$ as saturating flash for a duration of 1 s. Measurements were done only for the warm season, from November 2016 to May 2017 on 30 young fully expanded leaves of both species and each of the four treatments.

IV.1.2.7. Stomatal density

Five fully expanded leaves for each species and treatment were randomly collected to determine the stomatal density. For *A. marina*, because of a dense layer of trichomes obscuring stomata, the leaves were macerated in a 5:1 solution of hydrogen peroxide and glacial acetic acid for 1 hour at 70°C. Then, the abaxial epidermis was peeled and stained with Safranin O. The number of stomata were counted from the interior surface of the epidermis (Nguyen *et al.* 2015). For *R. stylosa*, nail varnish imprints of the abaxial side of the leaves were taken. The number of stomata were then counted under a light microscope (Leica DM500B, Leica Microsystems, Wetzlar, Germany) on three fields of view per leaf at a x200 magnification.

IV.1.2.8. Statistical analysis

Normality and equality of variance were analyzed using Shapiro and Levenne tests, respectively. Following results, either a two-way analysis of variance (ANOVA), followed by a Scheffe post-hoc test or a Kruskal-Wallis test was applied to identify significant differences ($p \leq 0.05$), between treatments of gas-exchange parameters, F_v/F_m and stomatal density. Both species were analyzed independently. All statistical analysis were performed using R software version 3.3.1 (R Development Core Team 2008) with the 'agricolae' package.

IV.1.3. Results

IV.1.3.1. Leaf-gas exchange response to elevated CO_2 and flooding

The results of leaf gas-exchanges for *A. marina* and *R. stylosa* are presented in Fig. IV-3. For *A. marina*, mean annual net photosynthesis rate (P_n) was significantly higher under elevated CO_2 than under ambient CO_2 concentrations (Table IV-2), either with normal or longer TFD. However, within each CO_2 treatment, longer TFD slightly decreased P_n (Fig. IV-3a). Furthermore, transpiration rates (T_r) were significantly reduced under elevated CO_2 in both tidal duration treatments (Fig. IV-3b and Table IV-2). Consequently, water-use efficiency (WUE) significantly increased (Table IV-2) under elevated CO_2 for both TFD, but was lowered for the longer tidal duration treatment within both CO_2 concentrations (Fig. IV-3c). Concerning the stomatal conductance (g_s), elevated CO_2 significantly decreased it (Table IV-2) for both TFD treatments (Fig. IV-3d). No significant differences (Table IV-2) were observed for dark respiration rates (R_d) with CO_2 or TDF treatments (Fig. IV-3e). For *R. stylosa*, elevated CO_2 significantly increased P_n (Table IV-2) for both natural and longer TFD treatments (Fig. IV-3f). Transpiration rates were significantly reduced at elevated CO_2 (Table IV-2), and also reduced with longer tidal duration within both CO_2 treatments (Fig. IV-3g). As a result, WUE for *R. stylosa* was significantly higher for trees grown under elevated than under ambient CO_2 concentrations (Table IV-2). Considering each CO_2 treatment, longer TFD increased WUE in trees grown under elevated CO_2, and decreased WUE for trees grown under ambient CO_2 concentrations (Fig. IV-3h). Stomatal conductance was significantly reduced in both TFD treatments under elevated CO_2 (Table IV-2). However, no differences were observed with TFD within each CO_2 concentrations (Fig. IV-3i). No significant differences (Table IV-2) were observed for dark respiration rates (R_d) between treatments (Fig. IV-3j).

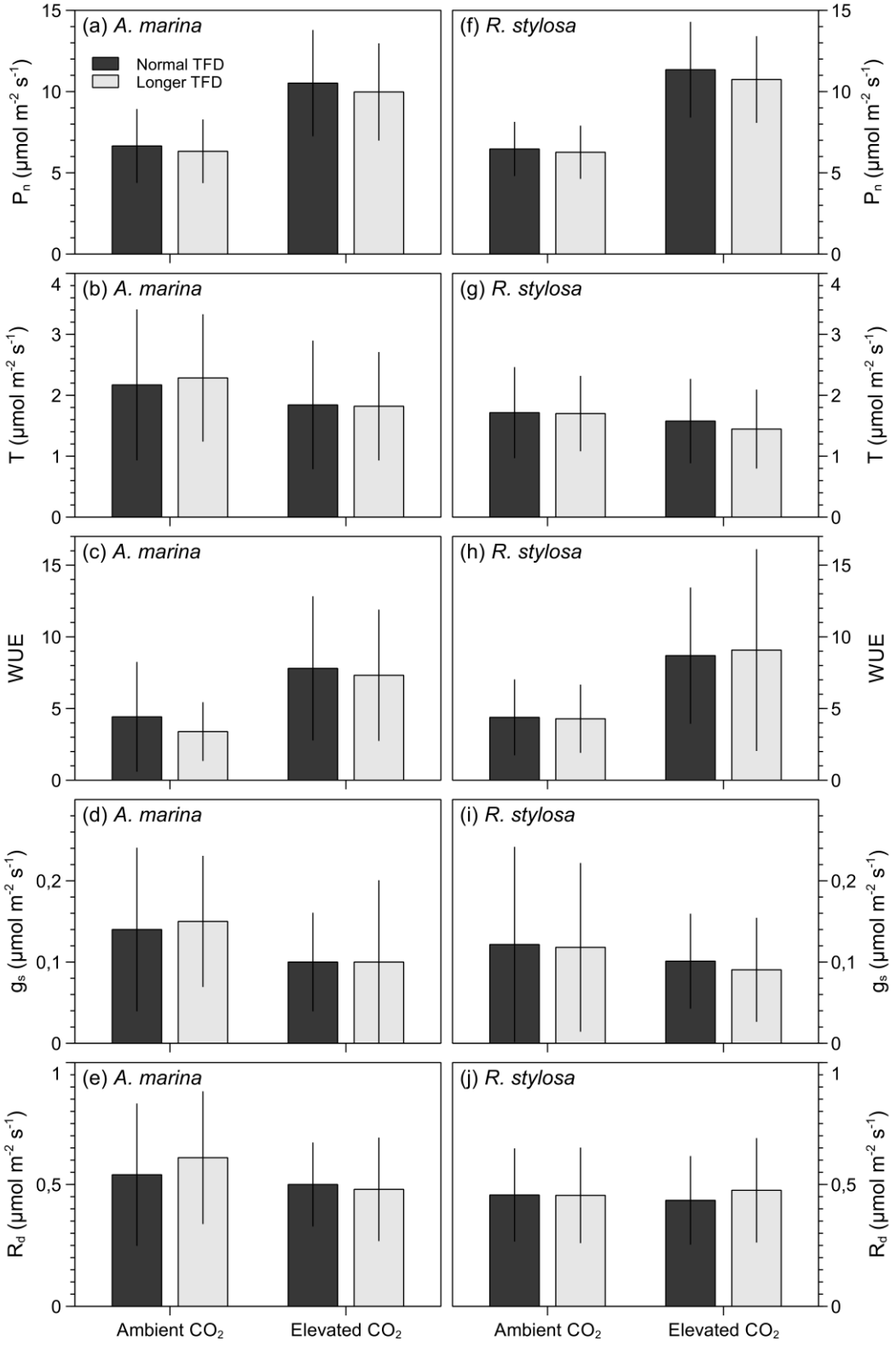

Fig. IV-3: Mean values (± SD) of leaf gas exchange parameters for *A. marina* and *R. stylosa* grown in ambient (400 ppm) or elevated (800 ppm) CO_2, and under normal (dark-grey bars) and longer TFD (grey bars), for 12 months. (a and f) photosynthetic rates (µmol m^{-2} s^{-1}), (b and g) transpiration rates (µmol m^{-2} s^{-1}), (c and h) water-use efficiency, (d and i) stomatal conductance (µmol m^{-2} s^{-1}), and (e and j) dark respiration rates (µmol m^{-2} s^{-1}).

IV.1.3.2. Seasonal response of the net photosynthetic rates

Different seasonal responses of net photosynthetic rates were observed between the cool season and the warm season (Fig. IV-4). From June to November, mean temperature was 22.30 °C, whereas from November to May, it was 26.68°C (Table IV-1). For *A. marina*, elevated CO_2 enhanced P_n by 32 and 33% for natural and longer TFD during the cool season, whereas during the warm season, P_n was enhanced by 40 and 39% for natural and longer TFD, respectively (Fig. IV-4a). For *R. stylosa*, a similar response as for *A. marina* was observed. During the cool season, an increase in P_n of 40 and 37% was observed for natural and longer TFD, whereas an increase of P_n of 45% was observed during the warm season, for both TFD treatments (Fig. IV-4b).

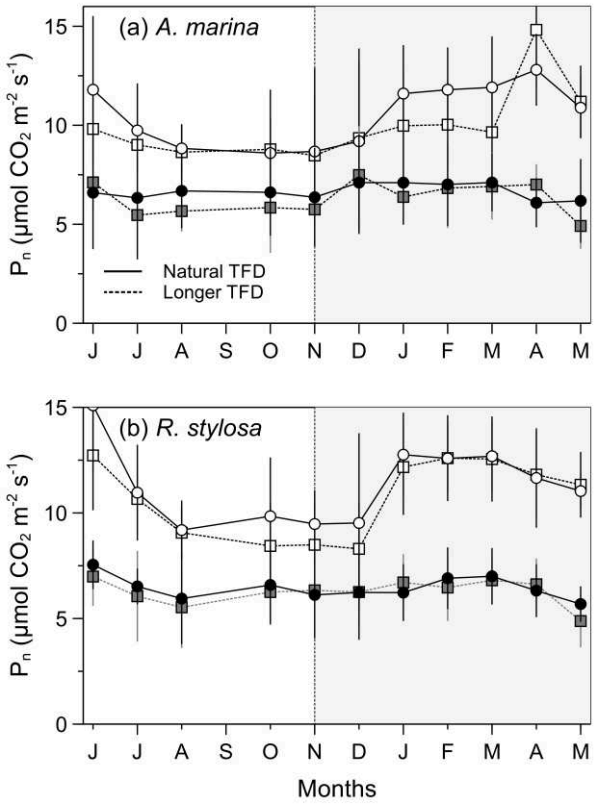

Fig. IV-4: Annual evolution (± SD) of leaf net photosynthetic rates (P_n, µmol m^{-2} s^{-1}) for (a) *A. marina*, and (b) *R. stylosa*. Colored markers: ambient CO_2 concentrations, white markers: elevated CO_2 concentrations. Shaded area represents the warm season.

IV.1.3.3. Specific leaf area after 12 months of enrichment

Specific leaf area (SLA) was significantly higher for both species under elevated CO_2, either with natural or longer TFD (Fig. IV-5a, b and Table IV-2). Within each CO_2 treatment, no significant effects of longer TFD on SLA were observed for *A. marina* (Fig. IV-5a). For *R. stylosa*,

SLA decreased under ambient CO_2 and longer TFD, whereas it significantly increased with longer TFD under elevated CO_2 (Fig. IV-5b and Table IV-2).

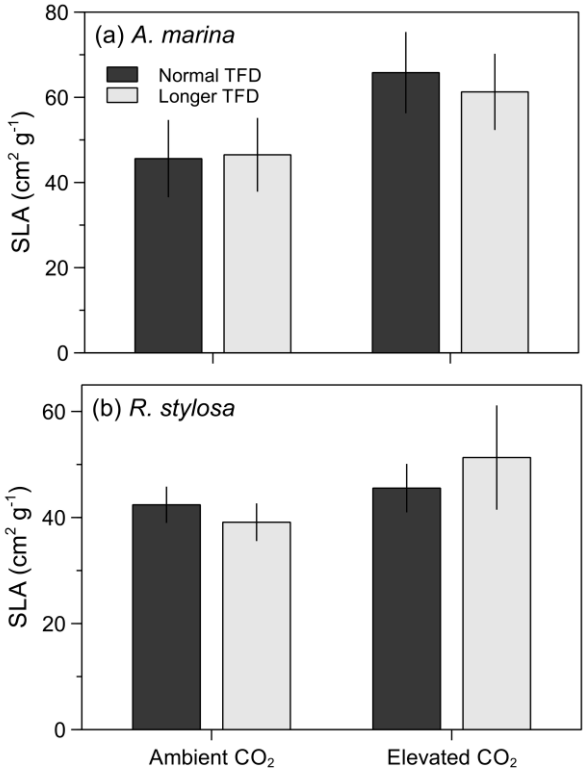

Fig. IV-5: SLA ($cm^2\ g^{-1}$) of (a) *Avicennia marina* and (b) *Rhizophora stylosa* grown in ambient or elevated CO2, and under normal (dark-grey bars) and longer TFD (grey bars), for 12 months. Values are means ± SD (*n*=30).

Table. IV-2. Significance values reported by two-way analysis of variance (ANOVA), followed by a Scheffe post-hoc test or a Kruskal-Wallis test.

	Avicennia marina			*Rhizophora stylosa*		
	CO_2	TFD	Interaction	CO_2	TFD	Interaction
P_n	667.70***	8.86**	0.55^{NS}	1401.48**	10.37***	2.63^{NS}
T_r	45.78***	0.718^{NS}	1.304^{NS}	28.33***	3.919*	2.511^{NS}
WUE	41.10***	0.196^{NS}	7.62**	67.74***	1.50^{NS}	6.23*
g_s	80.03***	3.78*	0.71^{NS}	74.25***	2.42^{NS}	0.05^{NS}
D_r	0.05^{NS}	0.01^{NS}	0.07^{NS}	1.77^{NS}	0.017^{NS}	0.241^{NS}
SLA	114.49***	1.260^{NS}	2.75^{NS}	51.61***	1.35^{NS}	18.00^{NS}
SD	94.97***	0.426^{NS}	0.05^{NS}	83.06***	0.535^{NS}	0.05^{NS}

***, **, * indicates significant effects at p<0.001, 0.01, and 0.05, respectively. *NS*: non-significant

IV.1.3.4. Net photosynthesis light curves responses (Pn/PPFD)

The net photosynthesis response to light was similar for both species (Fig. IV-6a and b). From 0 to100 µmol photon m^{-2} s^{-1}, P_n showed no difference between all the four treatments either for *A. marina* or *R. stylosa*. For PPFD values higher than 100 µmol photon m^{-2} s^{-1}, both *A. marina* and *R. stylosa* showed higher P_n values when growing under elevated than under ambient CO_2 concentrations. When compared to natural TFD, longer TFD slightly reduced P_n under ambient CO_2 concentrations, whereas under elevated CO_2, P_n was higher from 100 to 800 µmol photon m^{-2} s^{-1}, but lower at 1,200 µmol photon m^{-2} s^{-1}. Regarding the light saturation points, for *A. marina*, they were, under ambient CO_2 concentrations, 872 and 785 µmol photon m^{-2} s^{-1} for natural and longer TFD, respectively whereas under elevated CO_2 concentrations, they were 1490 and 1224 µmol photon m^{-2} s^{-1}. For *R. stylosa*, the light saturation points were, under ambient CO_2 concentrations, 751 and 676 µmol photon m^{-2} s^{-1}, and under elevated CO_2 concentrations, 1591 and 1283 µmol photon m^{-2} s^{-1}, for natural and longer TFD, respectively.

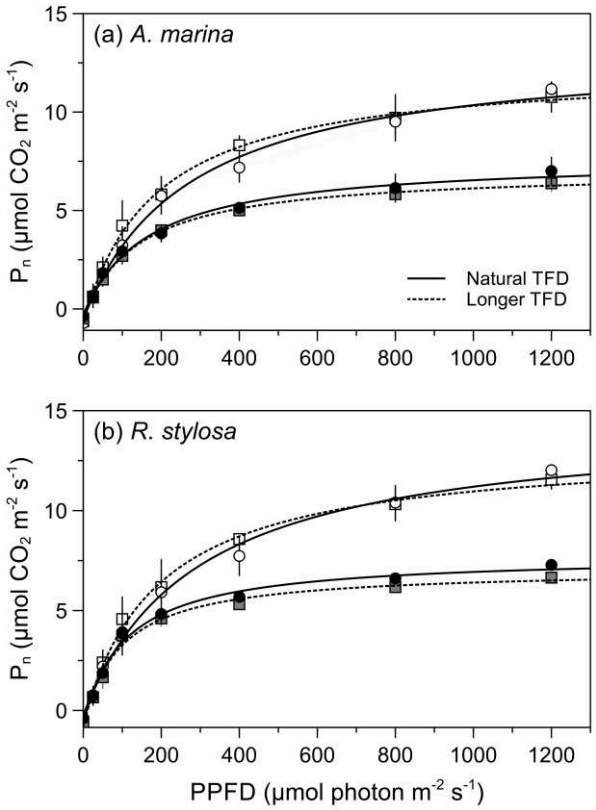

Fig. IV-6: P_n/PPFD curves for *A. marina* (a) and *R. stylosa* (b) at the end of the experiment. (*n*=3 ± SD). Colored markers: ambient CO_2 concentrations, white markers: elevated CO_2 concentrations.

IV.1.3.5. Maximum quantum efficiency of PSII photochemistry (F_v/F_m) during the warm season

During the warm season, similar variations of F_v/F_m were observed for both species and each treatment (Fig. IV-7a and b). For both species, elevated CO_2 had a slightly positive effect on F_v/F_m, either with natural or longer TFD, whereas within the CO_2 treatment, longer TFD slightly reduced F_v/F_m. For *A. marina*, mean values of F_v/F_m under ambient CO_2 concentrations were 0.81 ± 0.02 and 0.78 ± 0.03 for natural and longer TFD, respectively. Under elevated CO_2 concentrations, F_v/F_m had mean values of 0.82 ± 0.03 and 0.80 ± 0.03, for natural and longer TFD, respectively (Fig. IV-7a). For *R. stylosa*, mean values of F_v/F_m were, under ambient CO_2 concentrations, 0.81 ± 0.03 and 0.79 ± 0.03, and under elevated CO_2 concentrations, 0.82 ± 0.03 and 0.80 ± 0.05, for natural and longer TFD, respectively (Fig. IV-7b).

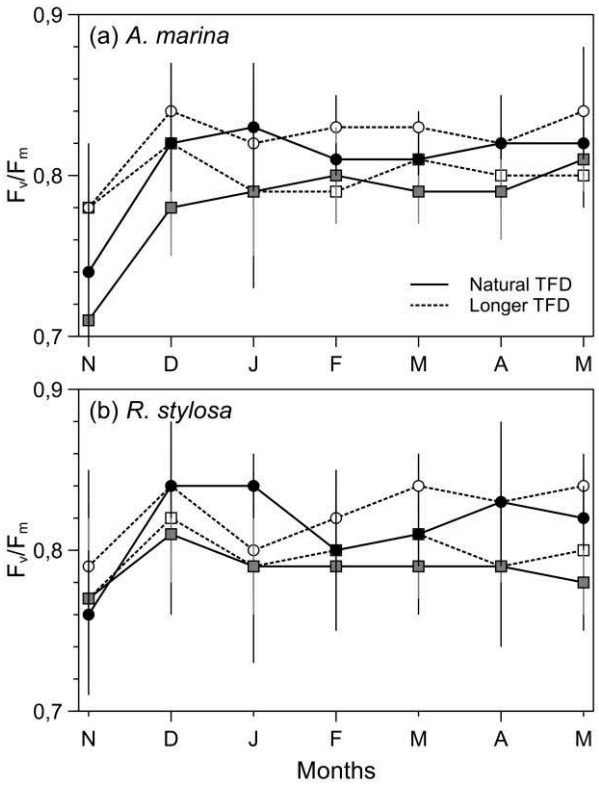

Fig. IV-7: Maximum quantum efficiency of PSII photochemistry (F_v/F_m) for *A. marina* (a) and *R. stylosa* (b) from November 2016 to May 2017. (*n*=30 ± SD). Colored markers: ambient CO_2 concentrations, white markers: elevated CO_2 concentrations.

IV.1.3.6. Stomatal density

For both species, the stomatal density was significantly reduced (Fig. IV-8a, b and Table IV-2) under elevated CO_2 in comparison to ambient CO_2 concentrations, whereas within each CO_2 treatment, no significant differences (Table IV-2) in stomatal density were observed under natural or longer TFD (Fig. IV-8a and b). For *A. marina*, mean stomatal density under ambient CO_2 concentrations were 227.84 ± 15.91 and 223.86 ± 15.13 mm^{-2} for natural and longer TFD, respectively. Under elevated CO_2 concentrations, mean stomatal density was 183.06 ± 19.00 and 181.18 ± 19.11 mm^{-2}, for natural and longer TFD, respectively (Fig. IV-8a). For *R. stylosa*, mean stomatal density were, under ambient CO_2 concentrations, 120.51 ± 10.40 and 118.21 ± 13.8279 mm^{-2}, whereas under elevated CO_2 concentrations, mean stomatal density were 91.86 ± 12.47 and 89.55 ± 11.79 mm^{-2}, for natural and longer TFD, respectively (Fig. IV-8b).

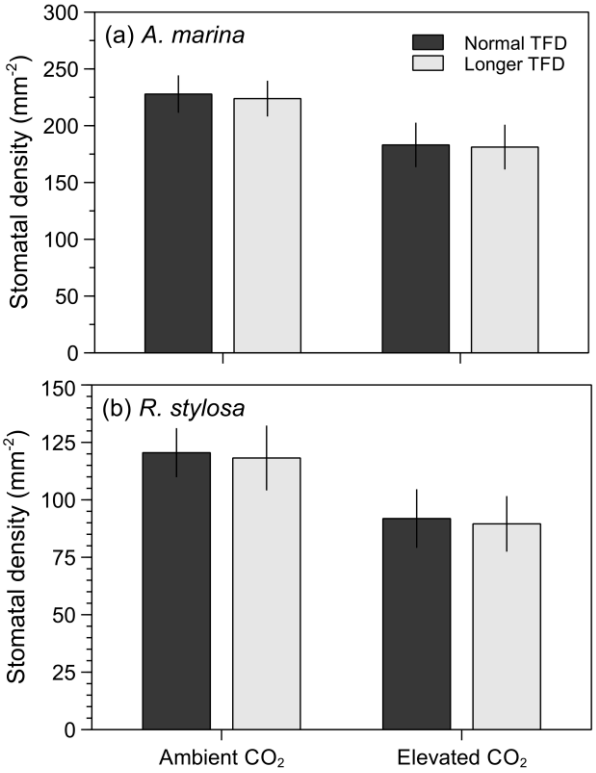

Fig. IV-8: Stomatal density (mm^{-2} ± S.D.) (*n*=15) of (a) *Avicennia marina* and (b) *Rhizophora stylosa* grown in ambient or elevated CO_2, and under normal (dark-grey bars) and longer TFD (grey bars), for 12 months.

IV.1.4. Discussion

IV.1.4.1. Future sea-level rise will affect mangrove photosynthesis

Sea-level rise will result in an increase of the tidal flooding duration for mangroves. In our experiment, applying a longer tidal duration to *Avicennia marina* and *Rhizophora stylosa* seedlings resulted in a decrease of 5% and 3% in photosynthesis, and of 23% and 2% in WUE, for *A. marina* and *R. stylosa*, respectively. Under ambient CO_2 concentrations, photosynthesis decreased from 6.65 ± 2.24 to 6.33 ± 2.24 µmol m^{-2} s^{-1} and from 6.47 ± 1.63 to 6.27 ± 1.60 µmol m^{-2} s^{-1}, and WUE decreased from 4.42 ± 3.79 to 3.39 ± 2.01 and from 4.38 ± 2.61 to 4.29 ± 2.34 for *A. marina* and *R. stylosa*, respectively. However, these reductions in photosynthesis and WUE were lower than those reported for other stressing factors, such as salinity or WUE, as demonstrated by Ball *et al.* (1997) on *R. stylosa* and *R. apiculata*. Tidal flooding may induce a rapid deficit in oxygen in the soil due to roots and micro-organisms respiration (Naidoo *et al.* 1997). Depending on studies, a decrease of 28% of oxygen could be observed after 6h of flooding (Skelton and Allaway 1996), or of 100% after 3.5 hours, as reported for *A. marina* seedlings (Hovenden *et al.* 1995). In this later case, the deficit of oxygen led to a complete anoxia of the root system. During flooding events, mangrove roots may use all their internal oxygen content, and then start to metabolize anaerobically (Krauss *et al.* 2008). Mangroves are well-adapted to waterlogging condition of their soil, and generally respond by producing lenticels on basal stems or root structures to help offset the effects of low soil oxygen levels (Krauss *et al.* 2008). However, in our study, *A. marina* and *R. stylosa* were three-years-old at the end of the experiment, and their number of lenticels was limited due to their size and only a few seedlings started to produce pneumatophore or prop roots. Similar results of a decrease in photosynthesis and water-use efficiency with increasing tidal flood duration were previously observed on seedlings but also on mature mangrove trees (Youssef and Saenger 1996; Naidoo *et al.* 1997; Chen *et al.* 2005). In their work on *Kandelia candel*, Chen *et al.* (2005) showed that during anaerobic conditions, the production of abscisic acid (ABA) increased. The latter stimulates stomatal closure, and thus reduces photosynthesis (Kozlowski 1984). No hormone measurements were made in our study, but we suggest that a similar mechanism may be involved in the observed decrease of photosynthesis for *A. marina* and *R. stylosa* when subjected to longer tidal flooding, as observed by Chen *et al.* (2005). Reduced photosynthesis

during longer immersion time may also result from the inhibition of the RuBisCO enzyme activity (Ellison and Farnsworth 1997; Pezeshki *et al.* 1997).

All F_v/F_m values reported in our study for *A. marina* and *R. stylosa*, either with elevated CO_2 or longer tidal flooding, indicated that leaves were photosynthetically actives, with ratios between 0.78 to 0.82 (Fig. IV-7), indicative of healthy photosystems and absence of significant stressing factors damaging the photosynthetic functions (Lichtenthaler *et al.* 2005; Sobrado 2008; Orekhov *et al.* 2015). However, for both species, we could observe a slightly decrease in F_v/F_m with longer tidal duration treatment in comparison to natural duration, either with ambient or elevated CO_2 concentrations. We, thus, hypothesize that longer tidal flooding may have induced a light stress, which not significantly impacted trees response.

IV.1.4.2. Elevated atmospheric CO_2 concentrations will increase mangrove net productivity

According to our initial hypothesis, elevated CO_2 had a significant positive effect on photosynthesis, which was enhanced by more than 37% for *A. marina* (6.65 ± 2.24 vs. 10.52 ± 3.24 µmol m^{-2} s^{-1}) and by more than 45% for *R. stylosa* (6.47 ± 1.63 vs. 10.74 ± 2.63 µmol m^{-2} s^{-1}). In our study, the initial stimulation of photosynthesis was maintained after one year of enrichment, and no downregulation was observed, contrary to some previous observations of photosynthetic acclimation after long-term exposure to elevated CO_2 (Farnsworth *et al.* 1996). In addition, dark respiration was not affected by elevated CO_2 concentrations, either for *A. marina* (0.54 ± 0.29 vs. 0.50 ± 0.17 µmol m^{-2} s^{-1}), or for *R. stylosa* (0.46 ± 0.19 vs. 0.44 ± 0.18 µmol m^{-2} s^{-1}), which is different from the results of (Farnsworth *et al.* 1996) who observed a slight decrease of dark respiration with elevated CO_2. Consequently, elevated CO_2 induced a stimulation of photosynthesis but did not influence plant dark respiration, suggesting that the productivity of mangroves seedlings may be further enhanced with future climate change, which is in accordance with previous studies showing increase of the net CO_2 exchange rate (Farnsworth *et al.* 1996; Ball *et al.* 1997; Reef *et al.* 2015).

In addition, our results showed a clear positive response of photosynthesis to light in both *A. marina* and *R. stylosa* seedlings grown under elevated CO_2 concentrations (Fig. IV-6). However, under elevated CO_2, the light saturation point was higher for both species, indicating that the effect of CO_2 concentrations on the rate of photosynthesis was maximal at the highest

light levels, whereas at low light levels, rate of photosynthesis was limited by the availability of light. These findings are consistent with previous work which demonstrated that the response of C3 plants with elevated CO_2 is also light dependent (Ziska *et al.* 1990; Drake and Leadley 1991; Kubiske and Pregitzer 1996; Herrick and Thomas 1999). In addition, it was surprising to observed that SLA increased for both species under elevated CO_2 (Fig. IV-5), opposite to the results of other studies (Ball *et al.* 1997; McKee and Rooth 2008; Reef and Lovelock 2014). This is an important result as an increase in SLA will lead to a higher potential for carbon acquisition by photosynthesis but also for light interception. Consequently, even if elevated CO_2 had no effect on photosynthesis in low light conditions, the increase of SLA may promote the growth of *A. marina* and *R. stylosa* seedlings in shaded area.

IV.1.4.3. Increase in temperature will raise the beneficial effect of elevated CO_2

We observed a clear difference in the photosynthetic response to elevated CO_2 between the cool season and the warm season, which increased from 32% to 40% and from 38% to 45% for *A. marina* and *R. stylosa*, respectively (Fig. IV-4). Although photosynthesis of tropical C3 species such as *A. marina* and *R. stylosa* can operate between 15 to 45°C, there is a temperature optimum for which it will be maximal (Sage and Kubien 2007). In their review, Gilman *et al.* (2008) indicated that this optimum lies between 28 to 32°C for mangroves species, however, it appears to be species-specific, as lower values of 24.5°C has been reported for *A. germinans* (Reef *et al.* 2016) and of 26.8°C for *A. marina* (Leopold *et al.* 2016). In our study, mean monthly temperatures increased from 22.30 to 26.68°C during the warm season, which is close to the optimal temperatures reported above, therefore confirming the hypothesis of temperature as a limiting factor for photosynthesis during the cool season under elevated CO_2. With future climate change, the global temperatures are predicted to rise by 0.3 to 4.8°C, depending on prediction models (Stocker *et al.* 2013), and our work suggests that the combination of elevated CO_2 with the increase of temperature may further promote the CO_2 fixation by mangrove trees. However, it seems that this beneficial effect may be inhibited if temperatures increase to more than 40°C (Andrews *et al.* 1984; Gilman *et al.* 2008; Reef *et al.* 2016), which may happen with future climate changes, particularly in the actual arid or semi-arid regions.

IV.1.4.4. Elevated CO_2 will help mangroves trees to resist drought

We observed that growth under elevated atmospheric CO_2 resulted in a significant reduction of stomatal density, with more than 19% and 23% for *A. marina* and *R. stylosa*, respectively. The more likely is that this effect was induced by the decrease of stomatal conductance, as previously reported by Lammertsma *et al.* (2011), which was already observed in mangrove trees grown under elevated CO_2 (Snedaker and Araújo 1998; Reef *et al.* 2015). Decrease in stomatal density, and thus in stomatal conductance, probably contributed to the decrease in transpiration rates (Fig. IV-3). The combination between higher net photosynthetic rates and lower transpiration rates leaded to an increase in water-use efficiency, and our results showed that this parameter was enhanced by more than 45% for *A. marina* and more than 50% for *R. stylosa* under elevated CO_2, consistently with previous observations (Reef *et al.* 2015). As atmospheric CO_2 concentrations will continue to rise in the future (Collins *et al.* 2014), it is possible that the stomatal density will continue to decline, thereby preventing water loss by further reduction of transpiration rates. Improving water-use efficiency might be a key for mangroves to resist drought episodes, which will increase in frequency with future climate change (Dai 2013). Due to the semi-arid climate, mangrove trees in New Caledonia are often stunted in growth, suffering from the lack of water, and, thus, they have a limited productivity (Leopold *et al.* 2016). Enhancement of water-use efficiency with future climate change will, in return, promote growth and productivity of these trees, and finally will improve their carbon fixation and as so, their role in climate change mitigation. Expanding mangrove forests within arid and semi-arid regions is another major challenge, as it could be the case, for example, on the west coast of South Africa. In this region, mangrove expansion is limited to the tropics, notably due to the aridity of the Sahara Desert in the north, and the Namib Desert in the south (Ward *et al.* 2016) preventing mangroves seedlings from colonizing the northern and southern subtropical areas.

IV.1.5. Conclusion

Our results highlight that future climate changes, and particularly elevated CO_2 and increased tidal flooding duration, will strongly affect mangroves physiology. In this study, elevated CO_2 (800 ppm) significantly enhanced photosynthesis by more than 37% and 45% for *A. marina* and *R. stylosa*. However, our results do not support the previous observations of a downregulation of photosynthesis. Additionally, dark respiration was not affected by elevated

CO_2, therefore implying a higher carbon gain for the mangrove seedlings studied. Season was also a key driver of the leaf-gas exchanges, with an increase of photosynthesis during the warm period for both species. Consequently, future increase in global temperatures with climate change will further enhance the productivity of the trees, as long as it does not exceed the species-specific optimal temperature for photosynthesis. When increasing tidal flooding duration, photosynthetic rates were slightly reduced but not enough to offset the carbon gain induced by the elevated CO_2 concentrations. Additionally, elevated CO_2 reduced transpiration rates, leading to a significant increase in water-use efficiency, which may favor mangrove expansion, specifically in arid or semi-arid regions. As both species responded similarly to the experiment, we suggest that climate changes may not favor the development of one species over the other, and thus may not affect their relative repartition along the intertidal areas. This study thus provided useful information about the response of mangrove seedlings to future climate change. Further research will now be needed to evaluate the effects of future climate change on the carbon storage capacities of the whole ecosystem. Indeed, mangroves are recognized for their major role in carbon sequestration in their biomass, but also and mainly in their soils. Therefore, understanding how elevated CO_2 and prolonged water flooding will affect mangrove plant tissues composition, and thus the diagenesis of mangrove-derived organic matter in soils could help to understand the future role of mangrove ecosystems in climate change mitigation.

Acknowledgments

This research was supported by the Province Sud of New Caledonia, the City of Mont Dore, KNS Koniambo Nickel SAS, and Vale NC. We are grateful to the IFRECOR Committee for having attributed to this study the IFRECOR Palme National Distinction. We thank Eric Gay, the mayor of Mont-Dore, for his continuous support during the study. We also thank Jacky Mermoud and Diana Burns for assistance with managing the facilities, as well as Laure Barrabe, Tracy Rolland and Inès Gayral for their help in field work. We are also very grateful to Emeritus Pr Karen L. Mckee for her helpful comments on the manuscript.

Partie 2.

Effects of elevated atmospheric CO_2 and longer tidal flooding on growth, biomass, and C:N ratios of two common mangrove species: *Avicennia marina* and *Rhizophora stylosa*

Adrien Jacotot, Cyril Marchand, Simon Gensous, Michel Allenbach

Abstract

The effects of CO_2 enrichment and increased tidal flooding on more than 1,000 two-years old *A. marina* and *R. stylosa*, the most widespread mangrove species within the Indo-Pacific region, were investigated during a one-year experiment. Plants were grown in greenhouses for ambient CO_2 and in CO_2-controlled closed chambers, placed inside the greenhouses, for elevated CO_2 (800 ppm). Tidal flooding duration was set-up conformingly to their specific distribution in New Caledonia, and increased by 1h45 in the longer treatment. Growth, above and below-ground biomass, as well as C:N ratios were determined. We observed a net positive effect of elevated CO_2, which stimulated final biomass by more than 46% and 32 % for *A. marina* and *R. stylosa*, respectively. In addition, the C:N ratios increased for both species. Longer tidal flooding had contrasting effects on *A. marina* and *R. stylosa*. Growth and biomass of *R. stylosa* was reduced with longer tidal flooding, probably due to more anaerobic conditions in the soil that resulted in a photosynthesis decrease. Conversely, growth and biomass of *A. marina* were stimulated, suggesting that *A. marina*, developing at higher elevation than *Rhizophora*, experience a strong water stress in its actual position in the intertidal area in the specific semi-arid climate of New Caledonia. These results provide useful information that may help to understand the future evolution of mangrove ecosystems. In addition, they suggest that the colonization capacity of mangrove seedlings in available accommodation spaces may be enhanced with future climate change.

Keywords: Mangrove, Elevated CO_2, Sea-level rise, Growth, Biomass, Climate change

IV.2.1. Introduction

The steady increase in anthropogenic greenhouse gas emissions since the preindustrial age resulted to a substantial augmentation of the atmospheric CO_2 concentrations, from 280 ppm to over 400 ppm currently (Betts *et al.*, 2016). This increase implies a strong global

warming (Cook *et al.*, 2016), which, in turn, leads to an increase of the mean sea-level. Projections agree that atmospheric CO_2 concentrations will continue to rise in the future, and, depending on simulation model, they are more likely to range from 794 to 1,150 by the end of the 21st (Collins *et al.*, 2014). As a result, the global mean sea-level is expected to increase from 0.26 to 0.98 m by 2100 (Church *et al.*, 2013).

Many studies investigated the response of C3 terrestrial plants to elevated CO_2 concentrations, which mainly results to photosynthesis stimulation and higher productivity (Norby *et al.*, 2005; Prior *et al.*, 2011). Mangrove ecosystems are constituted of halophytes C3 trees developing along tropical and subtropical coastlines. Due to their high primary productivity (average of 218 ± 72 Tg C yr^{-1}) (Bouillon *et al.*, 2008), they are considered as major ecosystems in the coastal carbon cycle, and have therefore been named "blue carbon" sinks (Mcleod *et al.*, 2011). Only a few studies have focused on the response of mangroves to elevated CO_2 concentrations, also showing an increase in productivity (Ball *et al.*, 1997; Farnsworth *et al.*, 1996; Luo *et al.*, 2010; McKee and Rooth, 2008; Reef *et al.*, 2016), and highlighting their valuable role on climate change mitigation. However, mangrove response to elevated CO_2 concentrations may be strongly dependent of other biotic and abiotic factors such as temperature, nutrient availability, or flooding (Alongi, 2015).

Although the increase of atmospheric CO_2 concentrations may have positive effects on mangroves, the major threat of climate change may come from the increase in global mean sea-level due to their position between land and sea (Ellison, 2015; Ward *et al.*, 2016). Mangrove ecosystems have the capacity to cope with sea-level rise through surface elevation change processes (Krauss *et al.*, 2014), however this capacity is influenced by several factors (Ward *et al.*, 2016) and may be specific to each mangrove forest. In fact, Lovelock *et al.* (2015) reported that 69% of mangroves surveyed in the Indo-Pacific region were not building surface elevation at rates that equal or exceed sea-level rise. As a consequence, these mangroves will experience major changes in their tidal flooding duration if their inland migration is prevented by coastal human activities (Gilman *et al.*, 2008).

Consequently, future climate changes may have several positive or negative effects on the evolution of mangrove ecosystems. Due to their interactive effects and potential feedback, the different parameters of climate changes have to be studied jointly. To our knowledge, only a handful studies were interested in the evolution of mangroves with climate change, and they

focused on elevated CO_2 in interaction with salinity (Reef *et al.*, 2015), nutrient availability (McKee and Rooth, 2008; Reef *et al.*, 2016) or species competition (McKee and Rooth, 2008), and to date, no study investigated the interactive effect of elevated CO_2 concentrations and tidal flooding duration.

Within this context, this study aimed to evaluate the response of *Avicennia marina* and *Rhizophora stylosa* to the long-term effects of elevated CO_2 and tidal flooding duration. *Avicennia marina* and *Rhizophora stylosa* are two common and widespread mangrove species throughout the Indo-Pacific region (Buchmann *et al.*, 2008; Ellison *et al.*, 2008). The questions we wanted to answer were: (i) Does atmospheric CO_2 enrichment lead to a stimulation of growth and biomass? (ii) Does tidal flooding duration conduct to a reductionof growth due to waterlogging stress? (iii) What will be the effects of these two parameters to the C:N ratios of the different plant tissues? To reach our goals, we designed a closed chambers experiment, where more than 1,000 two-year-old mangrove seedlings were grown at two CO_2 concentrations (400 vs 800 ppm), over two tidal flooding durations (one typical of New Caledonian mangroves, and one longer) during one complete year. Plants heights and basal diameters were monitored throughout the year, and plant biomass, as well as carbon and nitrogen contents were measured after harvest at the end of the experiment.

IV.2.2. Materials and Methods

IV.2.2.1. Description of the facility

The experiment was conducted in New Caledonia (22°13'49"S, 166°31'09"E) from June 2016 to May 2017 in three semi-open greenhouses of 72m² each (12 m x 6 m, 6 m height). Inside each greenhouse, a circular closed chamber of 36 m² (2.4 m height) area was built to maintain elevated atmospheric CO_2 concentrations. The atmospheric CO_2 concentrations in each of the three closed chambers was supplied from 5:00 am to 7:00 pm and was continuously monitored using CO_2 probes connected to a CO_2 central unit, which controlled the entire system (MAXICLIM NG 08/3Z, Anjou Automation).

Air temperature and humidity were recorded every 5 min inside the greenhouses and the closed chambers with HOBO sensors (Onset, Cape Cod, Massachusetts, USA). Temperature and humidity were allowed to fluctuate naturally inside the greenhouses, however air cooling units were installed in the closed chambers to prevent high variations of temperatures. Mean

temperatures during the experiment period were 25.14 ± 2.93 and 25.00 ± 3.31 °C for inside the greenhouses and the closed chambers, respectively. Relative humidity was 82.62 ± 13.56 % inside the greenhouse and 79.91 ± 12.55 % inside the closed chambers.

All mangrove seedlings were placed in custom tidal tables made of a 700 liters polypropylene water reserve (1 m² area over 0,7 m height), surmounted by a 300 liters planting tray (1 m² area over 0.3 m height), working as an individual unit. Fresh seawater was pumped from the adjacent sea and stored in the water reserve, which was replaced twice a month during the entire study. During high tide periods, an aquarium pump placed in each water reserves sent the water to the planting tray. During low tide periods, a siphon pipe allowed the planting tray to drain the water back to the reserve. To control the tidal treatment attributed to each tank, the aquarium pumps were connected to three open-source Arduino Uno cards (one per greenhouse) coupled to currents relays, which were programmed according to the needs of the experiments.

IV.2.2.2. Plant material

A total of 720 *R. stylosa* and 400 *A. marina* propagules were collected from the pristine mangrove of Oundjo, in New Caledonia (21°4'8"S, 164°42'51"E) during the optimum fruiting period, from February to March 2014. They were then planted individually in 2.5 liters polyethylene bags in a 1:1 hand mixed mangrove peat and sand, and grown for two years before the beginning of the experiment. The mangrove seedlings were allocated randomly between the tidal tables, with 25 *A. marina* or 30 *R. stylosa* in each tidal table, resulting in 100 *A. marina* (4 tidal tables) and 180 *R. stylosa* (6 tidal tables) for each of the four treatments (see below). The tidal tables were then distributed between the three greenhouses and the three closed chambers, according to their CO_2 treatment. During the experiment, the mangrove seedlings were regularly rotated within each tidal table, and were rotated three times between the greenhouses to minimize the greenhouse effect.

IV.2.2.3. Experimental design

The experiment was setup as a split-plot design with CO_2 atmospheric concentrations as the whole-plot (Ambient, 400 ppm vs. Elevated, 800 ppm) and tidal flood duration (TFD) as the split-plot nested within CO_2 (Natural vs. Longer). Elevated atmospheric CO_2 concentrations were maintained between 780 and 820 ppm CO_2. Natural TFD were set-up according to the

average flooding duration observed in New Caledonian mangroves for both species (unpublished data). In New Caledonia, mangroves develop in semi-arid conditions with a specific zonation of the ecosystem: *Rhizophora* spp. colonizes the seaward side, while *Avicennia marina* develops at higher elevations. As a result, the flooding duration for *Rhizophora* trees is higher than for *Avicennia*. Consequently, in the experiment, natural TFD were 3h15 for *A. marina* and 6h00 for *R. stylosa* for each high tide cycle. Simulated tidal cycles were semi-diurnal, meaning that there were two high tides and two low tides each day. We hypothesize that an increase in mean sea-level will similarly affect the flooding duration of both species; thus, in the experiment, longer TFD was simulated by increasing the natural times by 1h45. This increase in duration has been randomly defined, but however remains realistic given the expected sea-level rise at the end of the century. Nevertheless, an increase of 1h45 of tidal duration will have different implication for both species, as it corresponds to an increase of 45% of the natural tidal duration of *A. marina*, whereas it is only to 25% for *R. stylosa*. During high tide, the water level in the planting trays was identical for all tidal tables, 5 cm up to the surface sediment of the trees. At low tide, all the water in the planting tray was drained.

IV.2.2.4. Growth and biomass

All mangrove seedlings were measured for height and basal diameter. Measurement were realized five times during the experiment period: at the beginning, after 90, 180 and 260 days, and at the end of the experiment, when seedlings were three-years old. Destructing measurements were only realized at the end of the experiment. For each species and treatment, 30 seedlings were randomly selected for biomass measurements. All seedlings were separated into below and above-ground parts and were then carefully washed with deionized water. One fully expended leaf per seedling was scanned and analyzed for leaf area (SLA) using ImageJ (Schneider *et al.*, 2012). Then, all plant materials were dried at 60°C during 72 hours before being weighted for dry mass (g). Leaf mass area (LMA, g cm^{-2}) was calculated as the ratio of leaf dry mass to the corresponding leaf area. Relative growth rates (RGR) were calculated as the difference between final and initial biomass over the length of the experiment.

IV.2.2.5. Carbon and nitrogen content

Leaves, stems and roots were separately mixed in batches of ten individuals, totaling three batches per plant part for each treatment and each species. All batches were ground using a ball mill, and then homogenized. Three subsamples (approximately 2 mg) of each lot of leaves, stems and roots, were then analyzed for total carbon (TC) and nitrogen (TN) contents (%) using an elemental analyzer (Integra2, Sercon, UK). All the analyses were performed at the French Institute for the Sustainable Development (IRD) of Noumea, New Caledonia (France). The analytical precision was checked using IAEA-600 caffeine standard (IAEA Nucleus) and was 0.3% for C and 0.15% for N.

IV.2.2.6. Statistical analysis

Growth, biomass and C:N ratios were analyzed for significant differences ($p<0.05$) between treatments within each species. Normality and equality of variance were verified using Shapiro and Levenne tests, respectively. Following results, either a two-way analysis of variance (ANOVA), followed by a Scheffe post-hoc test or a Kruskal-Wallis test was applied. All statistical analysis were performed using R software version 3.3.1 (R Development Core Team, 2008) with the 'agricolae' package.

IV.2.3. Results and discussion

Elevated atmospheric CO_2 concentrations produced significant and positive effects on growth and biomass of *Avicennia marina* and *Rhizophora stylosa* (Fig. IV-9, Fig. IV-10 and Table. IV-3). Differential responses between elevated and ambient CO_2 were observed since the beginning of the experiment on both basal diameter and height (Fig. IV-9). However, the effect was significant only after six months of enrichment. At the end of the experiment, basal diameters increased from 7.65 ± 1.04 to 9.14 ± 1.38 mm, and from 7.43 ± 0.78 to 9.92 ± 0.89 mm for *A. marina* and *R. stylosa* respectively (Fig. IV-9a and b). Meanwhile, seedling heights increased from 211.74 ± 37.44 to 264.48 ± 41.46 mm for *A. marina* (Fig. IV-9b) and from 127.78 ± 20.60 to 185.35 ± 27.94 mm for *R. stylosa* (Fig. IV-9c). Consequently, final biomass of *A. marina* and *R. stylosa* increased from 18.19 ± 7.14 to 35.56 ± 3.77 g and from 42.87 ± 10.37 to 63.23 ± 10.11 g, respectively (Fig. IV-10a and b). Considering the entire experiment period, relative growth rates (RGR) increased by 35% and 56% for *A. marina* and *R. stylosa*, respectively. These increases in biomass and RGR are suggested to derive from the enhanced photosynthesis, which increased by more than 58% and 66%, for *A. marina* and *R. stylosa*,

respectively (Chap. II). However, this result may be surprising considering that it was reported that an increase of 30% of the photosynthesis resulted only in a 10% increase of the RGR (Kirschbaum, 2011). The same authors suggested that the excess of carbohydrates produced by photosynthesis enhancement may not be converted into plant tissues due to other resource limitations. Therefore, carbohydrates may accumulate in leaves as sugar and starch, resulting in an increase of the leaf mass area (LMA) (Poorter and Navas, 2003). However, in our experiment, a LMA decrease was observed for both species under elevated CO_2 concentrations, by 33% for *A. marina* (from 23.01 ± 6.14 to 15.50 ± 2.25 mg cm^{-2}) and by 21% for *R. stylosa* (from 25.76 ± 2.21 to 20.27 ± 4.39 mg cm^{-2}). Therefore, we consider that in our experiments, due to tide simulation and frequent water renewal, *A. marina* and *R. stylosa* growth were not limited by other resources, explaining the high RGR values measured.

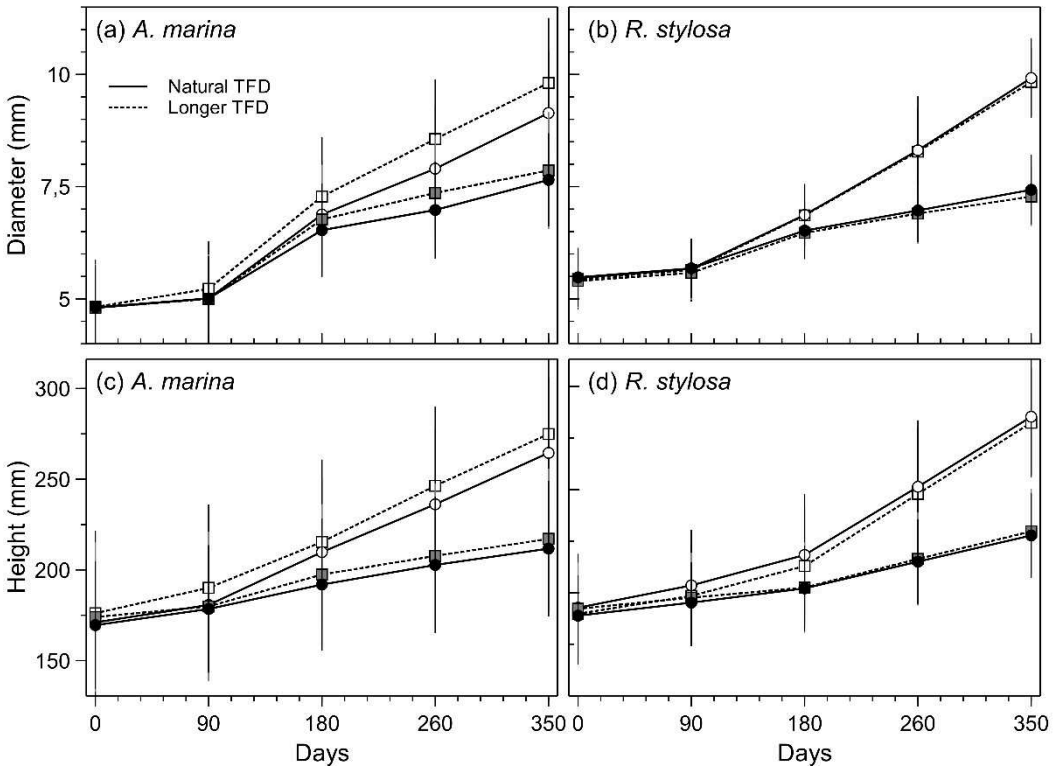

Fig. IV-9: Changes in basal stem diameter and heights of *Avicennia marina* and *Rhizophora stylosa* grown in ambient (closed symbols) or elevated (open symbols) CO_2, and two lengths of tidal flooding: normal (solid lines) and longer (dotted lines). Values are means ± SD (*A. marina n*=125; *R. stylosa n*=180).

Elevated CO_2 altered the above to below-ground ratio by further increasing the above-ground parts than the below-ground ones (Fig. IV-10c and d). This carbon allocation with elevated CO_2 has been previously observed for *A. germinans* by Reef *et al.* (2016). This newly gained carbon investment reveals a strategy of light capture and photosynthesis optimization

at the expense of soil resources utilization through roots uptake This result was consistent to our previous observation of an increase of the specific leaf area for both species grown under elevated CO_2 (Chap. II). Although more carbon was invested in above-ground parts, significant increase was also observed in the below-ground biomass for both species (Fig. IV-10a and b). This result may lead to several benefic implications for the future evolution of the ecosystem with climate changes: (i) the soil carbon storage potential of the ecosystem may increase, (ii) the increase in root development may facilitates seedings establishment in intertidal sediments (Balke *et al.*, 2011), which may, in turn, promote the ecosystem expansion, and (iii) the capacity of mangrove ecosystems to face sea-level rise may be improved, as higher root density will increase the soil volume and the soil organic matter content, which are two important factors contributing to the vertical accretion of mangrove soils (Cahoon *et al.*, 2006; Krauss *et al.*, 2014, 2017; McKee *et al.*, 2007; McKee, 2011).

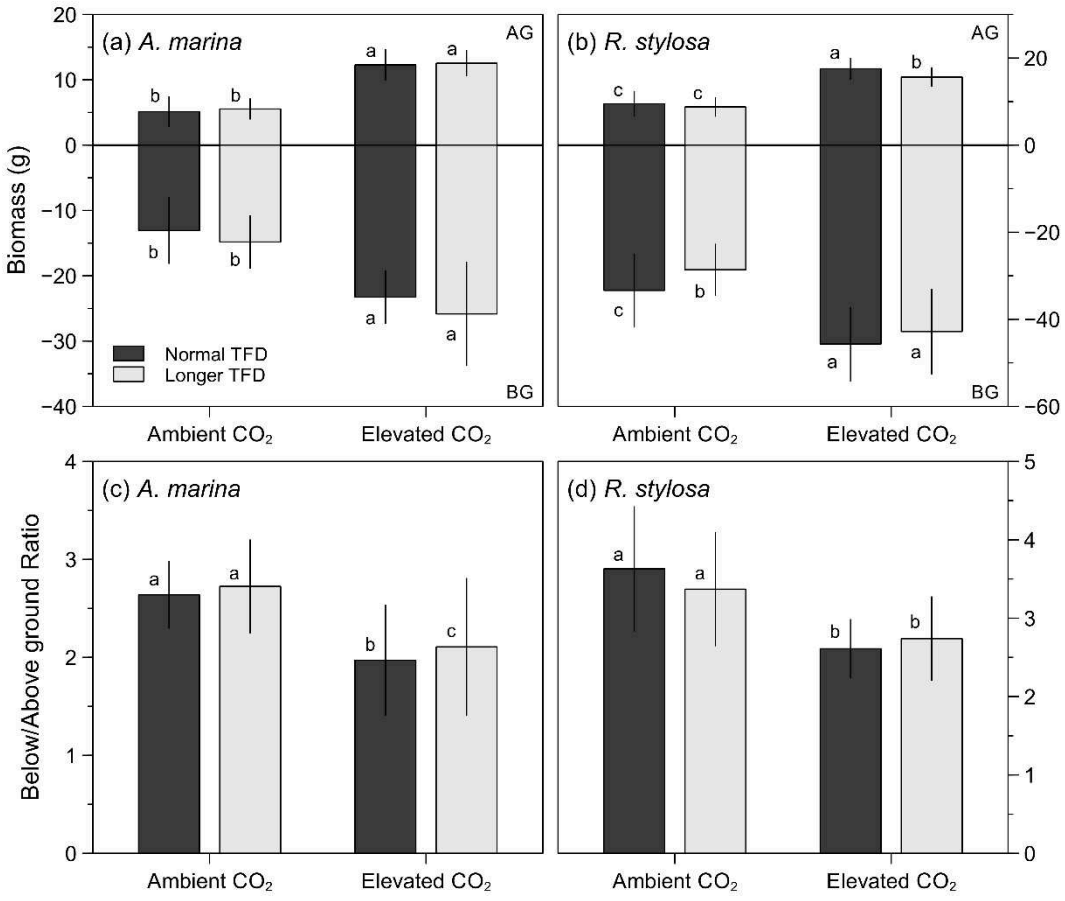

Fig. IV-10: Final above-ground (AG) and below-ground (BG) biomass (g), and below/above ground biomass ratios of (a, and c) *Avicennia marina* and (b, and d) *Rhizophora stylosa* grown in ambient or elevated CO_2, and under normal (dark-grey bars) and longer TFD (grey bars), for 12 months. Values are means ± SD (n=30). Different letters indicate significant differences after ANOVA and Scheffe post-hoc test (p<0.05).

McKee and Rooth (2008) demonstrated that species competition may be an important offset of growth under elevated CO_2. In their study, growth of *A. germinans* was partially inhibited when grown in a mixture with a C4 saltmarsh grass *Spartina alterniflora*. This later result is of importance, considering that, in New Caledonia, the mangrove ecotone is composed of a succession of different mangrove species, including a saltmarsh C4 grass, *Sarcocornia quinqueflora,* which compete for suitable spaces for expansion, and future climate may change their specific distribution.

Table. IV-3. Significance values reported by two-way analysis of variance (ANOVA), followed by a Scheffe post-hoc test or a Kruskal-Wallis test.

	Avicennia marina			*Rhizophora stylosa*		
	CO_2	TFD	Interaction	CO_2	TFD	Interaction
Height	203.115***	4.122*	0.422^{NS}	973.178***	0.062^{NS}	1.803^{NS}
Diameter	202.216***	17.143***	1.303^{NS}	1830.189***	4.385*	0.198^{NS}
Biomass	179.689***	2.224^{NS}	0.078^{NS}	134.827***	8.294**	0.037^{NS}
C:N						
Leaves	14.865***	0.007^{NS}	0.446^{NS}	28.363***	0.011^{NS}	0.083^{NS}
Stems	43.518***	3.243^{NS}	6.096***	87.655***	0.281^{NS}	0.074^{NS}
Roots	0.133^{NS}	0.846^{NS}	0.071^{NS}	115.124***	3.769^{NS}	0.689^{NS}

***, **, * indicates significant effects at p<0.001, 0.01, and 0.05, respectively. *NS*: non-significant

In addition to differences in growth and biomass, we also observed a significant evolution of plant composition, notably with an increase in the C:N ratios for both *A. marina* and for *R. stylosa* under elevated CO_2, at the exception of *A. marina* stem that remained unaffected (Table. IV-3 and Table. IV-4). The response of C:N ratios to elevated CO_2 has been extensively examined in natural ecosystems, however the available literature shows contrasting results (Gifford *et al.*, 2000; Luo *et al.*, 2006). C:N ratios may increase, decrease or be unaffected under elevated CO_2, but the most common result is a 15% increase (Gifford *et al.*, 2000). In our study, the increase in C:N ratios was mainly due to a decrease in nitrogen content in the plant tissues (Table. IV-3). Such a response of a decrease of nitrogen content with elevated CO_2 has often been observed in terrestrial plants (Ainsworth and Long, 2005; Cotrufo *et al.*, 1998; De GRAAFF *et al.*, 2006; Yin, 2002), including mangroves (McKee and Rooth, 2008), but remains poorly understood (Lotfiomran *et al.*, 2016; Taub and Wang, 2008). Decrease in N concentrations may result from the decrease of roots ability to supply N due to a lower development of the root system relatively to the above-ground parts under elevated CO_2 (Fig. IV-9).

In addition, some authors showed a general decrease in the specific uptake rates of N by roots under elevated CO_2 (Lotfiomran *et al.*, 2016; McDonald *et al.*, 2002; Taub and Wang, 2008). These authors suggested that this decrease results from both a decrease in N demand by shoots and of a reduce ability of the soil-root system to supply N. They also suggested that the best-supported mechanism for decreased N supply is a decrease in transpiration-driven mass flow of N in soils due to decreased stomatal conductance at elevated CO_2. In fact, such a decrease in stomatal conductance was effectively observed for *A. marina* and *R. stylosa* grown under elevated CO_2 (Chap. II), therefore adding to this last hypothesis. Higher C:N ratios implies lower rates of organic matter decomposition in soils (Hättenschwiler and Gasser, 2005; Jacob *et al.*, 2010; Zhang *et al.*, 2008; Zimmermann *et al.*, 2009), which may lead to a reduction in the greenhouse gas production, and, in turn, to a higher carbon storage capacity.

Table. IV-4. Results of C:N ratios in leaves, stems and roots of *A. marina* and *R. stylosa* grown in ambient or elevated CO_2, and under normal (N) and longer (L) TFD, for 12 months. Values are means ± SD. (*n*=3).

C:N	Ambient CO_2 (400ppm)		Elevated CO_2 (800 ppm)	
	N TFD	L TFD	N TFD	L TFD
Avicennia marina				
Leaves	36.53 ± 3.28	35.41 ± 3.56	41.30 ± 1.77	42.18 ± 0.57
Stems	72.65 ± 5.99	71.27 ± 0.73	72.45 ± 3.68	69.94 ± 1.82
Roots	52.56 ± 0.67	53.20 ± 1.30	61.22 ± 1.51	57.14 ± 2.56
Rhizophora stylosa				
Leaves	61.75 ± 0.96	62.02 ± 3.67	70.06 ± 1.59	69.47 ± 3.05
Stems	130.85 ± 2.90	119.26 ± 4.92	172.26 ± 12.94	167.61 ± 3.56
Roots	101.57 ± 3.57	100.02 ± 7.28	159.64 ± 5.87	154.80 ± 18.32

Accordingly to our initial hypothesis, growth and biomass of *R. stylosa* were slightly reduced with longer, relative to natural, tidal flooding duration (TFD) (Fig. IV-9 and Fig. IV-10). However, this effect was not significant (Table. IV-4). Under longer TFD, basal diameters decreased by 13% and by 5% for ambient and elevated CO_2, respectively. Seedlings heights were also reduced, by 6% and 11%, respectively (Fig. IV-9b and d). Consequently, final biomass of *R. stylosa* decreased from 7.36 ± 0.88 to 6.51 g and from 9.71 ± 0.66 to 9.26 ± 0.65 g under ambient and elevated CO_2, respectively (Fig. IV-10b). This decrease may result from the photosynthesis decrease that was observed for *R. stylosa* under longer TFD (Chap. II). In addition, longer TFD probably resulted in a more anoxic soil, with enhanced sulfate-reduction decay processes (Balk *et al.*, 2016; Kristensen *et al.*, 2008). Sulfides compounds, produced

during organic matter decomposition in marine environments, are strongly toxic to plants (Lamers *et al.*, 2013; Reef *et al.*, 2010), and thereby negatively affect their growth. Although no oxygen or sulfur measurements were realized in our experiment, the dark color of the sediment, as well as the strong rotten egg odor typical of H_2S gas, observed during harvest of *R. stylosa* seedlings grown with longer TFD added to the hypothesis of growth inhibition due to the more anoxic environment.

In contrast, final biomass of *A. marina* seedlings increased with longer TFD from 18.19 ± 7.14 to 20.36 ± 5.23 g and from 35.56 ± 3.77 to 38.38 ± 7.99 g under ambient and elevated CO_2 concentrations, respectively (Fig. IV-10a). Natural TFD were based on our field observations and measurements (unpublished data), and thus were representative of the natural conditions in which both species develop in New Caledonia, with *A. marina* at a higher elevation than *R. stylosa* along the intertidal gradient. This position, in combination with the semi-arid climate, implies *A. marina* to suffer from the lack of water and thus to have a limited productivity (Leopold *et al.*, 2016). In addition, due to the lower frequency of tidal submersion, soil salinity is higher under *A. marina* than under *R. stylosa* (Marchand *et al.*, 2011, 2012). Therefore, we suggest that increase in TFD for *A. marina* resulted in an increase in water availability, and to a decrease in soil salinity, which are two stressing parameters affecting growth and biomass. Consequently, due to the positive response of the seedlings in growth and biomass to increased TFD and CO_2 concentrations, *A. marina* colonization abilities could be enhanced with future climate change.

IV.2.4. Conclusion

Our results suggest that future climate changes, and specifically the increase of atmospheric CO_2 concentrations will have positive effects on *A. marina* and *R. stylosa* seedlings, as growth and biomass of both species were strongly stimulated under elevated CO_2 concentrations. Although a slight reduction effect of longer tidal flooding duration was observed for *R. stylosa*, this effect did not significantly affect the initial enhancement of growth and biomass due to elevated CO_2. This negative effect was not observed for *A. marina*, suggesting that this later may have stronger capacities in seedling recruitment and thus area expansion in the future. As below-ground biomass was also significantly enhanced by elevated CO_2 concentrations, we suggest that the capabilities of mangroves in vertical soil accretion will be further improve in the future, helping them to face sea-level rise, or to colonize new

available spaces by increasing seedlings establishment. In addition, elevated CO_2 concentrations significantly modified tissues quality by increasing the C:N ratios, indicating that, in the future, the role of mangrove ecosystems in carbon sequestration may be further enhanced with the production of organic matter more refractory to decomposition. We suggest that this latter hypothesis should be a main topic of future research on the evolution of mangrove ability to store carbon with future climate changes.

Acknowledgments

This research was supported by the Province Sud of New Caledonia, the City of Mont Dore, KNS Koniambo Nickel SAS and Vale NC. We are very grateful to the IFRECOR Committee for having attributed to this study the IFRECOR Palme National Distinction. We thank Eric Gay, the mayor of Mont-Dore, for his continuous support during the study. We also thank Jacky Mermoud and Diana Burns for assistance with managing the facilities, as well as Laure Barrabe, Tracy Rolland and Inès Gayral for their help in field work.

CHAPITRE V Synthèse générale et perspectives

En conséquence des changements climatiques générés par les activités anthropiques, et en prévision de leurs effets futurs, l'attention internationale s'est récemment tournée vers les écosystèmes capables de contribuer à leur atténuation. Ce nouvel intérêt a notamment permis de mettre en évidence le rôle que jouent les écosystèmes côtiers dans la régulation du climat. C'est notamment le cas des mangroves qui ont une productivité primaire élevée, couplée d'une part à des grandes capacités de stockage du carbone organique dans leur sol et qui, d'autre part, sont en capacité de le piéger sur de longues périodes de temps. En outre, malgré un sol riche en matière organique, la mangrove est un écosystème qui émet peu de gaz à effet de serre, lorsque l'on compare à d'autres écosystèmes. Toutefois, ce service écosystémique pourrait être partiellement modifié par les changements climatiques. Plus précisément, certains paramètres tels que l'augmentation du CO_2 atmosphérique, des températures et du niveau marin pourraient impacter l'écosystème. Malheureusement, la mangrove reste relativement peu étudiée et son fonctionnement est encore trop énigmatique pour conclure précisément sur son futur. C'est particulièrement le cas dans certaines régions du monde où la mangrove fait front, non seulement à des profonds changements environnementaux, mais aussi à une pression anthropique directe qui participe à sa disparition. Dès lors, définir des problématiques de recherche en liaison avec l'étude de l'impact des changements climatiques s'imposait comme une véritable nécessité. Les recherches menées durant ce travail ont consisté à : (i) comprendre l'impact de la régression marine de la fin de l'Holocène sur la distribution de la végétation de surface, et, par conséquent, sur les stocks de carbone organique enfouis dans les sols ; (ii) évaluer l'amplitude des émissions de dioxyde de carbone et de méthane émis vers l'atmosphère, depuis les sols et la colonne d'eau, et déterminer les différents facteurs qui influent sur ces émissions ; et (iii), déterminer l'impact des augmentations des concentrations en CO_2 atmosphérique et du niveau marin sur les échanges gazeux foliaires, ainsi que sur la croissance et la biomasse de jeunes plantules d'*Avicennia marina* et de *Rhizophora stylosa*. Le travail ainsi mené, autour de ces trois objectifs, nous permet d'écrire une synthèse reprenant les résultats majeurs obtenus. Cette synthèse sera suivie d'une proposition de perspectives de recherches qui font directement suite à cette étude.

V.1. Résultats majeurs

Effets de l'augmentation des concentrations en CO_2 atmosphérique, du niveau marin et des températures sur la dynamique du carbone dans l'écosystème mangrove

Élévation du CO_2 atmosphérique (800 ppm)

L'impact de l'augmentation du CO_2 atmosphérique sur le développement et la physiologie d'*Avicennia marina* et de *Rhizophora stylosa* a principalement été testé dans des serres à atmosphère contrôlée, dans lesquelles les concentrations en CO_2 atmosphérique ont été fixées à 800 ppm, le double des concentrations actuelles (400 ppm), afin de simuler celles attendues pour la fin du XXI^{e} siècle. Nous avons pu constater que les jeunes plants d'*A. marina* et de *R. stylosa* se sont montrés hautement réactifs à cette augmentation. Leur activité photosynthétique a notamment fortement augmenté, de 37% pour *A. marina* et de 40% pour *R. stylosa*, en comparaison à des plants témoins placés sous CO_2 ambiant (*c.f.* Chapitre IV Partie 1). À l'opposé, l'augmentation du CO_2 atmosphérique n'a pas affecté le taux de respiration. Cet accroissement de la quantité de carbone fixé, sans augmentation de la perte par respiration, implique un gain en carbone supplémentaire pour les deux juvéniles étudiés. Ce gain se fait directement ressentir dans les taux de croissance, qui ont augmenté de 35% et 56% pour *A. marina* et *R. stylosa*, respectivement (*c.f.* Chapitre IV Partie 2). En conséquence, après une année complète d'enrichissement en CO_2 atmosphérique, la biomasse d'*A. marina* et de *R. stylosa* a augmenté respectivement de 46% et de 32%, en comparaison aux plants qui ont grandi sous CO_2 actuel (400 ppm) (*c.f.* Chapitre IV Partie 2). Ainsi, il est possible que la croissance des jeunes plantules de palétuvier soit plus rapide avec les futurs changements climatiques, ce qui, par conséquent, pourrait augmenter la quantité de carbone stockée dans la biomasse de l'écosystème.

Par ailleurs, on constate que le rapport entre les parties aériennes et les parties souterraines a été modifié par l'augmentation du CO_2 atmosphérique. En effet, après une année d'enrichissement, une plus grande quantité de carbone a été investie dans les parties aériennes (tiges et feuilles) que dans les parties souterraines (système racinaire), ce qui n'est pas le cas des plantules qui ont grandi sous des concentrations ambiantes en CO_2 atmosphérique. Cependant, même si la biomasse aérienne a été préférentiellement stimulée par les augmentations de CO_2, la biomasse racinaire a tout de même été significativement

augmentée (*c.f.* Chapitre IV Partie 2). Cette augmentation de la biomasse racinaire avec la hausse des concentrations en CO_2 atmosphérique pourrait faciliter la lutte de l'écosystème contre la hausse du niveau marin en accroissant le volume du sol, et, par conséquent, en facilitant l'accrétion verticale du sédiment.

À de plus petites échelles, l'augmentation du CO_2 atmosphérique a significativement stimulé la surface foliaire des deux espèces étudiées (*c.f.* Chapitre IV Parties 1 et 2). Cet accroissement de la surface foliaire se révèle être une stratégie d'investissement du carbone qui permet aux deux palétuviers d'optimiser leur potentiel photosynthétique, et par conséquent, d'augmenter davantage leur gain en carbone par la photosynthèse. Cette stratégie d'investissement du carbone, adoptée à la fois par *A. marina* et par *R. stylosa* signifie aussi que leur croissance n'est pas limitée par d'autres ressources, telles que la disponibilité en nutriments dans les sols. Par conséquence, la capture d'azote par le système racinaire est réduite et la quantité d'azote présent dans les tissus végétaux diminue. Ce phénomène se traduit par des rapports C/N plus forts lorsque les plantes ont grandi sous CO_2 atmosphérique élevé. On a, en effet, pu constater qu'après un an complet d'enrichissement, les rapports C/N ont significativement augmenté dans les trois principaux compartiments (*i.e.* dans les feuilles, dans les tiges, et dans le système racinaire) d'*A. marina* et de *R. stylosa* (*c.f.* Chapitre IV Parties 1 et 2). Cette augmentation des rapports C/N peut avoir des répercussions importantes sur les taux de décomposition de la matière organique du sol. En effet, il a été montré que plus les rapports C/N sont importants, plus la matière organique est difficile à dégrader par les micro-organismes. Ainsi, il est possible que l'accroissement des concentrations en CO_2 atmosphérique augmente davantage le stock en carbone organique de l'écosystème, déjà élevé à l'heure actuelle (*c.f.* Chapitre II). Cela sera dû, premièrement, à l'intensification de la productivité d'*A. marina* et de *R. stylosa*, et donc de leur biomasse, aérienne et racinaire, et, deuxièmement, à la diminution de la vitesse de dégradation de la matière organique dans le sol, qui pourra, par conséquent, s'accumuler en plus grande quantité et sur de grandes échelles de temps.

<u>Augmentation de la durée d'immersion par la marée due à la hausse du niveau marin</u>

Avec la hausse du niveau marin, il est probable que les zones intertidales soient recouvertes par les marées pendant de plus longues périodes. Ainsi, les mangroves, qui se développent le long de ces zones, subiront des périodes d'immersions prolongées, ce qui

pourrait impacter la physiologie des palétuviers qui les composent. L'augmentation de la durée de chaque marée haute de 1h45 (*c.f.* Chapitre IV) a provoqué une réduction de l'activité photosynthétique de 5% et de 3 % chez *A. marina* et chez *R. stylosa*, respectivement (*c.f.* Chapitre IV Partie 1). Il semblerait que cette réduction provienne du déficit en oxygène du sol, induit par la prolongation des durées d'immersion. En effet, ce déficit en oxygène semble provoquer la fermeture des stomates due à la production d'acide abscissique. En revanche, même si l'augmentation de la durée d'immersion tidale réduit légèrement la photosynthèse, des effets contrastés ont été observés sur la croissance, et par conséquent, sur la biomasse, des deux espèces étudiées. En effet, alors que la biomasse de *R. stylosa* a été réduite de 11% lorsqu'il a grandi sous une longue durée d'immersion tidale, celle d'*A. marina* a, au contraire, augmenté de 12% (*c.f.* Chapitre IV Partie 2). Cette dissymétrie s'explique par les zones d'occupation actuelles de ces deux espèces sur les zones intertidales. En Nouvelle-Calédonie, *Rhizophora* occupe principalement la partie infralittorale (*c.f.* Chapitre I § 1.2.2) et est donc soumis à une immersion régulière par les marées, et sur une période de temps relativement longue (en moyenne 6h à chaque marée haute). L'augmentation de cette durée provoque une diminution de la quantité d'oxygène dans le sol. Cette anoxie favorise les processus de sulfato-réduction, qui produisent des composés sulfurés toxiques pour la plante, qui, à leur tour, limitent la croissance de cette dernière (*c.f.* Chapitre IV Partie 2). Par conséquent, il semblerait que *Rhizophora* se développe, de nos jours en Nouvelle-Calédonie, à la limite de sa zone de confort. C'est tout le contraire pour *A. marina* qui se développe plus en amont de la zone intertidale (*c.f.* Chapitre I § 1.2.2). Cette position est immergée moins fréquemment par les marées, ce qui diminue la disponibilité en eau qui est alors insuffisante pour maintenir une croissance optimale du palétuvier. En outre, la salinité de cette zone est plus élevée, relativement à la zone où se développe *R. stylosa*, à cause de l'évaporation intense induite par la radiation solaire et la canopée peu densifiée de cette espèce. Ainsi, la productivité et la croissance *d'A. marina* sont fortement limitées dans son milieu naturel en Nouvelle-Calédonie. L'augmentation de la durée d'immersion temporise ces stress naturels, et par conséquent, augmente la croissance et la biomasse des plantules (*c.f.* Chapitre IV Partie 2). Cet accroissement de la biomasse chez *A. marina* dû à l'augmentation du niveau marin est également observé lorsque les plantules sont soumises à l'augmentation du CO_2 atmosphérique. (*c.f.* Chapitre IV Partie 2). Ces différences dans la croissance et la biomasse peuvent avoir des répercussions importantes sur les stocks en carbone organique de

l'écosystème, qui, dès lors, devraient augmenter davantage dans la zone à *Avicennia* que dans la zone à *Rhizophora*. Toutefois, étant donné que le stock en carbone organique du sol lié au développement racinaire des palétuviers est, à l'heure actuelle, plus important sous *Avicennia* que sous *Rhizophora* (*c.f.* Chapitre III), cette différence de productivité ne modifiera pas la répartition du stock de carbone organique le long du gradient intertidal.

Cette hypothèse peut être appuyée par le fait que le recouvrement du substrat pendant de plus longues périodes de temps limite la diffusion de l'oxygène de l'atmosphère dans le sol qui, dès lors, peut devenir rapidement très anoxique. Par conséquent, la décomposition anaérobique de la matière organique va devenir de plus en plus dominante dans les sols des forêts actuelles. On constate, en effet, que les émissions moyennes de CO_2 vers l'atmosphère diminuent de 12% lorsque le sédiment est inondé par la marée alors, qu'au contraire, les émissions de CH_4 – issues de la méthanogénèse, un processus strictement anaérobique – sont, elles, multipliées par quatre (*c.f.* Chapitre IV Parties 1 et 2). Toutefois, comme les processus anaérobiques de décomposition de la matière organique sont moins efficaces que les processus aérobiques, le stock en carbone organique du sol devrait augmenter encore davantage.

Finalement, les variations du niveau marin provoquent des modifications plus globales de l'écosystème, qui se traduisent par une migration de l'ensemble des espèces qui tentent de rester dans leur zone d'accommodation préférentielle. Ces migrations se font sur des échelles de temps beaucoup trop longues pour être simulées. Cependant, en étudiant l'évolution passée de l'écosystème, il peut être possible d'avoir une idée de son avenir. En effet, l'enregistrement de certains indicateurs, tels que des tissus rouges caractéristiques des racines de *Rhizophora*, ainsi que des marqueurs géochimiques, tels que le rapport C/N et les signatures isotopiques $\delta^{13}C$ et $\delta^{15}N$ nous ont permis d'étudier l'impact engendré par les variations passées du niveau marin sur l'écosystème (*c.f.* Chapitre II). Ainsi, nous avons pu constater que pendant près de 3000 ans, durant l'Holocène tardif, lorsque le niveau marin était stable à environ 1 m de plus qu'actuellement, la mangrove se développait sur une position plus haute de la zone intertidale. En effet, *Rhizophora* se développait à cette époque au niveau de l'actuel tanne. Cette stabilité du niveau marin à, en outre, permis la stabilité de la forêt qui a accumulé des quantités très importantes de carbone organique (550 MgC ha^{-1}) dans son sol. La régression marine qui a fait suite à cette période de stabilité a permis aux différentes espèces de

palétuvier de progresser vers l'aval de la zone intertidale, au fur et à mesure que ce secteur devenait propice à leur développement (*c.f.* Chapitre II). Ainsi, il est fort probable que la future hausse du niveau marin provoque l'effet inverse, c'est-à-dire une migration vers l'intérieur des terres par les palétuviers. Toutefois, cette migration ne pourra se faire qu'à la stricte condition qu'aucun ouvrage anthropique ne bloque leur progression.

Température

La température n'est pas un paramètre qui a directement été testé dans les expériences que nous avons menées. Cependant, la variabilité climatique annuelle en Nouvelle-Calédonie impose une saison chaude et une saison fraîche. L'augmentation de la température pendant la saison chaude a notamment permis d'observer deux résultats contrastés. Premièrement, lorsque l'augmentation de température est combinée à des concentrations en CO_2 atmosphérique élevées, la capacité photosynthétique des jeunes plants d'*A. marina* et de *R. stylosa* est stimulée, ceux-ci fixent 40% de CO_2 atmosphérique supplémentaire en comparaison à leur taux de fixation durant la saison fraîche (*c.f.* Chapitre IV Partie 1). Deuxièmement, les émissions de CO_2 et de CH_4 depuis le sol vers l'atmosphère ont, elles-aussi, augmenté durant la saison chaude (*c.f.* Chapitre III Partie 1). De plus, le CH_4 s'est montré particulièrement sensible à l'élévation de la température en comparaison au CO_2, comme en témoignent les valeurs de Q_{10} – facteur par lequel il convient de multiplier les émissions pour une augmentation de 10°C en température – calculées à 7,61 pour le CH_4 et 2,39 pour le CO_2. En effet, l'élévation de la température a pour conséquence d'accroître les taux de décomposition de la matière organique dans le sol, à la fois par la respiration bactérienne, mais aussi par la méthanogénèse, et par conséquent les émissions de CO_2 et de CH_4 à la surface. Ainsi, il est probable que les augmentations futures des températures avec les changements climatiques vont agir sur l'écosystème. Ainsi, considérant les effets observés durant nos expériences, il est possible que l'augmentation des températures avec les futurs changements climatiques modifie, à la fois, les quantités de carbone stockées dans la biomasse, mais aussi les émissions de CO_2 et de CH_4 vers l'atmosphère. Toutefois, la hausse du niveau marin pourrait tempérer ces effets. Dans ce cas, des expériences de décomposition de la matière organique en fonction de ces différents paramètres du changement climatique permettraient d'apporter des éclairages sur ces questions.

Conquête de nouveaux espaces d'accommodation par *A. marina* et *R. stylosa*

Les différents paramètres des changements climatiques que nous avons étudiés dans ce travail s'accordent à montrer que la conquête de nouveaux espaces pour les jeunes plantules d'*A. marina* et de *R. stylosa* sera facilitée dans le futur. En Nouvelle-Calédonie, la zone d'arrière mangrove est constituée par un pré hypersalé que l'on nomme localement « tanne » (*c.f.* Chapitre I § 1.2.2). Cette zone, uniquement immergée lors des grandes marées d'équinoxe, est sursaturée en sel, et la disponibilité en eau y est très limitée. De fait, le tanne n'est actuellement colonisé que par une plante grasse halophile, *Sarcocornia quinqueflora* qui s'accommode de ces conditions stressantes, et notamment, sur la partie la plus aval de la zone. Avec les futures hausses du niveau marin et des concentrations en CO_2 atmosphérique, cette configuration pourrait se trouver modifiée. En effet, la hausse du niveau marin va réduire les concentrations en sel du tanne, et augmenter la disponibilité en eau dans le substrat. De plus, l'augmentation des concentrations en CO_2 atmosphérique va améliorer la gestion de l'eau chez les deux espèces de palétuviers étudiés (*c.f.* Chapitre IV Partie 1) et réduire leurs besoins en nutriments (*c.f.* Chapitre IV Partie 2). Par conséquent, la colonisation du tanne devrait être facilitée dans le futur, et il est possible que sa partie amont soit colonisée par *Sarcocornia quinqueflora*, alors que sa partie aval pourrait se faire coloniser par *A. marina* qui se développe à sa périphérie.

Ensuite, l'accroissement de la surface foliaire, et par conséquent du potentiel de capture de lumière, dû à l'augmentation du CO_2 atmosphérique (*c.f.* Chapitre IV Parties I et II), devrait permettre aux plantules d'*A. marina* et de *R. stylosa* de pouvoir coloniser des zones où la luminosité est faible. C'est, par exemple, le cas des zones de denses canopées, comme dans les strates à *Rhizophora* qui se développent sur les zones basses de la zone intertidale.

Finalement, le processus de colonisation de nouveaux espaces devrait être davantage facilité dans le futur, grâce à l'effet positif des augmentations en CO_2 atmosphérique sur la croissance du système racinaire (*c.f.* Chapitre IV Partie 1). En effet, il apparaît que le succès de l'établissement des plantules de palétuviers dépend fortement de l'expansion du système racinaire dans les premiers stades de croissance.

V.2. Perspectives de recherche

Ce travail s'inscrit parfaitement dans la compréhension de l'évolution de la mangrove face aux changements climatiques. Il a permis d'éclaircir certaines zones d'ombre et il ouvre la porte à de futurs questionnements, dont l'objectif final reste la compréhension du cycle du carbone actuel et futur de cet écosystème complexe et singulier.

Stockage de carbone organique à très long terme

Les sondages réalisés sur la mangrove de La Foa ont permis d'évaluer l'impact de la régression marine de l'Holocène tardif sur la distribution de la végétation de surface. Cette étude a montré la progression de la mangrove le long de la zone intertidale afin de se maintenir dans sa zone de confort. Toutefois, en cela, nous avons couvert seulement la moitié de cette période récente. En effet, on sait que l'Holocène est majoritairement caractérisé par une vaste transgression marine qui fait suite à la fonte des inlandsis de l'hémisphère nord. Le niveau marin a considérablement augmenté entre la période -10000 à -5000 ans, et la Nouvelle-Calédonie n'a pas échappé à ce phénomène (voir Cabioch *et al.*, 1989; Wirrmann *et al.*, 2011; Yamano *et al.*, 2014). Il est d'ailleurs possible que cette période ait vu apparaître les mangroves sur les zones où nous les connaissons actuellement. En effet, Baltzer (1982) décrit « un lit transgressif à restes de palétuviers » se développant sur des sédiments marins, eux-mêmes déposés sous les sols des actuelles mangroves qui forment la partie supérieure de la colonne sédimentaire (*c.f.* Chapitre II). C'est dans ce contexte qu'un forage profond vient d'être initié en collaboration entre l'IRD et l'Université de la Nouvelle-Calédonie. Cette future étude permettra – parmi d'autres objectifs secondaires – d'évaluer la capacité de séquestration du carbone organique de la mangrove sur le très long terme, en prenant en compte les variations eustatiques. En outre, retracer l'évolution passée de l'écosystème durant la transgression marine de l'Holocène pourra permettre de mieux comprendre comment la future hausse du niveau marin pourrait impacter son développement futur.

Minéralisation du carbone au sein des sédiments

Les études réalisées dans la mangrove de Ouemo (*c.f.* Chapitre III) font suite à des travaux précédents qui ont permis une première évaluation des émissions de CO_2 depuis les sols de mangrove en Nouvelle-Calédonie. Ces travaux ont, en outre, mis en évidence le rôle du biofilm de surface dans la régulation de ces émissions (voir Leopold *et al.*, 2015, 2013). L'apport

de l'instrumentation de pointe (analyseur CRDS) permet d'aller plus en avant dans l'évaluation de ces émissions et du rôle du biofilm, notamment grâce à l'évaluation simultanée du CO_2, du $\delta^{13}C\text{-}CO_2$, et du CH_4 (*c.f.* Chapitre III). Toutefois, il reste encore beaucoup de travail avant de pouvoir arriver à évaluer la contribution relative des différentes sources de production du CO_2 dans les émissions vers l'atmosphère, et c'est vers cette suite que devraient s'orienter les prochaines études lancées sur ce sujet.

Parallèlement aux mesures de flux de CO_2 et de CH_4, nous avons tenté de mesurer les flux de gaz sulfurés (*e.g.* le sulfure d'hydrogène H_2S, l'oxysulfure de carbone COS, et le disulfure de diméthyle DMDS) depuis les sols de la mangrove vers l'atmosphère. En effet, les sols de mangroves sont des environnements fortement anoxiques (*c.f.* Chapitres III et IV), et, de fait, la sulfato-réduction y a été reconnue comme étant le processus anaérobique dominant dans la dégradation de la matière organique (Alongi *et al.*, 2001; Balk *et al.*, 2016; Kristensen *et al.*, 1994, 2008). Par conséquent, les émissions de gaz sulfurés depuis les sols de mangrove vers l'atmosphère pourraient être élevées. Ce travail annexe a permis la mise au point d'une méthodologie d'analyse de ces composés grâce à l'utilisation d'une chromatographie gazeuse équipée d'un détecteur à photométrie de flamme (GC-PFPD). Cette méthodologie s'est révélée efficace et nous a permis de réaliser des mesures préliminaires de concentrations d'H_2S, de COS, et de DMDS dans les sols de la mangrove. Toutefois, du fait des concentrations très faibles, relativement au CO_2 ou au CH_4, la méthode développée nécessite encore quelques approfondissements avant de pouvoir être appliquée aux mesures d'émissions. L'utilisation de pièges cryogéniques afin de concentrer les gaz émis depuis le sédiment, mais aussi, de les préserver le temps de réaliser les analyses, semble être la piste à suivre pour terminer le développement de cette nouvelle étude. À ce jour, très peu d'informations existent sur l'étendue des émissions de gaz sulfurés depuis les sols de mangrove, et il est fort probable qu'elles soient davantage augmentées dans le futur, en liaison avec la hausse attendue du niveau marin qui pourrait rendre les sols de mangrove plus anoxiques à cause des périodes d'immersion prolongées.

<u>Simulation des changements climatiques</u>

Du fait du temps restreint imposé à la réalisation d'un travail de thèse, l'intégralité des résultats récoltés n'a pas pu être inclue dans ce manuscrit. Ces résultats contiennent notamment des analyses de fractionnement isotopique du carbone au sein du continuum

photosynthèse-plante-respiration. Ces résultats supplémentaires font l'objet d'une publication en cours de réflexion, qui sera prochainement préparée pour le journal *New Phytologist*.

Les serres à atmosphère contrôlée se sont révélées être une installation puissante dans la simulation des changements climatiques. Elles nous ont permis de progresser dans la compréhension de l'impact de l'augmentation du CO_2 atmosphérique et du niveau marin sur les palétuviers ; notamment sur les premiers stades de vie qui sont primordiaux dans le succès de l'établissement d'un individu et donc, dans le succès de l'extension de l'écosystème. Toutefois, le cycle du carbone en mangrove est régi par des processus complexes et interactifs et tous ces derniers n'ont pas été considérés au cours de ce travail. Par conséquent, bien d'autres expériences demandent encore à être réalisées au sein de cette installation. Par exemple, des expériences de décomposition de la matière organique en fonction des augmentations des concentrations en CO_2 atmosphérique, des températures et de la durée d'immersion, permettraient d'apporter des réponses sur son devenir dans les sols de mangrove et par conséquent, sur les émissions de gaz à effet de serre dans le futur. De telles expériences devraient, par ailleurs, nécessairement prendre en compte le biofilm de surface, étant donné l'impact qu'il semble avoir sur les émissions (*c.f.* Chapitre III Partie 1). De plus, dans notre étude, la croissance et la biomasse des juvéniles n'ont été testées que de façon individuelle. Cependant, en Nouvelle-Calédonie, *Avicennia* et *Rhizophora* se développent de façon successive sur les zones intertidales (*c.f.* Chapitre I § 1.2.2). Ainsi, la compétition entre ces espèces est un paramètre important qu'il convient de tester afin d'évaluer l'impact des changements climatiques sur leur répartition relative au sein de l'écosystème. C'est d'autant plus important qu'*Avicennia* est bordée dans sa partie amont par *Sarcocornia quinqueflora*, une halophyte qui peut impacter sévèrement son développement (voir par exemple McKee and Rooth, 2008).

Finalement, cette installation de simulation de l'impact des changements climatiques pourra évoluer vers un véritable laboratoire d'observation de la mangrove au sens large, dans le but d'explorer d'autres thématiques. L'impact des métaux lourds sur la croissance des palétuviers est l'idée première, considérant l'activité minière importante qui a lieu en Nouvelle-Calédonie (*c.f.* Chapitre I § 1.2.2). Les mines orphelines subissent une érosion importante dont le matériel latéritique fin, chargé en métaux lourds, finit irrémédiablement dans la mangrove, et il est fort possible que le fonctionnement du milieu soit impacté par

l'accumulation de ces métaux. Par exemple, des études ont montré que certains métaux (*e.g.* le cuivre, le fer, le manganèse, le zinc) pouvaient avoir des effets notables sur la photosynthèse (*e.g.* Prasad and Strzałka, 1999; Yruela, 2013). De plus, le fer est utilisé dans les processus de diagénèse précoce, et son apport en grande quantité, dû au lessivage des sols des massifs miniers, pourrait modifier significativement les processus de minéralisation du carbone au sein de la mangrove.

Références

A

Abril, G., Commarieu, M.-V., Guérin, F., 2007. Enhanced methane oxidation in an estuarine turbidity maximum. Limnol. Oceanogr. 52, 470–475. doi:10.4319/lo.2007.52.1.0470

Adame, M.F., Kauffman, J.B., Medina, I., Gamboa, J.N., Torres, O., Caamal, J.P., Reza, M., Herrera-Silveira, J.A., 2013. Carbon Stocks of Tropical Coastal Wetlands within the Karstic Landscape of the Mexican Caribbean. PLoS ONE 8, e56569. doi:10.1371/journal.pone.0056569

Agrawala, S., Ota, T., Risbey, J., Hagenstad, M., Smith, J., van Aalst, M., Koshy, K., Prasad, B., 2003. Development and Climate Change in Fiji: Focus on coastal mangroves. OECD.

Ainsworth, E.A., Long, S.P., 2005. What have we learned from 15 years of free-air CO2 enrichment (FACE)? A meta-analytic review of the responses of photosynthesis, canopy properties and plant production to rising CO2. New Phytol. 165, 351–371. doi:10.1111/j.1469-8137.2004.01224.x

Allen, D., Dalal, R.C., Rennenberg, H., Schmidt, S., 2011. Seasonal variation in nitrous oxide and methane emissions from subtropical estuary and coastal mangrove sediments, Australia. Plant Biol. 13, 126–133.

Allen, D.E., Dalal, R.C., Rennenberg, H., Meyer, R.L., Reeves, S., Schmidt, S., 2007. Spatial and temporal variation of nitrous oxide and methane flux between subtropical mangrove sediments and the atmosphere. Soil Biol. Biochem. 39, 622–631. doi:10.1016/j.soilbio.2006.09.013

Alongi, D.M., 2015. The Impact of Climate Change on Mangrove Forests. Curr. Clim. Change Rep. 1, 30–39. doi:10.1007/s40641-015-0002-x

Alongi, D.M., 2014. Carbon Cycling and Storage in Mangrove Forests. Annu. Rev. Mar. Sci. 6, 195–219. doi:10.1146/annurev-marine-010213-135020

Alongi, D.M., 2012. Carbon sequestration in mangrove forests. Carbon Manag. 3, 313–322. doi:10.4155/cmt.12.20

Alongi, D.M., 2008. Mangrove forests: Resilience, protection from tsunamis, and responses to global climate change. Estuar. Coast. Shelf Sci. 76, 1–13. doi:10.1016/j.ecss.2007.08.024

Alongi, D.M., 1998. Coastal ecosystem processes.

Alongi, D.M., 1994. Zonation and seasonality of benthic primary production and community respiration in tropical mangrove forests. Oecologia 98, 320–327. doi:10.1007/BF00324220

Alongi, D.M., Boto, K.G., Tirendi, F., 1989. Effect of exported mangrove litter on bacterial productivity and dissolved organic carbon fluxes in adjacent tropical nearshore sediments. Mar. Ecol. Prog. Ser. 133–144.

Alongi, D.M., Pfitzner, J., Trott, L.A., Tirendi, F., Dixon, P., Klumpp, D.W., 2005. Rapid sediment accumulation and microbial mineralization in forests of the mangrove Kandelia candel in the Jiulongjiang Estuary, China. Estuar. Coast. Shelf Sci. 63, 605–618. doi:10.1016/j.ecss.2005.01.004

Alongi, D.M., Sasekumar, A., Chong, V.C., Pfitzner, J., Trott, L.A., Tirendi, F., Dixon, P., Brunskill, G.J., 2004. Sediment accumulation and organic material flux in a managed mangrove ecosystem: estimates of land–ocean–atmosphere exchange in peninsular Malaysia. Mar. Geol., Material Exchange Between the Upper Continental Shelf and

Mangrove Fringed Coasts with Special Reference to the N. Amazon-Guianas Coast 208, 383–402. doi:10.1016/j.margeo.2004.04.016

Alongi, D.M., Tirendi, F., Clough, B.F., 2000. Below-ground decomposition of organic matter in forests of the mangroves *Rhizophora*stylosa and *Avicennia*marina along the arid coast of Western Australia. Aquat. Bot. 68, 97–122.

Alongi, D.M., Wattayakorn, G., Pfitzner, J., Tirendi, F., Zagorskis, I., Brunskill, G.J., Davidson, A., Clough, B.F., 2001. Organic carbon accumulation and metabolic pathways in sediments of mangrove forests in southern Thailand. Mar. Geol. 179, 85–103. doi:10.1016/S0025-3227(01)00195-5

Alongi, M.D., 2009. The Energetics of Mangrove Forests | Daniel Alongi | Springer. Springer.

Andersen, F., Kristensen, E., 1988. Oxygen microgradients in the rhizosphere of the mangrove *Avicennia marina*. Mar. Ecol. Prog. Ser. 44, 201–204. doi:10.3354/meps044201

Andrews, T.J., Clough, B.F., Muller, G.J., 1984. Photosynthetic gas exchange properties and carbon isotope ratios of some mangroves in North Queensland. Physiol. Manag. Mangroves Tasks Veg. Sci. 9, 15–23.

Atwood, T.B., Connolly, R.M., Almahasheer, H., Carnell, P.E., Duarte, C.M., Ewers Lewis, C.J., Irigoien, X., Kelleway, J.J., Lavery, P.S., Macreadie, P.I., Serrano, O., Sanders, C.J., Santos, I., Steven, A.D.L., Lovelock, C.E., 2017. Global patterns in mangrove soil carbon stocks and losses. Nat. Clim. Change 7, 523–528. doi:10.1038/nclimate3326

B

Balk, M., Keuskamp, J.A., Laanbroek, H.J., 2016. Potential for Sulfate Reduction in Mangrove Forest Soils: Comparison between Two Dominant Species of the Americas. Front. Microbiol. 7. doi:10.3389/fmicb.2016.01855

Balke, T., Bouma, T.J., Horstman, E.M., Webb, E.L., Erftemeijer, P.L., Herman, P.M., 2011. Windows of opportunity: thresholds to mangrove seedling establishment on tidal flats. Mar. Ecol. Prog. Ser. 440, 1–9.

Ball, M.C., Cochrane, M.J., Rawson, H.M., 1997. Growth and water use of the mangroves *Rhizophora* apiculata and *R. stylosa* in response to salinity and humidity under ambient and elevated concentrations of atmospheric CO2. Plant Cell Environ. 20, 1158–1166.

Baltzer, F., 1982. Géodynamique de la sédimentation et diagenèse précoce en domaine ultrabasique – Nouvelle Calédonie [WWW Document]. URL http://horizon.documentation.ird.fr/exl-doc/pleins_textes/pleins_textes_5/pt5/travaux_d/02460.pdf (accessed 6.5.17).

Barbier, E.B., 2006. Natural barriers to natural disasters: replanting mangroves after the tsunami. Front. Ecol. Environ. 4, 124–131. doi:10.1890/1540-9295(2006)004[0124:NBTNDR]2.0.CO;2

Barbier, E.B., Hacker, S.D., Kennedy, C., Koch, E.W., Stier, A.C., Silliman, B.R., 2011. The value of estuarine and coastal ecosystem services. Ecol. Monogr. 81, 169–193. doi:10.1890/10-1510.1

Barroso-Matos, T., Bernini, E., Eduardo Rezende, C., 2012. Decomposition of mangrove leaves in the estuary of Paraíba do Sul RiverRio de Janeiro, Brazil. Lat. Am. J. Aquat. Res. 40, 398–407.

Bastviken, D., Cole, J., Pace, M., Tranvik, L., 2004. Methane emissions from lakes: Dependence of lake characteristics, two regional assessments, and a global estimate:

LAKE METHANE EMISSIONS. Glob. Biogeochem. Cycles 18, n/a-n/a. doi:10.1029/2004GB002238

Bastviken, D., Cole, J.J., Pace, M.L., Van de Bogert, M.C., 2008. Fates of methane from different lake habitats: Connecting whole-lake budgets and CH_4 emissions: FATES OF LAKE METHANE. J. Geophys. Res. Biogeosciences 113, n/a-n/a. doi:10.1029/2007JG000608

Bastviken, D., Santoro, A.L., Marotta, H., Pinho, L.Q., Calheiros, D.F., Crill, P., Enrich-Prast, A., 2010. Methane Emissions from Pantanal, South America, during the Low Water Season: Toward More Comprehensive Sampling. Environ. Sci. Technol. 44, 5450–5455. doi:10.1021/es1005048

Betts, R.A., Jones, C.D., Knight, J.R., Keeling, R.F., Kennedy, J.J., 2016. El Nino and a record CO2 rise. Nat. Clim. Change 6, 806–810. doi:10.1038/nclimate3063

Billerbeck, M., Werner, U., Polerecky, L., Walpersdorf, E., DeBeer, D., Huettel, M., 2006. Surficial and deep pore water circulation governs spatial and temporal scales of nutrient recycling in intertidal sand flat sediment. Mar. Ecol. Prog. Ser. 326, 61–76.

Biswas, H., Mukhopadhyay, S.K., Sen, S., Jana, T.K., 2007. Spatial and temporal patterns of methane dynamics in the tropical mangrove dominated estuary, NE coast of Bay of Bengal, India. J. Mar. Syst. 68, 55–64. doi:10.1016/j.jmarsys.2006.11.001

Borges, A.V., Djenidi, D., Lacroix, G., Théate, J., Delille, B., Frankignoulle, M., 2003. Atmospheric CO_2 flux from mangrove surrounding waters. Geophys. Res. Lett. 30. doi:10.1029/2003GL017143

Bouchez, A., Pascault, N., Chardon, C., Bouvy, M., Cecchi, P., Lambs, L., Herteman, M., Fromard, F., Got, P., Leboulanger, C., 2013. Mangrove microbial diversity and the impact of trophic contamination. Mar. Pollut. Bull. 66, 39–46. doi:10.1016/j.marpolbul.2012.11.015

Bouillon, S., Borges, A.V., Castañeda-Moya, E., Diele, K., Dittmar, T., Duke, N.C., Kristensen, E., Lee, S.Y., Marchand, C., Middelburg, J.J., others, 2008. Mangrove production and carbon sinks: a revision of global budget estimates. Glob. Biogeochem. Cycles 22.

Bouillon, S., Connolly, R.M., Lee, S.Y., 2008. Organic matter exchange and cycling in mangrove ecosystems: Recent insights from stable isotope studies. J. Sea Res. 59, 44–58. doi:10.1016/j.seares.2007.05.001

Bouillon, S., Dahdouh-Guebas, F., Rao, A., Koedam, N., Dehairs, F., 2003a. Sources of organic carbon in mangrove sediments: variability and possible ecological implications. Hydrobiologia 495, 33–39.

Bouillon, S., Frankignoulle, M., Dehairs, F., Velimirov, B., Eiler, A., Abril, G., Etcheber, H., Borges, A.V., 2003b. Inorganic and organic carbon biogeochemistry in the Gautami Godavari estuary (Andhra Pradesh, India) during pre-monsoon: The local impact of extensive mangrove forests. Glob. Biogeochem. Cycles 17, n/a-n/a. doi:10.1029/2002GB002026

Bouillon, S., Koedam, N., Raman, A., Dehairs, F., 2002. Primary producers sustaining macro-invertebrate communities in intertidal mangrove forests. Oecologia 130, 441–448.

Bouillon, S., Middelburg, J.J., Dehairs, F., Borges, A.V., Abril, G., Flindt, M.R., Ulomi, S., Kristensen, E., 2007. Importance of intertidal sediment processes and porewater exchange on the water column biogeochemistry in a pristine mangrove creek (Ras Dege, Tanzania). Biogeosciences Discuss. 4, 317–348.

Breithaupt, J.L., Smoak, J.M., Smith, T.J., Sanders, C.J., Hoare, A., 2012. Organic carbon burial rates in mangrove sediments: Strengthening the global budget: MANGROVE ORGANIC CARBON BURIAL RATES. Glob. Biogeochem. Cycles 26. doi:10.1029/2012GB004375

Bronk Ramsey, C., 2009. Bayesian Analysis of Radiocarbon Dates. Radiocarbon 51, 337–360. doi:10.1017/S0033822200033865

Bubier, J.L., Moore, T.R., Bellisario, L., Comer, N.T., Crill, P.M., 1995. Ecological controls on methane emissions from a Northern Peatland Complex in the zone of discontinuous permafrost, Manitoba, Canada. Glob. Biogeochem. Cycles 9, 455–470. doi:10.1029/95GB02379

Buchmann, N., Kathiresan, K., Salmo III, S.G., Fernando, E.S., Peras, J.R., Sukardjo, S., Miyagi, T., Koedam, N.E., Wang, Y., Primavera, J., Jin Eong, O., Wan-Hong Yong, J., Ngoc Nam, V., 2008. *Avicennia marina*. The IUCN Red List of Threatened Species 2010: e.T178828A7619457. doi:10.2305/IUCN.UK.2010-2.RLTS.T178828A7619457.en

Bulmer, R.H., Lundquist, C.J., Schwendenmann, L., 2015. Sediment properties and CO_2 efflux from intact and cleared temperate mangrove forests. Biogeosciences 12, 6169–6180. doi:10.5194/bg-12-6169-2015

C

Cabezas, A., Mitsch, W.J., MacDonnell, C., Zhang, L., Bydałek, F., Lasso, A., n.d. Methane emissions from mangrove soils in hydrologically disturbed and reference mangrove tidal creeks in southwest Florida. Ecol. Eng. doi:10.1016/j.ecoleng.2017.08.041

Cabioch, G., Thomassin, A., Lecolle, F.L., 1989. Age d'émersion des récifs frangeants holocènes autour de la (< Grande Terre)) de Nouvelle-Calédonie (SO Pacifique); nouvelle interprétation de la courbe des niveaux marins depuis 8 O00 ans BP. Académie Sci. Paris 308, 419–425.

Cahoon, D.R., Hensel, P.F., Spencer, T., Reed, D.J., McKee, K.L., Saintilan, N., 2006. Coastal Wetland Vulnerability to Relative Sea-Level Rise: Wetland Elevation Trends and Process Controls, in: Wetlands and Natural Resource Management, Ecological Studies. Springer, Berlin, Heidelberg, pp. 271–292. doi:10.1007/978-3-540-33187-2_12

Call, M., Maher, D.T., Santos, I.R., Ruiz-Halpern, S., Mangion, P., Sanders, C.J., Erler, D.V., Oakes, J.M., Rosentreter, J., Murray, R., Eyre, B.D., 2015. Spatial and temporal variability of carbon dioxide and methane fluxes over semi-diurnal and spring–neap–spring timescales in a mangrove creek. Geochim. Cosmochim. Acta 150, 211–225. doi:10.1016/j.gca.2014.11.023

Canadell, J.G., Raupach, M.R., 2008. Managing Forests for Climate Change Mitigation. Science 320, 1456–1457. doi:10.1126/science.1155458

Castañeda-Moya, E., Twilley, R.R., Rivera-Monroy, V.H., Marx, B.D., Coronado-Molina, C., Ewe, S.M.L., 2011. Patterns of Root Dynamics in Mangrove Forests Along Environmental Gradients in the Florida Coastal Everglades, USA. Ecosystems 14, 1178–1195. doi:10.1007/s10021-011-9473-3

Castillo, J.A.A., Apan, A.A., Maraseni, T.N., Salmo, S.G., 2017. Soil C quantities of mangrove forests, their competing land uses, and their spatial distribution in the coast of Honda Bay, Philippines. Geoderma 293, 82–90. doi:10.1016/j.geoderma.2017.01.025

Chanda, A., Akhand, A., Manna, S., Dutta, S., Das, I., Hazra, S., Rao, K.H., Dadhwal, V.K., 2013. Measuring daytime CO2 fluxes from the inter-tidal mangrove soils of Indian Sundarbans. Environ. Earth Sci. 72, 417–427. doi:10.1007/s12665-013-2962-2

Chauhan, R., Datta, A., Ramanathan, A., Adhya, T.K., 2015. Factors influencing spatio-temporal variation of methane and nitrous oxide emission from a tropical mangrove of eastern coast of India. Atmos. Environ. 107, 95–106. doi:10.1016/j.atmosenv.2015.02.006

Chen, G., Chen, B., Yu, D., Tam, N.F.Y., Ye, Y., Chen, S., 2016a. Soil greenhouse gas emissions reduce the contribution of mangrove plants to the atmospheric cooling effect. Environ. Res. Lett. 11, 124019. doi:10.1088/1748-9326/11/12/124019

Chen, G., Chen, B., Yu, D., Ye, Y., Tam, N.F.Y., Chen, S., 2016b. Soil greenhouse gases emissions reduce the benefit of mangrove plant to mitigating atmospheric warming effect. Biogeosciences Discuss. 1–22. doi:10.5194/bg-2015-662

Chen, G.C., Tam, N.F.Y., Ye, Y., 2012. Spatial and seasonal variations of atmospheric N2O and CO2 fluxes from a subtropical mangrove swamp and their relationships with soil characteristics. Soil Biol. Biochem. 48, 175–181. doi:10.1016/j.soilbio.2012.01.029

Chen, G.C., Tam, N.F.Y., Ye, Y., 2010. Summer fluxes of atmospheric greenhouse gases N2O, CH4 and CO2 from mangrove soil in South China. Sci. Total Environ. 408, 2761–2767. doi:10.1016/j.scitotenv.2010.03.007

Chen, G.C., Ulumuddin, Y.I., Pramudji, S., Chen, S.Y., Chen, B., Ye, Y., Ou, D.Y., Ma, Z.Y., Huang, H., Wang, J.K., 2014. Rich soil carbon and nitrogen but low atmospheric greenhouse gas fluxes from North Sulawesi mangrove swamps in Indonesia. Sci. Total Environ. 487, 91–96. doi:10.1016/j.scitotenv.2014.03.140

Chen, L., Wang, W., Lin, P., 2005. Photosynthetic and physiological responses of Kandelia candel L. Druce seedlings to duration of tidal immersion in artificial seawater. Environ. Exp. Bot. 54, 256–266. doi:10.1016/j.envexpbot.2004.09.004

Cherry, J.A., McKee, K.L., Grace, J.B., 2009. Elevated CO2 enhances biological contributions to elevation change in coastal wetlands by offsetting stressors associated with sea-level rise. J. Ecol. 97, 67–77. doi:10.1111/j.1365-2745.2008.01449.x

Chmura, G.L., Anisfeld, S.C., Cahoon, D.R., Lynch, J.C., 2003. Global carbon sequestration in tidal, saline wetland soils. Glob. Biogeochem. Cycles 17, 1111. doi:10.1029/2002GB001917

Church, J.A., Clark, P.U., Cazenave, A., Gregory, J.M., Jevrejeva, S., Levermann, A., Merrifield, M.A., Milne, G.A., Nerem, R.S., Nunn, P.D., Payne, A.J., 2013. Sea Level Change, in: Climate Change 2013: The Physical Science Basis. Contribution of Working Group I to the Fifth Assessment Report of the Intergovernmental Panel on Climate Change [Stocker, T.F., D. Qin, G.-K. Plattner, M. Tignor, S.K. Allen, J. Boschung, A. Nauels, Y. Xia, V. Bex and P.M. Midgley (Eds.). PM Cambridge University Press.

Claus, A., George, E., 2005. Effect of stand age on fine-root biomass and biomass distribution in three European forest chronosequences. Can. J. For. Res. 35, 1617–1625. doi:10.1139/x05-079

Clough, B.F., 1992. Primary productivity and growth of mangrove forests. Trop. Mangrove Ecosyst. 225–249.

Coffin, R.B., Fry, B., Peterson, B.J., Wright, R.T., 1989. Carbon isotopic compositions of estuarine bacteria. Limnol. Oceanogr. 34, 1305–1310.

Collins, M., Arblaster, J., Dufresne, J.-L., Fichefet, T., Friedlingstein, P., Gao, X., Gutowski, W.J., Johns, T., Krinner, G., Tebaldi, C., Weaver, A.J., Wehner, M., 2014. Long-term Climate Change: Projections, Commitments and Irreversibility Pages 1029 to 1076, in: Intergovernmental Panel on Climate Change (Ed.), Climate Change 2013 - The Physical

Science Basis. Cambridge University Press, Cambridge, pp. 1029–1136. doi:10.1017/CBO9781107415324.024

Conant, R.T., Ryan, M.G., \AAgren, G.I., Birge, H.E., Davidson, E.A., Eliasson, P.E., Evans, S.E., Frey, S.D., Giardina, C.P., Hopkins, F.M., 2011. Temperature and soil organic matter decomposition rates–synthesis of current knowledge and a way forward. Glob. Change Biol. 17, 3392–3404.

Cook, J., Oreskes, N., Doran, P.T., Anderegg, W.R.L., Verheggen, B., Maibach, E.W., Carlton, J.S., Lewandowsky, S., Skuce, A.G., Green, S.A., Nuccitelli, D., Jacobs, P., Mark Richardson, Winkler, B., Painting, R., Rice, K., 2016. Consensus on consensus: a synthesis of consensus estimates on human-caused global warming. Environ. Res. Lett. 11, 048002. doi:10.1088/1748-9326/11/4/048002

Cotrufo, M.F., Ineson, P., Scott, A., 1998. Elevated CO2 reduces the nitrogen concentration of plant tissues. Glob. Change Biol. 4, 43–54.

Crill, P.M., Bartlett, K.B., Harriss, R.C., Gorham, E., Verry, E.S., Sebacher, D.I., Madzar, L., Sanner, W., 1988. Methane flux from Minnesota Peatlands. Glob. Biogeochem. Cycles 2, 371–384. doi:10.1029/GB002i004p00371

Dahdouh-Guebas, F., Jayatissa, L.P., Di Nitto, D., Bosire, J.O., Lo Seen, D., Koedam, N., 2005. How effective were mangroves as a defence against the recent tsunami? Curr. Biol. 15, R443–R447. doi:10.1016/j.cub.2005.06.008

Dai, A., 2013. Increasing drought under global warming in observations and models. Nat. Clim. Change 3, 52–58. doi:10.1038/nclimate1633

Davidson, E.A., Janssens, I.A., 2006. Temperature sensitivity of soil carbon decomposition and feedbacks to climate change. Nature 440, 165–173. doi:10.1038/nature04514

D

De GRAAFF, M.-A., Van GROENIGEN, K.-J., Six, J., Hungate, B., Van KESSEL, C., 2006. Interactions between plant growth and soil nutrient cycling under elevated CO2: a meta-analysis. Glob. Change Biol. 12, 2077–2091. doi:10.1111/j.1365-2486.2006.01240.x

Deborde, J., Marchand, C., Molnar, N., Patrona, L.D., Meziane, T., 2015. Concentrations and Fractionation of Carbon, Iron, Sulfur, Nitrogen and Phosphorus in Mangrove Sediments Along an Intertidal Gradient (Semi-Arid Climate, New Caledonia). J. Mar. Sci. Eng. 3, 52–72. doi:10.3390/jmse3010052

Decho, A.W., 2000. Microbial biofilms in intertidal systems: an overview. Cont. Shelf Res. 20, 1257–1273. doi:10.1016/S0278-4343(00)00022-4

DelVecchia, A.G., Bruno, J.F., Benninger, L., Alperin, M., Banerjee, O., Morales, J. de D., 2014. Organic carbon inventories in natural and restored Ecuadorian mangrove forests. PeerJ 2, e388. doi:10.7717/peerj.388

Di Nitto, D., Neukermans, G., Koedam, N., Defever, H., Pattyn, F., Kairo, J.G., Dahdouh-Guebas, F., 2014. Mangroves facing climate change: landward migration potential in response to projected scenarios of sea level rise. Biogeosciences 11, 857–871. doi:10.5194/bg-11-857-2014

Dittmar, T., Lara, R.J., 2001. Molecular evidence for lignin degradation in sulfate-reducing mangrove sediments (Amazonia, Brazil). Geochim. Cosmochim. Acta 65, 1417–1428.

Donato, D.C., Kauffman, J.B., Murdiyarso, D., Kurnianto, S., Stidham, M., Kanninen, M., 2011. Mangroves among the most carbon-rich forests in the tropics. Nat. Geosci. 4, 293–297. doi:10.1038/ngeo1123

Drake, B.G., Leadley, P.W., 1991. Canopy photosynthesis of crops and native plant communities exposed to long-term elevated CO2. Plant Cell Environ. 14, 853–860.

Duarte, C.M., Marbà, N., Gacia, E., Fourqurean, J.W., Beggins, J., Barrón, C., Apostolaki, E.T., 2010. Seagrass community metabolism: Assessing the carbon sink capacity of seagrass meadows. Glob. Biogeochem. Cycles 24, GB4032. doi:10.1029/2010GB003793

Duke, N., Ball, M., Ellison, J., 1998. Factors influencing biodiversity and distributional gradients in mangroves. Glob. Ecol. Biogeogr. Lett. 7, 27–47. doi:10.1111/j.1466-8238.1998.00269.x

Duke, N.C., 2010. Overlap of eastern and western mangroves in the South-western Pacific: hybridization of all three *Rhizophora* (*Rhizophora*ceae) combinations in New Caledonia. Blumea - Biodivers. Evol. Biogeogr. Plants 55, 171–188. doi:10.3767/000651910X527293

Duke, N.C., 1992. Mangrove floristics and biogeography. Trop. Mangrove Ecosyst. 63–100.

Duke, N.C., Meynecke, J.-O., Dittmann, S., Ellison, A.M., Anger, K., Berger, U., Cannicci, S., Diele, K., Ewel, K.C., Field, C.D., Koedam, N., Lee, S.Y., Marchand, C., Nordhaus, I., Dahdouh-Guebas, F., 2007. A World Without Mangroves? Science 317, 41–42. doi:10.1126/science.317.5834.41b

Dutta, M. kumar, Mukhopadhyay, S.K., 2016. Reviews and syntheses: Methane biogeochemistry in Sundarbans mangrove ecosystem, NE coast of India; a box modeling approach. Biogeosciences Discuss. doi:10.5194/bg-2016-58

Dutta, M.K., Bianchi, T.S., Mukhopadhyay, S.K., 2017. Mangrove Methane Biogeochemistry in the Indian Sundarbans: A Proposed Budget. Front. Mar. Sci. 4. doi:10.3389/fmars.2017.00187

Dutta, M.K., Chowdhury, C., Jana, T.K., Mukhopadhyay, S.K., 2013. Dynamics and exchange fluxes of methane in the estuarine mangrove environment of the Sundarbans, NE coast of India. Atmos. Environ. 77, 631–639. doi:10.1016/j.atmosenv.2013.05.050

Dutta, M.K., Mukherjee, R., Jana, T.K., Mukhopadhyay, S.K., 2015. Biogeochemical dynamics of exogenous methane in an estuary associated to a mangrove biosphere; The Sundarbans, NE coast of India. Mar. Chem. 170, 1–10. doi:10.1016/j.marchem.2014.12.006

E

Ellison, A.M., Farnsworth, E.J., 1997. Simulated sea level change alters anatomy, physiology, growth, and reproduction of red mangrove (*Rhizophora* mangle L.). Oecologia 112, 435–446.

Ellison, J., Duke, N., Kathiresan, K., Salmo III, S.G., Fernando, E.S., Peras, J.R., Sukardjo, S., Miyagi, T., 2008. *Rhizophora stylosa*: The IUCN Red List of Threatened Species 2010: e.T178850A7626520. doi:10.2305/IUCN.UK.2010-2.RLTS.T178850A7626520.en

Ellison, J.C., 2015. Vulnerability assessment of mangroves to climate change and sea-level rise impacts. Wetl. Ecol. Manag. 23, 115–137. doi:10.1007/s11273-014-9397-8

F

Fang, C., Moncrieff, J.B., 2001. The dependence of soil CO2 efflux on temperature. Soil Biol. Biochem. 33, 155–165. doi:10.1016/S0038-0717(00)00125-5

Farnsworth, E.J., Ellison, A.M., Gong, W.K., 1996a. Elevated CO 2 alters anatomy, physiology, growth, and reproduction of red mangrove (*Rhizophora* mangle L.). Oecologia 108, 599–609.

Farnsworth, E.J., Ellison, A.M., Gong, W.K., 1996b. Elevated CO 2 alters anatomy, physiology, growth, and reproduction of red mangrove (*Rhizophora* mangle L.). Oecologia 108, 599–609.

Farquhar, G.D., Ehleringer, J.R., Hubick, K.T., 1989. Carbon isotope discrimination and photosynthesis. Annu. Rev. Plant Biol. 40, 503–537.

Ferreira, T.O., Otero, X.L., Vidal-Torrado, P., Macías, F., 2007. Effects of bioturbation by root and crab activity on iron and sulfur biogeochemistry in mangrove substrate. Geoderma 142, 36–46. doi:10.1016/j.geoderma.2007.07.010

Fierer, N., Craine, J.M., McLauchlan, K., Schimel, J.P., 2005. Litter Quality and the Temperature Sensitivity of Decomposition. Ecology 86, 320–326. doi:10.1890/04-1254

G

Gifford, R.M., Barrett, D.J., Lutze, J.L., 2000. The effects of elevated [CO2] on the C:N and C:P mass ratios of plant tissues. Plant Soil 224, 1–14. doi:10.1023/A:1004790612630

Gill, A.M., Tomlinson, P.B., 1977. Studies on the Growth of Red Mangrove (*Rhizophora* mangle L.) 4. The Adult Root System. Biotropica 9, 145. doi:10.2307/2387877

Gilman, E.L., Ellison, J., Duke, N.C., Field, C., 2008. Threats to mangroves from climate change and adaptation options: A review. Aquat. Bot., Mangrove Ecology – Applications in Forestry and Costal Zone Management 89, 237–250. doi:10.1016/j.aquabot.2007.12.009

Giri, C., Ochieng, E., Tieszen, L.L., Zhu, Z., Singh, A., Loveland, T., Masek, J., Duke, N., 2011. Status and distribution of mangrove forests of the world using earth observation satellite data. Glob. Ecol. Biogeogr. 20, 154–159.

Grellier, S., Janeau, J.-L., Dang Hoai, N., Nguyen Thi Kim, C., Le Thi Phuong, Q., Pham Thi Thu, T., Tran-Thi, N.-T., Marchand, C., 2017. Changes in soil characteristics and C dynamics after mangrove clearing (Vietnam). Sci. Total Environ. 593–594, 654–663. doi:10.1016/j.scitotenv.2017.03.204

H

Ha, T.H., Marchand, C., Aimé, J., Dang, H.N., Phan, N.H., Nguyen, X.T., Nguyen, T.K.C., 2017. Belowground carbon sequestration in a mature planted mangroves (Northern Viet Nam). For. Ecol. Manag. doi:10.1016/j.foreco.2017.06.057

Hättenschwiler, S., Gasser, P., 2005. Soil animals alter plant litter diversity effects on decomposition. Proc. Natl. Acad. Sci. U. S. A. 102, 1519–1524. doi:10.1073/pnas.0404977102

Herrick, J.D., Thomas, R.B., 1999. Effects of CO2 enrichment on the photosynthetic light response of sun and shade leaves of canopy sweetgum trees (Liquidambar styraciflua) in a forest ecosystem. Tree Physiol. 19, 779–786.

Hogarth, P.J., 1999. The biology of mangroves. Oxford University Press.

Hogg, A.G., Hua, Q., Blackwell, P.G., Niu, M., Buck, C.E., Guilderson, T.P., Heaton, T.J., Palmer, J.G., Reimer, P.J., Reimer, R.W., Turney, C.S.M., Zimmerman, S.R.H., 2013. SHCal13 Southern Hemisphere Calibration, 0–50,000 Years cal BP. Radiocarbon 55, 1889–1903. doi:10.2458/azu_js_rc.55.16783

Hossain, M., 2014. Carbon pools and fluxes in Bruguiera parviflora dominated naturally growing mangrove forest of Peninsular Malaysia. Wetl. Ecol. Manag. 22, 15–23. doi:10.1007/s11273-013-9318-2

Hovenden, M.J., Curran, M., Cole, M.A., Goulter, P.F.E., Skelton, N.J., Allaway, W.G., 1995. Ventilation and respiration in roots of one-year-old seedlings of grey mangrove *Avicennia marina* (Forsk.) Vierh. Hydrobiologia 295, 23–29. doi:10.1007/BF00029107

Howard, J., Sutton-Grier, A., Herr, D., Kleypas, J., Landis, E., Mcleod, E., Pidgeon, E., Simpson, S., 2017. Clarifying the role of coastal and marine systems in climate mitigation. Front. Ecol. Environ. 15, 42–50. doi:10.1002/fee.1451

Hutchison, J., Manica, A., Swetnam, R., Balmford, A., Spalding, M., 2014. Predicting Global Patterns in Mangrove Forest Biomass. Conserv. Lett. 7, 233–240. doi:10.1111/conl.12060

I

Inglett, K.S., Inglett, P.W., Reddy, K.R., Osborne, T.Z., 2012. Temperature sensitivity of greenhouse gas production in wetland soils of different vegetation. Biogeochemistry 108, 77–90. doi:10.1007/s10533-011-9573-3

J

Jacob, M., Viedenz, K., Polle, A., Thomas, F.M., 2010. Leaf litter decomposition in temperate deciduous forest stands with a decreasing fraction of beech (Fagus sylvatica). Oecologia 164, 1083–1094. doi:10.1007/s00442-010-1699-9

Johnston, H., Kinnison, D., 1998. Methane photooxidation in the atmosphere: Contrast between two methods of analysis. J. Geophys. Res. Atmospheres 103, 21967–21984. doi:10.1029/98JD01213

K

Kaipiainen, E.L., 2009. Parameters of photosynthesis light curve in Salix dasyclados and their changes during the growth season. Russ. J. Plant Physiol. 56, 445–453. doi:10.1134/S1021443709040025

Karnosky, D.F., 2003. Impacts of elevated atmospheric CO2 on forest trees and forest ecosystems: knowledge gaps. Environ. Int., Future Directions in Air Quality Research : Ecological,Atmospheric,Regulatory/Policy/Economic, and Educational Issues 29, 161–169. doi:10.1016/S0160-4120(02)00159-9

Katayama, A., Kume, T., Komatsu, H., Ohashi, M., Nakagawa, M., Yamashita, M., Otsuki, K., Suzuki, M., Kumagai, T., 2009. Effect of forest structure on the spatial variation in soil respiration in a Bornean tropical rainforest. Agric. For. Meteorol. 149, 1666–1673. doi:10.1016/j.agrformet.2009.05.007

Kathiresan, K., 2003. How do mangrove forests induce sedimentation? Rev. Biol. Trop. 51, 355–360.

Kathiresan, K., Bingham, B.L., 2001. Biology of mangroves and mangrove ecosystems. Adv. Mar. Biol. 40, 81–251.

Kauffman, J.B., Heider, C., Cole, T.G., Dwire, K.A., Donato, D.C., 2011. Ecosystem Carbon Stocks of Micronesian Mangrove Forests. Wetlands 31, 343–352. doi:10.1007/s13157-011-0148-9

Keeling, C.D., 1961. The concentration and isotopic abundances of carbon dioxide in rural and marine air. Geochim. Cosmochim. Acta 24, 277–298. doi:10.1016/0016-7037(61)90023-0

Keeling, C.D., 1958. The concentration and isotopic abundances of atmospheric carbon dioxide in rural areas. Geochim. Cosmochim. Acta 13, 322–334.

Khan, N.S., Vane, C.H., Horton, B.P., 2015. Stable carbon isotope and C/N geochemistry of coastal wetland sediments as a sea-level indicator. Handb. Sea-Level Res. 295–311.

Kirschbaum, M.U.F., 2011. Does Enhanced Photosynthesis Enhance Growth? Lessons Learned from CO2 Enrichment Studies. Plant Physiol. 155, 117–124. doi:10.1104/pp.110.166819

Kirui, B., Huxham, M., Kairo, J., Mencuccini, M., Skov, 2009. Seasonal dynamics of soil carbon dioxide flux in a restored young mangrove plantation at Gazi Bay. Adv. Coast. Ecol. 20, 122–130.

Kirwan, M.L., Megonigal, J.P., 2013. Tidal wetland stability in the face of human impacts and sea-level rise. Nature 504, 53–60. doi:10.1038/nature12856

Kitaya, Y., Yabuki, K., Kiyota, M., Tani, A., Hirano, T., Aiga, I., 2002. Gas exchange and oxygen concentration in pneumatophores and prop roots of four mangrove species. Trees 16, 155–158. doi:10.1007/s00468-002-0167-5

Komiyama, A., Havanond, S., Srisawatt, W., Mochida, Y., Fujimoto, K., Ohnishi, T., Ishihara, S., Miyagi, T., 2000. Top/root biomass ratio of a secondary mangrove (Ceriops tagal (Perr.) C.B. Rob.) forest. For. Ecol. Manag. 139, 127–134. doi:10.1016/S0378-1127(99)00339-4

Komiyama, A., Ong, J.E., Poungparn, S., 2008. Allometry, biomass, and productivity of mangrove forests: A review. Aquat. Bot. 89, 128–137. doi:10.1016/j.aquabot.2007.12.006

Kozlowski, T.T. (Ed.), 1984. Flooding and Plant Growth, in: Flooding and Plant Growth, Physiological Ecology. Academic Press, San Diego, p. iii. doi:10.1016/B978-0-12-424120-6.50001-8

Krauss, K.W., Cormier, N., Osland, M.J., Kirwan, M.L., Stagg, C.L., Nestlerode, J.A., Russell, M.J., From, A.S., Spivak, A.C., Dantin, D.D., Harvey, J.E., Almario, A.E., 2017. Created mangrove wetlands store belowground carbon and surface elevation change enables them to adjust to sea-level rise. Sci. Rep. 7. doi:10.1038/s41598-017-01224-2

Krauss, K.W., Lovelock, C.E., McKee, K.L., López-Hoffman, L., Ewe, S.M.L., Sousa, W.P., 2008. Environmental drivers in mangrove establishment and early development: A review. Aquat. Bot. 89, 105–127. doi:10.1016/j.aquabot.2007.12.014

Krauss, K.W., McKee, K.L., Lovelock, C.E., Cahoon, D.R., Saintilan, N., Reef, R., Chen, L., 2014. How mangrove forests adjust to rising sea level. New Phytol. 202, 19–34. doi:10.1111/nph.12605

Kreuzwieser, J., Buchholz, J., Rennenberg, H., 2003. Emission of methane and nitrous oxide by Australian mangrove ecosystems. Plant Biol. 5, 423–431.

Kristensen, E., Alongi, D.M., 2006. Control by fiddler crabs (Uca vocans) and plant roots (*Avicennia marina*) on carbon, iron, and sulfur biogeochemistry in mangrove sediment. Limnol. Oceanogr. 51, 1557–1571. doi:10.4319/lo.2006.51.4.1557

Kristensen, E., Bouillon, S., Dittmar, T., Marchand, C., 2008a. Organic carbon dynamics in mangrove ecosystems: A review. Aquat. Bot., Mangrove Ecology – Applications in Forestry and Costal Zone Management 89, 201–219. doi:10.1016/j.aquabot.2007.12.005

Kristensen, E., Bouillon, S., Dittmar, T., Marchand, C., 2008b. Organic carbon dynamics in mangrove ecosystems: A review. Aquat. Bot. 89, 201–219. doi:10.1016/j.aquabot.2007.12.005

Kristensen, E., Flindt, M.R., Ulomi, S., Borges, A., Abril, G., Bouillon, S., 2008c. Emission of CO2 and CH4 to the atmosphere by sediments and open waters in two Tanzanian mangrove forests. Mar. Ecol. Prog. Ser. doi:10.3354/meps07642

Kristensen, E., Jensen, M.H., Banta, G.T., Hansen, K., Holmer, M., King, G.M., 1998. Transformation and transport of inorganic nitrogen in sediments of a southeast Asian mangrove forest. Aquat. Microb. Ecol. 15, 165–175.

Kristensen, E., King, G.M., Holmer, M., Banta, G.T., Jensen, M.H., Hansen, K., Bussarawit, N., 1994. Sulfate reduction, acetate turnover and carbon metabolism in sediments of the Ao Nam Bor mangrove, Phuket, Thailand. Mar. Ecol. Prog. Ser. 245–255.

Kubiske, M.E., Pregitzer, K.S., 1996. Effects of elevated CO2 and light availability on the photosynthetic light response of trees of contrasting shade tolerance. Tree Physiol. 16, 351–358.

L

Lallier-Verges, E., Perrussel, B.P., Disnar, J.-R., Baltzer, F., 1998. Relationships between environmental conditions and the diagenetic evolution of organic matter derived from higher plants in a modern mangrove swamp system (Guadeloupe, French West Indies). Org. Geochem. 29, 1663–1686.

Lamb, A.L., Wilson, G.P., Leng, M.J., 2006. A review of coastal palaeoclimate and relative sea-level reconstructions using δ13C and C/N ratios in organic material. Earth-Sci. Rev. 75, 29–57. doi:10.1016/j.earscirev.2005.10.003

Lamers, L.P.M., Govers, L.L., Janssen, I.C.J.M., Geurts, J.J.M., Van der Welle, M.E.W., Van Katwijk, M.M., Van der Heide, T., Roelofs, J.G.M., Smolders, A.J.P., 2013. Sulfide as a soil phytotoxin—a review. Front. Plant Sci. 4. doi:10.3389/fpls.2013.00268

Lammertsma, E.I., de Boer, H.J., Dekker, S.C., Dilcher, D.L., Lotter, A.F., Wagner-Cremer, F., 2011. Global CO2 rise leads to reduced maximum stomatal conductance in Florida vegetation. Proc. Natl. Acad. Sci. U. S. A. 108, 4035–4040. doi:10.1073/pnas.1100371108

Lee, S.Y., Primavera, J.H., Dahdouh-Guebas, F., McKee, K., Bosire, J.O., Cannicci, S., Diele, K., Fromard, F., Koedam, N., Marchand, C., Mendelssohn, I., Mukherjee, N., Record, S., 2014. Ecological role and services of tropical mangrove ecosystems: a reassessment. Glob. Ecol. Biogeogr. 23, 726–743. doi:10.1111/geb.12155

Leopold, A., Marchand, C., Deborde, J., Allenbach, M., 2015. Temporal variability of CO 2 fluxes at the sediment-air interface in mangroves (New Caledonia). Sci. Total Environ. 502, 617–626.

Leopold, A., Marchand, C., Deborde, J., Chaduteau, C., Allenbach, M., 2013. Influence of mangrove zonation on CO 2 fluxes at the sediment–air interface (New Caledonia). Geoderma 202, 62–70.

Leopold, A., Marchand, C., Renchon, A., Deborde, J., Quiniou, T., Allenbach, M., 2016. Net ecosystem CO 2 exchange in the "Coeur de Voh" mangrove, New Caledonia: Effects of water stress on mangrove productivity in a semi-arid climate. Agric. For. Meteorol. 223, 217–232. doi:10.1016/j.agrformet.2016.04.006

Lichtenthaler, H.K., Buschmann, C., Knapp, M., 2005. How to correctly determine the different chlorophyll fluorescence parameters and the chlorophyll fluorescence decrease ratio R Fd of leaves with the PAM fluorometer. Photosynthetica 43, 379–393.

Lin, G., Ehleringer, J.R., 1997. Carbon Isotopic Fractionation Does Not Occur during Dark Respiration in C3 and C4 Plants. Plant Physiol. 114, 391–394. doi:10.1104/pp.114.1.391

Litton, C.M., Giardina, C.P., Albano, J.K., Long, M.S., Asner, G.P., 2011. The magnitude and variability of soil-surface CO2 efflux increase with mean annual temperature in Hawaiian tropical montane wet forests. Soil Biol. Biochem. 43, 2315–2323. doi:10.1016/j.soilbio.2011.08.004

Livesley, S.J., Andrusiak, S.M., 2012. Temperate mangrove and salt marsh sediments are a small methane and nitrous oxide source but important carbon store. Estuar. Coast. Shelf Sci. 97, 19–27. doi:10.1016/j.ecss.2011.11.002

Lloyd, J., Taylor, J., 1994. On the temperature dependence of soil respiration. Funct. Ecol. 83, 315–323.

Lobo, F. de A., Barros, M.P. de, Dalmagro, H.J., Dalmolin, Â.C., Pereira, W.E., Souza, É.C. de, Vourlitis, G.L., Ortíz, C.E.R., 2014. Erratum to: Fitting net photosynthetic light-response curves with Microsoft Excel — a critical look at the models. Photosynthetica 52, 479–480. doi:10.1007/s11099-014-0045-6

Lobo, F. de A., Barros, M.P. de, Dalmagro, H.J., Dalmolin, Â.C., Pereira, W.E., Souza, É.C. de, Vourlitis, G.L., Ortíz, C.E.R., 2013. Fitting net photosynthetic light-response curves with Microsoft Excel — a critical look at the models. Photosynthetica 51, 445–456. doi:10.1007/s11099-013-0045-y

Lotfiomran, N., Köhl, M., Fromm, J., 2016. Interaction Effect between Elevated CO2 and Fertilization on Biomass, Gas Exchange and C/N Ratio of European Beech (Fagus sylvatica L.). Plants 5. doi:10.3390/plants5030038

Lou, Y.-S., Li, Z.-P., Zhang, T.-L., 2003. Soil CO2 flux in relation to dissolved organic carbon, soil temperature and moisture in a subtropical arable soil of China. J. Environ. Sci. China 15, 715–720.

Lovelock, C.E., 2008. Soil Respiration and Belowground Carbon Allocation in Mangrove Forests. Ecosystems 11, 342–354. doi:10.1007/s10021-008-9125-4

Lovelock, C.E., Cahoon, D.R., Friess, D.A., Guntenspergen, G.R., Krauss, K.W., Reef, R., Rogers, K., Saunders, M.L., Sidik, F., Swales, A., Saintilan, N., Thuyen, L.X., Triet, T., 2015. The vulnerability of Indo-Pacific mangrove forests to sea-level rise. Nature 526, 559–563. doi:10.1038/nature15538

Lunstrum, A., Chen, L., 2014. Soil carbon stocks and accumulation in young mangrove forests. Soil Biol. Biochem. 75, 223–232. doi:10.1016/j.soilbio.2014.04.008

Luo, Y., Hui, D., Zhang, D., 2006. Elevated Co2 Stimulates Net Accumulations of Carbon and Nitrogen in Land Ecosystems: A Meta-Analysis. Ecology 87, 53–63. doi:10.1890/04-1724

Luo, Z., Sun, O.J., Wang, E., Ren, H., Xu, H., 2010. Modeling Productivity in Mangrove Forests as Impacted by Effective Soil Water Availability and Its Sensitivity to Climate Change Using Biome-BGC. Ecosystems 13, 949–965. doi:10.1007/s10021-010-9365-y

Lüthi, D., Le Floch, M., Bereiter, B., Blunier, T., Barnola, J.-M., Siegenthaler, U., Raynaud, D., Jouzel, J., Fischer, H., Kawamura, K., Stocker, T.F., 2008. High-resolution carbon dioxide concentration record 650,000–800,000 years before present. Nature 453, 379–382. doi:10.1038/nature06949

Lyimo, T.J., Pol, A., Op den Camp, H.J.M., 2002. Sulfate Reduction and Methanogenesis in Sediments of Mtoni Mangrove Forest, Tanzania. AMBIO J. Hum. Environ. 31, 614–616. doi:10.1579/0044-7447-31.7.614

M

Mackey, A.P., Smail, G., 1996. The decomposition of mangrove litter in a subtropical mangrove forest. Hydrobiologia 332, 93–98. doi:10.1007/BF00016688

Maher, D.T., Cowley, K., Santos, I.R., Macklin, P., Eyre, B.D., 2015. Methane and carbon dioxide dynamics in a subtropical estuary over a diel cycle: Insights from automated in situ radioactive and stable isotope measurements. Mar. Chem. 168, 69–79. doi:10.1016/j.marchem.2014.10.017

Maher, D.T., Santos, I.R., Golsby-Smith, L., Gleeson, J., Eyre, B.D., 2013. Groundwater-derived dissolved inorganic and organic carbon exports from a mangrove tidal creek: The missing mangrove carbon sink? Limnol. Oceanogr. 58, 475–488. doi:10.4319/lo.2013.58.2.0475

Maitrepierre, L., 2012. Les types de temps et les cyclones, les éléments du climat. Atlas de la Nouvelle-Calédonie., in: Atlas de La Nouvelle-Calédonie. pp. 53–60.

Marchand, C., 2017. Soil carbon stocks and burial rates along a mangrove forest chronosequence (French Guiana). For. Ecol. Manag. 384, 92–99. doi:10.1016/j.foreco.2016.10.030

Marchand, C., Allenbach, M., Lallier-Vergès, E., 2011a. Relationships between heavy metals distribution and organic matter cycling in mangrove sediments (Conception Bay, New Caledonia). Geoderma 160, 444–456. doi:10.1016/j.geoderma.2010.10.015

Marchand, C., Fernandez, J.-M., Moreton, B., Landi, L., Lallier-Vergès, E., Baltzer, F., 2012. The partitioning of transitional metals (Fe, Mn, Ni, Cr) in mangrove sediments downstream of a ferralitized ultramafic watershed (New Caledonia). Chem. Geol. 300–301, 70–80. doi:10.1016/j.chemgeo.2012.01.018

Marchand, C., Lallier-Vergès, E., Allenbach, M., 2011b. Redox conditions and heavy metals distribution in mangrove forests receiving effluents from shrimp farms (Teremba Bay, New Caledonia). J. Soils Sediments 11, 529–541. doi:10.1007/s11368-010-0330-3

McDonald, E.P., Erickson, J.E., Kruger, E.L., 2002. Research note: Can decreased transpiration limit plant nitrogen acquisition in elevated CO2? Funct. Plant Biol. 29, 1115–1120.

McKee, K.L., 2011. Biophysical controls on accretion and elevation change in Caribbean mangrove ecosystems. Estuar. Coast. Shelf Sci. 91, 475–483. doi:10.1016/j.ecss.2010.05.001

McKee, K.L., 1996. Growth and physiological responses of neotropical mangrove seedlings to root zone hypoxia. Tree Physiol. 16, 883–889. doi:10.1093/treephys/16.11-12.883

McKee, K.L., Cahoon, D.R., Feller, I.C., 2007. Caribbean mangroves adjust to rising sea level through biotic controls on change in soil elevation. Glob. Ecol. Biogeogr. 16, 545–556. doi:10.1111/j.1466-8238.2007.00317.x

McKee, K.L., Rooth, J.E., 2008. Where temperate meets tropical: multi-factorial effects of elevated CO_2, nitrogen enrichment, and competition on a mangrove-salt marsh community. Glob. Change Biol. 14, 971–984. doi:10.1111/j.1365-2486.2008.01547.x

Mcleod, E., Chmura, G.L., Bouillon, S., Salm, R., Björk, M., Duarte, C.M., Lovelock, C.E., Schlesinger, W.H., Silliman, B.R., 2011. A blueprint for blue carbon: toward an improved understanding of the role of vegetated coastal habitats in sequestering CO_2. Front. Ecol. Environ. 9, 552–560. doi:10.1890/110004

Meier, M.F., Dyurgerov, M.B., Rick, U.K., O'Neel, S., Pfeffer, W.T., Anderson, R.S., Anderson, S.P., Glazovsky, A.F., 2007. Glaciers Dominate Eustatic Sea-Level Rise in the 21st Century. Science 317, 1064–1067. doi:10.1126/science.1143906

Metcalfe, D., Meir, P., Aragao, L.E.O.C., Malhi, Y., Costa, D., L, A.C., Braga, A., Goncalves, P.H.L., de Athaydes, J., Almeida, D., S, S., Williams, M., 2007. Factors controlling spatio-temporal variation in carbon dioxide efflux from surface litter, roots, and soil organic matter at four rain forest sites in the eastern Amazon. J. Geophys. Res. 112, 04001–04001. doi:http://dx.doi.org/10.1029/2007JG000443

Meyers, P.A., Lallier-Vergès, E., 1999. Lacustrine sedimentary organic matter records of Late Quaternary paleoclimates. J. Paleolimnol. 21, 345–372.

Mitrovica, J.X., Peltier, W.R., 1991. On postglacial geoid subsidence over the equatorial oceans. J. Geophys. Res. Solid Earth 96, 20053–20071. doi:10.1029/91JB01284

Mizanur Rahman, M., Nabiul Islam Khan, M., Fazlul Hoque, A.K., Ahmed, I., 2015. Carbon stock in the Sundarbans mangrove forest: spatial variations in vegetation types and salinity zones. Wetl. Ecol. Manag. 23, 269–283. doi:10.1007/s11273-014-9379-x

Molnar, N., 2012. Impact des effluents de la crevetticulture sur la dynamique de la matière organique benthique et leurs implications sur les processus biogéochimiques dans une mangrove (Nouvelle-Calédonie).

Moore, T.R., Knowles, R., 1990. Methane Emissions from Fen, Bog and Swamp Peatlands in Quebec. Biogeochemistry 11, 45–61.

Morat, P., Jaffré, T., Tronchet, F., Munzinger, J., Pillon, Y., Veillon, J.-M., Chalopin, M., Birnbaum, P., Rigault, F., Dagostini, G., Tinel, J., Lowry, P.P., 2012. Le référentiel taxonomique Florical et les caractéristiques de la flore vasculaire indigène de la Nouvelle-Calédonie. Adansonia 34, 179–221. doi:10.5252/a2012n2a1

Mukherjee, N., Sutherland, W.J., Dicks, L., Hugé, J., Koedam, N., Dahdouh-Guebas, F., 2014. Ecosystem Service Valuations of Mangrove Ecosystems to Inform Decision Making and Future Valuation Exercises. PLoS ONE 9. doi:10.1371/journal.pone.0107706

Mumby, P.J., Edwards, A.J., Arias-González, J.E., Lindeman, K.C., Blackwell, P.G., Gall, A., Gorczynska, M.I., Harborne, A.R., Pescod, C.L., Renken, H., 2004. Mangroves enhance the biomass of coral reef fish communities in the Caribbean. Nature 427, 533–536.

Myers, N., Mittermeier, R.A., Mittermeier, C.G., da Fonseca, G.A.B., Kent, J., 2000. Biodiversity hotspots for conservation priorities. Nature 403, 853–858. doi:10.1038/35002501

Myhre, G., Shindell, D., Bréon, F.-M., Collins, W., Fuglestvedt, J., Huang, J., Koch, D., Lamarque, J.-F., Lee, D., Mendoza, B., others, 2013. Anthropogenic and natural

radiative forcing. Clim. Change 2013 Phys. Sci. Basis Contrib. Work. Group Fifth Assess. Rep. Intergov. Panel Clim. Change Stock. TF Qin G-K Plattner M Tignor SK Allen J Boschung Nauels Xia V Bex PM Midgley Eds 423, 658–740.

N

Nagelkerken, I., Blaber, S.J.M., Bouillon, S., Green, P., Haywood, M., Kirton, L.G., Meynecke, J.-O., Pawlik, J., Penrose, H.M., Sasekumar, A., Somerfield, P.J., 2008. The habitat function of mangroves for terrestrial and marine fauna: A review. Aquat. Bot., Mangrove Ecology – Applications in Forestry and Costal Zone Management 89, 155–185. doi:10.1016/j.aquabot.2007.12.007

Naidoo, G., Rogalla, H., Willert, D.J. von, 1997. Gas exchange responses of a mangrove species, *Avicennia marina*, to waterlogged and drained conditions. Hydrobiologia 352, 39. doi:10.1023/A:1003088803335

Nguyen, H.T., Stanton, D.E., Schmitz, N., Farquhar, G.D., Ball, M.C., 2015. Growth responses of the mangrove *Avicennia marina* to salinity: development and function of shoot hydraulic systems require saline conditions. Ann. Bot. 115, 397–407. doi:10.1093/aob/mcu257

Nóbrega, G.N., Ferreira, T.O., Siqueira Neto, M., Queiroz, H.M., Artur, A.G., Mendonça, E.D.S., Silva, E.D.O., Otero, X.L., 2016. Edaphic factors controlling summer (rainy season) greenhouse gas emissions (CO2 and CH4) from semiarid mangrove soils (NE-Brazil). Sci. Total Environ. 542, 685–693. doi:10.1016/j.scitotenv.2015.10.108

Nonquet, G., 2005. Mwata rè nê, le gâteau du fruit de palétuvier.

Norby, R.J., DeLucia, E.H., Gielen, B., Calfapietra, C., Giardina, C.P., King, J.S., Ledford, J., McCarthy, H.R., Moore, D.J.P., Ceulemans, R., Angelis, P.D., Finzi, A.C., Karnosky, D.F., Kubiske, M.E., Lukac, M., Pregitzer, K.S., Scarascia-Mugnozza, G.E., Schlesinger, W.H., Oren, R., 2005. Forest response to elevated CO2 is conserved across a broad range of productivity. Proc. Natl. Acad. Sci. U. S. A. 102, 18052–18056. doi:10.1073/pnas.0509478102

Nunn, P.D., Carson, M.T., 2015. Sea-level fall implicated in profound societal change about 2570 cal yr bp (620 bc) in western Pacific island groups. Geo Geogr. Environ. 2. doi:10.1002/geo2.3

O

Oertel, C., Matschullat, J., Zurba, K., Zimmermann, F., Erasmi, S., 2016. Greenhouse gas emissions from soils—A review. Chem. Erde - Geochem. 76, 327–352. doi:10.1016/j.chemer.2016.04.002

O'Leary, M.H., 1988. Carbon isotopes in photosynthesis. Bioscience 38, 328–336.

Ong, J.E., Gong, W.K., Wong, C.H., 2004. Allometry and partitioning of the mangrove, *Rhizophora* apiculata. For. Ecol. Manag. 188, 395–408. doi:10.1016/j.foreco.2003.08.002

Orekhov, D.I., Yakovleva, O.V., Goryachev, S.N., Protopopov, F.F., Alekseev, A.A., 2015. The use of parameters of chlorophyll a fluorescence induction to evaluate the state of plants under anthropogenic load. Biophysics 60, 263–268. doi:10.1134/S0006350915020128

P

Parida, A.K., Jha, B., 2010. Salt tolerance mechanisms in mangroves: a review. Trees 24, 199–217.

Parkin, T.B., Kaspar, T.C., 2003. Temperature Controls on Diurnal Carbon Dioxide Flux. Soil Sci. Soc. Am. J. 67, 1763–1772. doi:10.2136/sssaj2003.1763

Pataki, D.E., Ehleringer, J.R., Flanagan, L.B., Yakir, D., Bowling, D.R., Still, C.J., Buchmann, N., Kaplan, J.O., Berry, J.A., 2003. The application and interpretation of Keeling plots in terrestrial carbon cycle research. Glob. Biogeochem. Cycles 17.

Patel, N.T., Gupta, A., Pandey, A.N., 2010. Salinity tolerance of *Avicennia marina* (Forssk.) Vierh. from Gujarat coasts of India. Aquat. Bot. 93, 9–16. doi:10.1016/j.aquabot.2010.02.002

Pezeshki, S.R., DeLaune, R.D., Meeder, J.F., 1997. Carbon assimilation and biomass partitioning in *Avicennia* germinans and *Rhizophora* mangle seedlings in response to soil redox conditions. Environ. Exp. Bot. 37, 161–171.

Polidoro, B.A., Carpenter, K.E., Collins, L., Duke, N.C., Ellison, A.M., Ellison, J.C., Farnsworth, E.J., Fernando, E.S., Kathiresan, K., Koedam, N.E., Livingstone, S.R., Miyagi, T., Moore, G.E., Nam, V.N., Ong, J.E., Primavera, J.H., Iii, S.G.S., Sanciangco, J.C., Sukardjo, S., Wang, Y., Yong, J.W.H., 2010. The Loss of Species: Mangrove Extinction Risk and Geographic Areas of Global Concern. PLOS ONE 5, e10095. doi:10.1371/journal.pone.0010095

Poorter, H., Navas, M.-L., 2003. Plant growth and competition at elevated CO2: on winners, losers and functional groups. New Phytol. 157, 175–198. doi:10.1046/j.1469-8137.2003.00680.x

Poungparn, S., Komiyama, A., Tanaka, A., Sangtiean, T., Maknual, C., Kato, S., Tanapermpool, P., Patanaponpaiboon, P., 2009. Carbon Dioxide Emission through Soil Respiration in a Secondary Mangrove Forest of Eastern Thailand. J. Trop. Ecol. 25, 393–400.

Prasad, M.B.K., Kumar, A., Ramanathan, A.L., Datta, D.K., 2017. Sources and dynamics of sedimentary organic matter in Sundarban mangrove estuary from Indo-Gangetic delta. Ecol. Process. 6. doi:10.1186/s13717-017-0076-6

Prasad, M.N.V., Strzałka, K., 1999. Impact of Heavy Metals on Photosynthesis, in: Heavy Metal Stress in Plants. Springer, Berlin, Heidelberg, pp. 117–138. doi:10.1007/978-3-662-07745-0_6

Prior, S.A., Runion, G.B., Marble, S.C., Rogers, H.H., Gilliam, C.H., Torbert, H.A., 2011. A Review of Elevated Atmospheric CO2 Effects on Plant Growth and Water Relations: Implications for Horticulture. HortScience 46, 158–162.

R

R Development Core Team, 2008. R: A language and environment for statistical computing. R Foundation for Statistical Computing. Vienna, Austria.

Radić, V., Hock, R., 2011. Regionally differentiated contribution of mountain glaciers and ice caps to future sea-level rise. Nat. Geosci. 4, 91–94. doi:10.1038/ngeo1052

Raich, J.W., Schlesinger, W.H., 1992. The global carbon dioxide flux in soil respiration and its relationship to vegetation and climate. Tellus Ser. B Chem. Phys. Meteorol. B 44, 81–99. doi:10.1034/j.1600-0889.1992.t01-1-00001.x

Redfield, A.C., Ketchum, B.H., Richards, F.A., 1963. The influence of organisms on the composition of sea-water. Sea Ideas Obs. Prog. Study Seas.

Reef, R., Feller, I.C., Lovelock, C.E., 2010. Nutrition of mangroves. Tree Physiol. 30, 1148–1160. doi:10.1093/treephys/tpq048

Reef, R., Lovelock, C.E., 2014. Historical analysis of mangrove leaf traits throughout the 19th and 20th centuries reveals differential responses to increases in atmospheric CO2. Glob. Ecol. Biogeogr. 23, 1209–1214. doi:10.1111/geb.12211

Reef, R., Slot, M., Motro, U., Motro, M., Motro, Y., Adame, M.F., Garcia, M., Aranda, J., Lovelock, C.E., Winter, K., 2016. The effects of CO2 and nutrient fertilisation on the growth and temperature response of the mangrove *Avicennia* germinans. Photosynth. Res. 129, 159–170. doi:10.1007/s11120-016-0278-2

Reef, R., Winter, K., Morales, J., Adame, M.F., Reef, D.L., Lovelock, C.E., 2015. The effect of atmospheric carbon dioxide concentrations on the performance of the mangrove *Avicennia germinans* over a range of salinities. Physiol. Plant. 154, 358–368. doi:10.1111/ppl.12289

Rivera-Monroy, V.H., Torres, L.A., Bahamon, N., Newmark, F., Twilley, R.R., 1999. The Potential Use of Mangrove Forests as Nitrogen Sinks of Shrimp Aquaculture Pond Effluents: The Role of Denitrification. J. World Aquac. Soc. 30, 12–25. doi:10.1111/j.1749-7345.1999.tb00313.x

Rollet, B., 1975. Les utilisations de la mangrove. Les usages forestiers. J. Agric. Trop. Bot. Appliquée 22, 297–340. doi:10.3406/jatba.1975.3217

S

Sage, R.F., Kubien, D.S., 2007. The temperature response of C3 and C4 photosynthesis. Plant Cell Environ. 30, 1086–1106. doi:10.1111/j.1365-3040.2007.01682.x

Saintilan, N., Rogers, K., Mazumder, D., Woodroffe, C., 2013. Allochthonous and autochthonous contributions to carbon accumulation and carbon store in southeastern Australian coastal wetlands. Estuar. Coast. Shelf Sci. 128, 84–92. doi:10.1016/j.ecss.2013.05.010

Sanders, C.J., Maher, D.T., Tait, D.R., Williams, D., Holloway, C., Sippo, J.Z., Santos, I.R., 2016. Are global mangrove carbon stocks driven by rainfall?: Mangrove Carbon Stocks. J. Geophys. Res. Biogeosciences 121, 2600–2609. doi:10.1002/2016JG003510

Sanders, C.J., Smoak, J.M., Naidu, A.S., Araripe, D.R., Sanders, L.M., Patchineelam, S.R., 2010. Mangrove forest sedimentation and its reference to sea level rise, Cananeia, Brazil. Environ. Earth Sci. 60, 1291–1301. doi:10.1007/s12665-009-0269-0

Santos, I.R., Eyre, B.D., Huettel, M., 2012. The driving forces of porewater and groundwater flow in permeable coastal sediments: A review. Estuar. Coast. Shelf Sci. 98, 1–15. doi:10.1016/j.ecss.2011.10.024

Schneider, C.A., Rasband, W.S., Eliceiri, K.W., 2012. NIH Image to ImageJ: 25 years of image analysis. Nat Meth 9, 671–675. doi:10.1038/nmeth.2089

Scholander, P.F., van Dam, L., Scholander, S.I., 1955. Gas Exchange in the Roots of Mangroves. Am. J. Bot. 42, 92–98. doi:10.2307/2438597

Segers, R., 1998. Methane production and methane consumption: a review of processes underlying wetland methane fluxes. Biogeochemistry 41, 23–51.

Sjögersten, S., Black, C.R., Evers, S., Hoyos-Santillan, J., Wright, E.L., Turner, B.L., 2014. Tropical wetlands: A missing link in the global carbon cycle? Glob. Biogeochem. Cycles 28, 1371–1386. doi:10.1002/2014GB004844

Skelton, N.J., Allaway, W.G., 1996. Oxygen and pressure changes measured in situ during flooding in roots of the Grey Mangrove *Avicennia marina* (Forssk.) Vierh. Aquat. Bot., Ventilation in Macrophytes 54, 165–175. doi:10.1016/0304-3770(96)01043-1

Smith, S.M., Snedaker, S.C., 1995. Salinity Responses in Two Populations of Viviparous *Rhizophora* mangle L. Seedlings. Biotropica 27, 435. doi:10.2307/2388955

Snedaker, S.C., Araújo, R.J., 1998. Stomatal conductance and gas exchange in four species of Caribbean mangroves exposed to ambient and increased CO2. Mar. Freshw. Res. 49, 325–327.

Sobrado, M.A., 2008. Leaf characteristics and diurnal variation of chlorophyll fluorescence in leaves of the 'Bana'vegetation of the Amazon region. Photosynthetica 46, 202.

Stieglitz, T., Ridd, P., Müller, P., 2000. Passive irrigation and functional morphology of crustacean burrows in a tropical mangrove swamp. Hydrobiologia 421, 69–76. doi:10.1023/A:1003925502665

Stieglitz, T.C., Clark, J.F., Hancock, G.J., 2013. The mangrove pump: The tidal flushing of animal burrows in a tropical mangrove forest determined from radionuclide budgets. Geochim. Cosmochim. Acta 102, 12–22. doi:10.1016/j.gca.2012.10.033

Stocker, T.F., Qin, D., Plattner, G.-K., Tignor, M., Allen, S.K., Boschung, J., Nauels, A., Xia, Y., Bex, B., Midgley, B.M., 2013. IPCC, 2013: climate change 2013: the physical science basis. Contribution of working group I to the fifth assessment report of the intergovernmental panel on climate change. Cambridge University Press.

Sun, Z., Jiang, H., Wang, L., Mou, X., Sun, W., 2013. Seasonal and spatial variations of methane emissions from coastal marshes in the northern Yellow River estuary, China. Plant Soil 369, 317–333. doi:10.1007/s11104-012-1564-1

T

Tamooh, F., Huxham, M., Karachi, M., Mencuccini, M., Kairo, J.G., Kirui, B., 2008. Below-ground root yield and distribution in natural and replanted mangrove forests at Gazi bay, Kenya. For. Ecol. Manag. 256, 1290–1297. doi:10.1016/j.foreco.2008.06.026

Taub, D.R., Wang, X., 2008. Why are nitrogen concentrations in plant tissues lower under elevated CO2? A critical examination of the hypotheses. J. Integr. Plant Biol. 50, 1365–1374. doi:10.1111/j.1744-7909.2008.00754.x

Tomlinson, P.B., 1986. The botany of mangroves. Cambridge University Press.

Trudeau, N.C., Garneau, M., Pelletier, L., 2013. Methane fluxes from a patterned fen of the northeastern part of the La Grande river watershed, James Bay, Canada. Biogeochemistry 113, 409–422. doi:10.1007/s10533-012-9767-3

Turetsky, M.R., Treat, C.C., Waldrop, M.P., Waddington, J.M., Harden, J.W., McGuire, A.D., 2008. Short-term response of methane fluxes and methanogen activity to water table and soil warming manipulations in an Alaskan peatland. J. Geophys. Res. Biogeosciences 113, G00A10. doi:10.1029/2007JG000496

Twilley, R.R., Chen, R.H., Hargis, T., 1992. Carbon sinks in mangroves and their implications to carbon budget of tropical coastal ecosystems, in: Natural Sinks of CO2. Springer, pp. 265–288.

U

UNESCO World Heritage Centre, 2009. UNESCO World Heritage Centre - 32nd session of the Committee (No. WHC-08/32.COM/24Rev).

Urban, O., 2003. Physiological Impacts of Elevated CO2 Concentration Ranging from Molecular to Whole Plant Responses. Photosynthetica 41, 9–20. doi:10.1023/A:1025891825050

V

Van Cappellen, P., Wang, Y., 1996. Cycling of iron and manganese in surface sediments; a general theory for the coupled transport and reaction of carbon, oxygen, nitrogen, sulfur, iron, and manganese. Am. J. Sci. 296, 197–243. doi:10.2475/ajs.296.3.197

Virly, S., 2006. Virly, 2008, Typologies et Biodiversité des mangroves.

W

Wang, C., Lai, D.Y.F., Tong, C., Wang, W., Huang, J., Zeng, C., 2015. Variations in Temperature Sensitivity (Q10) of CH4 Emission from a Subtropical Estuarine Marsh in Southeast China. PLoS ONE 10. doi:10.1371/journal.pone.0125227

Wang, G., Guan, D., Peart, M.R., Chen, Y., Peng, Y., 2013. Ecosystem carbon stocks of mangrove forest in Yingluo Bay, Guangdong Province of South China. For. Ecol. Manag. 310, 539–546. doi:10.1016/j.foreco.2013.08.045

Wang, H., Liao, G., D'Souza, M., Yu, X., Yang, J., Yang, X., Zheng, T., 2016. Temporal and spatial variations of greenhouse gas fluxes from a tidal mangrove wetland in Southeast China. Environ. Sci. Pollut. Res. 23, 1873–1885. doi:10.1007/s11356-015-5440-4

Ward, R.D., Friess, D.A., Day, R.H., MacKenzie, R.A., 2016. Impacts of climate change on mangrove ecosystems: a region by region overview. Ecosyst. Health Sustain. 2. doi:10.1002/ehs2.1211

Weiss, C., Weiss, J., Boy, J., Iskandar, I., Mikutta, R., Guggenberger, G., 2016. Soil organic carbon stocks in estuarine and marine mangrove ecosystems are driven by nutrient colimitation of P and N. Ecol. Evol. 6, 5043–5056. doi:10.1002/ece3.2258

Wirrmann, D., Sémah, A.-M., Debenay, J.-P., Chacornac-Rault, M., 2011. Mid- to late Holocene environmental and climatic changes in New Caledonia, southwest tropical Pacific, inferred from the littoral plain Gouaro-Déva. Quat. Res. 76, 229–242. doi:10.1016/j.yqres.2011.04.007

Woodroffe, C.D., Rogers, K., McKee, K.L., Lovelock, C.E., Mendelssohn, I.A., Saintilan, N., 2016. Mangrove Sedimentation and Response to Relative Sea-Level Rise. Annu. Rev. Mar. Sci. 8, 243–266. doi:10.1146/annurev-marine-122414-034025

Woodroffe, S.A., Long, A.J., Punwong, P., Selby, K., Bryant, C.L., Marchant, R., 2015. Radiocarbon dating of mangrove sediments to constrain Holocene relative sea-level change on Zanzibar in the southwest Indian Ocean. The Holocene 25, 820–831.

Wooller, M., Smallwood, B., Jacobson, M., Fogel, M., 2003. Carbon and nitrogen stable isotopic variation in Laguncularia racemosa (L.) (white mangrove) from Florida and Belize: implications for trophic level studies. Hydrobiologia 499, 13–23. doi:10.1023/A:1026339517242

X

Xu, M., Qi, Y., 2001. Soil-surface CO2 efflux and its spatial and temporal variations in a young ponderosa pine plantation in northern California. Glob. Change Biol. 7, 667–677. doi:10.1046/j.1354-1013.2001.00435.x

Y

Yamano, H., Cabioch, G., Chevillon, C., Join, J.-L., 2014. Late Holocene sea-level change and reef-island evolution in New Caledonia. Geomorphology 222, 39–45. doi:10.1016/j.geomorph.2014.03.002

Yin, X., 2002. Responses of leaf nitrogen concentration and specific leaf area to atmospheric CO2 enrichment: a retrospective synthesis across 62 species. Glob. Change Biol. 8, 631–642. doi:10.1046/j.1365-2486.2002.00497.x

Youssef, T., Saenger, P., 1996. Anatomical adaptive strategies to flooding and rhizosphere oxidation in mangrove seedlings. Aust. J. Bot. 297–313.

Yruela, I., 2013. Transition metals in plant photosynthesis. Met. Integr. Biometal Sci. 5, 1090–1109. doi:10.1039/c3mt00086a

Z

Zeebe, R.E., Ridgwell, A., Zachos, J.C., 2016. Anthropogenic carbon release rate unprecedented during the past 66 million years. Nat. Geosci. 9, ngeo2681. doi:10.1038/ngeo2681

Zhang, D., Hui, D., Luo, Y., Zhou, G., 2008. Rates of litter decomposition in terrestrial ecosystems: global patterns and controlling factors. J. Plant Ecol. 1, 85–93. doi:10.1093/jpe/rtn002

Zickfeld, K., Solomon, S., Gilford, D.M., 2017. Centuries of thermal sea-level rise due to anthropogenic emissions of short-lived greenhouse gases. Proc. Natl. Acad. Sci. 114, 657–662. doi:10.1073/pnas.1612066114

Zimmermann, M., Meir, P., Bird, M., Malhi, Y., Ccahuana, A., 2009. Litter contribution to diurnal and annual soil respiration in a tropical montane cloud forest. Soil Biol. Biochem. 41, 1338–1340. doi:10.1016/j.soilbio.2009.02.023

Ziska, L.H., Drake, B.G., Chamberlain, S., 1990. Long-term photosynthetic response in single leaves of a C3 and C4 salt marsh species grown at elevated atmospheric CO2 in situ. Oecologia 83, 469–472.

Liste des Figures

Chapitre I

Chapitre II

Chapitre III

Chapitre IV

Liste des Tableaux

Chapitre I

Chapitre II

Chapitre III

Chapitre IV

Résumé

La mangrove est un écosystème complexe qui se développe sur les zones intertidales, le long des littoraux (sub)tropicaux. Du fait de sa position, elle est considérée comme un écosystème majeur dans le cycle du carbone des zones côtières. Dû à sa production primaire élevée, couplée à une grande capacité de séquestration du carbone organique à la fois dans la biomasse, et dans les sols, la mangrove a été nommée écosystème à « Carbone Bleu ». Toutefois, le changement climatique à venir, et particulièrement les augmentations en CO_2 atmosphérique et en température ainsi que la hausse du niveau marin, pourraient modifier son fonctionnement. Dans de ce contexte, les objectifs étaient de (i) comprendre comment les variations eustatiques passées ont pu impacter les stocks de carbone enfouis dans les sols de mangrove, afin de mieux prévoir l'effet de la future hausse du niveau marin, (ii) caractériser l'influence des marées et de la température sur les émissions de CO_2 et de CH_4 depuis les sols mais aussi depuis la colonne d'eau au sein de la mangrove à marée haute, et (iii) évaluer l'impact de la hausse des concentrations en CO_2 atmosphérique et d'une prolongation de la durée d'immersion sur la physiologie de jeunes plantules de palétuviers. L'augmentation des concentrations CO_2 atmosphérique modifiera fortement la productivité des jeunes palétuviers, notamment en stimulant leur activité photosynthétique, facilitant ainsi leurs capacités à coloniser de nouveaux espaces disponibles du fait de la hausse des océans. Cette hausse aura également un effet conséquent sur les stocks de carbone dans les sols de mangrove, comme nous l'avons montré pour les variations eustatiques au cours de la fin de l'Holocène, impliquant également une migration des strates de mangrove. Finalement, les émissions de CO_2 et de CH_4 vers l'atmosphère sont non négligeables, tout particulièrement celles émises depuis la colonne d'eau, et devront être pris en compte dans les futurs bilans carbone de l'écosystème.

Mots-clés : Mangrove ; Changement climatique ; Productivité primaire ; Stock de carbone ; Gaz à effet de serre ; Nouvelle-Calédonie

Abstract

Mangroves are complex and unique ecosystems that develop on intertidal areas along (sub)tropical coastlines. Due to their position, they are considered as major ecosystems in the coastal carbon cycle. Thanks to their high primary productivity, coupled with a high carbon sequestrating capacity in both biomass and soils, mangroves have been called "Blue Carbon" ecosystems. However, future climate change, and particularly increases in atmospheric CO_2 concentrations, temperatures and sea-level rise, may alter its functioning. Within this context, the objectives were to (i) understand how eustatic variations may have impacted soil carbon stocks by the past, in order to better predict the effects of future sea-level rise, (ii) characterize CO_2 and CH_4 emissions from the soil and also from the water column within the mangrove forest, and (iii) evaluate the impact of future increase in atmospheric CO_2 concentrations and in sea-level may affect the physiology of young mangrove seedlings. Increases in atmospheric CO2 concentrations will modify either the seedlings productivity and photosynthetic activity, therefore facilitating their ability to colonize new accommodation spaces due to the rising sea-level. This increase in sea-level will also have a consequent impact on soil carbon stocks, as we showed for the past eustatic variations of the late Holocene, also implying a migration of mangroves stands. Eventually, CO_2 and CH_4 emissions to the atmosphere were non-neglectable, particularly the one emitted from the water column.

Keywords: Mangrove; Climate Change; Primary productivity; Carbon stock; Greenhouse gas; New Caledonia.